SYNTHESIS, CHARACTERIZATION AND FLUORESCENCE QUENCHING OF WATER-SOLUBLE CATIONIC CONJUGATED POLYMERS

FAN QULI

NATIONAL UNIVERSITY OF SINGAPORE

2003

SYNTHESIS, CHARACTERIZATION AND FLUORESCENCE QUENCHING OF WATER-SOLUBLE CATIONIC CONJUGATED POLYMERS

FAN QULI

(*MSc Nanjing Univ.*)

A THESIS SUBMITTED FOR THE DEGREE OF

DOCTOR OF PHILOSOPHY

INSTITUTE OF MATERIAL RESEARCH AND

ENGINEERING (IMRE)

NATIONAL UNIVERSITY OF SINGAPORE

2003

Name: Fan Quli

Degree: Ph D of Philosophy

Dept: Institute of Material Research and Engineering (IMRE)

Thesis Title: SYNTHESIS, CHARACTERIZATION AND FLUORESCENCE QUENCHING OF WATER-SOLUBLE CATIONIC CONJUGATED POLYMERS

Abstract

Water-soluble conjugated polyelectrolytes have attracted increasing attention recently due to their potential applications as high-sensitive fluorescent biosensors. However, the influence of the physical and chemical properties of these WSCPs on the quenching sensitivity is still a major concern that retards their application as biosensors. The aim of this thesis was to syntheses and characterization of novel water-soluble conjugated polyelectrolytes and to study the structure-quenching and environment-quenching relationship of those conjugated polyelectrolytes as biosensors. In all, many water-soluble cationic ammonium-functionalized poly(*p*-phneylenevinylene) and poly(*p*-phenyleneethynylene) derivatives were synthesized through Gilch and Wittig reaction and Heck reaction respectively, and characterized by various modern techniques. The relationships of their optical properties and quenching behaviors with molecular structures, polymer concentrations, anionic saturated polymers and pH values were highly investigated and some modified theories were proposed to explain those quenching behaviors.

Keywords: Water-soluble conjugated polymers, ammonium-functionalization, sensors, poly(*p*-phneylenevinylene) (PPV), poly(*p*-phenyleneethynylene) (PPE), fluorescence quenching.

ACKNOWLEDGEMENTS

My most sincere gratitude goes out to my supervisor, Dr Huang Wei, for his giving me the opportunity to pursue a Ph. D degree at the Institute of Materials Research and Engineering (IMRE). Also thanks him for his expert guidance, kind encouragement, unselfish support and persistent creation of free research environment during the years. Deepest appreciation goes to my co-supervisor, Assoc. Prof. Lai Yee Hing, for their guidance despite their busy schedules.

I wish to give special thanks to Dr Pei Jian, Dr Chen Zhikuan, Dr Yu Wanglin and Dr Liu Bin, who tried their best to afford me helpful discussions during my research. Their consistent attitudes towards research were deeply impressed me and enlightened me most. In addition, I want to thank all research staffs and students in the Polymeric Light-Emitting Device Group at IMRE, Mdm. Xiao, Cheng Min, Ding Ailin, Liu Xiaoling, Liu Shaoyong, Lu Su, Ni Jing, Pan Jingfang, and not forgetting Zeng Gang, for their great help, collaboration and friendship. Especially, I must express my great appreciate to Pan Jingfang and Lu Su, my best colleagues and friends who worked with me together to spend that most difficult period.

I would also like to express my gratitude to the National University of Singapore for the award of the research scholarship and IMRE for the top-up award and Department of Chemistry for using the facilities to carry out my research.

Last but not least, I am very thankful to my parents and girlfriend Lu Xiaomei for their warmest patience, encouragement and moral support during my study.

TABLE OF CONTENTS

ACKNOWLEDGEMENTS I

TABLE OF CONTENTS II

LIST OF TABLES IX

LIST OF SCHEMES X

LIST OF FIGURES XI

SUMMARY XVII

CHAPTER ONE 1

PART I: BACKGROUND 1

1.1.1 Conjugated Polymers 1

1.1.1.1 Structures of Conjugated Polymers 1

1.1.1.2 Applications of Conjugated Polymers 5

1.1.2 Light-Emitting Polymers (LEPs) and Devices (LEDs) 7

1.1.3 Conjugated Polymers Used as Chemo or Biosensors 12

1.1.4 Synthesis of PPV and Its Derivatives 17

1.1.4.1 Synthetic Routes for PPVs 17

1.1.4.2 Alkoxy-Substituted PPV Derivatives 20

1.1.4.3 Phenyl-Substituted PPV Derivatives 24

1.1.5 Synthesis of PPE and Its Derivatives 27

1.1.5.1 Synthetic Routes for PPEs 27

1.1.5.2 Alkoxy-Substituted PPE Derivatives 30

REFERENCES **35**

CHAPTER ONE **47**

PART II: INTRODUCTION **47**

1.2.1 Conjugated Polyelectrolytes *47*

1.2.1.1 Application of Conjugated Polyelectrolytes 47

1.2.1.2 Layer-by-Layer Self-Assembly of Conjugated Polyelectrolytes 48

1.2.1.3 Conjugated Polyelectrolytes Used as Chemo or Biosensors 53

1.2.2 Project Objectives *57*

REFERENCES **62**

CHAPTER TWO **68**

SYNTHESIS, CHARACTERIZATION, AND FLUORESCENCE QUENCHING OF NOVEL CATIONIC PHENYL-SUBSTITUTED POLY(*P*-PHENYLENEVINYLENE)S **68**

2.1 INTRODUCTION 68

2.2 MOLECULAR DESIGN 70

2.3 SYNTHESIS AND CHARACTERIZATION 71

2.3.1 Materials *71*

2.3.2 Characterization Methods *72*

2.4 RESULTS AND DISCUSSION 73

2.4.1 Synthesis of Monomers and polymers *73*

2.4.2 Solubility Studies *76*

2.4.3 FT-IR Analysis *78*

2.4.4 NMR Analysis *80*

2.4.5 Thermal Stability *82*

2.4.6 Optical Properties *83*

2.4.7 Fluorescent Quenching of P3' *88*

2.5 CONCLUSIONS 92

REFERENCES AND NOTES **94**

CHAPTER THREE **98**

PART I: SYNTHESIS, CHARACTERIZATION AND OPTICAL PROPERTIES OF CATIONIC PHENYL-SUBSTITUTED POLY(*P*-PHENYLENEVINYLENE) RELATED COPOLYMERS **98**

3.1.1 Introduction *98*

3.1.2 Molecular Design *100*

3.1.3 Materials and Characterization Methods *101*

3.1.3.1 Materials 101

3.1.3.2 Characterization Methods 101

3.1.4 Results and Discussion *102*

3.1.4.1 Synthesis of Monomers and Polymers 102

3.1.4.2 Color and Solubility 105

3.1.4.3 FT-IR Analysis 106

3.1.4.4 Gel Permeation Chromatography (GPC) 108

3.1.4.5 Thermal Stability 109

3.1.4.6 NMR Analysis 112

3.1.4.7 Optical Properties 114

3.1.5 Conclusions 117

REFERENCES AND NOTES 119

CHAPTER THREE 121

PART II: FLUORESCENCE QUENCHING OF CATIONIC POLY(*P*-PHENYLENEVINYLENE)S WITH DIFFERENT CONTENTS OF *CIS*-AND *TRANS*-VINYLIC LINKAGES 121

3.2.1 Introduction 121

3.2.2 Materials and Characterization Methods 123

3.2.2.1 Materials 123

3.2.2.2 Characterization Methods 124

3.2.3 Results and Discussion 124

3.2.4 Conclusions 136

REFERENCES AND NOTES 137

CHAPTER FOUR 139

PART I: SYNTHESIS, CHARACTERIZATION AND PH-SENSITIVE OPTICAL PROPERTIES OF CATIONIC WATER-SOLUBLE POLY(*P*-PHENYLENEETHYNYLENE)S 139

4.1.1 Introduction 139

4.1.2 Molecular Design *141*

4.1.3 Materials and Characterization Methods *142*

4.1.3.1 Materials 142

4.1.3.2 Characterization Methods 142

4.1.4 Results and Discussion *143*

4.1.4.1 Synthesis of Monomers and Polymers 143

4.1.4.2 Solubility and Color Study 145

4.1.4.3 NMR Spectroscopy 147

4.1.4.4 Thermal Stability 149

4.1.4.5 Optical Properties 150

4.1.4.6 pH-Sensitive Photoluminescence of P8' 152

4.1.4.7 Stern-Volmer Study at Different pH Values 158

4.1.5 Conclusions *161*

REFERENCES AND NOTES **163**

CHAPTER FOUR **165**

PART II: POLYMER-CONCENTRATION-DEPENDENT PHOTOLUMINESCENCE QUENCHING OF POLY(*P*-PHENYLENEETHYNYLENE) BY $FE(CN)_6^{4-}$ IN AQUEOUS SOLUTION **165**

4.2.1 Introduction *165*

4.2.2 Materials and Characterization Methods *167*

4.2.2.1 Materials 167

4.2.2.2 Characterization Methods 167

4.2.3 Results and Discussion 168

4.2.3.1 UV-vis Absorption and Emission 168

4.2.3.2 Stern-Volmer Studies 170

4.2.4 Conclusions 178

REFERENCES AND NOTES 180

PART III: STUDY ON OPTICAL PROPERTIES AND FLUORESCENCE QUENCHING OF CATIONIC WATER-SOLUBLE POLY(*P*-PHENYLENEETHYNYLENE) UNDER COMPLEXATION WITH ANIONIC SATURATED POLYELECTROLYTES 182

4.3.1 Introduction 182

4.3.2 Materials and Characterization Methods 183

4.3.2.1 Materials 183

4.3.2.2 Characterization Methods 184

4.3.3 Results and Discussion 184

4.3.3.1 UV-vis Absorption and Emission of Polyelectrolyte Complex 184

4.3.3.2 Stern-Volmer Study of PAANa/PPE-NEt_3Br and PMAANa/PPE-NEt_3Br Complexes 190

4.3.4 Conclusions 196

REFERENCES AND NOTES 198

CHAPTER FIVE **200**

EXPERIMENTAL SECTION **200**

5.1 GENERAL 200

5.2 MONOMERS AND POLYMERS SYNTHESIZED IN CHAPTER 2 200

5.3 MONOMERS AND POLYMERS SYNTHESIZED IN CHAPTER 3 216

5.4 MONOMERS AND POLYMERS SYNTHESIZED IN CHAPTER 4 228

CHAPTER SIX **247**

CONCLUSION REMARKS **247**

LIST OF TABLES

Table 1.1.1 Some common conjugated polymers _____ *2*

Table 2.1 GPC and Spectroscopic Data for Ph-PPVs _____ *86*

Table 3.1.1 GPC and Spectroscopic Data for all Neutral and Quaternized Polymers 109

Table 3.2.1 Photoluminescence Quenching of Cationic PPVs by $Fe(CN)_6^{4-}$ _____ *129*

Table 4.1.1 Characterization of neutral polymers and uaternized polymers _____ *147*

Table 4.3.1 Photoluminescence quenching of complexes of PPE-NEt_3^+ *and anionic saturated polymers by* $Fe(CN)_6^{4-}$ _____ *192*

LIST OF SCHEMES

Scheme 2.1 Synthetic Routes for Monomers 1 and 2 _____ *74*

Scheme 2.2 Synthetic Routes for Monomers 3 and 4 _____ *75*

Scheme 2.3 Synthetic Routes for the Polymers _____ *76*

Scheme 3.1.1 The synthetic routes for the monomers _____ *103*

Scheme 3.1.2 The synthetic routes for those neutral and quaternized polymers ____ *104*

Scheme 3.2.1 Chemical structure of neutral and quaternized PPVs used in our investigation _____ *123*

Scheme 3.2.2 The conformation of one unit of P1' and P2 _____ *134*

Scheme 4.1.1 The synthetic route for monomers _____ *144*

Scheme 4.1.2 The synthetic routes for neutral and quaternized PPEs _____ *145*

Scheme 4.3.1 Chemical structures of ionic polymers used in our investigation _____ *183*

LIST OF FIGURES

Figure 1.1.1 The scheme for photoluminescence (PL) and electroluminescence (EL) of conjugated polymers ____ 9

Figure 1.1.2 The schematic diagram of the EL process ____ 9

Figure 1.1.3 The structure of a single-layer polymer LED device ____ 10

Figure 1.1.4 Conjugated polymers used in PLEDs ____ 11

Figure 1.1.5 Typical CPs used for detecting alkali or alkaline-earth metal ions ____ 13

Figure 1.1.6 Pyiridyl-based conjugated polymers as chemosensors ____ 14

Figure 1.1.7 Band diagram illustrating the mechanism of quenching behavior for conjugated polymers ____ 15

Figure 1.1.8 A: The first reported molecular structure of conjugated polymer and quencher used as fluorescence chemosensor. B: the structure of PPE derivatives used for detecting TNT ____ 17

Figure 1.1.9 The structure of PPV ____ 17

Figure 1.1.10 The reaction schemes for SPR, Gilch route and CPR. ____ 18

Figure 1.1.11 The structure of MEH-PPV ____ 21

Figure 1.1.12 Some modifications of MEH-PPV ____ 22

Figure 1.1.13 Alkoxy-substituted PPV derivatives ____ 23

Figure 1.1.14 Examples of some phenyl-substituted PPVs. ____ 24

Figure 1.1.15 More examples of phenyl-substituted PPV derivatives ____ 25

Figure 1.1.16 Some typical poly(aryleneethynylene)s (PAEs) ____ 28

Figure 1.1.17 Palladium synthesis route 29

Figure 1.1.18 The general synthetic route for dialkoxy-PPEs monomers 32

Figure 1.1.19 The genernal synthetic route for dialkoxy-PPEs 32

Figure 1.2.1 The process of layer-by-layer adsorption 49

Figure 1.2.2 Schematic representation of the structures of the polymer interlayers 51

Figure 1.2.3 Diagram illustrating the detection mechanism of conjugated polyelectrolyte for biomolecules 54

Figure 1.2.4 Diagrammatic representation for the use of a water-soluble CP with a specific PNA-C optical reporter probe to detect a complementary ssDNA sequence.* 55

Figure 1.2.5 Molecular structure of WSCPs used as chemo or biosensors 56

Figure 2.1 The designed neutral polymers for the green light emitting cationic polymers 71

Figure 2.2 FT-IR spectra of the neutral and quaternized Ph-PPVs 79

Figure 2.3 ^{1}*H NMR spectra of the neutral and quaternized Ph-PPVs* 81

Figure 2.4 Thermalgravimetric analysis of the neutral and quaternized Ph-PPVs 82

Figure 2.5 UV-vis absorption and PL emission spectra of P1 in acetic acid $CHCl_3$ *solution (1 M), in acetic acid aqueous solution (1 M) and as films* 83

Figure 2.6 UV-vis absorption and PL emission spectra of P2 and P3 in THF, P2' and P3' in methanol and P3' in water 85

Figure 2.7 UV-vis absorption and PL emission spectra of P2, P3, P2' and P3' as films 87

Figure 2.8 Unmodified Stern-Volmer plot of P3' (1.25 μM) quenched by $Fe(CN)_6^{4-}$ 89

Figure 2.9 Modified Stern-Volmer plot for the system in Figure 2.8 _____ *90*

Figure 2.10 UV-vis absorption and PL emission spectra of P3' (1.25 μM) in the absence and presence of $Fe(CN)_6^{4-}$ _____ *91*

Figure 3.1.1 The designed neutral polymers for the cationic polymers _____ *100*

Figure 3.1.2 FT-IR spectra of the neutral PPVs _____ *107*

Figure 3.1.3 FT-IR spectra of the quaternized PPVs _____ *108*

Figure 3.1.4 Thermalgravimetric analysis of the neutral and quaternized PPVs ____ *110*

Figure 3.1.5 The DSC traces of P2 and P4-P6 in a nitrogen atmosphere _____ *111*

Figure 3.1.6 ^1H *NMR spectra of the neutral polymers in chloroform-d* _____ *111*

Figure 3.1.7 ^1H *NMR spectra of the quaternized polymers in methanol-*d_4 _____ *113*

Figure 3.1.8 The UV-vis and PL spectra of the neutral polymers in $CHCl_3$ _____ *114*

Figure 3.1.9 The UV-vis and PL spectra of the quaternized polymers in CH_3OH ___ *116*

Figure 3.2.1 Absorption of $Fe(CN)_6^{4-}$ *(10 μM) and emission spectra of P3' (1.25 μM) and P7' (1.25 μM) in aqueous solution* _____ *125*

Figure 3.2.2 Stern-Volmer plot of P3' (1.25 μM) and P7' (1.25 μM) quenched by $Fe(CN)_6^{4-}$ *in water* _____ *127*

Figure 3.2.3 Modified Stern-Volmer plot of P3' (1.25 μM) in Figure 3.2.2 _____ *128*

Figure 3.2.4 Stern-Volmer plot of P3' (1.25 μM) by $Fe(CN)_6^{4-}$ *in water and methanol* *130*

Figure 3.2.5 Stern-Volmer plot of quaternized polymer P3' (1.25 μM) by $Fe(CN)_6^{4-}$ *in water and HCl aqueous solution (1 mM) and neutral polymer P3 (1.25 μM) in* CH_3COOH *aqueous solution (1 mM)* _____ *131*

Figure 3.2.6 Stern-Volmer plot of P3 (1.25 μM) and P1 by $Fe(CN)_6^{4-}$ *in* CH_3COOH

aqueous solution _____ *133*

Figure 3.2.7 Stern-Volmer plot of P3', P5' and P6' by $Fe(CN)_6^{4-}$ *in methanol* _____ *135*

Figure 4.1.1 The designed neutral polymers for cationic PPEs _____ *141*

Figure 4.1.2. ^1H *NMR spectra of neutral polymers P8-P10 in* $CDCl_3$ _____ *148*

Figure 4.1.3 ^{13}C *NMR spectra of neutral polymers P8-P10 in* $CDCl_3$ _____ *148*

Figure 4.1.4 ^1H *NMR spectra of quaternized polymers P8' in* D_2O *and P9'-P10' in* CD_3OD _____ *149*

Figure 4.1.5 Thermalgravimetric analyses of the neutral and quaternized PPEs ____ *150*

Figure 4.1.6 UV-vis absorption and PL emission spectra of (a) neutral polymers P8-P10 in chloroform and (b) quaternized polymers P8'-P10' in water or methanol __ *151*

Figure 4.1.7 UV-vis absorption spectra of quaternized polymer P8' in aqueous solution with different pH values _____ *152*

Figure 4.1.8 ^1H *NMR spectra of (a) neutral polymer P8 in* CD_3COOD/D_2O *solution, (b) quaternized polymer P8' in* D_2O*, (c) quaternized polymer P8' in* CD_3COOD/D_2O *solution and (d) quaternized polymer P8' in* D_2O *after addition of NaOH solution and then neutralization by* CH_3COOH *solution.* _____ *153*

Figure 4.1.9 PL emission spectra of quaternized polymer P8' in aqueous solution with different pH values _____ *155*

Figure 4.1.10 The curve of relative PL intensity of P8' in aqueous solution versus pH values which was adjusted by adding HCl and NaOH solution into P8' solution at pH = 7 respectively (–•–), adding HCl solution into P8' solution at pH = 1 (realized through adding NaOH solution) (□), adding NaOH solution into P8'

solution at pH = 13 (realized through adding HCl solution) (Δ). Inset: the relative PL intensity of P8' at different pH environment after adding salt (sodium chloride) with different concentrations at 10^{-5} (■), 10^{-4} (▲) and 10^{-3} (♦) μM respectively _____ *157*

Figure 4.1.11 The curve of relative PL intensity versus pH value at different P8' concentration _____ *158*

Figure 4.1.12 Stern-Volmer plot of P8' (5 μM) quenched by $Fe(CN)_6^{4-}$ in aqueous solution. Inset: the part of Stern-Volmer plot of P8' (5 μM) quenched by $Fe(CN)_6^{4-}$ at low concentration _____ *159*

Figure 4.1.13 The plots of K_{sv} value and relative PL intensity of P8' (5 μM) versus pH value _____ *160*

Figure 4.1.14 The plots of K_{sv} value of P8' versus pH value at different P8' concentration _____ *161*

Figure 4.2.1 UV-vis absorption and emission spectra of PPE-NEt_3^+ in aqueous solution at different concentrations: [PPE-NEt_3^+] = 1, 10 and 50 μM _____ *168*

Figure 4.2.2 UV-vis absorption and emission spectra of PPE-NEt_3^+ in water quenched by added $Fe(CN)_6^{4-}$. [PPE-NEt_3^+] = 1 μM, [$Fe(CN)_6^{4-}$] = 0, 0.0025, 0.025, 0.05, 0.1, 0.15, 0.20 and 0.25 μM; [PPE-NEt_3^+] = 50 μM, [$Fe(CN)_6^{4-}$] = 0, 0.125, 1.25, 2.5, 5, 7.5, 10 and 12.5 μM. Absorption spectrum red-shifted and fluorenscence intensity decreased with increasing [$Fe(CN)_6^{4-}$]. _____ *169*

Figure 4.2.3 Stern-Volmer plots of PPE-NEt_3^+ at different concentrations quenched by $Fe(CN)_6^{4-}$. [PPE-NEt_3^+] = 1 μM (●), 5 μM (▲), 10 μM (▼), 20 μM (♦) and 50

μM (■). Inset: low quencher concentration regime and linear static Stern-Volmer fittings. 171

Figure 4.2.4 The plot of the static quenching constant K_{sv}^{S} versus the reciprocal of [PPE-NEt_3^+] ranging from 0.2 to 200 μM. 172

Figure 4.2.5 Fluorescence quenching of PPE-NEt_3^+ at different concentrations versus [$Fe(CN)_6^{4-}$]. [PPE-NEt_3^+] = 1, 10 and 50 μM. The concentration of $Fe(CN)_6^{4-}$ ranges from 1/200 to 1/20 in units of the ratio of [$Fe(CN)_6^{4-}$] to [PPE-NEt_3^+] 177

Figure 4.3.1 UV-vis absorption and emission spectra of PPE-NEt_3Br in the presence of PAANa with different concentration 186

Figure 4.3.2 UV-vis absorption and emission spectra of PPE-NEt_3Br in the presence of PMAANa with different concentration 188

Figure 4.3.3 Curves of relative fluorescence intensity (the intensity ratio of PAANa/PPE-NEt_3Br complexes to pure PPE-NEt_3Br in aqueous solution) vs. PAANa:PPE-NEt_3Br or PMAANa:PPE-NEt_3Br molar ratio 189

Figure 4.3.4 The Stern-Volmer plot of PAANa/PPE-NEt_3Br (5 μM) complex quenched by $Fe(CN)_6^{4-}$ in aqueous solution with different concentrations of PAANa 190

Figure 4.3.5 The Stern-Volmer plot of PMAANa/PPE-NEt_3Br (5μM) complex quenched by $Fe(CN)_6^{4-}$ in aqueous solution with different concentrations of PMAANa 191

Figure 4.3.6 The K_{sv}^{S} values of PPE-NEt_3Br at different concentrations of those ionic polymers, PAANa and PMAANa 193

Figure 4.3.7 The percentage of inaccessible fluorophore vs the relative concentration of PAANa and PMAANa 195

SUMMARY

The focus of this thesis was to syntheses and characterization of novel water-soluble conjugated polyelectrolytes and to study the structure-quenching and environment-quenching relationship of those conjugated polyelectrolytes as sensors.

The second chapter is focused on synthesis and characterization of a new series of water-soluble green light-emitting poly(*p*-phenylenevinylene)s (PPVs). Novel phenyl-substituted PPVs with tertiary amine functionality were prepared by using either Gilch or Wittig reactions. Water-solubility was rendered to these materials via post-quaterization on the neutral precursors. It was found that the content of *cis*-/*trans*-vinylic group in the backbones depended on the polymerization method employed and those corresponding polymers exhibited different optical properties and fluorescence quenching.

The third chapter is divided into two parts. The first part is related to synthesis, characterization and optical properties of cationic phenyl-substituted PPV related copolymers. Such copolymers with thiophene, benzene and fluorene moieties showed tunable electronic properties. Introducing fluorene unit into the main chain efficiently enhanced the fluorescence intensity of conjugated polyelectrolyte. The second part is focused on the quenching effects of $Fe(CN)_6^{4-}$ in water and methanol on cationic phenyl-substituted PPV related copolymers with *cis*-/*trans*- vinylic group via Wittig reaction and PPV homopolymers with entire *trans*-vinylic group prepared from Gilch reaction. Compared with each other, it was demonstrated that the existence of

cis-vinylic group in conjugated backbone indeed lower the quenching efficiency.

The fourth chapter is composed of three sections. The first section is referred to synthesis, characterization and optical properties of cationic water-soluble poly(*p*-phenyleneethynylene) (PPE-NEt_3^+). The results showed obvious pH-dependent fluorescence intensity and sensitivity of PPE-NEt_3^+. The next section is about the study on the fluorescence quenching of PPE-NEt_3^+ at different concentrations by $Fe(CN)_6^{4-}$ in aqueous solution. The static quenching constant K_{sv}^S of PPE-NEt_3^+ increased with the decrease of its concentration. To account for this phenomenon, the concept of local quencher concentration was introduced into the Stern-Volmer equation and a new equation which successfully presented the relationship between K_{sv}^S and [PPE-NEt_3^+] was obtained. The third section is focused on optical properties and fluorescence quenching of PPE-NEt_3^+ under complexation with anionic saturated polyelectrolytes. It was showed that the complex structure was highly related to the structure of the saturated polymer chosen. The quenching effects of those complexes were also significantly determined by the structure of saturated polymer.

All these results prove that the new design and the strategy for novel water-soluble conjugated polyelectrolytes had led to new materials which are very promising for applications as biosensors and in theoretical study on corresponding quenching behaviors.

Keywords: Water-soluble conjugated polymers, ammonium-functionalization, sensors, poly(*p*-phneylenevinylene) (PPV), poly(*p*-phenyleneethynylene) (PPE), fluorescence quenching.

CHAPTER ONE

Part I: Background

1.1.1 Conjugated Polymers

Since the discovery of highly conductive doped polyacetylene (PA) in 1977, The investigation of highly conjugated organic polymers has been developed swiftly.[1] The possession of good optoelectric properties made conjugated polymers excellent alternatives with those widely used inorganic materials for constructing various electrical devices. These polymers have low density, ease of fabrication, flexibility in design and good stability, and their conductivity can be controlled by doping and by modification the chemical structures. Using appropriate chemical and material processes, the electronic, chemical and physical properties needed for a given device can be controlled appropriately. During the past two decades, conjugated polymers have become the focus of scientific research not only because of their theoretically interesting properties but also because of their technologically promising future.

1.1.1.1 Structures of Conjugated Polymers

The term conjugated refers to organic macromolecules represented by alternating double and single bonds, and is indicative of an σ-bonded C-C backbone with π-electron delocalization. It is useful to define the extent over which the π-electrons are delocalized as the conjugation length.[2] In fact, conjugated polymers are polymeric semiconductors which combine the desirable processing characteristics inherent of

polymer systems with the sought-after electrical, electro-optic and non-linear optical properties of semiconductors.[3,4]

Table 1.1.1 Some common conjugated polymers[5]

Polymer	Chemical Name	Formula	Bandgap (ev)
PA	trans-polyacetylene	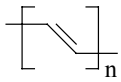	1.5
PPP	poly(*p*-phenylene)	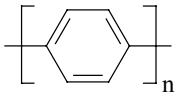	3.0
PF	polyfluorene	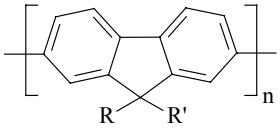	3.2
PPV	poly(*p*-phenylene vinylene)	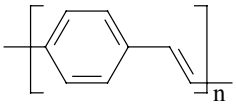	2.5
RO-PPV	poly(2,5-dialkoxy-*p*-phenylene vinylene)	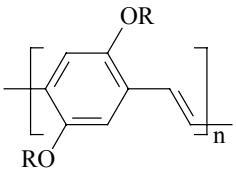	2.2
PT	polythiophene	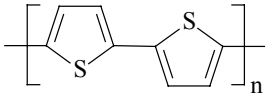	2.0
P3AT	poly(3-alkylthiophene)	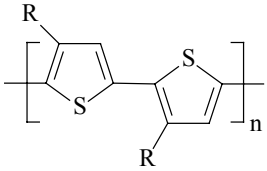	2.0
PTV	poly(2,5-thiophenylene vinylene)	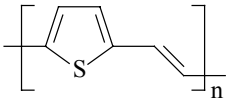	1.8
PPy	polypyrrole	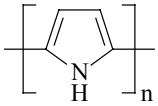	3.1
PANi	polyaniline	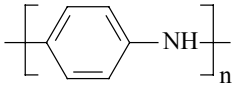	3.2

The semiconducting behaviour of conjugated polymers is easily understood from the

bonding. The double or triple bonds between carbon atoms in the polymer chain each have an electron excess to that normally required for bonding. These extra electrons are in p_z orbitals and are mainly perpendicular to the bonds between adjacent carbon atoms. These electrons overlap with adjacent p_z orbitals to form a delocalized π-electron cloud that spreads over several atomic sites along the polymer backbone. When this happens, delocalised π valence (bonding) and π* conduction (anti-bonding) bands with defined bandgap are formed–the requirements for semiconducting behaviour. Normally the electrons reside in the lower energy valence band but, if given sufficient energy, they can be excited into the normally empty upper conduction band, giving rise to a π–π* transition. Intermediate states are forbidden by quantum mechanics. The delocalised π-electron system confers the semiconducting properties on the polymer and gives it the ability to support positive and negative charge carriers with relatively high mobilities along the chain.[6]

However, a polymer must also satisfy two other conditions for it to work as a semiconductor.[7] One is that the σ bonds should be much stronger than the π bonds so that they can hold the molecule intact even when there are excited states – such as electrons and holes–in the π bonds. These semiconductor excitations weaken the π bonds and the molecule would split apart were it not for the σ bonds. The other requirement is that π-orbitals on neighbouring polymer molecules should overlap with each other so that electrons and holes can move in three dimensions between molecules. Fortunately many polymers satisfy these three requirements. Most conjugated polymers have semiconductor band gaps of 1.5–3 eV, which means that

they are ideal for optoelectronic devices which emit light.

Recently, different types of conjugated polymers (structure are showed in **Table 1.1.1**) such as polyacteylene (PA), poly(*p*-phenylene) (PPP), poly(*p*-phenylenevinylene) (PPV), polyaniline (PAni), polypyrrole (PPy) and polythiophene (PT) have been developed and intensively investigated.

Poly(*p*-phenylene) and its derivatives (PPPs) have found considerable interest over the past years since it acts as an excellent organic conductor upon doping whereas neutral PPP is a good insulator. A second major interest arises from the fact that PPP can be used as the active component in blue light-emitting diodes (LEDs).[8,9] Oligo(*p*-phenylene)s have played a dominant role as model compounds for PPPs in the study of physical mechanisms related to intra- and inter-chain charge transport or distribution and stabilization of charges and spins on π-conjugated chains. These mechanisms are of special interest in regard to the potential application of PPPs in rechargeable batteries.[10,11] PPV and its derivatives are among the most extensively studied systems since the first reported light-emitting devices (LEDs) using PPV as the emission layer.[12] The tremendous advantages in the chemistry and physics of PPVs over recent years have stimulated further interest in related types of structures such as poly(*p*-phenyleneethynylene) (PPE) polymers, which exhibit large photoluminescence efficiencies both in solution and in the solid state as a consequent of their high degree of rigidity, and their extremely stiff, linear backbones.[13]

1.1.1.2 Applications of Conjugated Polymers

Due to their unique structures, conjugated polymers display unusual electronic properties such as low ionization potential and high electron affinity, and the ability to be oxidized or reduced more reversibly than conventional polymers. These polymers may combine the electrical and optical properties of metals, the mechanical properties of the semiconductors, and the processing advantages of the traditional polymers. Therefore, this creative combination formed the basis and the potential applications of the conducting polymers.

Generally, the properties of the conducting polymers can be mainly divided into two parts. The first is focused on their reversible redox properties (i.e. electroactivity), while the other is focused on their electrically conductive properties (i.e. conductivity). In the former case, each application exploits the fact that the electrical and optical properties of conducting polymers depend, in a controllable manner, on their level of oxidation or reduction. As a result, the conducting polymers with this characteristic can be used as electronic devices,[14] rechargeable batteries,[15] controlled drug release systems.[16] The combination of electroactivity and reasonable stability in aqueous solutions makes feasible the use of selected conjugated polymers in the application of biomedical interest.[17] One example is that PPyhas been exploited as an electroactive film for the timed release of chemicals.[18] Since the conductivity of some conjugated polymers such as PA rise quite dramatically with exposure to small amounts of "dopants", they offer high sensitivity for detection of these dopants.

In the area of sensors, considerable attention has also been directed towards

amperometric sensors, primarily for monitoring of glucose.[19-21] It was also found that their applications as chemosensors,[22] biosensors[23] based on a variety of schemes including conductormetric sensors,[24] potentiometric sensors, colorimetric sensors,[25] and fluorescent sensors.[26] In addition, conducting polymers were also potential candidates as electrically conducting textiles by incorporation of conductive fillers,[27] and candidates as artificial muscles based on transition change caused dimensional changes.[28] The use of conducting polymers in industrial separation is gaining increased popularity due to the cost and energy conservation advantage. Electronically conducting polymers such as polymethylpyrrole and PAni are promising materials for industrial gas separation.

On the other hand, the application simply takes advantages of the electrical conductivity of doped conjugated polymers, which makes them attractive alternatives for certain materials currently used in microelectronics. The conductivity of these materials can be tuned by chemical manipulation of the polymer backbone, by the nature of the dopant, by the degree of doping, and by blending with other polymers. In addition, they offer advantages such as light-weight, processibility, and flexibility, which entitle them potential applicants ranging from the device level to the final electronic product. It is reported that PAni,[29] PA,[30] PPy[31] can be widely used as conducting resists in the lithiographic applications, PAni as the material for shielding electromagnetic radiation and reducing or eliminating electromagnetic interference shielding.[32-34]

One of the most advanced applications of conducting polymers is their use as active

materials in photoelectronic devices, such as light-emitting diodes,[35] light-emitting electrochemical cells,[36,37] photodiodes,[38-40] field effect transitors,[41-44] polymer rigid triodes,[45] optocouplers,[46] and laser diodes,[47] etc. Some of these polymer-based devices have reached performance levels comparable to or even better than those of their inorganic counterparts. In particular, polymer light emitting diodes have aroused special interest in recent years.

In addition, conjugated polymers can also be used for applications such as electrostatic shielding, non-linear optics,[48,49] electrochromic windows,[50] photodetectors,[40,51] and field effect transistors.[52-54]

1.1.2 Light-Emitting Polymers (LEPs) and Devices (LEDs)

Electroluminescence was first discovered for inorganic materials in 1936, when Destriau et al. observed high field electroluminescence from a ZnS phosphor powder dispersed in an isolator and sandwiched between two electrodes.[55] In the early 1960s, General Electric introduced commercially available light-emitting devices (LED) based on the inorganic semiconductor GaAsP.[56] Since the energy of the emitted photons and therefore the colour of the diode is determined by the energy gap of the semiconducting material in the active region of the LED, early LEDs only emitted red. The development of further materials granted access to colours other than red and made orange, yellow and green, as well as infrared accessible.[57] Materials that were generally used for inorganic LEDs are compounds of elements from groups III and V of the periodic table such as GaAs, GaP, AlGaAs, InGaP, GaAsP, GaAsInP, and more

recently AlInGaP. Blue LEDs, however, were difficult to obtain since semiconductors with large energy gaps are required. Nevertheless, blue diodes based on SiC, ZnSe, or GaN were developed, but exhibited distinctly lower efficiencies in comparison to other diodes. Since those inorganic materials used to fabricate LEDs are more complex than elemental silicon and are more difficult to produce and to process, the evolution of an analogous technology is still far behind technologies evolved for silicon.

Electroluminescence from organic crystals was first observed for anthracene in 1963.[58] Since the efficiencies and lifetimes of resulting devices were significantly lower than those obtained for inorganic systems at the same time, research activities were focused on the inorganic materials. In the late 1980s, Tang and VanSlyke,[59] as well as Saito and Tsutsui et al.[60] revived the research on electroluminescence of organic compounds, developing a new generation of light-emitting diodes with organic fluorescent dyes.

A significant breakthrough came with the discovery of EL in a conjugated polymer, PPV, by Burroughes et. al. in 1990. The demonstration of LEDs using a soluble conjugated polymer, poly(2-methoxy-5-(2'-ethylhexyloxy)-1,4-phenylene vinylene) (MEH-PPV)[12,61] and flexible LEDs[35] sparked further interest in polymer light-emitting devices (PLEDs).

In order to understand the process of light emission in organic conjugated polymeric materials, the processes of photoluminescence (PL) and electroluminescence (EL) are compared in **Figure 1.1.1**.

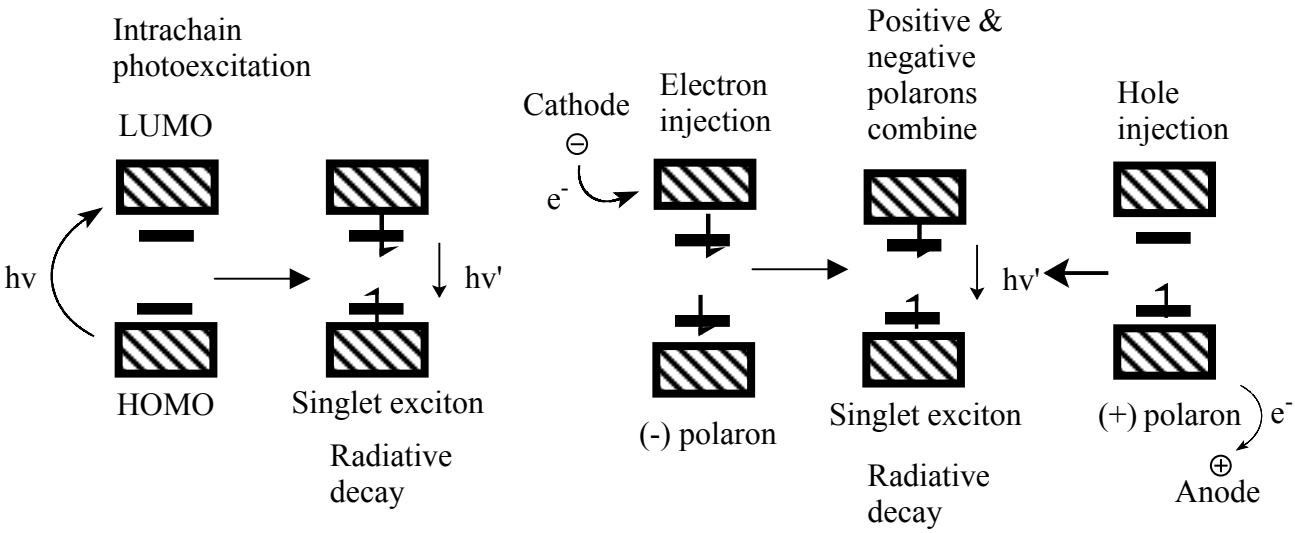

Figure 1.1.1 The scheme for photoluminescence (PL) and electroluminescence (EL) of conjugated polymers

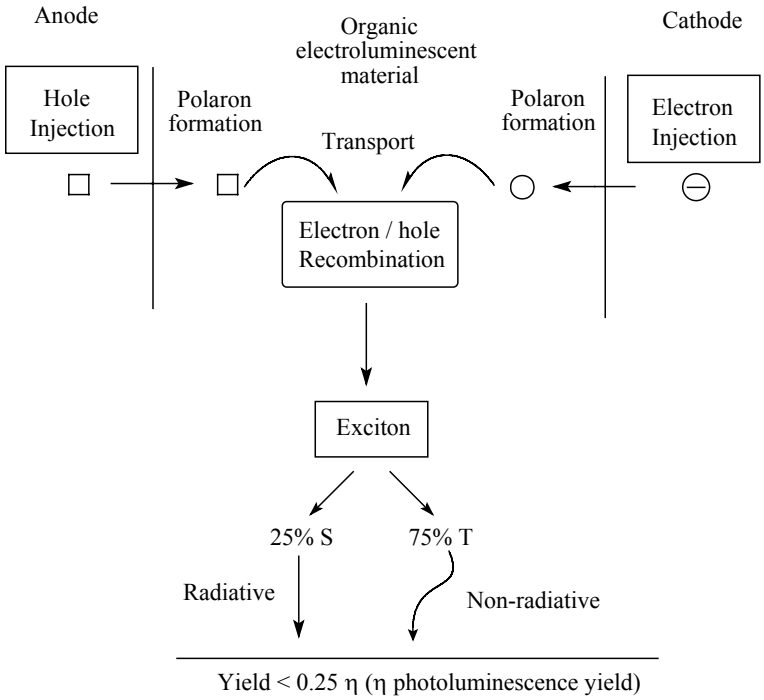

Figure 1.1.2 The schematic diagram of the EL process

In PL, light is converted into visible light using an organic compound as the active material whereas in EL, the organic compound converts an electric current into visible light.[62] Photoexcitation of an electron from the highest occupied molecular orbital

(HOMO) to the lowest unoccupied molecular orbital (LUMO) generates a singlet exciton (a neutral excitation) which can decay radiatively with emission of light at a longer wavelength (the Stokes shift) than that absorbed. Charged species (bipolarons) and triplet excitons (detected by photo-induced absorption) provide the main channels for non-radiative decay processes which can of course compete with and reduce efficiencies for radiative decay of the singlet exciton (**Figure 1.1.2**).[63-65]

In an EL experiment, injection of electrons from the cathode into the LUMO and holes from the anode into the HOMO generates negative and positive polarons, respectively, which migrate under the influence of the applied electric field and combine on a segment of the polymer chain to form the same singlet exciton as is produced in the PL experiment. The emitted light again exhibits a Stokes shift. If one of the electrodes is transparent, the generated light can escape.

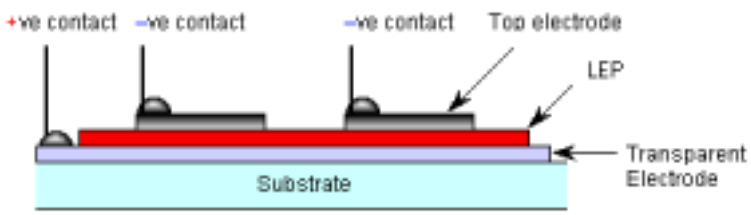

Figure 1.1.3 The structure of a single-layer polymer LED device

The simplest device configuration, consisting of a typical electrode/emitter/ electrode sandwich structure, is schematically depicted in **Figure 1.1.3**. The basic structure of an organic EL device[66] consists of one or more organic films deposited between two electrodes, one of which is transparent. A high work function (ϕ) material, typically indium tin oxide (ITO) (ϕ_w ~ 4.6 eV) or Au (ϕ_w = 5.1 eV), deposited on a glass substrate serves as the anode and is designed to be transparent so that emission from

the organic layer can escape the device. The luminescent material is deposited as a thin film on the surface of the electrode by using a variety of methods. The most common method being spin-coating[67] for processable polymeric materials and chemical vapour deposition (CVD) for low molecular weight materials and oligomers.[68] Finally a low work function metal such as Al (ϕ_w = 4.3 eV), In (ϕ_w = 4.1 eV), Mg (ϕ_w = 3.7 eV) or Ca (ϕ_w = 2.9 eV), among others,[69] is evaporated onto the luminescent material by vacuum metal vapour deposition. However since many LEPs are rather poor electron transporters, modification of the basic PLED device structure has been to include an electron-conducting hole-blocking layer between the luminescent layer and the metallic electrode.[70]

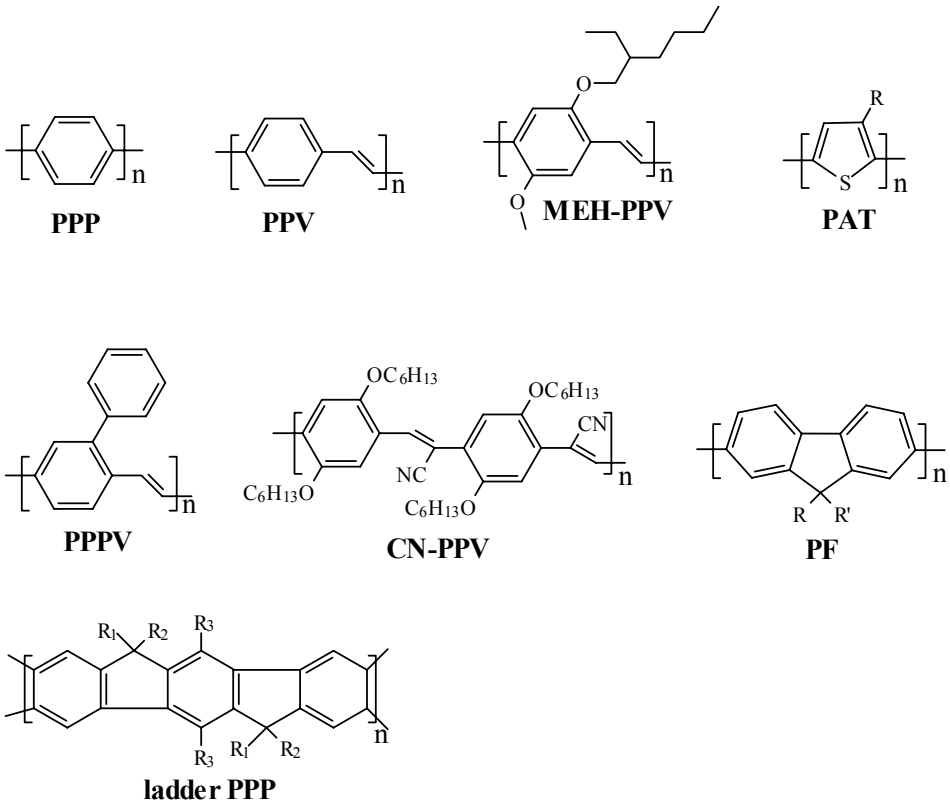

Figure 1.1.4 Conjugated polymers used in PLEDs

So far, numerous polymers with different type of π-conjugation moieties have been utilized in LEDs as the electroluminescent layer. The polymers that have attracted most attention are poly(*p*-phenylenevinylene) (PPV),[12,35,71,72] poly(*p*-phenylene) (PPP)[73] polyfluorene (PF) and polythiophene (PT) and their derivatives.[74,75] Some conjugated polymers used as emissive layers in PLEDs are shown in **Figure 1.1.4**.

1.1.3 Conjugated Polymers Used as Chemo or Biosensors

Conjugated polymers (CPs) offer a myriad of opportunities to couple analyte receptor interactions, as well as nonspecific interactions, into observable (transducible) responses. A key advantage of CP-based sensors over devices using small molecule (chemosensor) elements is the potential of the CP to exhibit collective properties that are sensitive to very minor perturbations. In particular, the CP's transport properties, electrical conductivity or rate of energy migration, provide amplified sensitivity.[23] CP-based sensors have been formulated in a variety of schemes, which includes conductometric, potentiometric, colorimetric and fluorescence sensors. Conductometric sensors display changes in electrical conductivity in response to an analyte interaction. Potentiometric sensors rely on analyte-induced changes in the system's chemical potential. Colorimetric sensors refer to changes in a material's absorption properties. Fluorescence is a widely used and rapidly expanding method in chemical sensing. Aside from inherent sensitivity, this method offers diverse transduction schemes based upon changes in intensity, energy transfer, wavelength (excitation and emission), and lifetime. There are advantages to using CPs in

fluorescent sensory schemes due to amplification resulting from efficient energy migration. The combination of amplification and sensitivity in CP-based sensors is evolving to produce new systems of unparalleled sensitivity.[76,77]

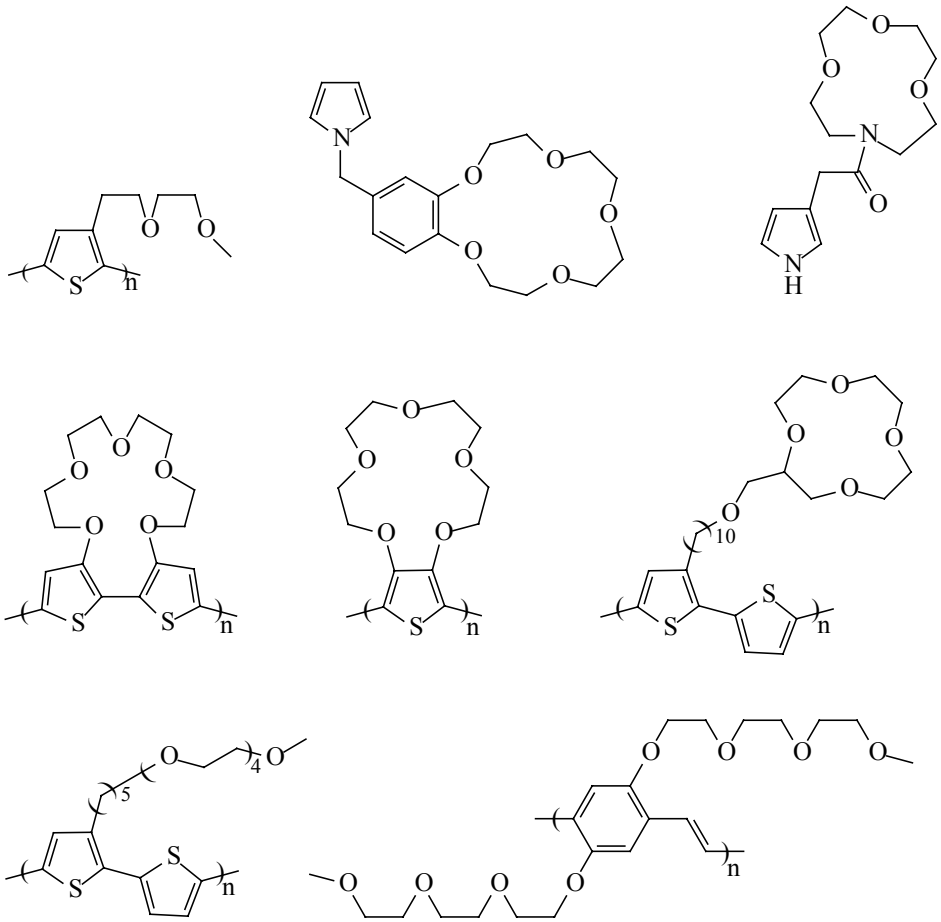

Figure 1.1.5 Typical CPs used for detecting alkali or alkaline-earth metal ions

Analyte specificity in CP-based sensors results from the covalent or physical integration of receptors, imprinting, and/or the CP's overall electrostatic and chemical characteristics. CPs functionalized with polyalkyl ether chains, crown ether, and aza crown ether moieties have been the most thoroughly studied covalently modified systems.[78] In 1989, Roncali and co-workers reported the synthesis of poly[3-(3,6-dioxaheptyl)thiophene] (1) and examined its voltammetric properties in

the presence of $Bu4N^+$ and Li^+ electrolytes.[79,80] This was said to be the first conjugated polymer system with a covalently attached functional group for ion complexation. After this report, a lot of CPs (polythiophene and polypyrrol) with crown ether were synthesized to selectively detect alkali or alkaline-earth metal ions.[81-92] (**Figure 1.1.5**)

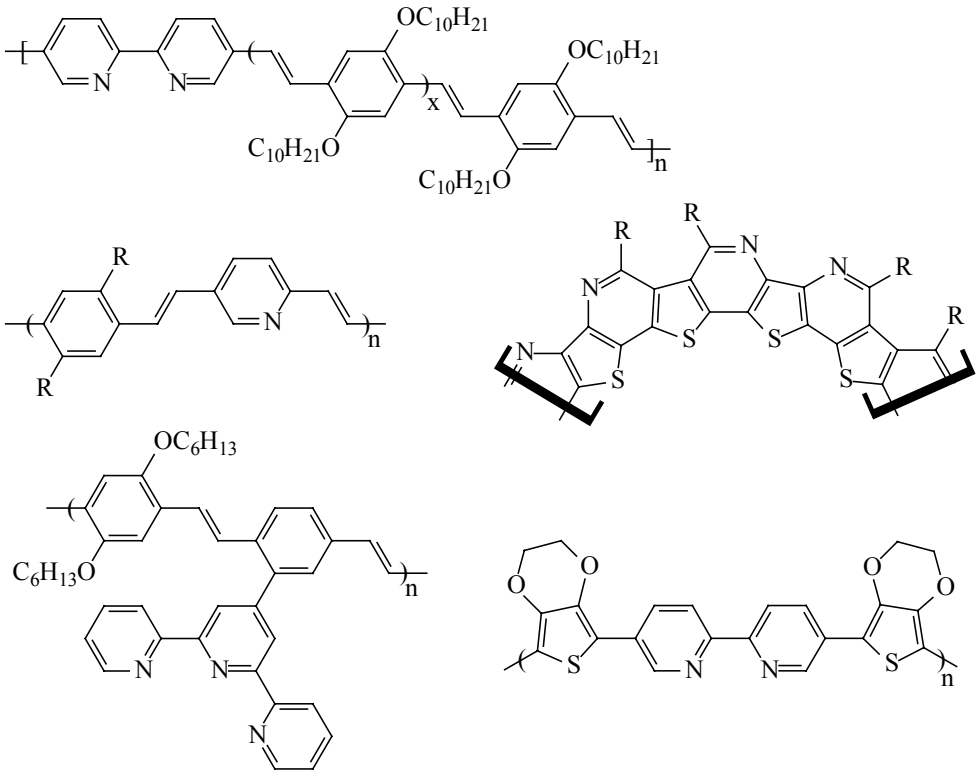

Figure 1.1.6 Pyiridyl-based conjugated polymers as chemosensors

The ability of pyridyl-based ligands to coordinate a large array of transition metal ions makes them an attractive functionality to be incorporated into CP sensors. Ligands of this general class can be placed in direct π-communication with the polymeric and/or backbone tethered by extended alkyl chains (**Figure 1.1.6**). In both cases, chelation of transition metal ions planarizes the pyridyl recognition sites to increase the conjugation and reduce the local band gap and thus lead to conformational, optical, or electrochemical changes in the CP. A significant amount of research has been devoted

to the study of bipyridine-based conjugated polymers due to their photophysical and electrochemical properties.[93-97]

Those CPs with crower ether or pyridyl groups were the most widely used materials as conductometric, potentiometric and colorimetric sensors for detecting metal ions. Now fluorescence quenching used in chemical or biochemical sensing has been paid much more attention because of its real-time and amplified response. The utility of CPs for fluorescence-based sensing was first demonstrated by Zhou and Swager.[98,99] A general finding of these studies is that the act of "wiring receptors in series" creates superior sensitivity over a small molecule indicator. The observed amplification is a result of the ability of the CP's delocalized electronic structure (i.e., energy bands) to facilitate efficient energy migration over large distances (**Figure 1.1.7**).

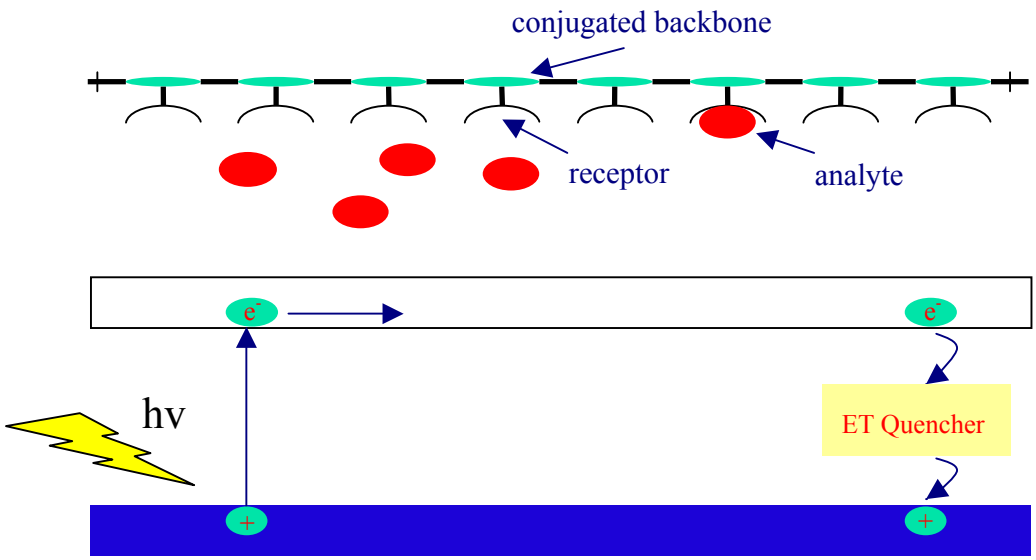

Figure 1.1.7 Band diagram illustrating the mechanism of quenching behavior for conjugated polymers

To demonstrate this principle, studies were conducted in parallel on a small molecule indicator containing a fluorescent monomeric cyclophane receptor. The cyclophane receptors were chosen to bind paraquat and related compounds that are very effective electron-transfer quenching agents. (**Figure 1.1.8 A**) By conducting detailed photophysical studies, these investigators were able to determine that both the monomer and polymer displayed quenching resulting from the binding of the paraquat by the cyclophane to form a rotaxane complex. Comparisons in solution of the quenching demonstrated a greatly enhanced sensitivity of the polymer over the monomeric compound. The proposed origin of this effect is facile energy migration along the polymer backbone to the occupied receptor sites (**Figure 1.1.7**). The signal amplification resulting from energy migration in CPs was also applied in 1998 by Yang and Swager for the detection of explosives, specifically 2,4,6-trinitrotoluene (TNT) and 2,4-dinitrotoluene (DNT).[76,77] (**Figure 1.1.8 B**)

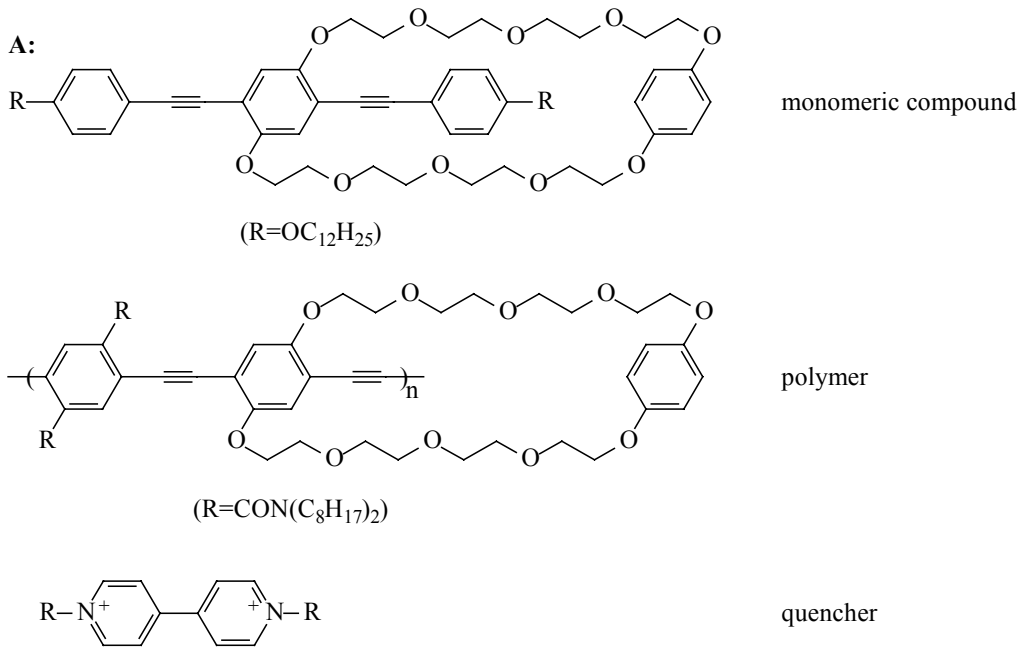

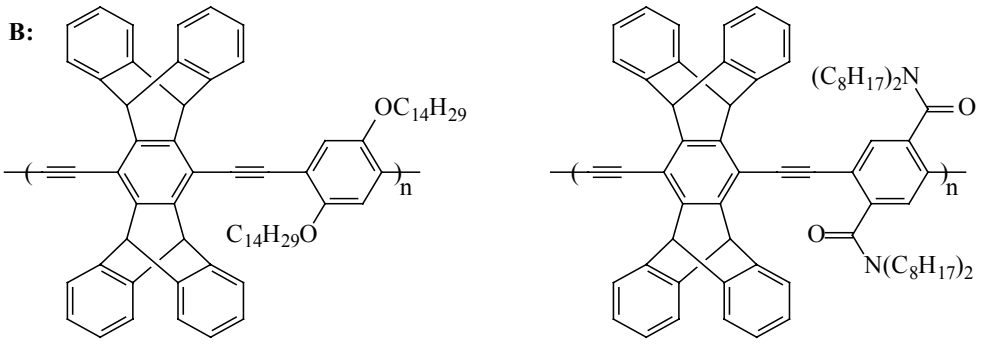

Figure 1.1.8 A: The first reported molecular structure of conjugated polymer and quencher used as fluorescence chemosensor. B: the structure of PPE derivatives used for detecting TNT

1.1.4 Synthesis of PPV and Its Derivatives

1.1.4.1 Synthetic Routes for PPVs

Poly(*p*-phenylene vinylene), more commonly known as PPV (**Figure 1.1.9**), has also been named poly(xylylidene) or by its IUPAC designations of poly(1,4-phenylene-1,2-ethenediyl) or poly(1,4-phenylene-1,2-ethenylene). It is a conjugated polymer composed of alternating repeating units of poly(acetylene) and poly(phenylene). Since the first report[12] of an EL device fabricated using PPV as the emissive layer, PPV and its derivatives have become the most extensively investigated conjugated polymers for application in light emitting devices.

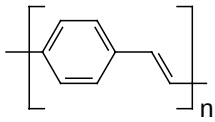

Figure 1.1.9 The structure of PPV

The synthesis of PPV was reported all the way back in 1960[100] and since then, numerous synthetic routes as well as a couple of comprehensive review articles[101-104] on the synthetic routes to PPV and its derivatives have appeared. The various synthetic routes to PPVs can be roughly divided into three categories: precursor approach, side-chain derivatization and polycondensation methods.

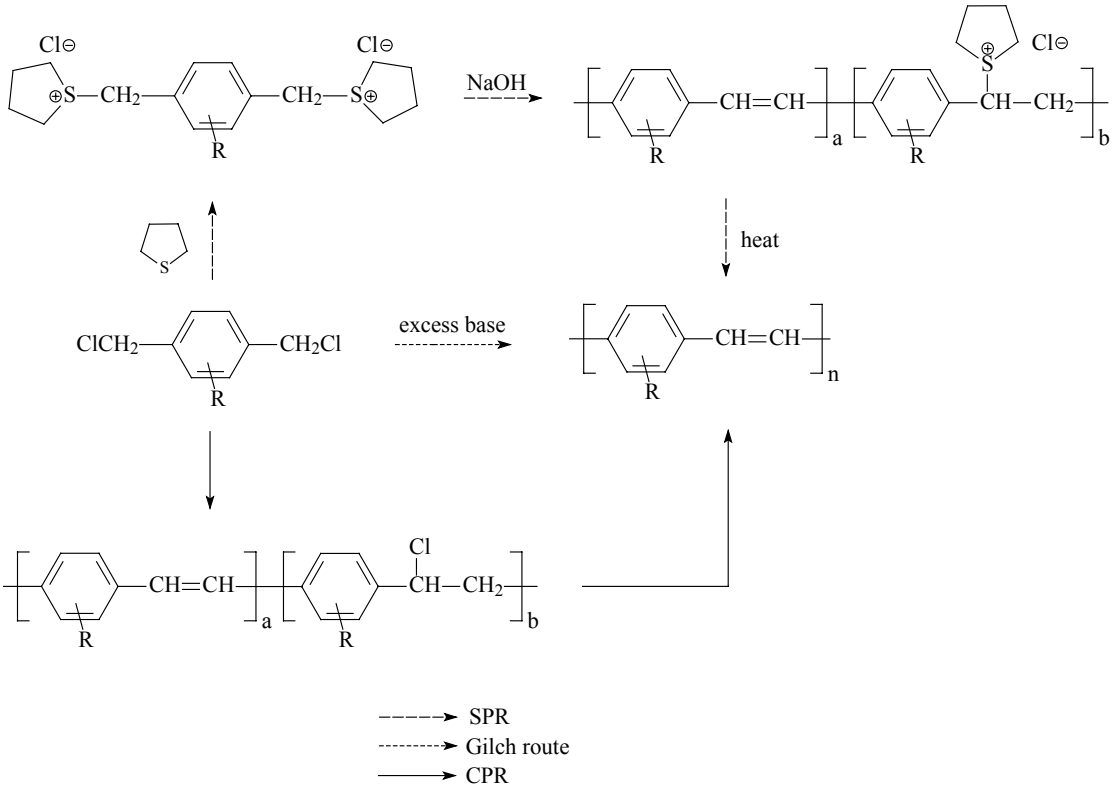

Figure 1.1.10 The reaction schemes for SPR, Gilch route and CPR.

The precursor approach relies on the preparation of a soluble precursor polymer that can be cast into thin films and then be transformed into the final conjugated polymer films through solid state thermo- or photo-conversion. The sulfonium precursor route (SPR) to PPV[105] is particularly well-known and involves the polymerization of *p*-xylene bis(tetrahydrothiophenium chloride) or one of its analogues or derivatives (**Figure 1.1.10**), in the presence of a base in water or methanol to give the

corresponding sulfonium precursor polymer. After purification, the sulfonium precursor polymer solution is used to cast films that are then converted thermally to give PPV thin films. This method was employed to fabricate the first conjugated polymer LED.

The side chain approach involves the polymerization of a highly substituted monomer to a soluble conjugated polymer that can be cast into thin films directly without conversion. The polymerization of bis(halomethyl)benzenes in the presence of a large excess of potassium *tert*-butoxide to PPVs is referred to as the Gilch route.[106] The Gilch route has been widely used for the preparation of soluble PPV derivatives in order to avoid the conversion step and the many problems associated with SPR.

A modification of the Gilch route – namely the chlorine precursor route (CPR) – was introduced by Swatos and Gordon[107] in 1990 to avoid polymer precipitation. They polymerized the monomer with about 1 equivalent of potassium *tert*-butoxide, instead of an excess of base as in the Gilch route, to give a soluble chlorine precursor polymer that was then converted to desired polymer. This approach should also be applicable to bis(bromomethyl)benzene monomers to give the corresponding bromine precursor polymers and can thus be referred to as the halogen precursor route in a more general sense. According to B.R. Hsieh,[101] the CPR is very simple, general, versatile and reproducible and is superior to the SPR and the Gilch route for the preparation of PPV derivatives.

Polycondensation methods refer to step-growth methods and can be differentiated into two types[104]: where the carbon skeleton of PPV is generated in an olefinic reaction (e.g.

the Knoevenagel, Wittig-Horner and McMurray reactions) with formation of the olefinic bond or where the PPV backbone is synthesized via a transition metal-catalyzed aryl-olefin-coupling (e.g. the Heck reaction) with formation of the aryl-vinyl single bond. The most common polycondensation method for the preparation of PPVs is the Wittig method, which typically involves the addition of terephthaldehyde with *p*-xylylenebis(triphenylphosphonium chloride). This method tends to produce a low molecular weight infusible yellowish fluorescent powder. The low molecular weight is due mainly to the fact that high molecular weight PPV is insoluble and by precipitating out of the reaction medium, the propagation step is effectively terminated. An advantage of the Wittig step is that the structure of the resulting polymer is well-defined and it allows a careful control of the molecular weight. A modified Wittig reaction, the Wittig-Horner reaction, starting from bisphosphonate or aromatic bisphosphine oxide monomers allows coupling not only with aromatic dialdehydes but also with aromatic diketones to the corresponding PPV derivatives. Other widely used polycondensation methods include the Heck reaction which involves a palladium-catalyzed coupling reaction between an aryl halide and a vinyl compound, the Knoevenagel condensation using dialdehydes, dimethylbenzenes and/or other heterocyclic monomers and the McMurry reaction, a form of reductive coupling polymerization involving the use of low-valent Ti reagents as catalysts.

1.1.4.2 Alkoxy-Substituted PPV Derivatives

The most common class of PPV derivatives are alkoxy-substituted PPVs, among

which, MEH-PPV[108] (**Figure 1.1.11**) is the most widely investigated. It has been almost a decade since the first report on a LED based on MEH-PPV but new data related to the improvement in synthetic route,[109-112] molecular weight studies[113] and stability studies[114] are still being published only very recently.

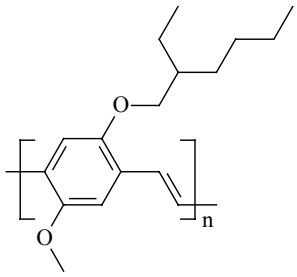

Figure 1.1.11 The structure of MEH-PPV

MEH-PPV has the advantage of being soluble in the conjugated form in common organic solvents and emits orange light. This simplifies the device fabrication because of the direct casting of the polymer from solution is possible. The major problem with this polymer is its relatively low stability against oxidation and air. This low stability demands careful handling of the polymer during synthesis and device fabrication. Hence, one of the main research goals in this field is to establish the structure-property relationship of PPV derivatives with the aim of improving the stability, efficiency and colour tuning of electroluminescent devices fabricated with the polymers as an emitting layer.

Based on the success of MEH-PPV as a light-emitting layer in PLEDs, it is no wonder that numerous modifications of MEH-PPV have been designed in order to model or even surpass it. Modifications of MEH-PPV include various side-chain and main chain modifications (**Figure 1.1.12**) leading to monomethoxy substituted PPV –

poly(2-methoxy-1,4-phenylene vinylene) (PMPV),[115] monoalkoxy-substituted PPV – poly[2-(2-ethyl hexyloxy)-1,4-phenylene vinylene] (EH-PPV),[116] poly(2-(2'-ethylhexylthio-5-methoxy-1,4-phenylene vinylene) (PMEHTPV),[117] poly[2-(5-cyclo-hexylmethoxypentyloxy)-5-methoxy-1,4-phenylene vinylene] (PMCYHPV),[118] and poly[2-methoxy-5-(2-ethyl hexyloxy)-1,4-phenylene-1,3-butadiene-1,4-diyl] (MEH-PPB).[119]

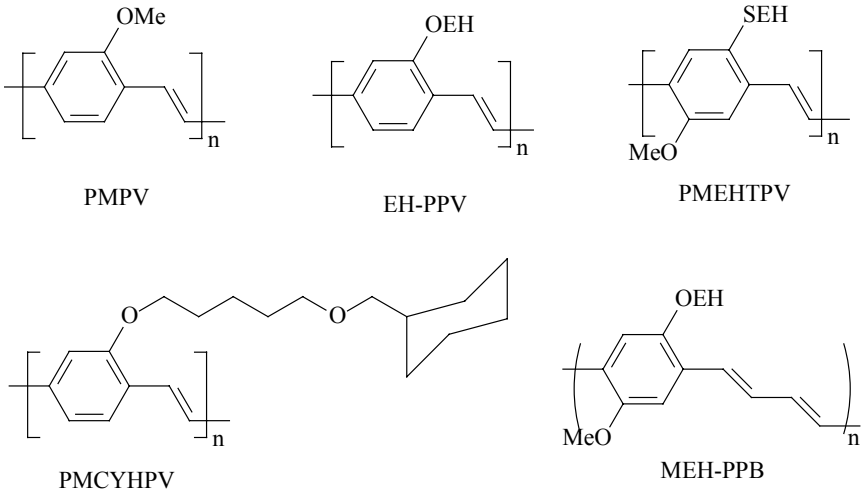

Figure 1.1.12 Some modifications of MEH-PPV

Besides MEH-PPV, many alkoxy-substituted PPVs have also been reported (**Figure 1.1.13**). These PPV derivatives possess alkoxy side chains,[120] dialkoxy side chains[121-125] and branched, macrocyclic and cyclic polyethereal alkoxy chains.[126] In addition, desirable properties in polymers can be achieved by copolymerization incorporating dialkoxy PPV units.[127-130]

The best LED performance is obtained from alkoxy derivatives of PPV. These polymers turn-on below 2 V (d.c.) and reach 100 cd/m^2 at 2.4 V (the brightness of a colour TV), 4000 cd/m^2 for V < 4 V (the brightness of a fluorescent lamp) and over 10 000 cd/m^2 for V > 5 V. The external quantum efficiency of these polymer LEDs has

been improved to greater than 2% photon per electron with excellent reproducibility and the luminous efficiency is 1.5 – 1.8 cd/A; values which are competitive with existing display technologies.[131]

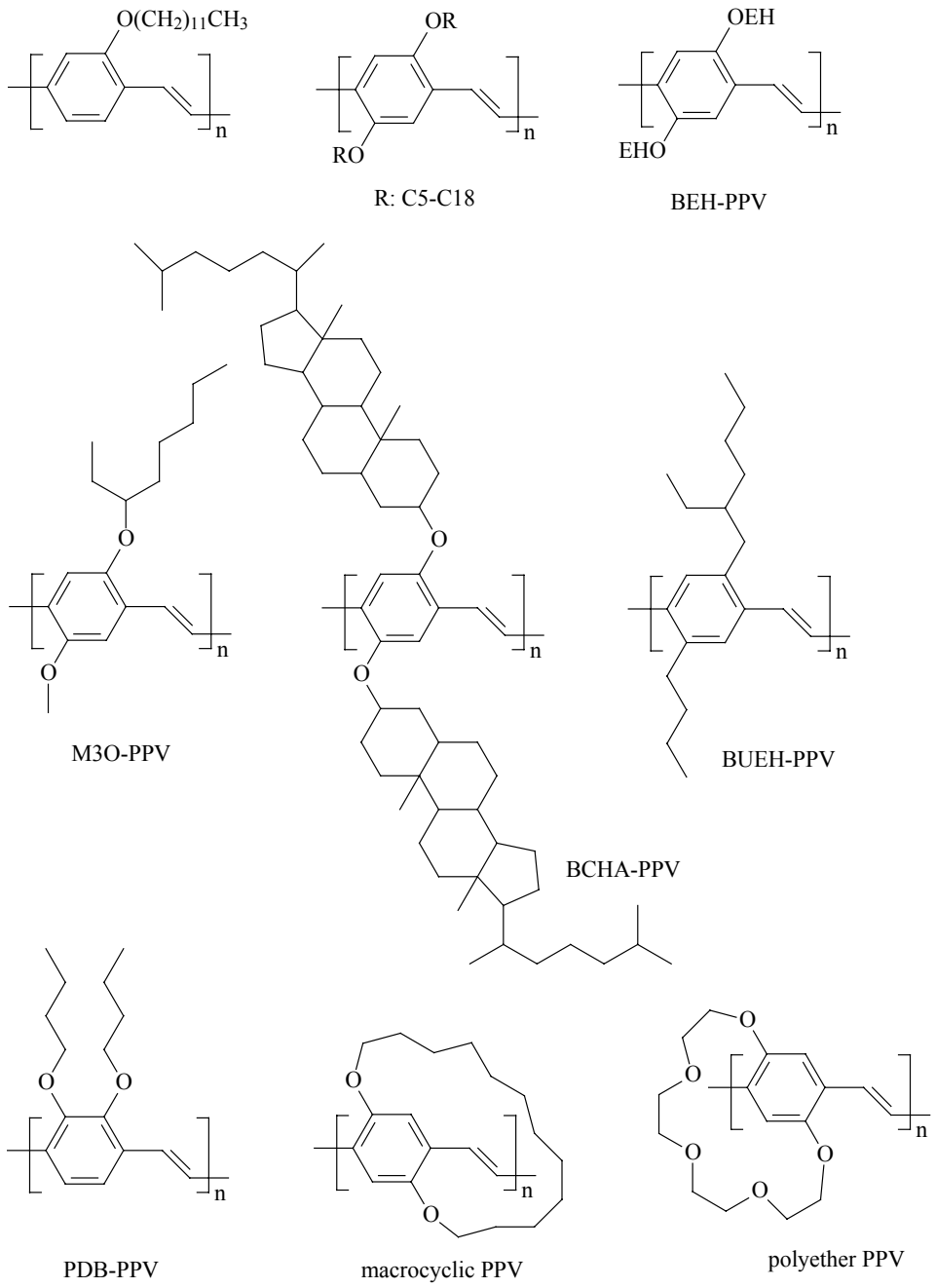

Figure 1.1.13 Alkoxy-substituted PPV derivatives

1.1.4.3 Phenyl-Substituted PPV Derivatives

The first phenyl-substituted PPVs were synthesized even before the discovery of electroluminescence in conjugated polymers was reported. Some examples of several of these well-known phenyl-substituted PPVs and their corresponding acronyms are shown in **Figure 1.1.14**.

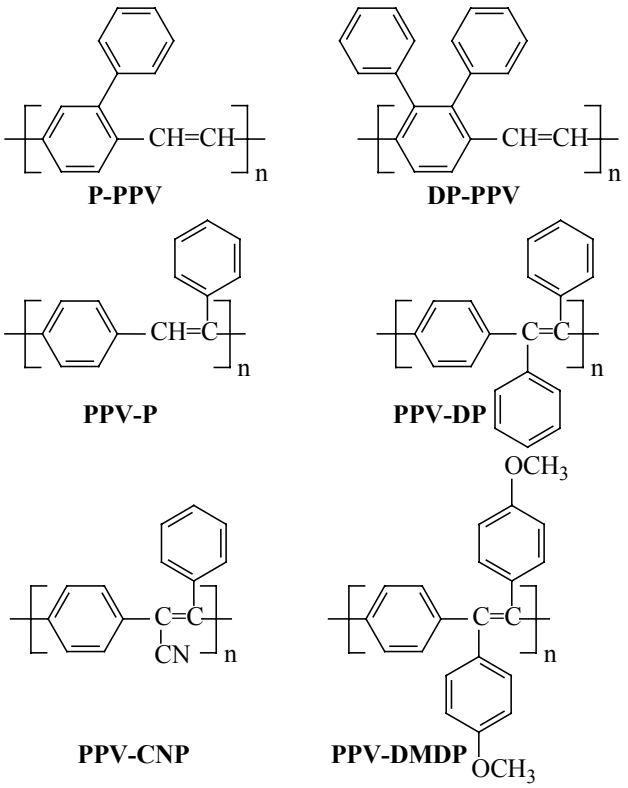

Figure 1.1.14 Examples of some phenyl-substituted PPVs.

It was only later that Vestweber et. al. reported green LEDs fabricated using P-PPV as the active electroluminescent layer.[132] Also, B.R. Hsieh et.al. reported for the first time the use of CPR to fabricate thin film EL devices containing DP-PPV[133] as well as the photophysical properties of the polymer.[134] In addition, several highly phenylated PPVs prepared *via* CPR[135,136] and diphenyl-substituted PPVs with flexible solubilizing side chains[137] have also been reported. One of the diphenyl-substituted PPVs with

flexible solubilizing side chains polymers, DP6-PPV, shows a PL emission peak of 490 nm which may represent the bluest emission peak for a fully conjugated PPV and a PL efficiency of 65% in the solid state, among the highest values reported for a fully conjugated PPV.

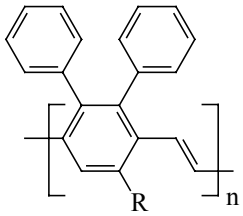

R: phenyl (1i)
R: 4-fluorophenyl (1ii)
R: 4-biphenyl (1iii)

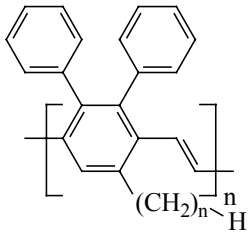

n = 6 (DP6-PPV) (2i)
n = 8 (DP8-PPV) (2ii)
n = 10 (DP10-PPV) (2iii)

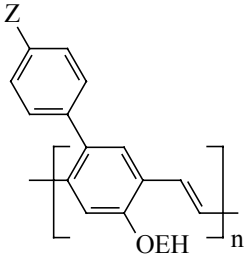

Z = H (3i)
Z = SO_2Me (3ii)

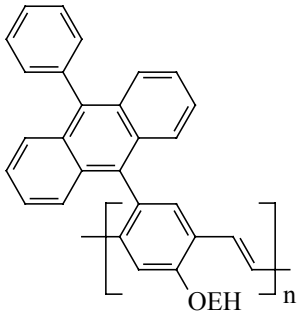

(4)

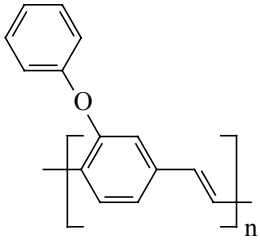

(5)

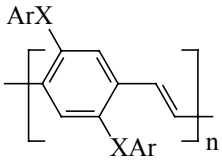

	X	Ar
(6i)	O	phenyl
(6ii)	O	biphenyl
(6iii)	O	*tert*-butylphenyl
(6iv)	S	phenyl
(6v)	S	*tert*-butylphenyl

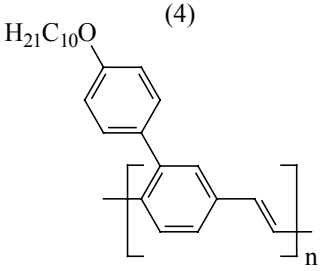

DOP-PPV

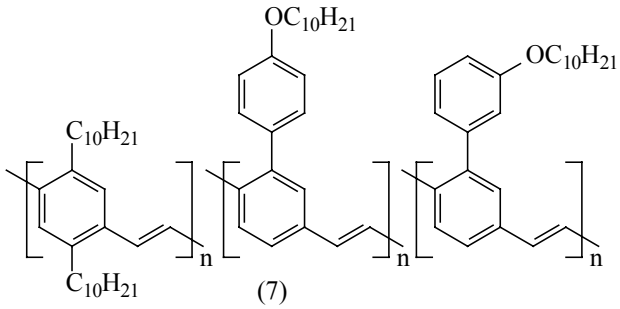

(7)

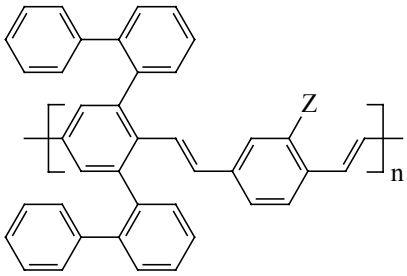

R: H (8i)
R: $OC_{12}H_{25}$ (8ii)

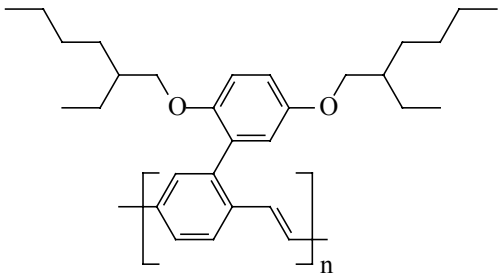

BEHP-PPV

Figure 1.1.15 More examples of phenyl-substituted PPV derivatives

Many other research groups have also presented various results from other phenyl-substituted PPVs. The electronic properties of poly[2-(2'-ethylhexyloxy)-5-phenyl-1,4-phenylene vinylene] and its methylsulfonyl derivative, poly[2-(2'-ethylhexyloxy)-5-(4"-methylsulfonylphenyl)-1,4-phenylene vinylene] were studied but it was found that the latter made no difference to the efficiency of the single layer EL devices and appeared qualitatively to reduce their lifetimes.[138] On a more optimistic note, it was found that a PPV derivative with phenylanthracene and branched alkoxy pendants, poly[2-(2'-ethyl)hexyloxy-5-(10'-phenyl)anthryl-9'-yl-1,4-phenylene vinylene], was soluble and of enhanced PLED efficiency.[139] The preparation and characterization of a series of novel PPVs containing phenoxy and thiophenoxy substituents has been reported.[140] Much closer to home, J. Pei et. al. reported the synthesis and characterization of poly[2-(4'-decyloxyphenyl)-1,4-phenylene vinylene] (DOP-PPV) which emits bright green light from a single layer LED with an emission maximum at 520 nm and an external quantum efficiency of *ca.* 0.3%.[141]

Copolymers of PPV derivatives have recently been shown to exhibit excellent properties. H. Spreitzer et. al. synthesized copolymers of different phenyl-substituted PPVs and obtained polymers with high molecular weights, complete solubility in standard organic solvents, no phenomenon of gelation at room temperature and luminance and power efficiencies unprecedented in the field of PLEDs.[142] Copolymers of biphenyl-substituted PPVs were synthesized[143,144] and shown to be highly soluble in spite of their highly phenylated structures. Also these polymers

possessed high molecular weights with narrow molecular weight distribution and high PL efficiencies (>50%) in both solution and as solid film, which are among the highest ever reported for PPVs. In order to improve the stability of PPVs, D.M. Johansson et. al. synthesized poly(2-(2',5'-bis-(ethylhexyloxy)phenyl)-1,4-phenylene vinylene) (BEHP-PPV) and its copolymers with MEH-PPV[145,146] and found that not only were the polymers of high molecular weight and good solubility, they were also more stable to air and light compared to poly(2-butyl-5-(2'-ethylhexyl)-1,4-phenylenevinylene) (BUEH-PPV) and showed high PL efficiency (84%) in solution. The structures of the various polymers are shown in **Figure 1.1.15**.

1.1.5 Synthesis of PPE and Its Derivatives

1.1.5.1 Synthetic Routes for PPEs

The class of conjugated polymers which has found the most attention in the past are undoubtedly the PPVs which "made it big" since Friend's 1990 report of organic polymeric LEDs.[9,12] However, the structurally closest relative to PPV, the PPEs have attracted much less attention in the polymer community, despite their fascinating properties. Only recently the groups of Swager,[77] Mullen,[147]and Weder[148,149] demonstrated that PPEs with their unique property profile are fantastic materials in such different areas as explosive detection, molecular wires in bridging nanogaps,[150,151] and polarizers for LC displays. **Figure 1.1.16** shows the types of poly(aryleneethynylene)s (PAEs).

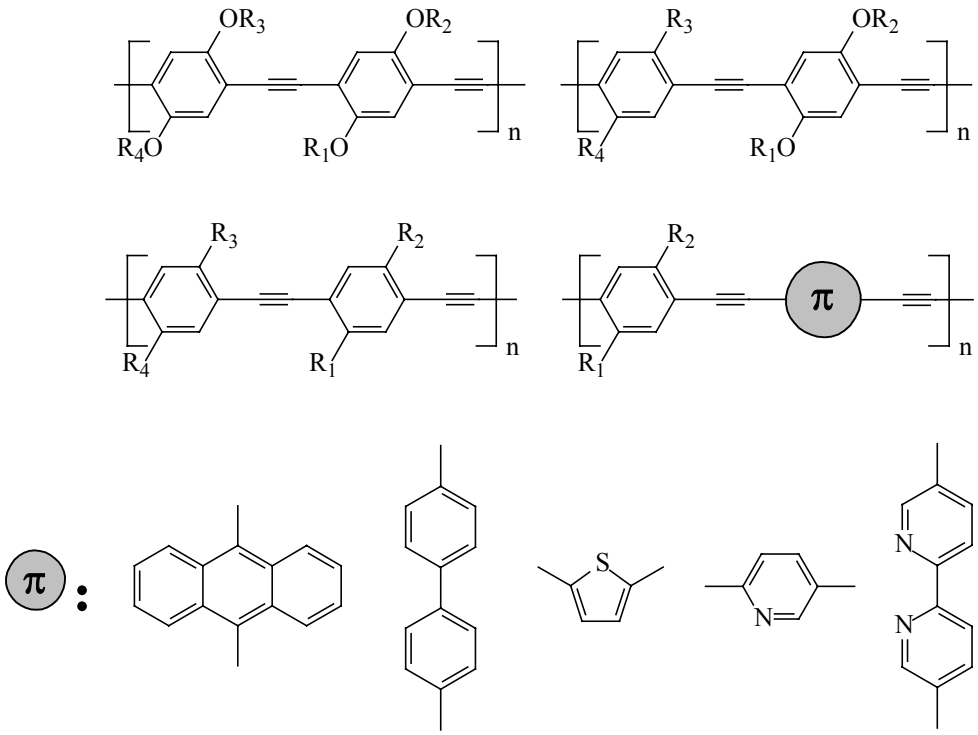

Figure 1.1.16 Some typical poly(aryleneethynylene)s (PAEs)

There are two ways to synthesize PPEs that are palladium methodologies and alkyne metathesis. The Pd-catalyzed coupling of terminal alkynes to aromatic bromides or iodides in amine solvents has been known since 1975. It is called the Heck-Cassar-Sonogashira-Hagihara reaction and is probably one of the most frequently used C-C bond forming processes in organic chemistry.[152-154] This coupling is powerful to form C-C single bonds between an sp- and an sp^2- hybridized carbon center. The generally accepted mechanism of this reaction is depicted in **Figure 1.1.17** and will be discussed here with respect to its implications in polymer synthesis.

In most cases (both for the synthesis of low-molecular-weight organic targets and for the preparation of PAEs) the commercially available $(Ph_3P)_2PdCl_2$ is the catalytic source of Pd. In its oxidized form this catalyst is inactive. In the first step, two molecules of a cuprated alkyne, **A**, transmetalate the Pd catalyst precursor and form **B**.

B is not stable under the reaction conditions but reductively eliminates a symmetrical butadiyne and creates the active catalyst **C**. In an oxidative addition the aromatic bromide or iodide forms the intermediate **D**, which after transmetalation with **A** leads to the diorgano-Pd species **E**. This species undergoes reductive elimination to the product and reforms the active catalyst **C**.

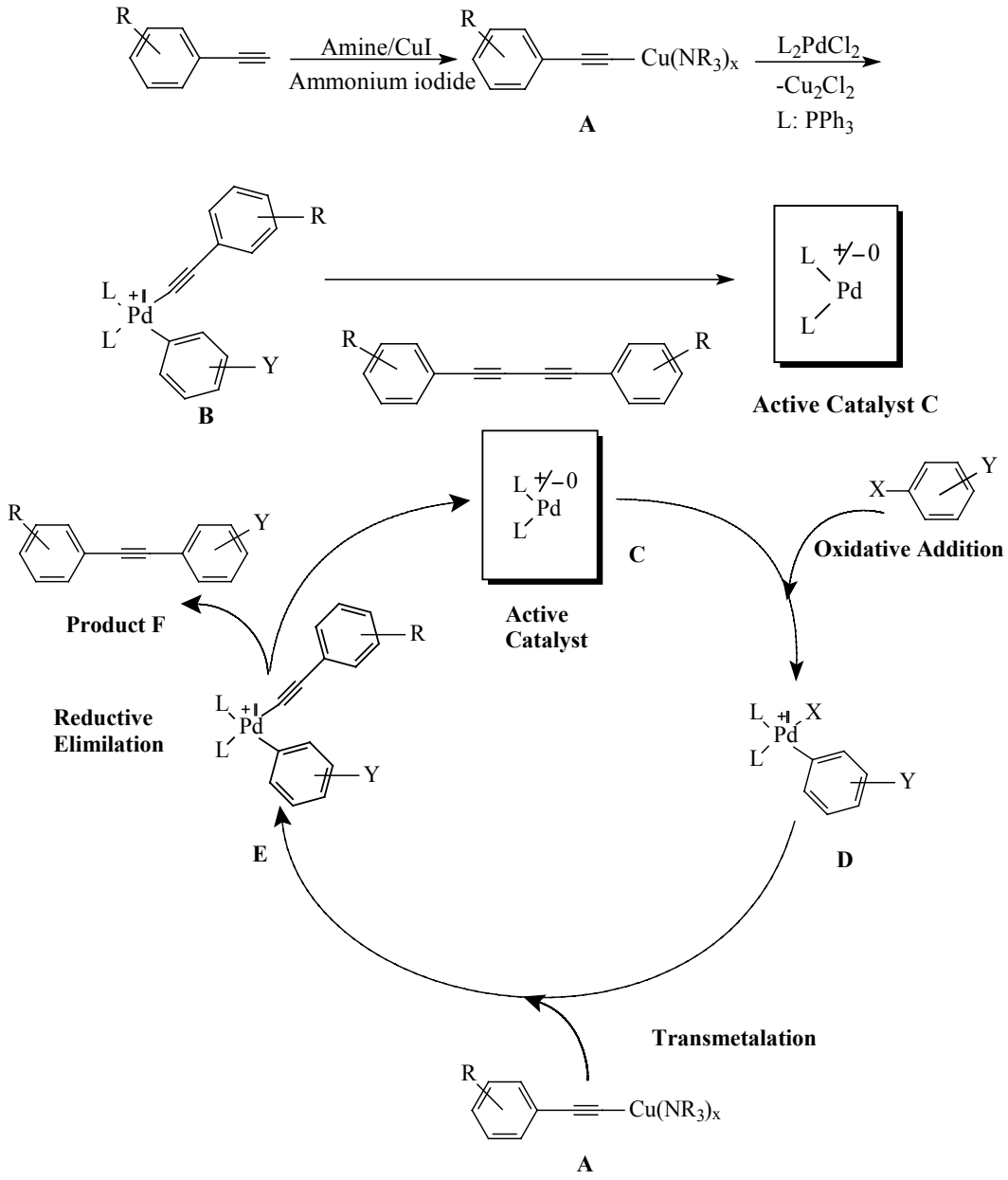

Figure 1.1.17 Palladium synthesis route

The classic Pd-catalyzed Heck-Cassar-Sonogashira-Hagihara reaction forms the single bond between the arene ring and the alkyne triple bond. It should be equally possible to form the C-C triple bond during the polymerization reaction. In the case of double bonds this has been achieved by McMurry[155] coupling, condensation reactions,[156] and alkene metathesis.[157] However, there is no analogue of the McMurry reaction in alkyne chemistry, and likewise, high-yielding condensation methods are not well-developed for the synthesis of triple bonds. Alkyne metathesis in homogeneous solution on the other hand has been known since 1974. It was discovered by Mortreux and Blanchard, who treated tolanes with a mixture of molybdenum hexacarbonyl and 4-chlo-rophenol. In 1997, Bunz, Weiss, and Mullen[158] reported the first use of Schrock's tungsten-carbyne[159] for the preparation of some PPEs including 2,5-dihexyl-PPE. Kloppenburg, Pschirer, and Bunz[160,161] optimized the reaction conditions of alkyne metathesis utilizing $Mo(CO)_6$ and 4-chlorophenol by increasing the reaction temperature from 105 to 130-150 °C. The polymer synthesized from alkyne metathesis got higher molecular weight than that from Heck reaction. Using the more solubilizing ethylhexyl, dodecyl, or dihydrocitronellyl (chiral) substituents as the side chains furnished PPEs with a DP of up to 1.2×10^3 (ethylhexyl), which is remarkable[162] and even surpasses the molecular weights of acceptor-substituted PPEs made by Swager.[99]

1.1.5.2 Alkoxy-Substituted PPE Derivatives

Early attempts to prepare the parent PPE led to the formation of infusible, insoluble, low-molecular-weight oligomers.[163] The first success of preparing soluble PPE

derivatives was achieved by Giesa.[164] The attachment of long alkoxy groups to the linear, rigid PPE backbone was expected to furnish polymers with increased solubility. The choice of alkoxy groups was based on the simplicity of the synthetic access to the corresponding monomers, and dialkoxy-substituted PPEs are the most easily synthesized representatives of the PPE class. Giesa's synthesis started with the alkylation of dibromohydroquinone, **1**, to obtain the monomer **2**[164] (**Figure 1.1.18**). Alkynylation of **2** and standard deprotection lead to the second monomer **3**. Palladium/CuI-catalyzed coupling of **2** to **3** in a mixture of triethylamine/pyridine furnished polymers with a degree of polymerization (DP) of 10-15 as deeply colored solids, the dissolvable fractions of which formed highly fluorescent solutions in aromatic hydrocarbons. Despite the long alkoxy groups (R, R' = hexyl, decyl, heptadecyl) attached, the solubility of the polymers **1** was not high, and in some cases even low. The minute solubility in combination with the deep coloring of their products suggests that Schulz' PPEs were substantially cross-linked. Structurally defined and defect-free derivatives of **1** are brilliantly yellow-orange powders, which show a green tinge in daylight due to efficient fluorescence, but are never brown or rusty-red materials.[165]

An improved synthesis of **1** was developed by Moroni et al.,[166] who coupled **2** and **3** (R= dodecyl) in the presence of $PdCl_2$, $Cu(OAc)_2$, and triphenylphosphine in a triethylamine/THF (**Figure 1.1.19**) mixture. The authors claimed to have formed PPEs with a DP of approximately 150 and attributed the high molecular weight to the presence of THF as solubilizing cosolvent.

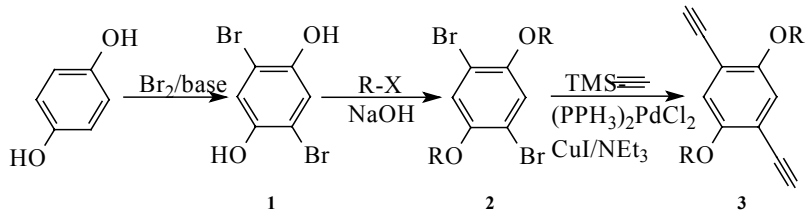

Figure 1.1.18 The general synthetic route for dialkoxy-PPEs monomers

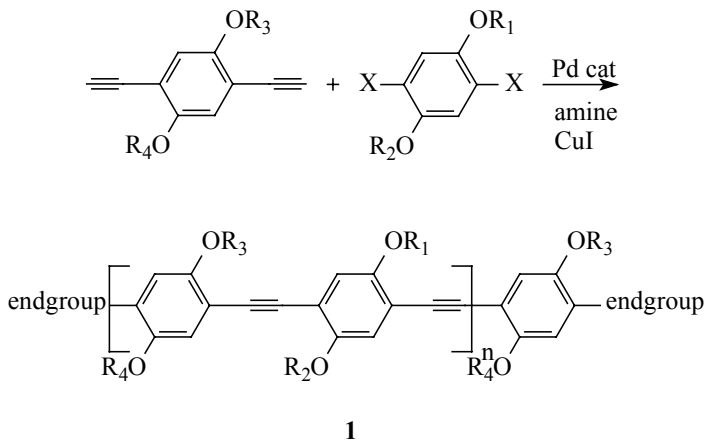

Figure 1.1.19 The genernal synthetic route for dialkoxy-PPEs

Their claim with respect to molecular weights is unsubstantiated: (a) In the (displayed) ^{13}C NMR spectrum of their "high-molecular-weight polymer", end group signals are clearly visible. The sensitivity of ^{13}C NMR spectroscopy is such that approximately 5-10% of an impurity can be detected. As a consequence, the DP of Le Moigne's material cannot exceed 20-25 PE units. (b) In the experimental part of their paper the authors state that 1.8 mmol of **2** and 1.8 mmol of **3** are treated with 0.2 mmol of $PdCl_2$ and 0.03 mmol of $Cu(OAc)_2$.[166] To form the active catalyst, 0.23 mmol of diyne **3** will have to be used to reduce both the Cu^{2+} and the Pd^{2+} species into their active zerovalent form. The presence of diyne defects is thus necessary, consequence, these PPEs **1** are expected to show a DP not exceeding 20, even after fractionation, and that

is exactly what is seen in the ^{13}C NMR spectrum. The authors describe their dialkoxy-PPEs as red-orange materials, suggesting at least some cross-linking to have occurred under these relatively harsh reaction conditions. The cross-linking may be responsible for the GPC and light-scattering data and the massive overestimation of their molecular weights.

By a similar method, utilizing 2,5-bis(2-(S)-methylbutoxy)-1,4-diethynylbenzene (**3**) and 2,5-bis(2-(S)-methylbutoxy)-1,4-dibromobenzene (**2**), Scherf[167] prepared a chiral dialkoxy-PPE, utilizing $Pd(PPh_3)_4$ and CuI in boiling triethyl- amine/THF. The chiral polymer had a DP of approximately 40 according to GPC, reinforcing the notion that it is difficult to make high-molecular-weight PPEs by the use of brominated monomers.

Cross-linking seems to be a general problem when working at elevated temperatures. The problem is circumvented if the coupling can be conducted at room temperature or up to 70 °C. Wrighton reported the coupling of the reactive 2,5-diiodo-1,4-dialkoxybenzenes to 2,5-di-ethynyl-1,4-dialkoxybenzenes in a diisopropylamine/toluene mixture under $Pd(PPh_3)_4$/CuI catalysis. This protocol furnishes PPEs which according to GPC measurements have DPs of up to 100.[168,169] The authors of that study prepared end-capped PPEs in which either anthracene or bromoalkyl-substituted dialkoxybenzenes are the chain terminators. The DP of these polymers is dependent on the amount of end-capper used, and end-functionalized PPEs with a DP of 20-40 were reported. Weder and Wrighton prepared a series of dialkoxy-substituted copolymers **1** with interesting side chains including ones with 3-(dimethylamino)propyl and 7-carboxy-heptyl groups.[170,171] To control molecular

weight, the authors added iodobenzene as end capper and isolated PPEs **1** with DPs of 20-30. These PPEs seem well defined and only have phenyl end groups according to ^{1}H NMR spectroscopy and elemental analysis. Weder[172] accessed a polymer by the same method with ethylhexyloxy and octyloxy solubilizing groups. He produced a high-molecular-weight polymer, which according to gel permeation chromatography (GPC) shows a DP of 230 phenyleneethynylene units. His rationalization for the high molecular weight is the supposed solubility-enhancing power of the branched ethylhexyl side chain. While that is certainly true, a DP of >200 is quite surprising for these Pd-catalyzed polycondensations, because it suggests that the efficiency of the coupling reaction must exceed 99.5% per coupling step. However, the reported yield is not quantitative but only 87%, suggesting fractionation. Similar PPEs have been made by Swager,[173] who reported a DP of approximately 50 for a dialkoxy-PPE, after fractionation. To limit the molecular weight, Swager had used 1.1 equiv of the diiodide to ensure the complete consumption of the diyne and the presence of defined iodine end groups.

References

1 Chiang, C. K.; Fincher, C. R.; Park, Y. W.; Heeger, A. J.; Shirakawa, H.; Louis, E. J.; Gau, S. C.; MacDiarmid, A. G. *Phys. Rev. Lett.*, **1977**, *39*, 1098.

2 Brown, A. R. *Electroluminescence in Poly(p-phenylenevinylene) and Derivatives*, Ph. D. dissertation, University of Cambridge, **1992**.

3 Bradley, D. D. C. *Chem. Br.*, **1991**, *21*, 719.

4 Bradley, D. D. C.; Brown, A. R.; Burn, P. L.; Burroughes, J. H.; Friend, R. H.; Greenham, N. C.; Gymer, R. W.; Holmes, A. B.; Kraft, A. M.; Marks, R. N. *"Conjugated Polymer Electro-optic Devices"* in *Photochemistry and Polymeric Systems*, Royal Society of Chemistry, **1993**, 120.

5 Friend, R. H.; Greenham, N. C. *"Conjugated Polymer Electroluminescence"* in *Physical Properties of Polymers Handbook*, AIP Press, **1996,** *35*, 479.

6 May, P. *Physics World*, **1995**, 52.

7 Friend, R. H.; Burroughes, J. H.; Shimoda, T. *Physics World*, **1999**, 35.

8 Kraft, A.; Grimsdale, A. C.; Holmes, A. B. *Angew. Chem.*, **1998**, *110*, 416.

9 Kraft, A.; Grimsdale, A. C.; Holmes, A. B. *Angew. Chem. Int. Ed.*, **1998**, *37*, 403.

10 Novák, P.; Müllen, K.; Santhanam, K. S. V.; Hass, O. *Chem. Rev.*, **1997**, *97*, 207.

11 Bohnen, A.; Heitz, W.; Müllen, K.; Räder, H. J.; Schenk, R. *Makromol. Chem.*, **1991**, *192*, 1679.

12 Burroughes, J. H.; Bradley, D. D. C.; Brown, A. R.; Marks, R. N.; Mackay, K.; Friend, R. H.; Burn, P. L.; Holmes, A. B. *Nature*, **1990**, *347*, 539.

13 Chen, W. *Design, Synthesis*, *Characterization and Study of Novel Conjugated*

Polymers, Ph. D dissertation, Iowa State University, **1997**.

14 Potember, R. S.; Hoffmann, R. C.; Hu, H. S.; Cocchiaro, J. E.; Viands, C. V.; Murphy, R. A.; Poehler, T. O. *Polymer*, **1987**, *28*, 574.

15 Bond, S. F.; Howie, A.; Friend, R. H. *Sur. Sci.*, **1995**, *333*, 196.

16 Blankespoor, R. L.; Miller, L. L. *J. Chem. Soc., Chem. Commum.*, **1985**, 90.

17 Couves, L. D.; Porter, S. J. *Synth. Met.*, **1989**, *28*, C761.

18 Zinger, B.; Miller, L. L. *J. Am. Chem. Soc.*, **1984**, *106*, 6861.

19 Umana, M.; Weller, *J. Anal. Chem.,* **1986**, *58*, 2979.

20 Barlett, P. N.; Whitaker, R. G. *J. Electroanal. Chem.*, **1987**, *37*, 224.

21 Caglar, P.; Wnek, G. E. *J. Macromol. Sci. Pure. Appl. Chem.*, **1995**, *A32*, 349.

22 Jung, S. K.; Wilson, G. S. *Anal. Chem.*, **1996**, *68*, 591.

23 Swager, T. M. *Acc. Chem. Res.*, **1998**, *31*, 201.

24 Paul, E. W.; Ricco, A. J.; Wrighton, M. S. *J. Phys. Chem.*, **1985**, *89*, 1441.

25 McQuade, D. T.; Pullen, A. E.; Swager, T. M. *Chem. Rev.*, **2000**, *100*, 2537.

26 Thomas, K. G.; Thomas, K. J.; Das, S.; George, M. V. *Chem. Commun.*, **1997**, 597.

27 Okoniewski, M. *Modifizerung der Synthesefasern zur Erzielung von leitfahigen*, Ferromagnetischen, Anderen Eigenschaften, Melliand textilber, **1990**, *71*, 94.

28 Kuhn, W.; Hargitay, B.; Katchalsky, A.; Eisenberg, H. *Nature*, **1950**, *165*, 514.

29 Angelopoulos, M.; Shaw, J. M.; Kaplan, R. D.; Perreault, S. *J. Vac. Sci. Technol. B*, **1989**, *7*, 1519.

30 Clarke, T. C.; Krounbi, M. T.; Lee, V. Y.; Street, G. B. *J. Chem. Soc., Chem.*

Commun., **1981**, *8*, 384.

31 Pitchumani, S.; Willig, F. *J. Chem. Soc., Chem. Commun.*, **1983**, *13*, 809.

32 Colaneri, N. F.; Shacklette, L. W. *IEEE Trans. Instrum. Meas.*, **1992**, *IM-41*, 291.

33 Taka, T. *Synth. Met.*, **1991**, *41*, 1777.

34 Joo, J.; Epstein, A. J. *Appl. Phys. Lett.*, **1994**, *65*, 2278.

35 Gustafsson, G.; Cao, Y.; Treacy, G. M.; Klavetter, F.; Colaneri, N.; Heeger, A. J. *Nature*, **1992**, *357*, 1789.

36 Pei, Q.; Yu, G.; Zhang, C.; Yang, Y.; Heeger, A. J. *Science*, **1995**, *269*, 1086.

37 Pei, Q.; Yang, Y.; Yu, G.; Zhang, C.; Heeger, A. J. *J. Am. Chem. Soc.*, **1996**, *118*, 3922.

38 Yu, G.; Heeger, A. J. *J. Appl. Phys.*, **1995**, *78*, 4510.

39 Hals, J. J. M.; Walsh, C. A.; Marseglia, E. A.; Friend, R. H.; Moratti, S. C.; Holmes, A. B. *Nature*, **1995**, *396*, 498.

40 Yu, G.; Cao, Y.; Hummelen, J. C.; Wudl, F.; Heeger, A. J. *Science*, **1995**, *270*, 1789.

41 Burroghes, J. H.; Jones, C. A.; Friend, R. H. *Nature*, **1998**, *335*, 137.

42 Garnier, F.; Hajlaoui, R.; Yasser, A.; Srivastava, P. *Science*, **1994**, *265*, 1684.

43 Brown, A. R.; Pomp, A.; Hart, C. M.; de Leeuw, D. M. *Science*, **1995**, *270*, 972.

44 Torsi, L.; Dodabalapur, A.; Rothberg, L. J.; Fung, A. W. P.; Katz, H. E. *Science*, **1996**, *272*, 1462.

45 Yang, Y.; Heeger, A. J. *Nature*, **1994**, *372*, 344.

46 Yu, G.; Pakbaz, K.; Heeger, A. J. *J. Electron. Mater.*, **1994**, *23*, 925.

47 Hide, F.; Diaz-Garcia, M. A.; Schwartz, B. J.; Heeger, A. J. *Acc. Chem. Res.*, **1997**, *30*, 430.

48 Halvorson, C.; Hays, A.; Kraabel, B.; Wu, R.; Wudl, F.; Heeger, A. J. *Science*, **1992**, *265*, 1215.

49 Halger, T. W.; Heeger, A. J. *Phys. Rev. B*, **1994**, *49*, 7313.

50 Reynolds, J. R.; Kumar, A.; Reddinger, J. L.; Sankaran, B.; Sapp, S. A.; Sotzing, G. A. *Synth. Met.*, **1997**, *85*, 1295.

51 Yu, G.; Wang, J.; McElvain, J.; Heeger, A. J. *Adv. Mater.,* **1998**, *10*, 1431.

52 Sirringhaus, H.; Tessler, N.; Friend, R. H. *Science*, **1998**, *280*, 1741.

53 Horowitz, G. *Adv. Mater.*, **1998**, *10*, 365.

54 Drury, C. J.; Mutsaers, C. M. J.; Hart, C. M.; Matters, M.; deleeuw, D. M. *Appl. Phys. Lett.*, **1998**, *73*, 108.

55 Destriau, G. *J. Chem. Phys.*,**1936**, *33*, 587.

56 Holonyak Jr, N.; Bevacqua, S. F. *Appl. Phys. Lett.*, **1962**, *1*, 82.

57 Craford, M. G.; Steranka, F. M. *Light-Emitting Diodes in Encyclopedia of Applied Physics*, ed. Trigg, G. L., VCH, Weinheim, **1994**, *8*, 485.

58 Pope, M.; Kallmann, H. P.; Magnante, P. *J. Chem. Phys.*, **1963**, *38*, 2042.

59 Tang, C. W.; VanSlyke, S. A. *Appl. Phys. Lett.*, **1987**, *51*, 913.

60 Adachi, C.; Tsutsui, T.; Saito, S. *Appl. Phys. Lett.*, **1990**, *56*, 799.

61 Braun, D.; Heeger, A. J. *Appl. Phys. Lett.*, **1991**, *58*, 1982.

62 Salbeck, J.; *Ber. Bunsenges. Phys. Chem.*, **1996**, *100*, 1667.

63 Colaneri, N. F.; Bradley, D. D. C.; Friend, R. H.; Burn, P. L.; Holmes, A. B.;

Spangler, C. W. *Phys. Rev. B*, **1990**, *42*, 11670.

64 Woo, H. S.; Graham, S. C.; Halliday, D. A.; Bradley, D. D. C.; Friend, R. H.; Burn, P. L.; Holmes, A. B. *Phys. Rev. B*, **1992**, *46*, 7379.

65 Dubois, J. C.; Le Barny, P.; Bouché, C. M.; Berdagué, P.; Facoetti, H.; Robin, P. *"Organic Electroluminescence and Applications"* in *Photoactive Organic Materials*, Kluwer Academic Publishers, **1996**, 313.

66 Segura, J. L.; *Acta. Polym.*, **1998**, *49*, 319.

67 Weill, A. *Springer Proceedings in Physics*, Vol. 13, Springer, **1986**, 51.

68 Sakakibara, Y.; Iijima, M.; Tsukagoshi, K.; Takahashi, Y. *Jpn. J. Appl. Phys.*, **1993**, *32*, L332.

69 Kido, J.; Nagai, K.; Okamoto, Y. *IEEE Trans. Electron Devices*, **1993**, *40*, 1000.

70 Sheats, J. R.; Antoniadis, M.; Hueschen, M.; Leonard, W.; Miller, J.; Moon, R.; Roitman, D.; Stocking, A. *Science*, **1996**, *273*, 884.

71 Greenham, N. C.; Moratti, S. C.; Bradley, D. D. C.; Friend, R. H.; Burn, P. L.; Holmes, A. B. *Nature*, **1993**, *365*, 628.

72 Son, S.; Dodabalapur, A.; Lovinger, A. J.; Galvin, M. E. *Science*, **1995**, *269*, 376.

73 Yang, Y.; Pei, Q.; Heeger, A. J. *J. Appl. Phys.*, **1996**, *79*, 934.

74 Uchida, M.; Ohmori, Y.; Morishima, C.; Yoshino, K. *Polym. Prepr.*, **1997**, *38*, 357.

75 Kim, D. Y.; Kim, J. K.; Cho, H. N.; Kim, C. Y. *Polym. Prep.,* **1997**, *38*, 417.

76 Yang, J.-S.; Swager, T. M. *J. Am. Chem. Soc.* **1998**, *120*, 5321.

77 Yang, J.-S.; Swager, T. M. *J. Am. Chem. Soc.* **1998**, *120*, 11864.

78 Moutet, J.-C.; Saint-Aman, E.; Tran-Van, F.; Angibeaud, P.; Utille, J.-P. *Adv. Mater.* **1992**, *4*, 511.

79 Roncali, J.; Garreau, R.; Delabouglise, D.; Garnier, F.; Lemaire, M. *J. Chem. Soc., Chem. Commun.* **1989**, 679.

80 Shi, L. H.; Garnier, F.; Roncali, J. *Synth. Met.* **1991**, *41-43*, 547.

81 Bartlett, P. N.; Benniston, A. C.; Chung, L.-Y.; Dawson, D. H.; Moore, P. *Electrochim. Acta* **1991**, *36*, 1377.

82 Youssoufi, H. K.; Hmyene, M.; Garnier, F.; Delabouglise, D. *J. Chem. Soc., Chem. Commun.* **1993**, 1550.

83 Garnier, F.; Korri, H.; Hmyene, M.; Yassar, A. *Polym. Prepr.* **1994**, *35* (1), 205.

84 Youssoufi, H. K.; Yassar, A.; Baý¨teche, S.; Hmyene, M.; Garnier, F. *Synth. Met.* **1994**, *67*, 251.

85 Marsella, M. J.; Swager, T. M. *J. Am. Chem. Soc.* **1993**, *115*, 12214.

86 Swager, T. M.; Marsella, M. J. *Adv. Mater.* **1994**, *6*, 595.

87 Swager, T. M.; Marsella, M. J.; Bicknell, L. K.; Zhou, Q. *Polym. Prepr.* **1994**, *35* (1), 206.

88 Marsella, M. J.; Swager, T. M. *Polym. Prepr.* **1994**, *35* (1), 271.

89 Marsella, M. J.; Newland, R. J.; Swager, T. M. *Polym. Prepr.* **1995**, *36* (1), 594.

90 Bäuerle, P.; Scheib, S. *Acta Polym.* **1995**, *46*, 124.

91 Scheib, S.; Bäuerle, P. *J. Mater. Chem.* **1999**, *9*, 2139.

92 Inoue, M.; Sotelo, M.; Machi, L.; Inoue, M. B.; Nebesny, K. W.; Fernando, Q. *Synth. Met.* **1989**, *32*, 91.

93 Wang, B.; Wasielewski, M. R. *J. Am. Chem. Soc.* **1997**, *119*, 12.

94 Zhang, Q. T.; Tour, J. M. *J. Am. Chem. Soc.* **1997**, *119*, 9624.

95 Fu, D.-K.; Xu, B.; Swager, T. M. *Tetrahedron* **1997**, *53*, 15487.

96 Kimura, M.; Horai, T.; Hanabusa, K.; Shirai, H. *Adv. Mater.* **1998**, *10*, 459-.

97 Zotti, G.; Zecchin, S.; Schiavon, G.; Berlin, A.; Penso, M. *Chem. Mater.* **1999**, *11*, 3342.

98 Zhou, Q.; Swager, T. M. *J. Am. Chem. Soc.* **1995**, *117*, 7017.

99 Zhou, Q.; Swager, T. M. *J. Am. Chem. Soc.* **1995**, *117*, 12593.

100 McDonald, R. N.; Campbell, T. W. *J. Am. Chem. Soc.*, **1960**, *82*, 4669.

101 Hsieh, B. R. *"Poly(p-phenylene vinylenes)s (Methods of Preparation and Properties)"* in *Polymeric Materials Encyclopedia*, CRC Press, Inc., **1996**, 6537.

102 Leung, L. M. *"Polyphenylene Vinylene"* in *Handbook of Thermoplastics*, Marcel Dekker, Inc., **1997**, *33*, 817.

103 Moratti, S. C. *"The Chemistry and Uses of Polyphenylenevinylenes"* in *Handbook of Conducting Polymers*, 2nd ed., Marcel Dekker, Inc., **1998**, *13*, 343.

104 Scherf, U. *Top. Curr. Chem.*, **1999**, *201*, 163.

105 Wessling, R. A. *J. Polym. Sci, Polym. Symp.*, **1985**, *72*, 55.

106 Gilch, H. G.; Wheelwright, W. L. *J. Polym. Sci., Part A: Polym. Chem.*, **1966**, *4*, 1337.

107 Swatos, W. J.; Gordon III, B. *Polym. Prepr.*, **1990**, *31*, 505.

108 Braun, D.; Heeger, A. J. *Appl. Phys. Lett.*, **1991**, *58*, 1982.

109 Burn, P. L.; Grice, A. W.; Tajbakhsh, A.; Bradley, D. D. C.; Thomas, A. C. *Adv.*

Mater., **1997**, *9*, 1171.

110 Lo, S.-C.; Sheridan, A. K.; Samuel, I. D. W.; Burn, P. L. *J. Mater. Chem.*, **1999**, *9*, 2165.

111 Sanford, E. M.; Perkins, A. L.; Tang, B.; Kubasiak, A. M.; Reeves, J. T.; Paulisse, K.W. *Chem. Commun.*, **1999**, *23*, 2347.

112 Neef, C. J.; Ferraris, J. P. *Macromolecules*, **2000**, *33*, 2311.

113 McCallien, D. W. J.; Thomas, A. C.; Burn, P. L. *J. Mater. Chem.*, **1999**, *9*, 874.

114 Atreya, M.; Li, S.; Kang, E. T.; Neoh, K. G.; Ma, Z. H.; Tan, K. L.; Huang, W. *Polym. Degrad. Stabil.*, **1999**, *65*, 287.

115 Shim, H.-K.; Hwang, D.-H.; Lee, K.-S. *Macromol. Chem.*, **1993**, *194*, 1115.

116 Jang, M.-S.; Shim, H.-K. *Polym. Bull.*, **1995**, *35*, 49.

117 Yoon, C.-B.; Kang, I.-N.; Shim, H.-K. *J. Polym. Sci., Polym. Chem.*, **1997**, *35*, 2253.

118 Jang, M. S.; Song, S. Y.; Lee, J.-I.; Shim, H.-K.; Zyung, T. *Macromol. Chem. Phys.*, **1999**, *200*, 1101.

119 Pfeiffer, S.; Hörhold, H.-H. *Macromol. Chem. Phys.*, **1999**, *200*, 1870.

120 Liu, Y. B.; Lahti, P. M.; La, F. *Polymer*, **1998**, *39*, 5241.

121 Doi, S.; Kuwabara, M.; Noguchi, T.; Ohnishi, T. *Synth. Met.*, **1993**, *57*, 4174.

122 Andersson, M. R.; Yu, G.; Heeger, A. J. *Synth. Met.*, **1997**, *85*, 1275.

123 Brandon, K. L.; Bentley, P. G.; Bradley, D. D. C.; Dunmur, D. A. *Synth. Met.*, **1997**, *91*, 305.

124 Cacialli, F.; Chuah, B. S.; Kim, J. S.; dos Santos, D. A.; Friend, R. H.; Moratti, S.

C.; Holmes, A. B.; Brédas, J. L. *Synth. Met.*, **1999**, *102*, 924.

125 Chuah, B. S.; Cacialli, F.; dos Santos, D. A.; Feeder, N.; Davies, J. E.; Moratti, S. C.; Holmes, A. B.; Friend, R. H.; Brédas, J. L. *Synth. Met.*, **1999**, *102*, 935.

126 Babudri, F.; Cicco, S. R.; Chiavarone, L.; Farinola, G. M.; Lopez, L. C.; Naso, F.; Scamarcio, G. *J. Mater. Chem.*, **2000**, *10*, 1573.

127 Barashkov, N. N.; Novikova; T. S.; Ferraris, J. P. *Synth. Met.*, **1996**, *83*, 39.

128 Barashkov, N. N.; Novikova, T. S.; Ferraris, J. P. *Synth. Met.*, **1997**, *84*, 259.

129 Doi, S.; Osada, T.; Tsuchida, Y.; Noguchi, T.; Ohnishi, T. *Synth. Met.*, **1997**, *85*, 1281.

130 Ahn, T.; Jang, M. S.; Shim, H.-S.; Hwang, D.-H.; Zyung, T. *Macromolecules*, **1999**, *32*, 3279.

131 Heeger, A. J. *Solid State Commun.*, **1998**, *107*, 673.

132 Vestweber, H.; Greiner, A.; Lemmer, U.; Mahrt, R. F.; Richert, R.; Heitz, W.; Bässler, H. *Adv. Mater.*, **1992**, *4*, 661.

133 Hsieh, B. R.; Antoniadis, H.; Bland, D. C.; Feld, W. A. *Adv. Mater.*, **1995**, *7*, 36.

134 Antoniadis, H.; Roitman, D.; Hsieh, B. R.; Feld, W. A. *Polym. Adv. Technol.*, **1997**, *8*, 392.

135 Wan, W. C.; Gao, Y. L.; Goodwin, T. E.; Gonzalez, S. A.; Feld, W. A.; Hsieh, B. R. *Macromol. Symp.*, **1997**, *125*, 205-211.

136 Hsieh, B. R.; Wan, W. C.; Yu, Y.; Gao, Y. L.; Goodwin, T. E.; Gonzalez, S. A.; Feld, W. A. *Macromolecules*, **1998**, *31*, 631.

137 Hsieh, B. R.; Yu, Y.; Forsythe, E. W.; Schaaf, G. M.; Feld, W. A. *J. Am. Chem.*

Soc., **1998**, *120*, 231.

138 Boardman, F. H.; Grice, A. W.; Rüther, M. G.; Sheldom, T. J.; Bradley, D. D. C.; Burn, P. L. *Macromolecules*, **1999**, *32*, 111.

139 Chung, S.-J.; Jin, J.-I.; Lee, C.-H.; Lee, C.-E. *Adv. Mater.*, **1998**, *10*, 684.

140 Reisch, H. A.; Scherf, U. *Macromol. Chem. Phys.*, **1999**, *200*, 552.

141 Pei, J.; Yu, W. L.; Huang, W.; Heeger, A. J. *Chem. Lett.*, **1999**, *10*, 1123.

142 Spreitzer, H.; Becker, H.; Kluge, E.; Kreuder, W.; Schenk, H.; Demandt, R.; Schoo, H. *Adv. Mater.*, **1998**, *10*, 1340.

143 Peng, Z. H.; Zhang, J. H.; Xu, B. B. *Macromolecules*, **1999**, *32*, 5162.

144 Peng, Z. H.; Pan, Y. C.; Xu, B. B.; Zhang, J. H. *Macromol. Symp.*, **2000**, *154*, 245.

145 Johansson, D. M.; Srdanov, G.; Theander, M.; Yu, G.; Inganäs, O.; Andersson, M. R. *Synth. Met.*, **1999**, *101*, 56.

146 Johansson, D. M.; Srdanov, G.; Yu, G.; Theander, M.; Inganäs O.; Andersson, M. R. *Macromolecules*, **2000**, *33*, 2525.

147 Mangel, T.; Eberhardt, A.; Scherf, U.; Bunz, U. H. F.; Mullen, K. *Macromol. Rapid Commun.* **1995**, *16*, 571.

148 Weder, C.; Sarwa, C.; Montali, A.; Bastiaansen, G.; Smith, P. *Science* **1998**, *279*, 835.

149 (a) Montali, A.; Bastiaansen, G.; Smith, P.; Weder, C. *Nature* **1998**, *392*, 261. (b) Takui, T.; Itoh, K. *Macromolecules* **1993**, *26*, 3698.

150 Bumm, L. A.; Arnold, J. J.; Cygan, M. T.; Dunbar, T. D.; Burgin, T. P.; Jones, L.;

Allara, D. L.; Tour, J. M.; Weiss, P. S. *Science* **1996**, *271*, 1705.

151 (a) Samori, P.; Francke, V.; Mullen, K.; Rabe, J. P. *Chem. Eur. J.* **1999**, *5*, 2312. (b) Samori, P.; Sikharulidze, I.; Francke, V.; Mullen, K.; Rabe, J. P. *Nanotechnology* **1999**, *10*, 77. (c) Samori, P.; Francke, V.; Mullen, K.; Rabe, J. P. *Thin Solid Films* **1998**, *336*, 13. (d) Samori, P.; Francke, V.; Mangel, T.; Mullen, K.; Rabe, J. P. *Opt. Mater.* **1998**, *9*, 390. (e) Mullen, K.; Rabe, J. P. *Ann. N.Y. Acad. Sci.* **1998**, *852*, 205.

152 Dieck, H. A.; Heck, R. F. *J. Organomet. Chem.* **1975**, *93*, 259.

153 Cassar, I. *J. Organomet. Chem.* **1975**, *93*, 253.

154 Sonogashira, K.; Tohda, Y.; Hagihara, N. *Tetrahedron Lett.* **1975**, *16*, 4467.

155 *Active Metal*s; Furstner, A. Ed.; VCH: Weinheim, **1996**.

156 Scherf, U. *Top. Curr. Chem.* **1999**, *201*, 163.

157 Schuster, M.; Blechert, S. *Angew. Chem.* **1997**, *36*, 2037.

158 Weiss, K.; Michel, A.; Auth, E. M.; Bunz, U. H. F.; Mangel, T.; Mullen, K. *Angew. Chem.* **1997**, *36*, 506.

159 Schrock, R. R.; Clark, D. N.; Sancho, J.; Wengrovius, J. H.; Pederson, S. F. *Organometallics* **1982**, *1*, 1645.

160 Kloppenburg, L.; Song, D.; Bunz, U. H. F. *J. Am. Chem. Soc.* **1998**, *120*, 7973.

161 Pschirer, N. G.; Bunz, U. H. F. *Tetrahedron Lett.* **1999**, *40*, 2481.

162 Kloppenburg, L.; Jones, D.; Bunz, U. H. F. *Macromolecules* **1999**, *32*, 4194.

163 Giesa, R. *J. M. S.-Rev. Macromol. Chem. Phys.* **1996**, *36*, 631.

164 Giesa, R.; Schulz, R. C. *Macromol. Chem. Phys.* **1993**, *191*, 857.

165 Kloppenburg, L.; Song, D.; Bunz, U. H. F. *J. Am. Chem. Soc.* **1998**, *120*, 7973.

166 Moroni, M.; LeMoigne, J.; Luzzati, S. *Macromolecules* **1994**, *27*, 562.

167 Fiesel, R.; Scherf, U. *Macromol. Rapid Commun.* **1998**, *19*, 427.

168 Ofer, D.; Swager, T. M.; Wrighton, M. S. *Chem. Mater.* **1995**, *7*, 418.

169 Swager, T. M.; Gil, C. J.; Wrighton, M. S. *J. Phys. Chem.* **1995**, *99*, 4886.

170 Weder, C.; Wrighton, M. S. *Macromolecules* **1996**, *29*, 5157.

171 Weder, C.; Wrighton, M. S.; Spreiter, R.; Bosshard, C.; Gunter, P. *J. Phys. Chem.* **1996**, *100*, 18931.

172 Steiger, D.; Smith, P.; Weder, C. *Macromol. Rapid Commun.* **1997**, *18*, 643.

173 Kim, J. S.; McHugh, S. K.; Swager, T. M. *Macromolecules* **1999**, *32*, 1500.

CHAPTER ONE

Part II: Introduction

1.2.1 Conjugated Polyelectrolytes

1.2.1.1 Application of Conjugated Polyelectrolytes

The ionic nature, induced electrostatic potentials, and broad range of microscopic architectures available with polyelectrolytes (PE's) make them interesting candidates for use in a variety of redox and electroactive systems,[1] including solid-state device applications. PE's can enhance or hinder chemical reactions by their ability to increase or decrease the concentration of ionic reactants.[2,3] PE's have also proven useful as reaction media for photoinduced electro-transfer events; photoinduced charge separation has been enhanced in the presence of PE's which may retard back electron transfer.[4,5]

Recent studies show that water-soluble conjugated polymers may offer a lot of new application opportunities. Potential applications of water-soluble conjugated polymers include the construction of active layers in organic light-emitting diodes through layer-by-layer self-assembly approach,[6] as buffer layer and emissive layer materials in inkjet printing fabricated organic LEDs,[7] and as highly sensitive fluorescent sensory materials in living bodies.[8,9] The applications generally favor high molecular weights and high photoluminescence (PL) efficiencies and require different ionic types. Water-solubility of semiconducting conjugated polymers was first demonstrated in

3-substituted PTs[10,11] and was then extended to poly(*para*-phenylene vinylene) (PPV)-based[12] and poly(*para*-phenylene) (PPP)-based polymers.[13,14] Among them, water-soluble PPP derivatives have been widely investigated. In 1990, Kim and Webster synthesized a trifunctional benzene-based monomer, (3,5-dibromophenyl)boronic acid, which could be self-condensed to a hyperbranched macromolecule that is water soluble.[15] Novak et al subsequently reported the synthesis of a water soluble, rigid rod PPP derivative using a water-soluble Pd(0) catalyst.[16] This PPP derivative contains two carboxylic acid groups directly attached to each quaterphenylene repeat unit and all *para* linkages along its backbone. In addition, Rehahn et al. prepared a series of PPP-based polyelectrolytes containing both carboxylate and tetralkylammonium functionality,[13,17,18] while Wegner prepared directly sulfonated PPP's via an organic soluble precursor and Reynolds et al synthesized the sulfonated PPP's through the Suzuki reaction with a water-soluble catalyst.[19,20] Recent publications have shown that PPP polyelectrolytes can be obtained with high molecular weights, controlled physical properties, and desired solubility.[18,21-24]

1.2.1.2 Layer-by-Layer Self-Assembly of Conjugated Polyelectrolytes

Among all the applications of conjugated ions, layer-by-layer self-assembly is most attractive recently. Through the attractive electrostatic interaction between the chains, pairs of oppositely charged polyelectrolytes in aqueous solution are well-known to form complexes. The process, which is extremely simple, is depicted in **Figure 1.2.1**

for the case of polyanionpolycation deposition on a positively charged surface.

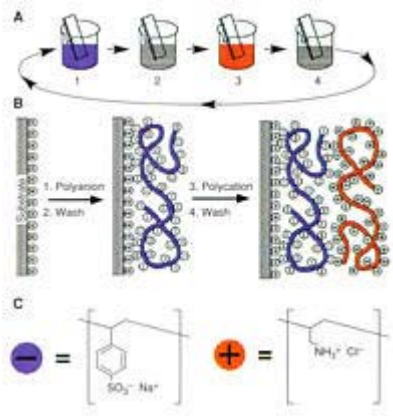

Figure 1.2.1 The process of layer-by-layer adsorption

Strong electrostatic attraction occurs between a charged surface and an oppositely charged molecule in solution. In principle, the absorption of molecules carrying more than one equal charge allows for charge reversal on the surface, which has two important consequences: (i) repulsion of equally charged molecules and thus self-regulation of the adsorption and restriction to a single layer, and (ii) the ability of an oppositely charged molecule to be adsorbed in a second step on top of the first one. Cyclic repetition of both adsorption steps leads to the formation of multilayer structures.

The incorporation of proteins in multilayers films may lead to the application of polyelectrolyte multilayers as biosensors[25] or in biotechnology[26,27], the latter may even provide the base for new developments in multistep chemical catalysis. A crucial point in this type of application will be the control of transport in multilayer films.[28,29] Multilayer microcapsules may have biomedical applications as well. Multilayer films can also be fabricated on colloids, which may have implications for photovoltaics.[30]

Other possible applications include the incorporation of dye molecules to tailor the optical properties of polyion films.[31-37] In the case of rodlike amphiphiles carrying hydrophilic head groups at both ends and a central diacetylene group, multilayer systems may also have high inplane order, because the topochemical polymerization of the diacetylene group only works in a single crystal.[38]

The use of multilayers as gas separation membranes is a currently developing technology.[39] As of today, the most advanced development of polyion-based films is probably their potential for the fabrication of light-emitting diodes.[40-49] This interest was kindled by the demonstration that a water-soluble polyelectrolyte precursor of the intractable electroluminescent polymer PPV can be incorporated into polyelectrolyte films and subsequently thermally converted to PPV.[40] The nuetron reflectivity scan shows that the multilayer structure of such films, which contain hydrophobic PPV layers after elimination, remains intact.

Conjugated polymers have been incorporated as active materials into several kinds of electronic, optical, magnetic and miscellaneous devices. The development and utilization of conjugated polymers as the active elements of thin-film electronic and optical devices continue to be a highly pursued area of research. These materials are generally manipulated into thin films via simple spin-casting techniques. However, it is becoming increasingly more apparent that more control over the molecular and supramolecular organizations of these materials is needed to fully exploit their novel optical and electrical properties. For example, multilayer thin films comprised of separate hole and electron transport layers are currently being considered for use in

light-emitting diodes based on conjugated polymers.[50,51]

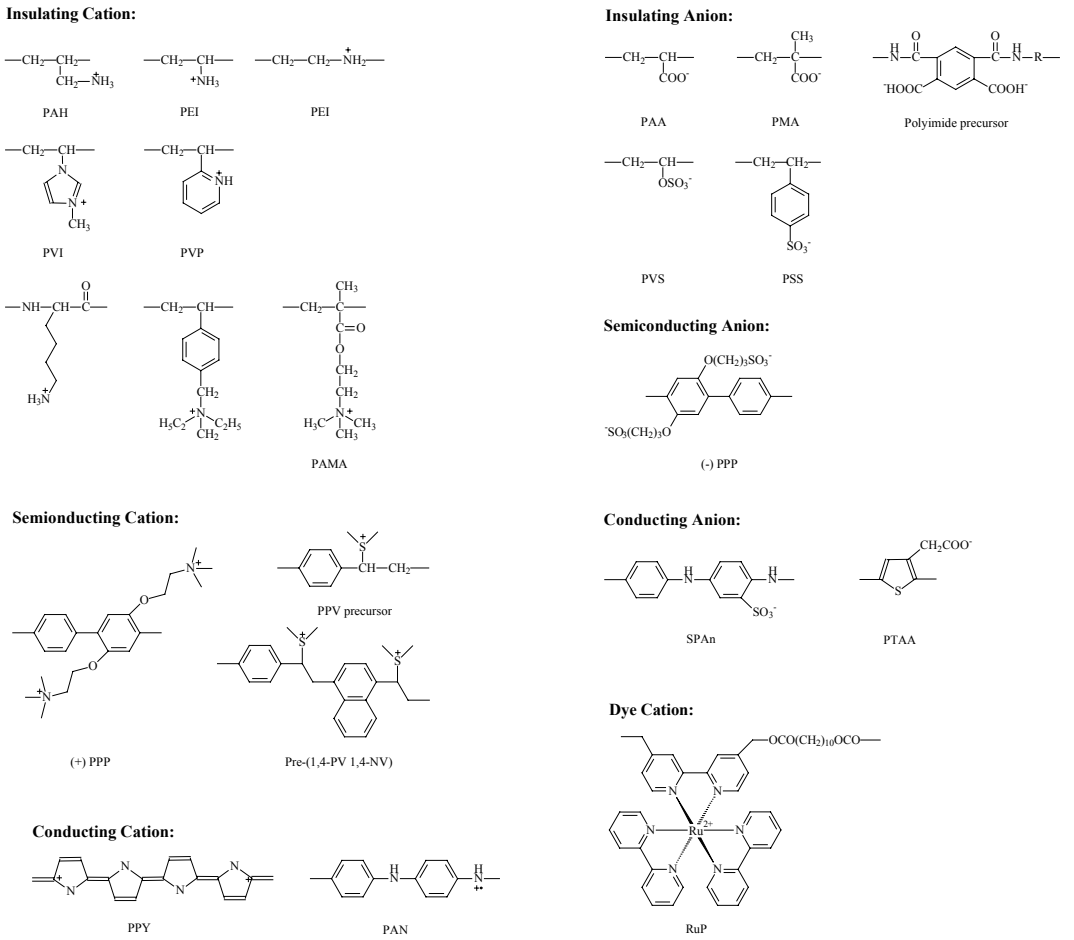

Figure 1.2.2 Schematic representation of the structures of the polymer interlayers

The ultimate realization of this particular approach would be the ability to manipulate conjugated polymers into layers with molecular dimensions in a highly controlled manner. The layer-by-layer processing technique, which is a viable means to manipulate polymers into multilayer thin films, provides molecular-level control over the thickness and architecture of multilayer thin films and is readily extended to a wide variety of polymers including many different electroactive polymers (**Figure 1.2.2**). In 1994, M. F. Rubner *et al.* first reported the manipulation of conjugated polymers via this technique.[52,53] In his group work, conducting polymers, poly(thiophene-3-acetate)

(PTAA), sulfonated polyaniline (SPAN) and polypyrrol and light-emitting polymer, PPV precursor were successfully fabricated into multilayer thin films with non-conjugated polyelectrolyte via self-assembly. Then besides Rubner's group, a number of other groups have utilized this approach to fabricate light-emitting devices from both PPV precursor materials and non-conjugated polyelectrolyte[54,46,48] or fully conjugated polyions, such as PPV/SPAN[55] and Bu-PHPyV/SPAN.[45] In 1998, M.F. Rubner *et al.* reported the first sequentially adsorbed multilayer devices in which both the polycation and polyanion layers are based on the same emitting polymer, PPP.[6] Recently, M.F. Rubner *et al.* have fabricated light emitting devices based on sequentially adsorption of an electrochemiluminescent active $Ru(bpy)_3^{2+}$ polyester and various polyanion including a small molecule Ru(II) dye, sulfonated poly(*p*-phenylene) (SPPP), sulfonated polystyrene (PSS), poly(methacrylic acid) (PMA) and poly (acrylic acid) (PAA) and external device efficiencies in the range of 1-3% have been achieved.[56,59] Now the self-assembly multilayers fabricated from conjugated polymers have been used to modify the electrode as the hole or electronic injection or transporting layer in the device. P.K.H. Ho et al. interposed a well-defined, continuous and ultrathin polymer layer at the interface between the indium tin oxide electrode layers and the emissive polymer.[60] They fabricated separate devices with a conducting polymer interlayer of self-doped PAni, a semiconducting polymer interlayer containing PPV or an insulating polymer interlayer of saturated main chain polymers. The results show that interlayer significantly alters charge injection and enhances the device electroluminescence efficiency. M. F. Rubner has recently studied the Forster energy

transferred between PPV and PPP monolayers using the sequential adsorption process to adjust the layer number between those two layers.[61]

1.2.1.3 Conjugated Polyelectrolytes Used as Chemo or Biosensors

Although previous studies on conjugated polymers demonstrated amplified quenching to allow trace detection of analytes, the systems are limited because the polymers only dissolve in organic solvents. A sensor would be more useful if it operates in an aqueous environment. Recently, water-soluble conjugated polymers (WSCPs) show potential for use as a new class of high-sensitivity rapid-response chemical and biological sensors.[62] Through electrostatic attraction, WSCPs could attach quenchers with oppositely charge more closely and their fluorescence can be quenched by those very small amounts of charged molecules (quenchers) that quench the excited state by energy transfer or electron transfer. In 1999, L. H. Cheng first reported the amplification of quenching sensitivity of MPS-PPV (PPV-SO_3^{2-}) to methyl viologen (MV^{2+}), in which $K_{sv} = 1.2 \times 10^7\ M^{-1}$.[62]

This quenching can be adapted to biosensing by coupling a quencher to a biological ligand. In aqueous solution, the photoluminescence (PL) from the polymer is quenched when the quencher–ligand conjugate associates with the polyelectrolyte to form a relatively weak conjugate–polymer complex, as a consequence of electrostatic and hydrophobic interactions. Exposure of the conjugate–polymer complex to a biological receptor results in formation of a biospecific receptor–conjugate complex and release of the polymer with concomitant unquenching of the polymer fluorescence.[62] (**Figure**

1.2.3) In 2002, biosensing of the anti-DNP lgG with a charge neutral complex (CNC) formed in aqueous solution by combining PPV-SO_3^- and a saturated cationic polyelectrolyte at a 1:1 ratio (per repeat unit) was demonstrated by D. L. Wang et al.[63] This modified mechanism could efficiently minimize nonospecific interactions between conjugated polyelectrolytes and biopolymers.

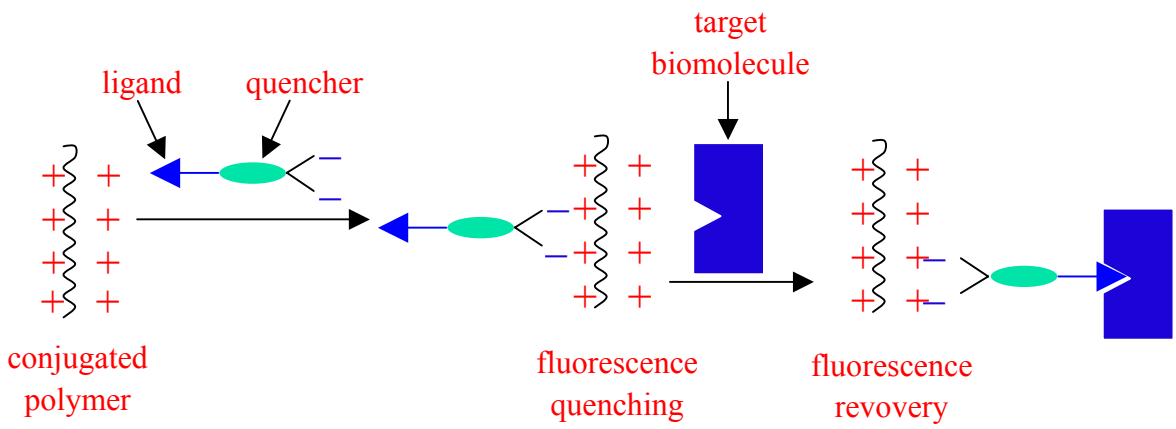

Figure 1.2.3 Diagram illustrating the detection mechanism of conjugated polyelectrolyte for biomolecules

Soon after that report, the light-harvesting properties of cationic conjugated polymers (PF) are used to sensitize the emission of a dye on a specific peptide nucleic acid (PNA) sequence for the purpose of homogeneous, real-time DNA detection by G. C. Bazan et al and detection of target DNA at concentrations of 10 pM was realized successfully.[64] **Figure 1.2.4** showed the mechanism of such a detection method. This method made it possible to take advantage of the optical amplification of WSCPs to detect DNA hybridization to a singly labeled PNA strand.

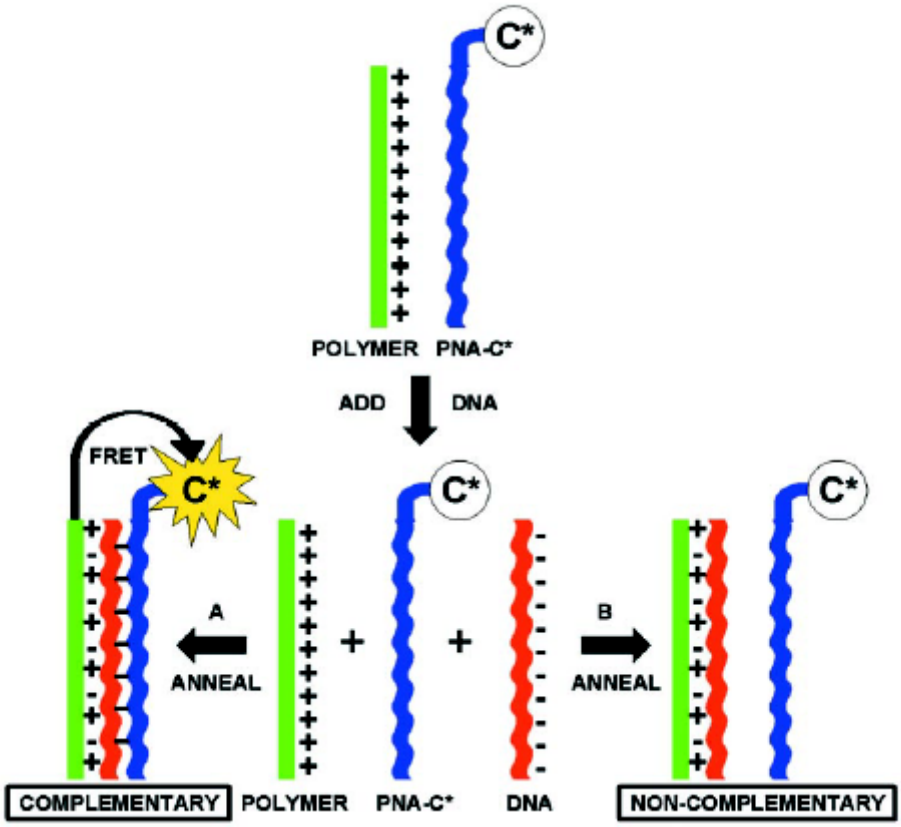

Figure 1.2.4 Diagrammatic representation for the use of a water-soluble CP with a specific PNA-C* optical reporter probe to detect a complementary ssDNA sequence.

Based on their potential applications as biosensors in the future, the fluorescence quenching of WSCPs were significantly investigated. Under preliminary studies, it was shown that the amplified sensitivity of WSCPs was highly related to its conjugated length,[65] charge of quenching,[66] ionic strength,[67] substrate,[68] complex of WSCPs with oppositely charged surfactant[69,70] or polyelectrolytes[68,71] and aggregation statutes.[72] Studies of PPV-SO_3^- showed that the higher conjugated length of WSCPs and the greater the opposite charge on the quencher, the more amplified quenching will be obtained.[65] By layering fluorescent polyelectrolytes onto oppositely charged surfaces, one could tune superquenching effects, for example, when PPV-SO_3^- was deposited on

the surface of polystyrene microsphere, it can be used to detect quencher with the same charge instead of that with opposite charge.[68]

The complex, which was formed through combining PPV-SO_3^- with cationic surfactant, showed higher sensitivity to neutral quenchers (such as trinitrotoluene) while swiftly decreased sensitivity to oppositely charged quenchers.[69] More recently, energy transfer between oppositely charges polyelectrolytes has been used to obtain fluorescence superquenching.[68] These mixtures offer possibilities of "charge reversal", where it is also possible to encourage interactions between a given polyelectrolyte and a fluorescence quencher with similar charge.

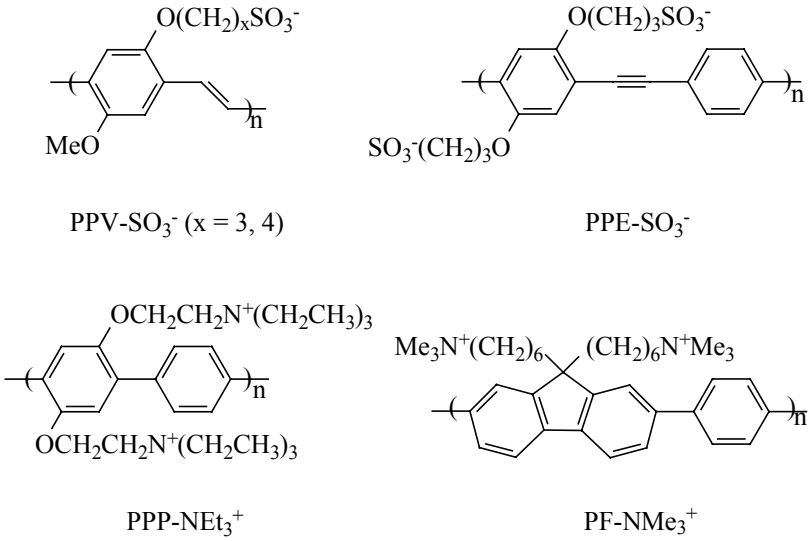

Figure 1.2.5 Molecular structure of WSCPs used as chemo or biosensors

Although a lot of information related to the quenching behavior of WSCPs has been collected by scientists recently, the relationship between quenching behavior and physical and chemical properties of conjugated polymers is still a major concern. Meanwhile, most of the above researches were focused on anionic WSCPs, especially on PPV-SO_3^-.[65-71] **Figure 1.2.5** showed the molecular structures of WSCPs which have

been used to study the quenching behavior.[64-70, 72,73] For cationic WSCPs, only M. F. Rubner reported fluorescent quenching of cationic PPP-NEt_3^+ by several anionic quencher, such as $Ru(phen')_3^{4-}$ and $Fe(CN)_6^{4-}$ in aqueous solution[73] and G.. C. Bazan proposed to detect DNA with cationic conjugated polymer PF-NEt_3^+.[71] Thus, preparation of novel cationic WSCPs and detectation of their quenching behavior are more attractive to develop good biosensors with high sensitivity.

1.2.2 Project Objectives

It is well known that conjugated polyelectrolytes have wide applications in many fields, in which ionic conjugated polymers could be used in construction of active layers in organic light-emitting diodes through layer-by-layer self-assembly approach, as buffer layer and emissive layer materials in inkjet printing fabricated organic LEDs, and as highly sensitive fluorescence sensory materials. To realize the full color displays, all the three primary colors (red, green and blue) are required. Those ionic conjugated polymers used in LEDs have been realized to emit red and blue light. Up to now, there is no green light-emitting conjugated polyelectrolyte reported. Simultaneously, for the fabrication of multiplayer derivatives, in some cases, it is difficult to spin cast multilayers of polymers because the first layer that is deposited can be dissolved during the spin-casting of the subsequent layers. Designing and synthesizing polymers with high PL efficiencies but different solubility in common organic solvents is essential to prepare devices with good properties. As for self-assembly, the polyelectrolytes with opposite charges must be required to afford the electrostatic

attraction. But most of the water-soluble polymers achieved by now are functionalized with terminal carboxylate or sulfonate groups, which are anionic conjugated polyelectrolytes. Up to now, almost all kinds of conjugated polymers such as PT, PPP, PPV and PPE have their anionic polyelectrolytes. But for cationic conjugated polymers, only cationic PPP and PF are now existing. Thus it is very attractive to obtain new kinds of cationic conjugated polyelectrolytes. Meanwhile, novel water-soluble conjugated polyelectrolytes are dramatically required for studying the relationship between quenching behavior and the conformation of conjugated polymer at different environments.

To obtain cationic green light-emitting PPVs with high quantum efficiency, the phenyl-substituted group on the side chains was chosen due to its steric hindrance which minimizes the interchain interaction. Introducing ammonium-terminated group into the side chain of the phenyl-substituted PPVs is chosen to realize the water-solubility of those PPVs. Based on the analysis mentioned above, in effort to develop highly PL efficiency green light emission cationic conjugated polymers, we designed three neutral phenyl-substituted PPVs, which are composed of all (amino-terminated alkoxy) phenyl-substituted hydrophilic units (**P1**, prepared through Gilch reaction), (amino-terminated alkoxy) phenyl-substituted hydrophilic moieties alternating with dodecyloxy phenyl-substituted hydrophobic moieties (**P2**, prepared through Wittig reaction) and (amino-terminated alkoxy) phenyl-substituted hydrophilic moieties alternating with tri(ethylene glycol)methyl ether phenyl-substitutied hydrophilic moieties (**P3**, prepard through Wittig reaction). In the synthesis of cationic

polymers, tertiary amine is chosen as the functional group in the neutral polymer, which upon quaternization with bromoethane, water soluble polymers could be expected. **P1** is anticipated to may not be able to dissolved in common organic solvents because of its short alkoxy groups. Introducing long chains into **P2** and **P3** will be benefit for enhancing the solubility of the neutral polymer and make the quaternization successful. Furthermore, introduction of hydrophilic group into **P3** will promote the water-solubility of its quaternized polymer. Because of their different conformation structure of backbone (with different content of trans/cis vinylic group), their optical properties and fluorescence quenching behavior can be compared with each other to collect the useful information.

Copolymerization approach that has been widely used in the preparation of conjugated polymers so as to achieve specific electronic and physical properties is of special interest for conjugated polyelectrolytes. By copolymerization with different aryl co-monomers, the optical and electronic properties of the resultant neutral and quaternized polymers are expected tunable. In this thesis, a new series of tertiary amino-based alternating copolymers of PPVs and their quaternized cationic polymers are synthesized, in an effort to obtain cationic PPVs with higher fluorescence efficiency and further investigation of the relationship between the quenching behavior and the conformation of vinylic group on the conjugated backbone.

To obtain cationic PPVs with different main and side chain structure, dihalomethylide of alkyl-substituted thiophene, alkyloxy-substituted benzene, phenyl-substituted benzene and alkyl-substituted fluorene are selected as the comonomers for

polymerization. Since thiophene as an electron rich moiety, will cause a spectral red shift, one alkyl chain is introduced to the thiophene moieties to adjust the light emission. Alkoxy and phenyl-substituted benzenes are specially chosen for their different steric and electron-donating properties, whereas fluorene are chosen for its high quantum efficiency.

Conjugated polymers, PPEs, with aromatic groups that are linearly conjugated through acetylene linkages have been the center of much attention in the past few years. One of the most appealing attributes of PPEs comes from the efficient electronic communication that occurs along their linearly conjugated structures, which have been widely used in chemo and biosensor fields. Meanwhile, because of the free rotation and easily changeable torsional angle of phenyl group on PPE backbone and the corresponding conveniently changeable optical properties at different environments, PPEs are good candidates to be used to investigate quenching behavior of conjugated polymers in which the mechanism is still unclear for scientists. Thus, preparing water-soluble conjugated polymers will be significantly beneficial to study the relationship between the optical and fluorescence quenching behavior and conformation of conjugated polymers. Ammonium-functionalized PPE derivateives were selected to obtain cationic PPEs. Copolymerization approach is also chosen to prepare PPEs so as to introduce aromatic units with different side chains into the PPE backbones. Similarly, to investigate the solubility and the optical properties of those quaternized polymer with side chains containing different hydrophilic and hydrophobic groups, diethynyl of hydrophilic tertiary amino-terminated ethoxy, tri(ethylene

glycol)methyl-substituted and hydrophobic hexyloxy, octyloxy and dodecyloxy-substituted benzenes are selected as the co-monomers for polymerization. Different lengths of the hydrophobic alkoxy chains are chosen to investigate the changes of the quaternization situation and the optical properties accompanied with the changes of the ratio of hydrophobic group with hydrophilic group. Introduction of hydrophilic groups is used to increase the water-solubility of those PPE derivatives. The optical properties and fluorescence quenching of water-soluble cationic PPE by anionic quencher $Fe(CN)_6^{4-}$ at different environments, such as different pH values, different concentrations of conjugated polymer PPE used and different anionic saturated polymers were systematically studied to try to disclose the relationship of quenching behavior and conformation of conjugated polymer.

References

1 Yotaro, M. *Adv. Polym. Sci.* **1992**, *104*, 51.

2 Morawetz, H. *Acc. Chem. Res.* **1970**, *3*, 354.

3 (a) Okubo, T.; Ise, N. *Proc. R. Soc. London, Ser. A* **1972**, *327*, 413 (b) Okubo, T.; Ise, N. *Bull. Chem. Soc. Jpn.* **1973**, *46*, 2493 (c) Mita, K.; Kunugi, S.; Okubo, T.; Ise, N. *J. Chem. Soc. Faraday Trans. 1* **1975**, *71*, 936 (d) Okubo, T.; Ishiwatari, T.; Mita, K.; Ise, N. *J. Phys. Chem.* **1975**, *79*, 2108 (e) Ise, N.; Okubo, T. *Macromolecules* **1978**, *11*, 439.

4 (a) Meisel, D.; Matheson, M. S. *J. Am. Chem. Soc.* **1977**, *99*, 6577 (b) Meisel, D.; Rabani, J.; Meyerstein, D.; Matheson, M. S. *J. Phys. Chem.* **1978**, *82*, 985 (c) Meyerstein, D.; Rabani, J.; Matheson, M. S. *J. Phys. Chem.* **1978**, *82*, 1879 (d) Jonah, C. D.; Matheson, M. S.; Meisel, D. *J. Phys. Chem.* **1979**, *83*, 257.

5 Sassoon, R. E.; Rabani, J. *J. Phys. Chem.* **1980**, *84*, 1319.

6 (a) Ferreira, M.; Rubner, M. F. *Macromolecules*, **1995**, *28*, 7101. (b) Fou, A. C.; Onitsuka, O.; Ferreira, M.; Rubner, M. F. *J. Appl. Phys.*, **1996**, *79*, 7501. (c) Baur, J. W.; Kim, S.; Balanda, P. B.; Reynolds, J. R.; Rubner, M. F. *Adv. Mater.*, **1998**, *10*, 1452.

7 (a) Bharathan, J.; Yang, Y. *Appl. Phys. Lett.*, **1998**, *72*, 2660. (b) Chang, S. C.; Bharathan, J.; Yang, Y. *Appl. Phys. Lett.*, **1998**, *73*, 2561.

8 Garnier, F.; Korri-Youssoufi, H.; Srivastava, P.; Mandrand, B.; Delarr, T. *Synth. Met.*, **1999**, *100*, 89.

9 (a) Fäid, K; Leclere, M. *Chem. Commun.*, **1996**, 2761; (b) Fäid, K; Leclere, M. *J.*

Am. Chem. Soc., **1998**, *120*, 5274.

10 Patil, A. O.; Ikenoue, Y.; Wudl, F.; Heeger, A. J. *J. Am. Chem. Soc.*, **1987**, *109*, 1858.

11 Pickup, P. *J. Electroanal. Chem.*, **1987**, *225*, 273.

12 Shi, S.; Wudl, F. *Macromolecules*, **1990**, *23*, 2119.

13 Wallow, T. I.; Novak, B. M. *J. Am. Chem. Soc.*, **1991**, *113*, 7411.

14 Child, A. D.; Reynolds, J. R. *Macromolecules*, **1994**, *27*, 1975.

15 Kim, Y. H.; Webster, O. W. *J. Am. Chem. Soc.*, **1990**, *112*, 4592.

16 Kim, Y. H.; Webster, O. W. *Macromolecules*, **1992**, *25*, 5561.

17 Rau, I. U.; Rehahn, M. *Acta Polym.*, **1994**, *45*, 3.

18 Brodowski, G.; Horvath, A.; Ballauf, M.; Rehahn, M. *Macromolecules*, **1996**, *29*, 6962.

19 Rulkens, R.; Schulze, M.; Wegner, G. *Makromol. Rapid. Commun.* **1994**, *15*, 669.

20 Kim, S.; Jackiw, J.; Robinson, E.; Schanze, K. S.; Reynolds, J. R.; Baur, J.; Rubner, M. F.; Boils, D. *Macromolecules*, **1998**, *31*, 964.

21 Cimrova, V.; Schmidt, W.; Rulkens, R.; Schuize, M.; Meyer, W.; Neher, D. *Adv. Mater.,* **1996**, *8*, 585.

22 Kowitz, C.; Wegner, G. *Tetrahedron*, **1997**, *53*, 15553.

23 Rulkens, R.; Wegner, G.; Chu, B. *Macromolecules*, **1998**, *31*, 6119.

24 Petrekidis, G.; Vlassopoulos, D.; Fytas, G.; Rulkens, R.; Wegner, G. *Macromolecules*, **1998**, *31*, 6129.

25 Sun, Y.; Zhang, X.; Sun, C.; Wang, B.; Shen, J. *Macromol. Chem. Phys.*, **1996**, *197*,

147.

26 Onda, M.; Lvov, Y.; Ariga, K.; Kunitake, T. *Biotechnol. Bioeng.*, **1996**, *51*, 163.

27 Decher, G.; Ferment, J. *Bioeng.*, **1996**, *82*, 502.

28 von Klitzing R.; Mohwald, H. *Thin Solid Films*, **1996**, *284-285*, 352.

29 Decher, G. *Macromolecules*, **1996**, *29*, 6901.

30 Keller, S. W.; Johnson, S. A.; Brigham, E. S.; Yonemoto, E. H.; Mallouk, T. E. *J. Am. Chem. Soc.*, **1995**, *117*, 12879.

31 Zhang, X.; Gao, M.; Kong, X.; Sun, Y.; Shen, J. *J. Chem. Soc. Chem. Commun.*, **1994**, 1055.

32 Cooper, T. M.; Campbell, A. L.; Crane, R. L. *Langmuir*, **1995**, *11*, 2713.

33 Laschewsky, A. et al., *Thin Solid Films*, **1996**, *284-285*, 334.

34 Lee, J. K.; Yoo, D. S.; Handy, E. S.; Rubner, M. F. *Appl. Phys. Lett.*, **1996**, *69*, 1686.

35 Sun, Y. et al., *J. Chem. Soc. Chem. Commun.*, **1996**, *1996*, 2379.

36 Saremi, F.; Lange, G.; Tieke, B. *Adv. Mater.*, **1996**, *8*, 923.

37 Ariga, K.; Lvov, Y.; Kunitake, T. *J. Am. Chem. Soc.*, **1997**, *119*, 2224.

38 Saremi, F.; Maassen, E.; Tieke, B.; Jordan, G.; Rammensee, W. *Langmuir*, **1995**, *11*, 1068.

39 Stroeve, P.; Vasques, V.; Coelho, M. A. N.; Rabolt, J. F. *Thin Solid Films*, **1996**, *284-285*, 708.

40 Ferreira, M.; Rubner, M. F.; Hsieh, B. R. *Mater. Res. Soc. Symp. Proc.*, **1994**, *328*, 119.

41 Tian J. et al., *Polym. Prepr. Am. Chem. Soc. Div. Polym. Chem.*, **1994**, *35*, 761.

42 Fou, A. C.; Onitsuka, O.; Ferreira, M.; Rubner, M. F.; Hsieh, B. R. *Mater. Res. Soc. Symp. Proc.*, **1995**, *369*, 575.

43 Onoda M.; Yoshino, K. *J. Appl. Phys.*, **1995**, *78*, 4456.

44 Tian J. et al., *Adv. Mater.*, **1995**, *7*, 395.

45 Tian, J.; Wu, C. C.; Thompson, M. E.; Sturm, J. C.; Register, R. A. *Chem. Mater.*, **1995**, *7*, 2190.

46 Fou, A. C.; Onitsuka, O.; Ferreira, M.; Rubner, M. F.; Hsieh, B. R. *J. Appl. Phys.*, **1996**, *79*, 7501.

47 Lehr, B.; Seufert, M.; Wenz, G.; Decher, G.; *Supramol. Sci.*, **1996**, *2*, 199.

48 Onitsuka, O.; Fou, A. C.; Ferreira, M.; Hsieh, B. R.; Rubner, M. F. *J. Appl. Phys.*, **1996**, *80*, 4067.

49 Hong H. et al., *Supramol. Sci.*, **1997**, *4*, 67.

50 Brown, A. R.; Bradley, D. D. C.; Friend, R. H. et al., *Appl. Phys. Lett.*, **1992**, *61*, 2793.

51 Brown, A. R.; Bradley, D. D. C.; Friend, R. H. et al., *Chem. Phys. Lett.*, **1992**, *200*, 46.

52 Ferreira, M.; Cheung, J. H.; Rubner, M. F. *Thin Solid Films*, **1994**, *244*, 806.

53 Cheung, J. H.; Fou, A. F.; Rubner, M. F. *Thin Solid Films*, **1994**, *244*, 985.

54 Hong, H.; Davidov, D.; Neumann, R. et al., *Adv. Mater.*, **1995**, *7 (10)*, 846.

55 Onoda, M.; Yoshino, K. *Jpn. J. Appl. Phys.*, **1995**, *34*, 260.

56 Wu, A.; Lee J.; Rubner, M. F. *Thin Solid Films*, **1998**, *327-329*, 663.

57 Lyons, C. H.; Abbas, E. D.; Lee, J.-K.; Rubner, M. F. *J. Am. Chem. Soc.*, **1998**, *120*, 12100.

58 Handy, E. S.; Pal, A. J.; Rubner, M. F. *J. A. Chem. Soc.*, **1999**, *121*, 3525.

59 Wu, A.; Yoo, D.; Lee, J.-K.; Rubner. M. F. *J. A. Chem. Soc.*, **1999**, *121*, 4883.

60 Ho, P. K. H.; Granstrom, M. R.; Friend, H.; Greenham, N. C. *Adv. Mater.*, **1998**, *10 (10)*, 769.

61 Baur, J. W.; Rubner, M. F.; Reynolds, J. R.; Kim, S. *Langmuir*, **1999**, *15*, 6460.

62 Chen, L.; McBranch, D. W.; Wang, H.-L.; Helgeson, R.; Wudl, F.; Whitten, D. G. *Proc. Natl. Acad. Sci. U. S. A.* **1999**, *96*, 12287.

63 Wang, D.; Gong, X.; Heeger, P. S.; Rininsland, F.; Bazan, G. C.; Heeger, A. J. *Proc. Natl. Acad. Sci. U. S. A.* **2002**, *99*, 49.

64 Gaylord, B. S.; Heeger, A. J.; Bazan, G. C. *Proc. Natl. Acad. Sci. U. S. A.* **2002**, *99*, 10954.

65 Gaylord, B. S.; Wang, S.; Heeger, A. J.; Bazan, G. C. *J. Am. Chem. Soc.* **2001**, *123*, 6417.

66 Wang, D. L.; Wang, J.; Moses, D.; Bazan; G. C.; Heeger, A. J. *Langmuir* **2001**, *17*, 1262.

67 Wang, J.; Wang, D. L.; Miller, E. K.; Moses, D.; Bazan; G. C.; Heeger, A. J. *Macromolecules* **2000**, *33*, 5153.

68 Jones, R. M.; Bergstedt, T. S.; McBranch, D. W.; Whitten, D. G. *J. Am. Chem. Soc.* **2001**, *123*, 6726.

69 Chen, L.; McBranch, D.; Wang, R.; Whitten, D. G. *Chem. Phys. Lett.* **2000**, *330*,

27.

70 Chen, L.; Xu, S.; McBranch, D.; Whitten, D. G. *J. Am. Chem. Soc.* **2000**, *122*, 9302.

71 Stork, M.; Gaylord, B. S.; Heeger, A. J.; Bazan, G. C. *Adv. Mater.* **2002**, *14*, 361.

72 Tan, C.; Mauricio, R. P.; Schanze, K. S. *Chem. Commun.* **2002**, 446.

73 Harrison, B. S.; Ramey, M. B.; Reynolds, J. R.; Schanze, K. S. *J. Am. Chem. Soc.* **2000**, *122*, 8561.

CHAPTER TWO

Synthesis, Characterization, and Fluorescence Quenching of Novel Cationic Phenyl-Substituted Poly(*p*-phenylenevinylene)s

2.1 Introduction

Water-soluble conjugated polymers (WSCPs) have attracted increasing attention recently due to their versatile applications in optoelectronic[1-3] and biological research.[4] To endow conjugated polymers with water solubility, hydrophilic substituents such as quaternized ammonium, carboxylate or sulfonate must exist on the polymer backbone which produce conjugated polyelectrolytes. The optical and electronic properties of WSCPs can be easily tuned by designing the conjugated structure of the polymer main chain. Furthermore, the ionic functionality was also found to be useful in the construction of interesting supramolecular structures with electronic activity.[5-8]

Envisioned applications of WSCPs include optoelectronic devices fabricated through layer-by-layer self-assembly,[9] ink-jet printing[10] or screen printing techniques.[11] These new film deposition techniques may be promising in producing large area multilayer assemblies in a low-cost way. For example, Yang et al. developed blue and orange-red dual-color polymeric light-emitting pixels via hybrid ink-jet printing method (HIJP).[12] Rubner et al. reported sequentially adsorbed multilayer devices through layer-by-layer processing technique based on blue-light emitting polycation- and polyanion-type conjugated polymers.[2] The same strategy was also employed to study the Förster energy transfer between conjugated polymers of different band-gaps.[13] Another reason

for the current growing interest in these water-based techniques is to avoid the unfavorable interdiffusion or erosion between neighboring layers encountered in the organic solvent-based fabrication processes.[14] It is important to note, however, that polymers with red, green, and blue emission are required to obtain full-color displays. Water-soluble poly(*p*-phenylene) (PPP)[15-17] and poly(*p*-phenylenevinylene) (PPV)[18, 19] which are blue and red light-emitting materials respectively, have been investigated, while the preparation of water-soluble polymers with green emission is still a challenge.

Recently, WSCPs have also been found potential applications as high-sensitive biosensors which exhibit rapid and collective response to relatively small perturbations in local environment.[20] It has been shown that a low concentration of quencher is sufficient to extinguish the fluorescence from the conjugated segments through electron transfer or energy transfer due to facile energy migration along the conjugated backbone and relatively strong binding of the quencher with WSCPs. Although such an amplified quenching has been achieved by using a few WSCPs including water-soluble PPV[21] and PPP[22] systems, the influence of the physical and chemical properties of these WSCPs such as chemical structures, fluorescent quantum efficiencies, and emission wavelength on the quenching sensitivity is still a major concern. Therefore, it is crucial to develop novel WSCPs to evaluate a variety of polymer compositions for obtaining optimized sensory materials.

In this paper, we report our successful effort in synthesizing a new series of water-soluble green light-emitting polymers, which should shed some light on

problems raised above. Phenyl-substituted PPV derivatives are desired as they have proven to exhibit highly efficient green fluorescence and enhanced photostability due to the steric hindrance of the bulky phenyl groups which minimize the interchain interactions.[23-25] We are also very interested in cationic WSCPs because such system is less studied[17b, 21g, 26] than the anionic counterparts in optoelectronic devices and sensors. Therefore, novel phenyl-substituted PPVs with tertiary amine functionality were prepared by using either Gilch or Wittig reactions. Water-solubility was rendered to these materials via post-quaterization on the neutral precursors with bromoethane. Besides, the water solubility was further studied through adjusting the hydrophilicity of the substituents. The optical and thermal properties of these novel water-soluble phenyl-substituted PPVs were characterized. The quenching behavior with an inorganic compound was also investigated. Preliminary results indicate that these materials offer promising opportunities in optoelectronic and sensory applications.

2.2 Molecular Design

In order to synthesize the cationic water-soluble polymers, tertiary amine as the functional group was designed for the neutral polymer, which upon quaternization with bromoethane, could afford water-soluble green-light emitting polymers. Those PPVs which could emit pure green light generally contain phenyl-substituted or silicon-substituted groups on the side chains. In this paper, introducing amino-terminated group into the side chain of the phenyl-substituted PPVs is my final choice to synthesize the target water-soluble polymers. The chemical structures of one

designed neutral polymer **P1** is illustrated in **Figure 2.1**.

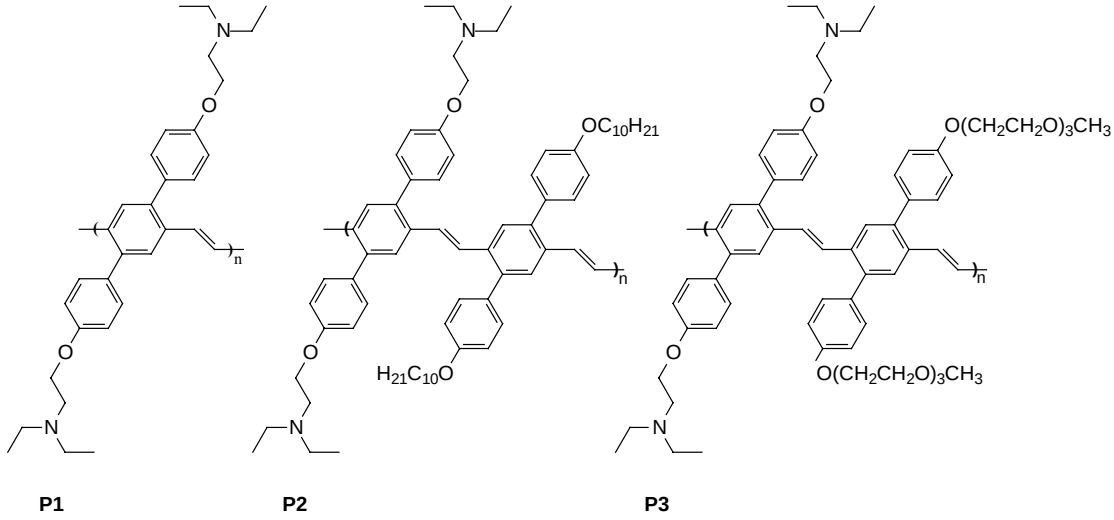

Figure 2.1 The designed neutral polymers for the green light emitting cationic polymers

It may bring about a big problem that the designed neutral polymer may not be able to dissolved in common organic solvents which results from the short alkyloxy group on the side chain. The possible poor solubility will make the post-quaternization very difficult. To prevent the occurring of the problem, we designed the other two polymers with long flexible side chains which may improve the corresponding solubility (**P2** and **P3** in **Figure 2.1**).

2.3 Synthesis and Characterization

2.3.1 Materials

All chemical reagents used were purchased from Aldrich Chemical Co. THF was purified by distillation from sodium in the presence of benzophenone. Other organic solvents were used without any further purification. Thionyl chloride was distilled

prior to use.

2.3.2 Characterization Methods

The NMR spectra were collected on a Bruker Advance 400 spectrometer with tetramethylsilane as the internal standard. FT-IR spectra were recorded on a Bio-Rad FTS 165 spectrometer by dispersing samples in KBr. Mass spectra (MS) were obtained using a micromass VG 7035E mass spectrometer at an ionizing voltage of 70 eV. UV-vis spectra were recorded on a Shimadzu 3101 PC spectrometer. The concentrations of copolymer solutions were adjusted to about 0.01 mg/mL or less. Fluorescence measurement was carried out on a Perkin-Elmer LS 50B photoluminescence spectrometer with a xenon lamp as a light source. TGA measurements were performed on a TA Instruments Hi-Res TGA 2950 Thermogravimetric Analyzer at a heating rate of 10 °C/min under N_2. Elemental microanalyses were carried out by the Microanalysis Laboratory of the National University of Singapore. Gel permeation chromatography (GPC) analysis was conducted with a Waters 2690 separation module equipped with a Waters 2410 differential refractometer HPLC system and three 5 μm Waters Styragel columns (pore size: 10^3, 10^4 and 10^5 Å) in series, using polystyrenes as the standard and tetrahydrofuran (THF) as the eluant at a flow rate of 1.0 mL/min and 35 °C.

The quenching behavior was studied by comparing the fluorescence intensities of polymer aqueous solutions in the presence of quenchers with different concentrations. The Milli-Q water used in preparing the aqueous solutions of those polymers and

quenchers was purged with nitrogen for 4 h before using.

2.4 Results and Discussion

2.4.1 Synthesis of Monomers and polymers

The preparation of monomers was shown in **Schemes 2.1** and **2.2**. Compound **3** was prepared from 2,5-dibromo-*p*-xylene according to the following reaction sequences: free-radical bromination with NBS, esterification, hydrolysis and protection of hydroxy groups with DHP. Compound **4** was prepared from 4-bromophenol by Williamson ether reaction with 2-chlorotriethylamine hydrochloride in refluxing acetone. Palladium-catalyzed aryl-aryl coupling between compounds **3** and **4** afforded compound **5** as white crystals, which was converted to the key monomer **1,** 2,5-bis[4'-2-(*N,N*-diethylamino)ethoxyphenyl]-1,4-bis(chloromethyl)benzene dihydrochloride, through acid-assisted deprotection and chlorification with thionyl chloride. It is worth noting that the tertiary amine groups must be protected with chloric acid before the formation of monomer **1** to prevent the self-quaternization with benzylchloride groups.[27] Monomer **2** was then obtained from monomer **1** by reaction with PPh_3. Monomers **3** and **4** were prepared in a similar way from compounds **7** and **13** respectively through consecutive NBS bromination, esterification, hydrolysis, and PCC oxidation. Compounds **7** and **13** were both obtained via Grignard coupling reaction. However, for compound **7,** a decyloxy group was introduced before the coupling reaction while the tri(ethylene glycol)methyl ether functionality was introduced for compound **13** after the coupling reaction.

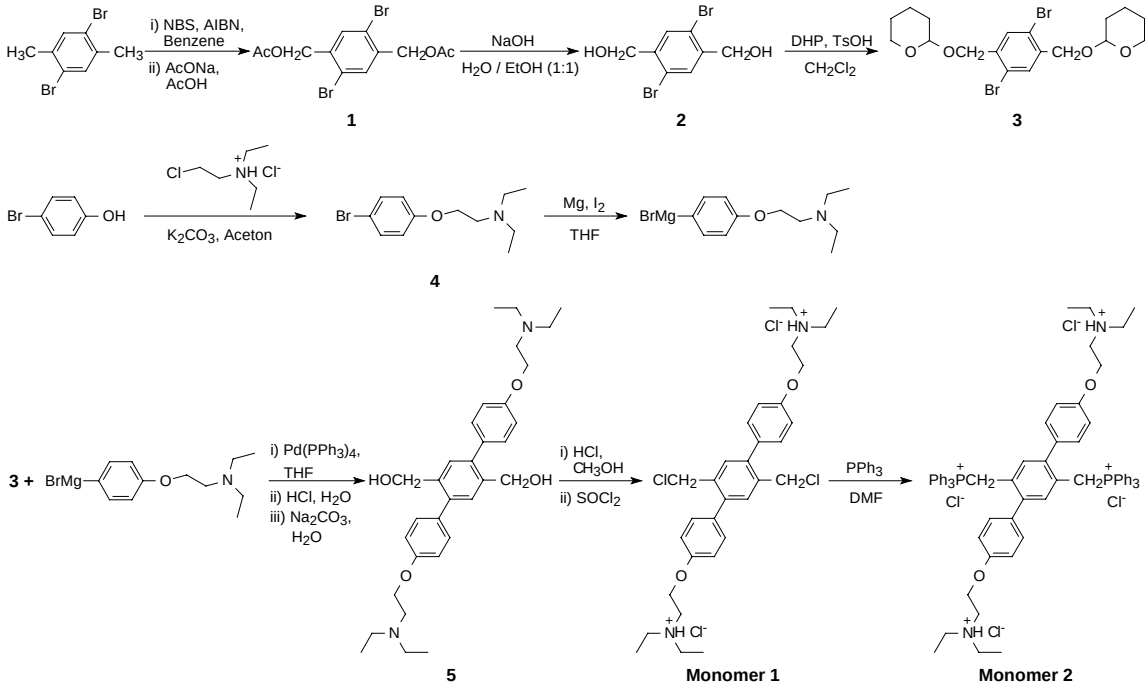

Scheme 2.1 Synthetic Routes for Monomers 1 and 2

Syntheses of the polymers were outlined in **Scheme 2.3**. **P1** was obtained through the general Gilch reaction that proceeded in THF solution under the injection of excess BuOK solution in THF (1M) accompanied with vigorous stirring at room temperature for one day. **P2** and **P3** were synthesized via Wittig reaction that proceeded in a mixture of chloroform and ethanol (1:1) under the injection of excess C_2H_5ONa solution in ethanol (1M) under vigorous stirring at room temperature for one day. Conversion of the neutral polymers to the final cationic polymers was achieved by treating them with bromoethane in dimethyl sulfoxide (DMSO) and tetrahydrofuran (THF) (1:4) by stirring at 50 ^{o}C for 5 days. Such a post-quaterization approach has the advantage that the neutral polymers, **P2** and **P3** here, can be purified easily and characterized clearly.[17b]

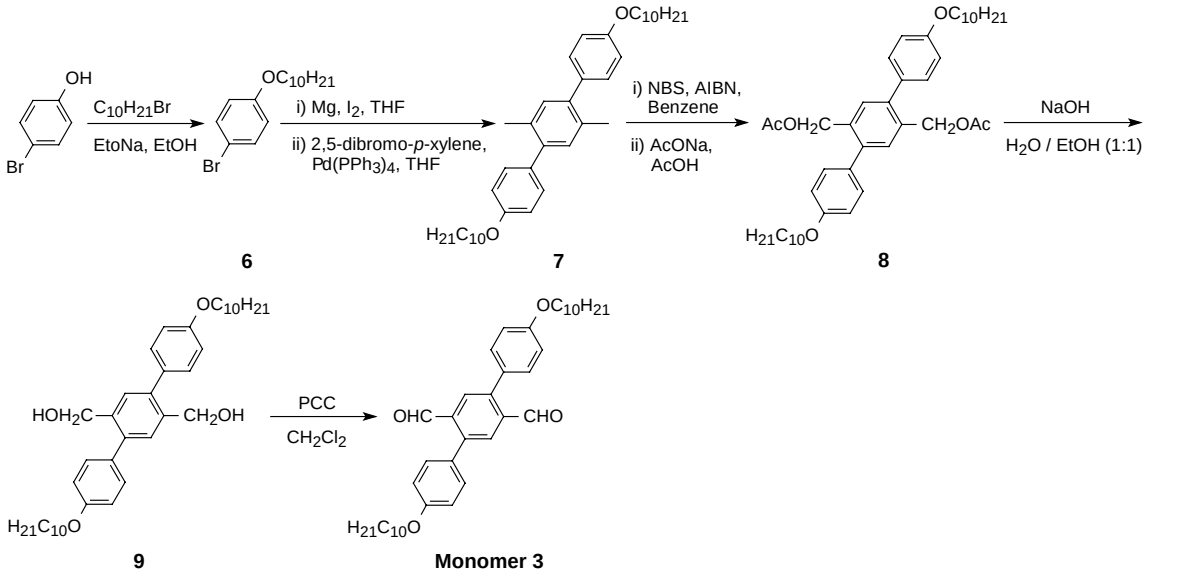

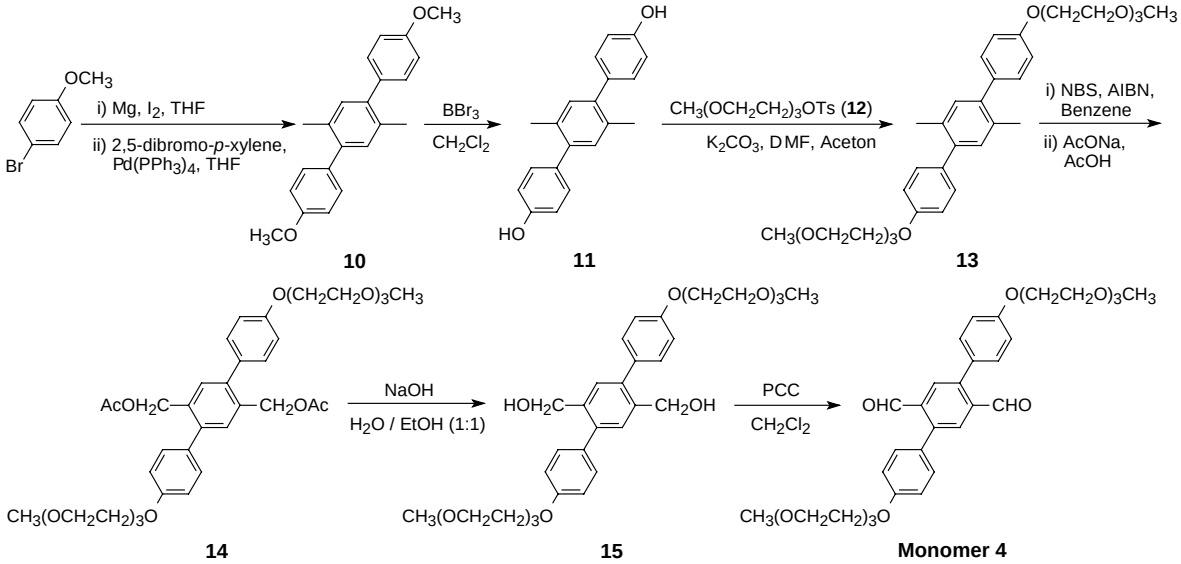

Scheme 2.2 Synthetic Routes for Monomers 3 and 4

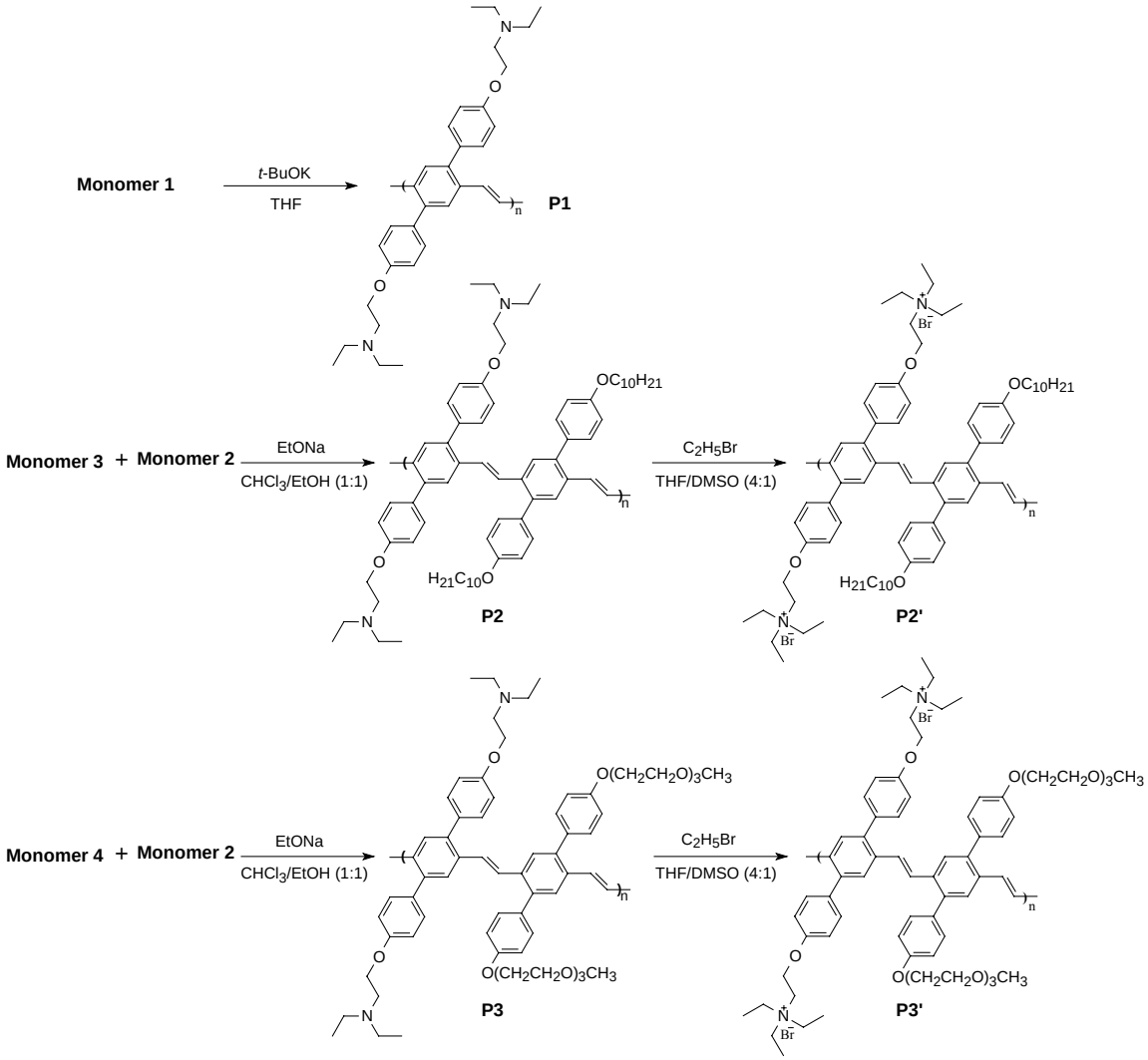

Scheme 2.3 Synthetic Routes for the Polymers

2.4.2 Solubility Studies

Although with tertiary amine side chains, **P1** was quickly precipitated in the potassium *tert*-butoxide-THF system during the Gilch reaction. The obtained bright yellow powder could not be dissolved in common solvents such as THF and $CHCl_3$, indicating that the tertiary amine side chains are not longer enough to make such rigid phenyl-substituted PPV soluble, although it appeared to be a little swelled in $CHCl_3$. Therefore, preparation of quaternized **P1** is impossible through post-quaternization due

to its insolubility. In an attempt to improve the solubility, **P2** and **P3** with longer flexible side chains were designed. To compare the effect of hydrophilicity of the side chains on water solubility of the polymers, decyloxy or tri(ethylene glycol)methyl ether groups were employed. Both **P2** and **P3** showed excellent solubility in common organic solvents such as THF and $CHCl_3$, but they were insoluble in polar ones such as DMSO, CH_3OH and H_2O. Quaternization of neutral **P2** and **P3** was thus performed in THF/DMSO (4:1) mixtures. The obtained **P2'** and **P3'** could be dissolved in DMSO, DMF, and CH_3OH, indicating enhanced polarity due to quaterization. In addition, while **P2'** was completely insoluble in water, **P3'** could be successfully dissolved in warm water at 50 ^{o}C and no precipitate was observed at room temperature even after standing still for three months, showing that a relatively stable aqueous solution was formed. Based on the above observation, it was suggested that the use of hydrophilic functionality such as tri(ethylene glycol)methyl ether groups as the side chains be crucial in obtaining intrinsically water-soluble conjugated polymers with an alternating substitution pattern.

The intractable **P1**, however, could be soluble in some polar solvents including $CHCl_3$, MeOH, and water by adding organic acid (1 M) such as acetic acid. Such an interesting phenomenon of acid-assisted solubility exhibited in many solvents for amine-functionalized conjugated polymers as described in our previous work,[26b] which may be attributed to relatively strong intermolecular interactions between the polymer and the acid introduced. In addition, it was also found that such a polymer/acid "complex" was unstable in vacuum. For example, when **P1** in acetic acid-$CHCl_3$

solution was precipitated in hexane and dried in vacuum at 60 ^{o}C for three days, the resulting solid could not be dissolved in $CHCl_3$ any more unless acetic acid was re-added. FT-IR spectrum of such **P1** precipitate was the same as that of pristine **P1** in which no carboxyl absorption attributable to acetic acid appeared at about 1680 cm^{-1}, indicating completely removal of the acid from the "complex". It is well known that conjugated polymers with similar solubility are unsuitable for construction of a multilayer light-emitting diode due to the unfavorable damage of the polymer-polymer interface which may influence the quantum efficiency of the device. Therefore, the versatile acid-assisted and interesting reversible solubility for **P1** may find applications in fabricating multiplayer optoelectronic devices through a spin-coating approach.

2.4.3 FT-IR Analysis

Infrared spectra for all polymers were shown in **Figure 2.2**. As the structure difference among **P1**-**P3** only lies in the different side chains attached to the phenylene rings, IR spectra of these polymers were similar to each other. It can be seen that a weak absorption, which can be attributed to the aldehyde end groups for **P2** and **P3**, occurs at 1680 cm^{-1}, indicating incomplete intermolecular condensation.

Interestingly, it was also found that the ratio of *trans*-CH=CH (~975 cm^{-1}) group to *cis*-CH=CH (~875 cm^{-1}) group in the IR spectrum of **P1** was rather different from that of **P2** and **P3**. A weak absorption peaked at 975 cm^{-1} was clearly visible for **P1** while no signals could be found at 875 cm^{-1}, indicating that **P1** predominantly contains *trans*-CH=CH group under Gilch conditions. On the contrary, a high ratio of

cis-CH=CH group to *trans*-CH=CH was observed based on the IR measurements for **P2** and **P3** which were obtained through Wittig reaction. Therefore, it is concluded that Gilch reaction is more suitable for developing polymers with regular molecular configurations than Wittig reaction. However, the ratio of *trans*- vs *cis*-configuration cannot be determined by FT-IR spectrum, which will be discussed in the next section.

Upon quaternization, all the quaternized polymers showed some spectral modifications due to new substitutents formed while the spectral features of the intact structures in the polymers remained unchanged in the FT-IR spectra. Besides, a broad and strong self-associated absorption peak of water at 3400 cm^{-1} can be observed, which reflects strong hydrophilicity of the resulting quaternized polymers.

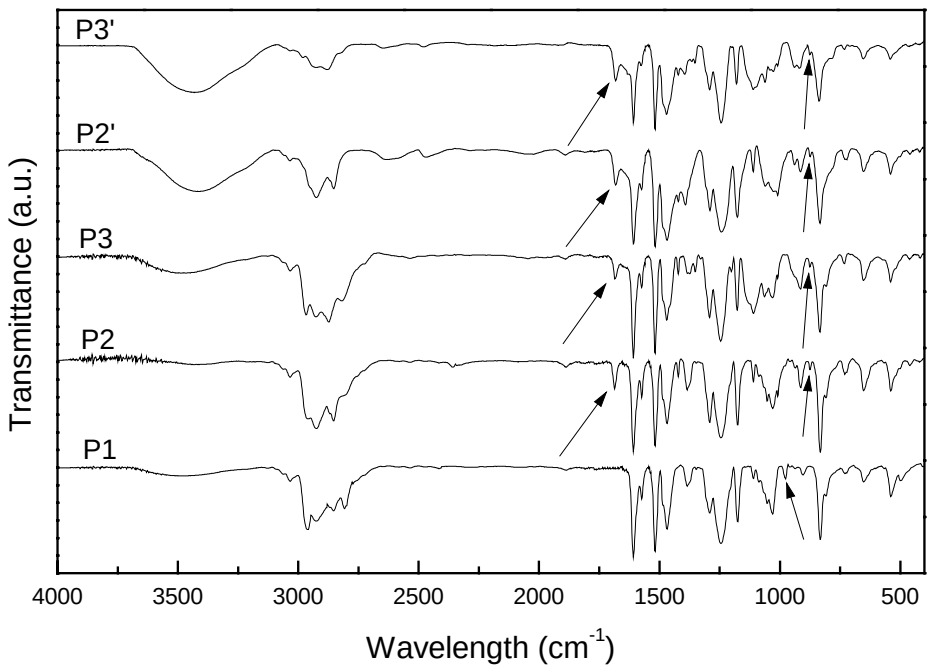

Figure 2.2 FT-IR spectra of the neutral and quaternized Ph-PPVs

2.4.4 NMR Analysis

^{1}H NMR spectra of all the neutral and quaternized polymers were shown in **Figure 2.3**. Integration ratios of the end aldehyde protons (10.01 ppm) to the -OCH$_2$C*H*$_2$N- protons for **P2** and **P3** (3.00-2.76 ppm) were found to be about 1/30 and 1/32 respectively, corresponding to 15 and 16 phenyl rings in the backbone respectively. These results are in good agreement with those measured by GPC (**Table 2.1**). Our FT-IR analysis showed that **P1** adopted predominantly *trans*-CH=CH configuration while for **P2** and **P3**, a high content of *cis*-CH=CH groups was present. Such a result was also substantiated by ^{1}H NMR measurements. The ^{1}H NMR spectrum of **P1** was rather simple compared with **P2** and **P3**, indicating a more regular structure for **P1**. Based on the spectral simplicity for **P1** as well as the structural similarity among **P1**, **P2**, and **P3**, it is easy to realize that there were two groups of resonances for the protons of **P2** and **P3**, in which the downfield and upfield ones caused by the *trans*- and *cis*-configurations respectively.[28] Although the *cis*- and *trans*-vinyl protons can be observed at 6.50 ppm and 7.36 ppm respectively with the former to be much more intensive, the ratios of *cis*- to *trans*-vinylic groups were determined by comparing the relative integrations of the *cis*-C*H*=C*H* resonance at 6.50 ppm with the -OCH$_2$C*H*$_2$N- resonance between 3.00 ppm and 2.78 ppm. As a result, the contents of *cis*-configurations for **P2** and **P3** were calculated to be 80 % and 81% respectively. It is well known that in normal Wittig reactions both *trans*- and *cis*-vinyl are formed. Such high values of *cis*-configuration in the present work may be related to the steric effect due to bulky phenylene substitutents which may also affect the main chain

conformations of such PPV-type polymers.

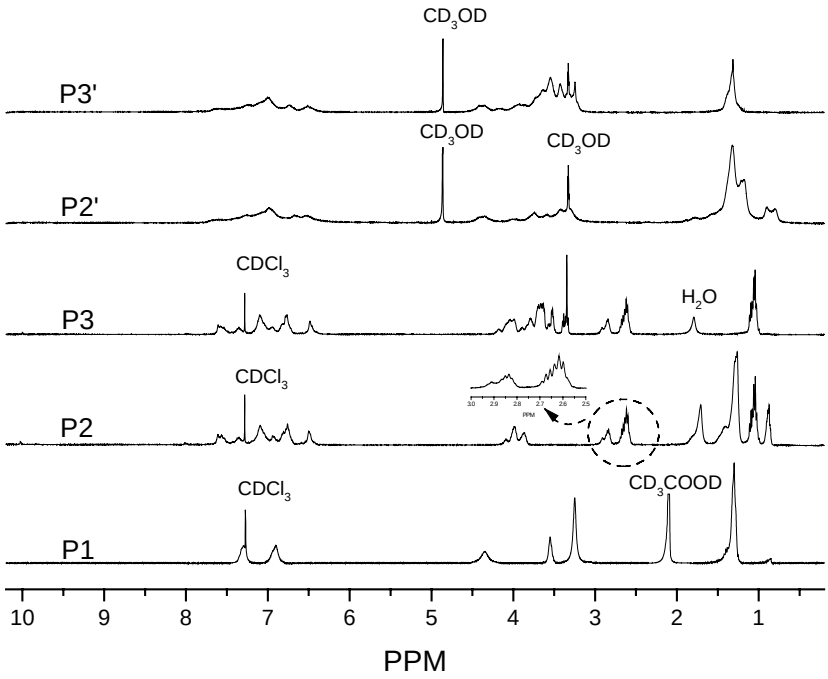

Figure 2.3 ^{1}H NMR spectra of the neutral and quaternized Ph-PPVs

Quaternization with bromoethane led to broadened proton peaks, some of which could not be identified. It can be seen in **Figure 2.3**, however, that the aromatic protons of the quaternized polymers resonance at the same chemical shifts compared with those of the corresponding neutral ones, whereas **P2'** and **P3'** exhibit spectra in which all the signals from -OCH_2CH_2N-, -NCH_2CH_3 and –NCH_2CH_3 groups are downshifted. The quaternization degrees (QD) could be determined from the ^{1}H NMR spectra by comparing the relative integrations of the aromatic peaks at 6.0-8.0 ppm (total aromatic and vinyl protons) with that of 0.5-2.0 ppm (total alkyl protons for –$OCH_2C_9H_{19}$ and –NCH_2CH_3 in **P2'** or –NCH_2CH_3 in **P3'**).[29] As a result, the QDs of **P2'** and **P3'** were calculated to be about 90% and 85% respectively, which were close

to the results from elemental analysis.

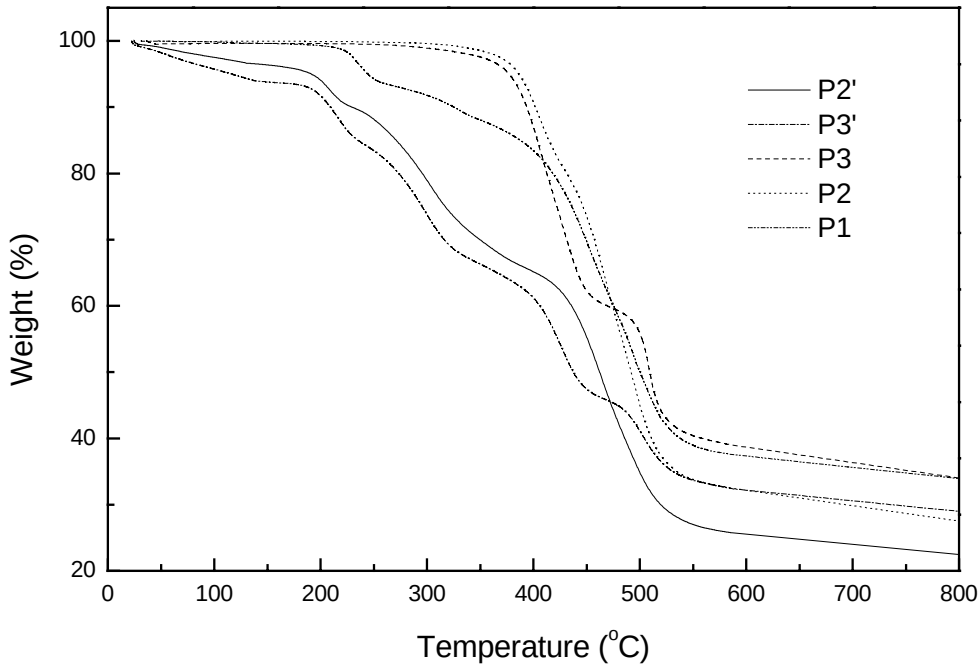

Figure 2.4 Thermalgravimetric analysis of the neutral and quaternized Ph-PPVs

2.4.5 Thermal Stability

Thermal properties of the polymers were studied by thermogravimetric analysis (TGA) under nitrogen atmosphere. The thermograms in **Figure 2.4** showed that the neutral polymers **P2** and **P3** exhibited good thermal stability with a weight loss of 3% at 340 ^{o}C. However, **P1** gave an initial degradation at 220 ^{o}C, which is considerable lower than those of **P2** and **P3**. Such a decrease of thermostability for **P1** may be attributed to the molecular impurities encapsulated by **P1** when it was precipitated from the reaction mixture. For the quaternized samples, the degradation onsets for **P2'** and **P3'** decreased to 200 ^{o}C with the initial weight loss deriving from associated water. This

variation can be explained by the lower stability of ethyl bromide than that of the other alkoxy side chains.[17b] The relatively high thermostabilitiy thus renders these polymers good candidates in light-emitting diodes and fluorescent sensor uses.

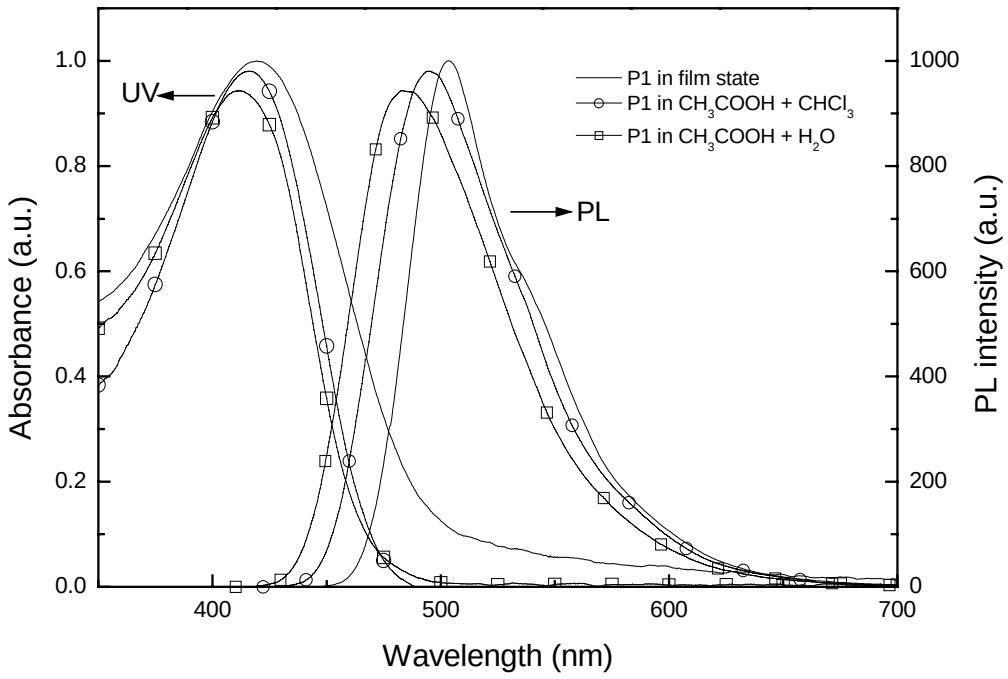

Figure 2.5 UV-vis absorption and PL emission spectra of P1 in acetic acid $CHCl_3$ solution (1 M), in acetic acid aqueous solution (1 M) and as films

2.4.6 Optical Properties

The optical properties of **P1** were investigated and the absorption and emission spectra in $CHCl_3$ or H_2O containing acetic acid (1M) and as film were shown in **Figure 2.5**. It was found that both of the absorption and emission spectra in $CHCl_3$ are more red-shifted than those in H_2O. Although the spectral changes in different solvents may result from the solvatochromism due to the polarity of the solvents, the observed bathochromic shift in $CHCl_3$ is unlikely caused by the stabilization of the ground state

as well as the excited state by the solvent based on the fact that $CHCl_3$ is less polar than water which would lead to a hypochromic shift in the spectra. It should be more reasonable to consider the different molecular conformation of the polymer in different solvents. It has been reported that the conformation of MEH-PPV varies from extended to coiled ones depending on the quality of the solvents.[30, 31] Accordingly, we performed ^{1}H NMR experiment for **P1** in $CDCl_3$ and D_2O respectively, both of which contained a small amount of acetic acid-d_4. While the proton signals obtained in $CDCl_3$ are clearly distinguishable, those in D_2O cannot be observed even when the number of scans was 10,000. It is generally accepted that decrease of solvent quality causes a corresponding reduction of magnetic resonance signature. Therefore, we believe that H_2O is a poor solvent and **P1** tends to be less solvated. The hypochromic shift of **P1** found in H_2O is consistent with the reduced solvent quality, indicating a coiled molecular conformation which causes a shorter average conjugation length.[30, 31] In addition, fluorescence quantum efficiencies (Φ_f) were also measured and the findings showed that **P1** gave a lower Φ_f of 18% in H_2O than that in $CHCl_3$ (52%). To examine the possible contribution of aggregation effects to that decrease, the absorption and emission spectra of **P1** as film (spin-cast from $CHCl_3$ solution) were studied, both of which (420 nm and 505 nm respectively) presented slightly red-shifted spectral maxima as compared with those in solutions. There is no evidence showing the formation of interchain dimmers or excimers. Φ_f of this film (51%) was found to be comparable with that in solution (52%). Based on the above observations, intermolecular aggregation should play a less important role in the lower fluorescence yield of **P1** in

water, although it may exist. Therefore, such a decrease in Φ_f may also be explained by the coiled molecular structure of the polymer backbone which contains a lot of torsional defects.[30]

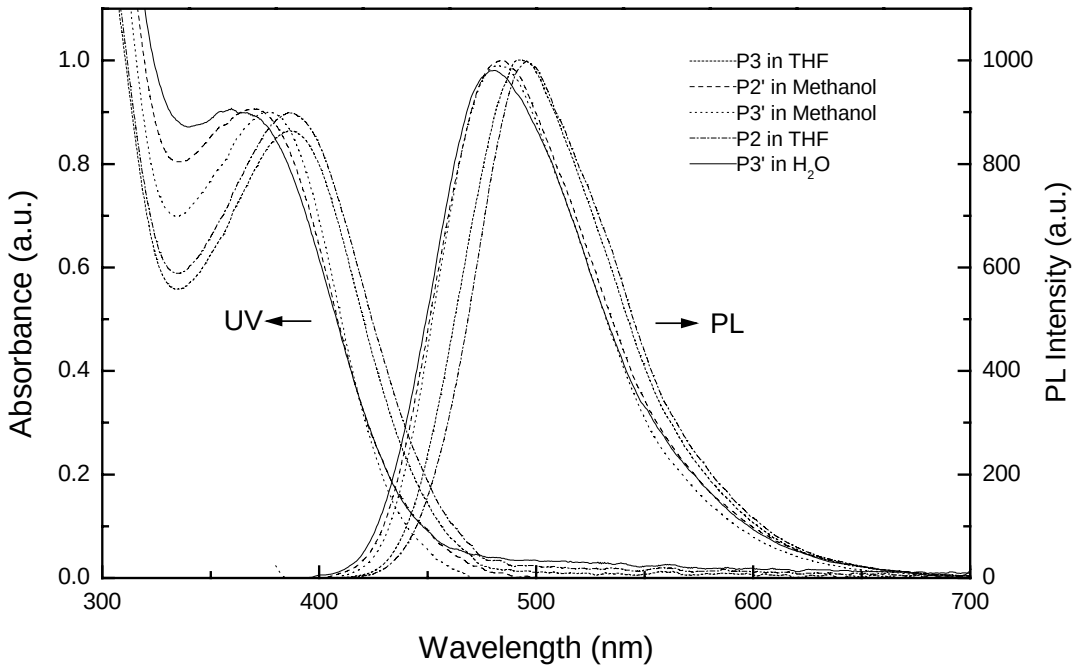

Figure 2.6 UV-vis absorption and PL emission spectra of P2 and P3 in THF, P2' and P3' in methanol and P3' in water

The UV-vis absorption and photoluminescence (PL) spectra of the neutral and quaternized polymers **P2**, **P3**, **P2'**, and **P3'** in solution were depicted in **Figure 2.6**. The same absorption maxima at 387 nm and emission maxima at 494 nm exhibited by both **P2** and **P3** imply that the electronic properties of these phenyl-substituted polymers are predominantly determined by the rigid PPV main-chain while those flexible chains play a minor role. The absorption maxima of the neutral polymers **P2** and **P3** in solution blue-shifted considerably as compared with that of *trans*-type

poly{2-(4'-decyloxyphenyl)-1,4-phenylenevinylene (DOP-PPV) (410 nm),[32] which is in agreement with the high content of *cis*-vinyl bonds in **P2** and **P3** with reduced effective conjugation length.

Table 2.1 GPC and Spectroscopic Data for Ph-PPVs

	GPC			absorbance		fluorescence			
				in solution	as film	in solution		film	
polymer	M_n[a]	M_w[a]	PDI[a]	$\lambda_{max\ (nm)}$	$\lambda_{max\ (nm)}$	$\lambda_{max\ (nm)}$	Φ_{pl}	$\lambda_{max\ (nm)}$	Φ_{pl}
P1	—	—	—	416[b]	420	494[b]	0.52	505	0.51
P1	—	—	—	412[c]	—	483[c]	0.18	—	—
P2	8600	12 000	1.40	387[d]	387	495[d]	0.51	507	0.58
P3	8200	10 600	1.29	387[d]	389	493[d]	0.51	505	0.56
P2'	—	—	—	370[e]	380	483[e]	0.28	496	0.17
P3'	—	—	—	377[e]	380	483[e]	0.25	495	0.13
P3'	—	—	—	368[f]	—	481[f]	0.15	—	—

[a] M_n, M_w and PDI of the polymers were determined by gel permeation chromatography using polystyrene standards. [b] The values listed were measured in acetic acid-$CHCl_3$ solution (1 M), [c] in acetic acid-H_2O solution (1 M), [d] in THF, [e] in methanol, and [f] in water, respectively. The Φ_f values of those polymers in solutions were measured using the quinine sulfate solution (ca. 1.0×10^{-5} M) in 0.10 M H_2SO_4 (Φ_f = 55%) as a standard. The Φ_f values of those polymers as films were measured using diphenylanthracene (dispersed in PMMA film with a concentration less than 10^{-3} M, assuming Φ_f = 81%) as a standard.

Quaternization was found to create more obvious blue-shifted absorption and fluorescence spectra and result in decreased Φ_f for **P2'** and **P3'** as shown in **Figure 2.6** and **Table 2.1**. Such a blue-shift, attributable to the mutual electrostatic repulsion of positive charges pendent on the alternating benzene rings which leads to an increased torsion of the conjugated main chain and a decreased effective conjugation length,[17b, 26b] was observed in other quaternized systems. We also found that qaternization resulted in reduced Φ_f of **P2'** and **P3'** which may be caused by the torsion induced quenching as the planarization in the excited state is impeded.[33] ^{1}H NMR measurement showed that water is a poorer solvent for **P3'** than methanol. As a result, the

blue-shifted electronic spectra and decreased Φ_f exhibited by **P3'** in water as compared with those measured in methanol suggested the more coiled structure adopted in water as we discussed for P1. We will demonstrate later that intermolecular aggregation may not contribute so much to such a decrease.

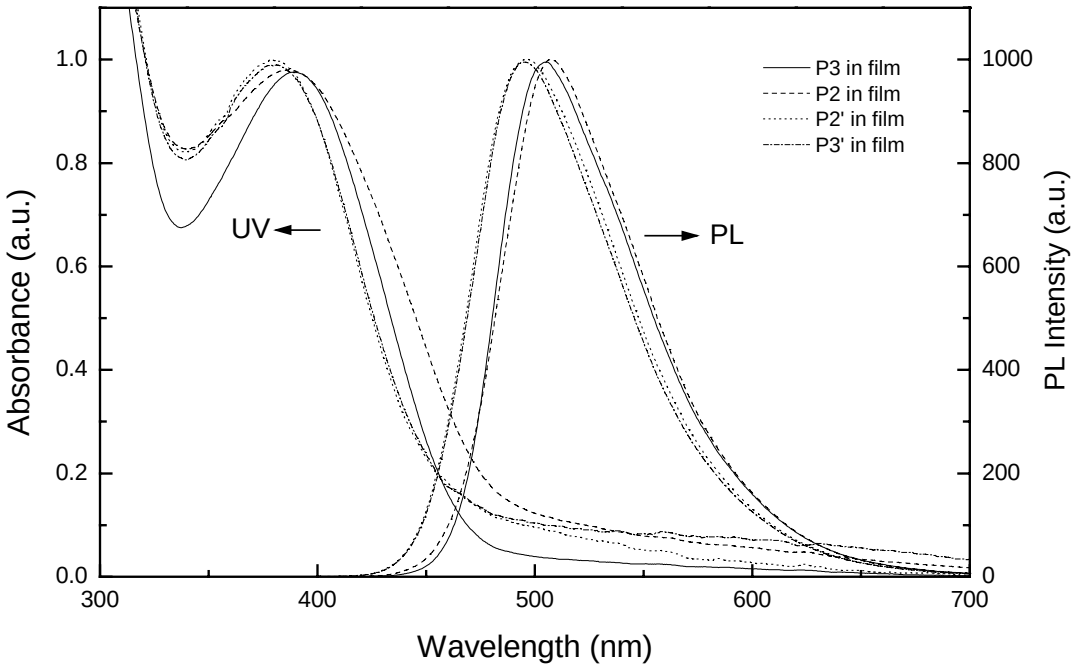

Figure 2.7 UV-vis absorption and PL emission spectra of P2, P3, P2' and P3' as films

When the absorption and emission spectra of these polymers as films were investigated, blue-shifted spectral maxima as shown in **Figure 2.7** were observed for quaternized polymers as compared with their respective precursors. This indicates that the modified conformation of the quaternized polymers in solution was maintained in their respective films. In addition, almost the same spectral features and Φ_f exhibited by the neutral polymers in both solution and the solid state suggest that the formation of

interchain dimmers and eximers is negligible due to the steric effect of the two phenyl rings and the strong intermolecular electrostatic repulsion as films. Therefore, although intermolecular aggregation (association) was observed with a few WSCPs in water,[34] such interchain interactions do not cause significant decrease in fluorescence yield in our systems.

2.4.7 Fluorescent Quenching of P3'

One promising application of WSCPs is for chemo- or biosensors due to their fluorescent superquenching by traces of analytes. The quenching of fluorescence generally includes static quenching and dynamic quenching. Each quenching behavior can be simply described by the Stern-Volmer equation[35]:

$$F_0/F = 1 + K_{sv}[Q] \quad (1)$$

In this equation, F_0 is the fluorescence intensity with no quencher present, F is the fluorescence intensity with quencher present, [Q] is the quencher concentration and K_{sv} is the Stern-Volmer constant. Both dynamic and static quenching follow linear Stern-Volmer plot (F_0/F~[Q]). However, if the dynamic quenching and static quenching exist simultaneously, Equation 1 must be modified and the plot shows an upward curve[35]:

$$F_0/F = (1 + K_{sv}^{S}[Q])(1 + K_{sv}^{D}[Q]) \quad (2)$$

where K_{sv}^{S} is the static quenching constant and K_{sv}^{D} is the dynamic quenching constant. Previously, both the linear and upward Stern-Volmer curves were observed with WSCPs.[20, 21c, 21d, 22]

As a cationic WCPS, **P3'** was employed to detect anionic analyte, $Fe(CN)_6^{4-}$, to study its sensing behavior. $Fe(CN)_6^{4-}$ has been used to investigate a cationic PPP polymer[22] as a quencher, of which both the energy transfer and photo-induced electron transfer processes may be involved in the quenching mechanism, depending on the type of the chromophores. **Figure 2.8** shows the Stern-Volmer plot for **P3'** with $Fe(CN)_6^{4-}$ as the quencher. It can be seen that an intriguing downward Stern-Volmer curve was observed, which has never been reported with fluorescent WSCPs. Therefore, it is reasonable to believe that some other influencing factors may work.

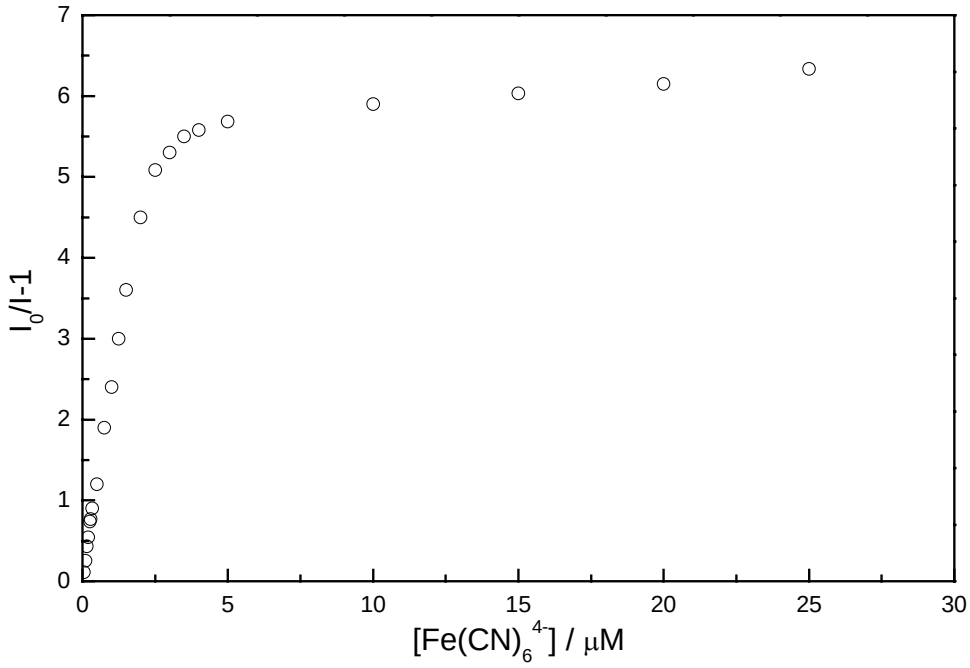

Figure 2.8 Unmodified Stern-Volmer plot of P3' (1.25 μM) quenched by $Fe(CN)_6^{4-}$

Such a downward Stern-Volmer plot was observed during the study of fluorescent quenching of tryptophan in proteins using iodide and explained by the existence of two populations of fluorophores, and one of which is inaccessible to the quencher.[36]

Therefore, with the introduction of a quencher, only those accessible fluorophores are quenched while the fluorescence from the inaccessible ones remains. Based on the above assumption, a quantitative expression was given to describe the relation between the fluorescence intensity and quencher concentration[37]:

$$F_0/(F_0 - F) = 1/(f_a K_{sv}[Q]) + 1/f_a \quad (3a)$$

$$f_a = F_{0a}/(F_{0a} + F_{0b}) \quad (3b)$$

where F_{0a} is the fluorescence intensity from an accessible fluorophore, F_{0b} is the fluorescence intensity from an inaccessible fluorophore and f_a is the fraction of fluorescence from an accessible fluorophore.

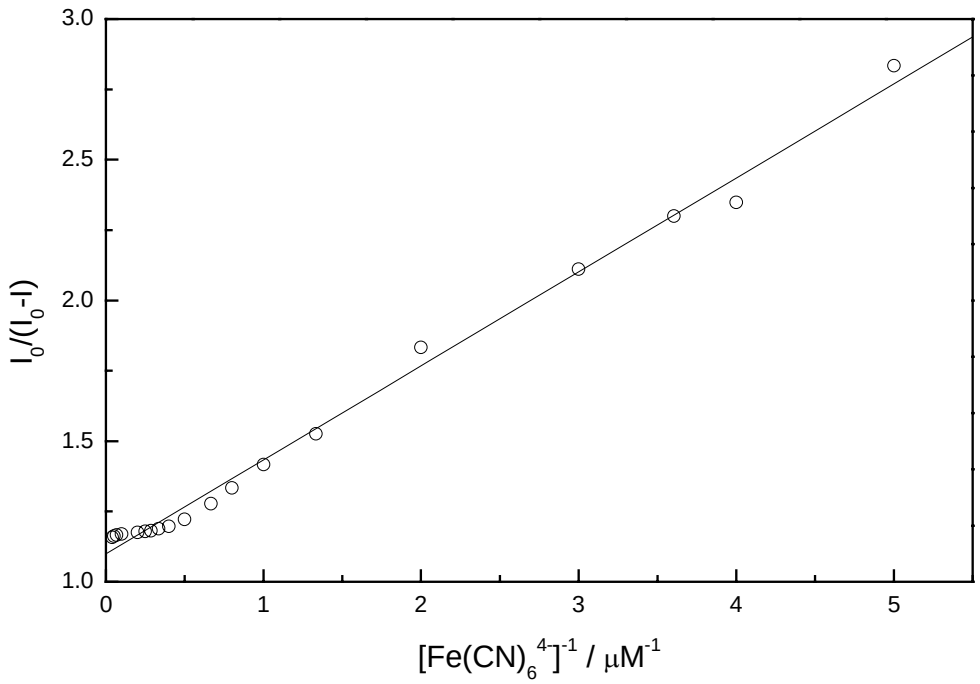

Figure 2.9 Modified Stern-Volmer plot for the system in Figure 2.8

The modified Stern-Volmer plot for **P3'** according to equation 3a was shown in **Figure 2.9** and a linear dependence of $F_0/(F_0 - F)$ on $1/[Fe(CN)_6^{4-}]$ can be observed. Based on the intercept and the slope, $f_a = 0.91$ and $K_{sv} = 3.3 \times 10^6$ M^{-1} were obtained. Such a

value of K_{sv} did indicate an efficient fluorescence quenching of **P3'** which was bound with the quencher through static electronic interaction. Approximately 7-8 phenyl rings in the polymer backbone per quencher can also be estimated, which corresponds to almost one polymer chain per two quenchers.[38] 9% of the inaccessible fluorophore might result from the proposed twisted and coiled backbone conformation and possible intermolecular aggregation due to poor solvent quality.

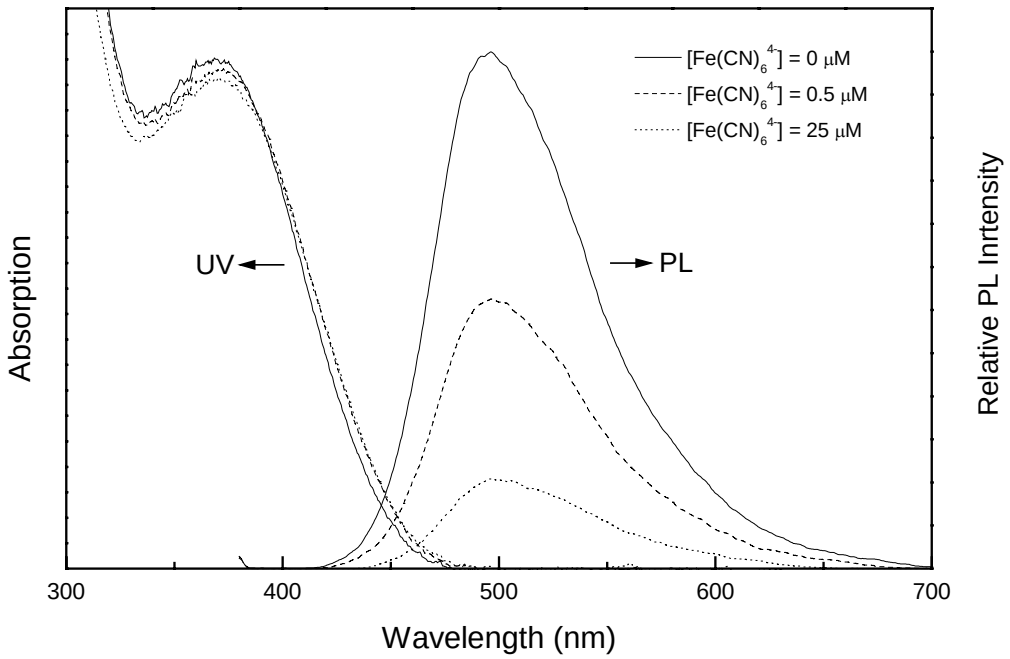

Figure 2.10 UV-vis absorption and PL emission spectra of P3' (1.25 μM) in the absence and presence of $Fe(CN)_6^{4-}$

It is important to note that additions of multivalent cations may tend to increase the aggregation resulting in interchain quenching.[20, 21d] However, as discussed earlier, such an additional aggregation does not significantly affect the quantum efficiency of **P3'** due to the bulky phenylene substituents. In addition, both absorption and emission

spectra for **P3'** obtained with the addition of $Fe(CN)_6^{4-}$ exhibited minor spectral changes in terms of the shape and wavelength of the peaks as shown in **Figure 2.10**,[39] indicating that intermolecular ground state and excited state complex were absent. It is also suggested that quencher-induced aggregation may be minimal, considering the relatively low concentration of **P3'** in the mixture (as low as 1.25 μM).[20] Therefore, it is fluorophore-quencher interaction (electron or energy transfer) that was involved in the quenching of **P3'**.

2.5 Conclusions

In this work we have shown that by means of suitable functional modifications, a series of novel water-soluble cationic green light-emitting polymers can be successfully synthesized through a post-quaternization approach. Two traditional polymerization techniques, Gilch and Wittig reactions, were employed and found to produce two types of polymer structures, in which *trans*- and *cis*-vinyl was the dominant composition respectively. Although the Gilch product **P1** was insoluble in common organic solvents, its interesting acid-assisted and reversible solubility make it very promising for application as green emissive material in light-emitting diodes. Increase of hydrophilicity of the side chains was found to be beneficial to water solubility of the polymers. The optical properties of **P1** were studied, which showed a solvent-dependent conjugation length. Quaterizaition also resulted in the more twisted conformation of the polymer main chain. The conformation change may be responsible for the decrease in quantum efficiency of the polymers in solution. The bulky phenyl

rings successfully suppressed interchain interactions, as evidenced by the absence of intermolecular dimmer and excimer. Quenching studies on water-soluble polymer **P3'** showed that efficient fluorescence quenching can be achieved by using an anionic quencher $Fe(CN)_6^{4-}$, which is very useful in chemo- and biosensor applications. However, a modified Stern-Volmer plot demonstrated that some of the fluophores can not be accessible to the quencher, probably due to a twisted conformation or intermolecular aggregation.

References and Notes

1 Cimrova, V.; Schmidt, W.; Rulkens, R.; Schulze, M.; Meyer, W.; Neher, D. *Adv. Mater.* **1996**, *8*, 585.

2 Baur, J. W.; Kim, S.; Balanda, P. B.; Reynolds, J. R.; Rubner, M. F. *Adv. Mater.* **1998**, *10*, 1452.

3 Ho, P. K. H.; Granstrom, M.; Friend, R. H.; Greenham, N. C. *Adv. Mater.* **1998**, *10*, 769.

4 McQuade, D. T.; Pullen, A. E.; Swager, T. M. *Chem. Rev.* **2000**, *100*, 2537.

5 Chen, L.; Yu, S.; Kagami, Y.; Gong, J.; Osada, Y. *Macromolecules* **1998**, *31*,787.

6 Decher, G. *Science* 1997, 277, 1232.

7 McCullough, R. D.; Ewbank, P. C.; Loewe, R. S. *J. Am. Chem. Soc.* **1997**, *119*, 633.

8 (a) Thünemann, A. F. *Adv. Mater.* **1999**, *11*, 127. (b) Thünemann, A. F.; Ruppelt, D. *Langmuir* **2001**, *17*, 5098.

9 (a) Ferreira, M.; Rubner, M. F. *Macromolecules* **1995**, *28*, 7107. (b) Fou, A. C.; Rubner, M. F. *Macromolecules* **1995**, *28*, 7115. (c) Fou, A. C.; Onitsuka, O.; Ferreira, M.; Rubner, M. F. *J. Appl. Phys.* **1996**, *79*, 7501.

10 Bharathan, J.; Yang, Y. *Appl. Phys. Lett.* **1998**, *72*, 2660.

11 Bao, Z.; Feng, Y.; Dodabalapur, A.; Raju, V. R.; Lovinger, A. J. *Chem. Mater*. **1997**, *9*, 1299.

12 Chang, S. C.; Bharathan, J.; Yang, Y. *Appl. Phys. Lett.* **1998**, *73*, 2561.

13 Baur, J. W.; Rubner, M. F.; Reynolds, J. R.; Kim, S. *Langmuir* **1999**, *15*, 6460.

14 Landfester, K.; Montenegro, R.; Scherf, U.; Güntner, R.; Asawapirom, U.; Patil, S.;

Neher, D.; Kietzke, T. *Adv. Mater.* **2002**, *14*, 651.

15 Brodowski, G.; Horvath, A.; Ballauf, M.; Rehahn, M. *Macromolecules* **1996**, *29*, 6962.

16 Rulkens, R.; Schulze, M.; Wegner, G. *Macromol. Rapid Commun.* **1994**, *15*, 669.

17 (a) Kim, S.; Jackiw, J.; Robinson, E.; Schanze, K. S.; Reynolds, J. R. *Macromolecules* **1998**, *31*, 964. (b) Balanda, P. B.; Ramey, M. B.; Reynolds, J. R. *Macromolecules* **1999**, *32*, 3970.

18 Shi, S.; Wudl, F. *Macromolecules* **1990**, *23*, 2119.

19 Wagaman, M. W.; Grubbs, R. H. *Macromolecules* **1997**, *30*, 3978.

20 Chen, L.; McBranch, D. W.; Wang, H.-L.; Helgeson, R.; Wudl, F.; Whitten, D. G. *Proc. Natl. Acad. Sci. U. S. A.* **1999**, *96*, 12287.

21 (a) Chen, L.; Xu, S.; McBranch, D.; Whitten, D. G. *J. Am. Chem. Soc.* **2000**, *122*, 9302. (b) Chen, L.; McBranch, D.; Wang, R.; Whitten, D. G. *Chem. Phys. Lett.* **2000**, *330*, 27. (c) Wang, J.; Wang, D. L.; Miller, E. K.; Moses, D.; Bazan; G. C.; Heeger, A. J. *Macromolecules* **2000**, *33*, 5153. (d) Wang, D. L.; Wang, J.; Moses, D.; Bazan; G. C.; Heeger, A. J. *Langmuir* **2001**, *17*, 1262. (e) Gaylord, B. S.; Wang, S.; Heeger, A. J.; Bazan, G. C. *J. Am. Chem. Soc.* **2001**, *123*, 6417. (f) Jones, R. M.; Bergstedt, T. S.; McBranch, D. W.; Whitten, D. G. *J. Am. Chem. Soc.* **2001**, *123*, 6726. (g) Stork, M.; Gaylord, B. S.; Heeger, A. J.; Bazan, G. C. *Adv. Mater.* **2002**, *14*, 361. (h) Wang, D.; Gong, X.; Heeger, P. S.; Rininsland, F.; Bazan, G. C.; Heeger, A. J. *Proc. Natl. Acad. Sci. U. S. A.* **2002**, *99*, 49. (i) Fan, C.; Plaxco, K. W.; Heeger, A. J. *J. Am. Chem. Soc.* **2002**, *124*, 5642.

22 Harrison, B. S.; Ramey, M. B.; Reynolds, J. R.; Schanze, K. S. *J. Am. Chem. Soc.* **2000**, *122*, 8561.

23 Spreitzer, H.; Becker, H.; Kluge, E.; Kreuder, W.; Schenk, H.; Demandt, R.; Schoo, H. *Adv. Mater.* **1998**, *10*, 1340.

24 (a) Wan, W. C.; Antoniadis, H.; Choong, V. E.; Razafitrimo, H.; Gao, Y.; Feld W. A.; Hsieh, B. R. *Macromolecules*, **1997**, 30, 6567. (b) Hsieh, B. R.; Yu, Y.; Forsythe, E. W.; Schaaf, G. M.; Feld, W. A. *J. Am. Chem. Soc.* **1998**, 120, 231.

25 Peng, Z.; Zhang, J.; Xu, B. *Macromolecules* **1999**, *32*, 5162.

26 (a) Liu, B.; Yu, W.; Lai, Y. H.; Huang, W. *Chem. Comm*. **2000**, 551. (b) Liu, B.; Yu, W.; Lai, Y. H.; Huang, W. *Macromolecules* **2002**, *35*, 4975.

27 Stenger-Smith, J. D.; Zarras, P.; Merwin, L. H.; Shaheen, S. E.; Kippelen, B.; Peyghambarian, N. *Macromolecules* **1998**, *31*, 7566.

28 (a) Liao, L.; Pang, Y.; Ding, L.; Karasz, F. E. *Macromolecules* **2001**, *34*, 7300. (b) Liao, L.; Pang, Y.; Ding, L.; Karasz, F. E. *Macromolecules* **2001**, *34*, 7300.

29 The QDs of **P2'** and **P3'** were calculated according to the following equations: $(50 + 6x)/24 = I_{0.5\text{-}2.0}/I_{6.0\text{-}8.0}$ and $(12 + 6x)/24 = I_{0.5\text{-}2.0}/I_{6.0\text{-}8.0}$, respectively, where x is the QD, $I_{0.5\text{-}2.0}$ is the integration of the peaks at 0.5-2.0 ppm and $I_{6.0\text{-}8.0}$ is the integration of the peaks at 6.0-8.0 ppm.

30 Nguyen, T.-Q.; Doan, V.; Schwartz, B. J. *J. Chem. Phys.* **1999**, *110*, 4070.

31 Nguyen, T.-Q.; Schwartz, B. J. J. Chem. P*hys.* **2002**, *116*, 8198.

32 Pei, J; Yu, W.-L.; Huang, W.; Heeger, A. J.; *Chem. Lett.* **1999**, *10*, 1123.

33 Oelkrug, D.; Tompert, A.; Gierschner, J.; Egelhaaf, H.-J.; Hanack, M.; Hohloch, M.;

Steinhuber, E. *J. Phys. Chem. B* **1998**, *102*, 1902.

34 Wang, D.; Lai, J.; Moses, D.; Bazan, G. C.; Heeger, A. J. *Chem. Phys. Lett.* **2001**, *348*, 411.

35 Lakowicz, J. R. in *Principles of Fluorescence Spectroscopy*, 2nd ed.; Plenum Press: New York, 1999.

36 Lehrer, S. S. *Biochemistry* **1971**, *10*, 3254.

37 Gong, Y.-K.; Miyamoto, T.; Nakashima, K.; Hashimoto, S. *J. Phys. Chem. B* **2000**, *104*, 5772.

38 The modified Stern-Volmer plot of **P3'** (1.25 μM) quenched by $Fe(CN)_6^{4-}$ showed that 50% quenching was achieved at $[Fe(CN)_6^{4-}] \approx 0.36$ μM, which corresponds to approximately 7-8 phenyl rings in the polymer backbone per quencher.

39 The UV absorption of 10 μM $Fe(CN)_6^{4-}$ in aqueous solution was very weak and can be negligible as compared with that of 2.5 μM **P3'** in water used in the quenching study.

CHAPTER THREE

Part I: Synthesis, Characterization and Optical Properties of Cationic Phenyl-Substituted Poly(*p*-phenylenevinylene) Related Copolymers

3.1.1 Introduction

Poly(*p*-phenylenevinylene) (PPV) and its derivatives have attracted a great deal of attention in recent years because of their interesting electroluminescent properties and their potential application as the active emitting layer in light-emitting diodes (LED).[1] Recently, considerable research has focused on an anionic PPV (sulfonated PPV, i.e., MPS-PPV), a type of polyelectrolytes which consist of both polyanions and fluorescent conjugated backbones, and shown that such ionic conjugated polymers (ICPs) are the good candidates as chemo or biosensors which exhibit rapid and collective response to relatively small perturbations in local environment.[2] Such amplified fluorescence quenching sensitivity is achieved through electron transfer or energy transfer due to the facile energy migration along the conjugated backbone[3] and relatively strong electrostatic binding of the oppositely charged quenchers with ICPs.[2] Although the optical and electronic properties of MPS-PPV are remarkable, and MPS-PPV was reported on detecting proteins for biological target through electron transfer[2a], this polymer suffers from its intrinsic shortcomings such as a relatively low photoluminescence quantum efficiency and their single anionic charges which can not be used to detect anionic DNA chain through electrostatic attraction.

Most recently, the effect of cationic fluorescent conjugated polymer on anionic quencher[4] and DNA sensing[5] is gaining high interesting, in which, especially, a cationic polyfluorene was successfully developed to identify anionic DNA through energy transfer.[5] To obtain high energy transfer and therefore improve the sensitivity, new types of cationic conjugated polymers with suitable emission wavelength and high photoluminescence quantum efficiency are required. PPV is very appropriate for the color tunability over the full visible range by the control of its HOMO-LUMO band gap and for enhancement of the PL quantum efficiency through introduction of bulky group into the side chain or incorporation of unit with high PL efficiency into the conjugated main chain. Therefore, it is crucial to develop cationic PPVs with higher PL quantum efficiency and different emission wavelength to evaluate a variety of polymer compositions for obtaining optimized sensory materials.

In this paper, we report on the syntheses and photoluminescence properties of cationic phenyl-substituted poly(*p*-phenylenevinylene) related copolymers containing thiophene, fluorene or alkoxy- or phenyl-substituted phenylene groups. We attempted to gain highly PL quantum efficiency by incorporating the bulky substitutent and the fluorene unit. Phenyl-substituted PPV derivatives are desired as they have proven to exhibit highly efficient fluorescence and enhanced photostability due to the steric hindrance of the bulky phenyl groups which minimize the interchain or intrachain interactions.[6-8] The fluorene unit is well known as a highly PL efficient material and has been used to enhance the PL efficiency of PPV derivatives.[9] In addition, the emission wavelength was changed by introduction of those units with different

electronic properties.[6-9] On the basis of these considerations, we successfully synthesized new cationic PPVs with relative high PL quantum efficiency and tunable emission wavelength.

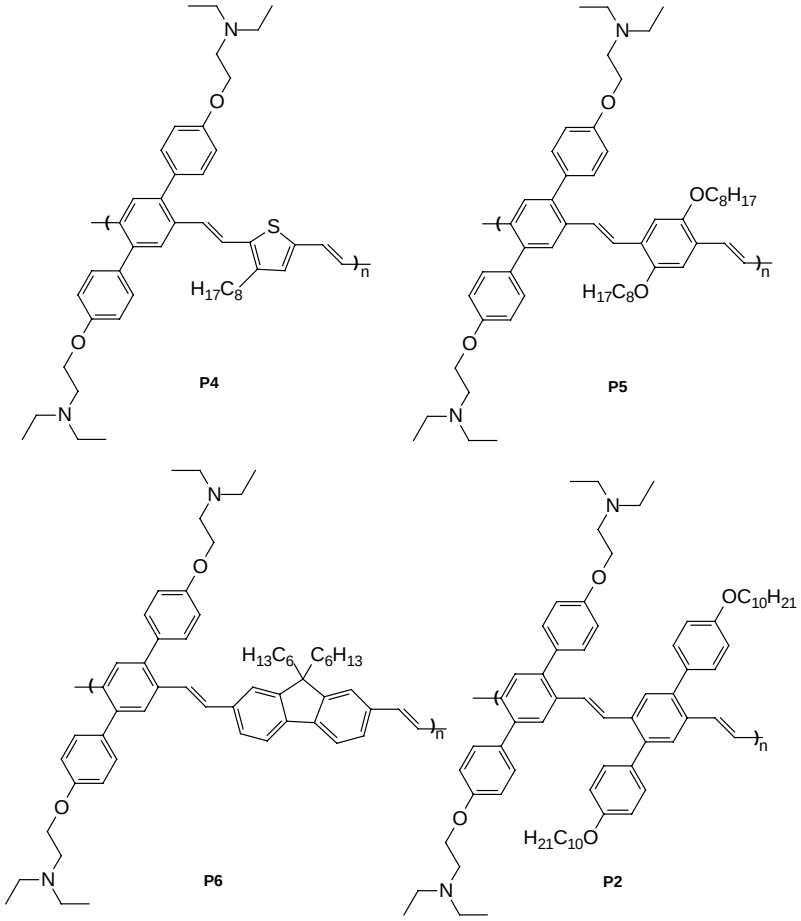

Figure 3.1.1 The designed neutral polymers for the cationic polymers

3.1.2 Molecular Design

To obtain phenyl-substituted PPV copolymers with different emission wavelength and higher fluorescence efficiency, several moieties, such as thiophene, benzene and fluorene were selected as the comonomers for the copolymerization. One alkyl chain were introduced to the thiophene moieties to adjust the light emission, since thiophene

as an electron rich moiety, will cause a spectral red shift. Alkoxylated benzene and phenyl-substituted benzene were specially chosen for their different steric properties and expected that the optical properties could be tuned via such modification. Alklated fluorene was chosen to cause the light emission blue shift.

In order to synthesize cationic copolymers, tertiary amine as the functional group was also designed for the neutral polymer, which is similar as what we referred in chapter 2. Meanwhile, long alkoxy chains or alkyl chains were introduced into the side chain of those four copolymers to enhance their corresponding solubility which will be conducive to their post-quaternization in the next step. All molecular structures of those PPV-copolymers are shown in **Figure 3.1.1**.

3.1.3 Materials and Characterization Methods

3.1.3.1 Materials

All chemical reagents used were purchased from Aldrich Chemical Co. THF was purified by distillation from sodium in the presence of benzophenone. Other organic solvents were used without any further purification. Thionyl chloride was distilled prior to use.

3.1.3.2 Characterization Methods

The NMR spectra were collected on a Bruker Advance 400 spectrometer with tetramethylsilane as the internal standard. FT-IR spectra were recorded on a Bio-Rad

FTS 165 spectrometer by dispersing samples in KBr. Mass spectra (MS) were obtained using a micromass VG 7035E mass spectrometer at an ionizing voltage of 70 eV. UV-vis spectra were recorded on a Shimadzu 3101 PC spectrometer. The concentrations of copolymer solutions were adjusted to about 0.01 mg/mL or less. Fluorescence measurement was carried out on a Perkin-Elmer LS 50B photoluminescence spectrometer with a xenon lamp as a light source. TGA measurements were performed on a TA Instruments Hi-Res TGA 2950 Thermogravimetric Analyzer at a heating rate of 10 °C/min under N_2. Elemental microanalyses were carried out by the Microanalysis Laboratory of the National University of Singapore. Gel permeation chromatography (GPC) analysis was conducted with a Waters 2690 separation module equipped with a Waters 2410 differential refractometer HPLC system and three 5 μm Waters Styragel columns (pore size: 10^3, 10^4 and 10^5 Å) in series, using polystyrenes as the standard and tetrahydrofuran (THF) as the eluant at a flow rate of 1.0 mL/min and 35 °C.

3.1.4 Results and Discussion

3.1.4.1 Synthesis of Monomers and Polymers

Monomer **5** was directly synthesized from 3-octylthiophene via reaction with *n*-butyllithium and TMEDA in hexane and then with DMF and HCl solution. 3-octylthioohene was synthesized from 3-bromothiophene with 1-bromooctane via Grignard reaction using [1,3-bis (diphenylphosphino)propane]dichloronickel(II) as the catalyst. Monomer **6** was prepared from 1,4-dioctylbenzene via dibromomethylation,

esterification, hydrolysis and hydroformylation. The 1,4-dioctylbenzene was obtained from 1,4-hydroquinone by reaction with 1-bromooctane in refluxing ethanol in the presence of $NaOC_2H_5$. Monomer **7** was prepared from 9,9-di-*n*-hexylfluorene via dibromomethylation, esterification, hydrolysis and hydroformylation. 9,9-di-*n*-hexylfluorene was synthesized from fluorene by reaction with 1-bromohexane in the presence of *n*-butyllithium at –78°C. Monomer **2** and Monomer **3** has been reported in chapter 2. All the synthetic routes except Monomer **2** and **3** are shown in **Scheme 3.1.1**.

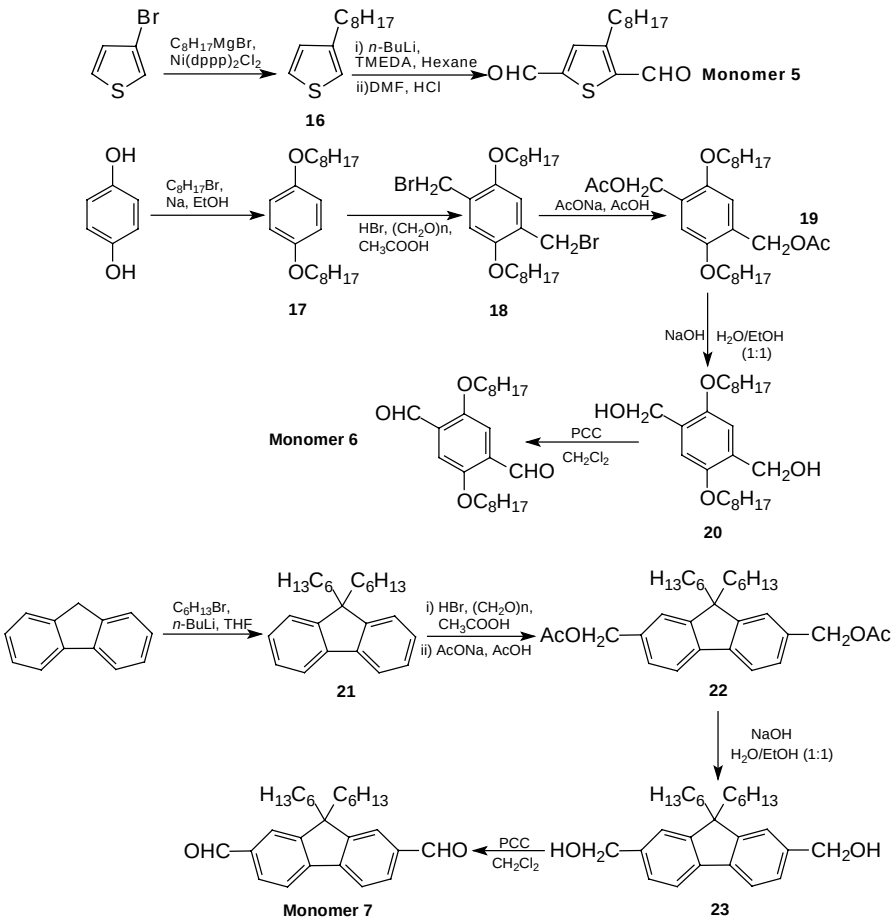

Scheme 3.1.1 The synthetic routes for the monomers

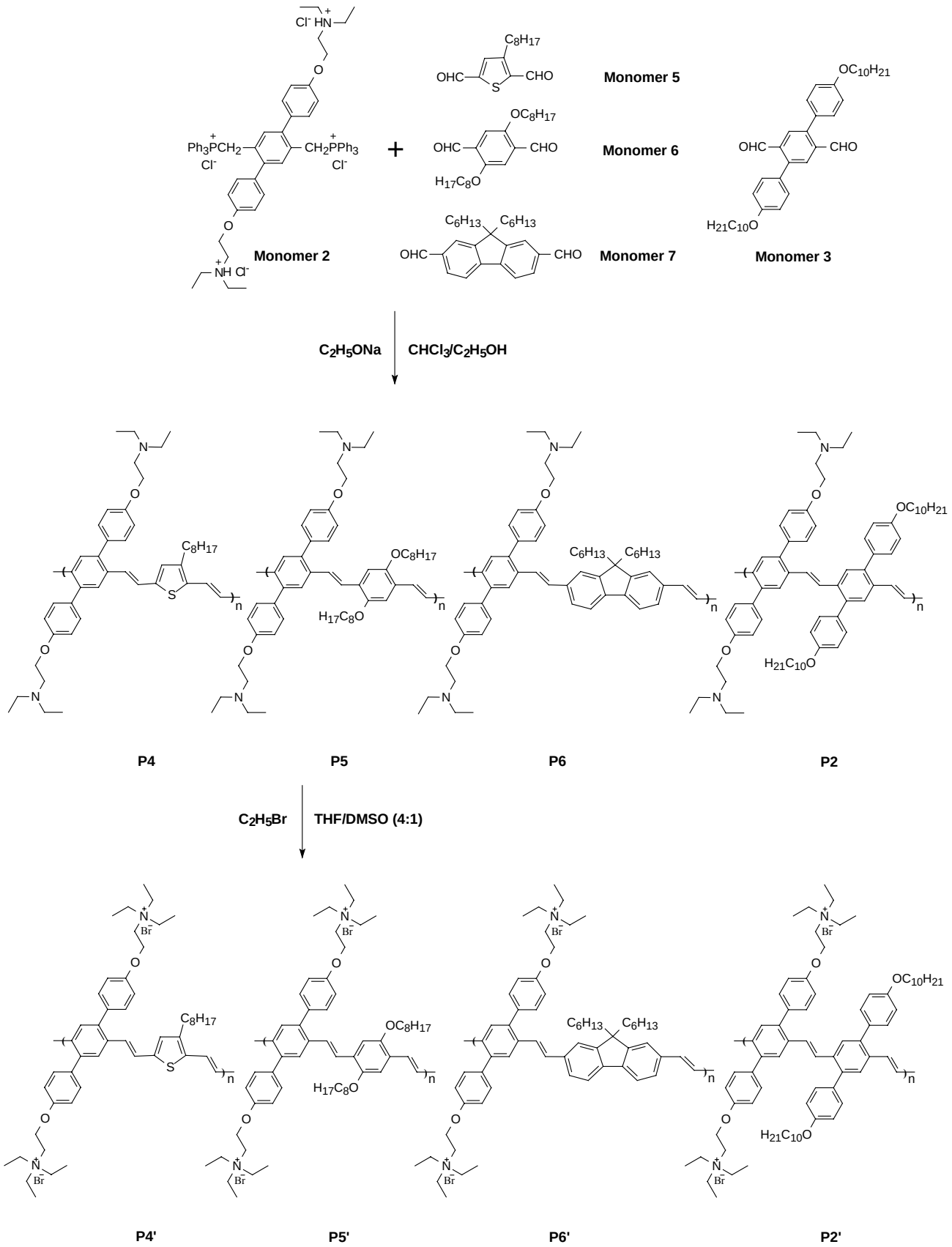

Scheme 3.1.2 The synthetic routes for those neutral and quaternized polymers

All polymers were synthesized via Wittig reaction that proceeded in a mixture of chloroform and ethanol (1:1) under the injection of excess C_2H_5ONa solution in ethanol (1M) under vigorous stirring at room temperature for one day (see **Scheme 3.1.2**). Conversion of the neutral polymers to the final cationic polymers was achieved by treating them with bromoethane in dimethyl sulfoxide (DMSO) and tetrahydrofuran (THF) (1:4) by stirring at 50 ^{o}C for 5 days, just as what we reported in chapter 2. In syntheses of all the neutral polymers, it was found that by using the Wittig reaction condition, precipitate was observed in the mixed solvent of ethanol and chloroform during polymerization. The poor solubility of the resultant polymers in the solvent mixture retarded the polymerization procession and might explain for the small molecular weights obtained by using this method.

3.1.4.2 Color and Solubility

In all neutral polymers, **P4** is a deep red solid, **P5** is a bright orange solid, **P6** is a bright blue-green solid and **P2** is a bright green solid. Compared with those neutral polymers, the obtained quaternized polymers show slight deeper colours, in which **P4'** is deep red, **P5'** is red, **P6'** is green and **P2'** is yellow-green color. All of the neutral polymers prepared through Wittig reaction are readily soluble in common organic solvents such as chloroform, tetrahydrofuran, 1,2-dichloroethane and so on, but have poor solubility in polar ones such as methanol, DMSO and DMF. After quaternized, **P2'** and **P4'-P6'** could be dissolved well in DMSO, DMF, and CH_3OH, indicating enhanced polarity from cationic groups due to quaternization.

In addition, **P4-P6** were dissolved well in methanol, DMSO or water containing acetic acid (1 M). This organic acid-assisted solubility has been reported by our group previously,[10,11] which may be attributed to relatively strong intermolecular interactions between the polymer and the acid introduced. However, it is noteworthy that although under the acid-assistance, **P2**, using bulky phenyl groups as all the substituents, can be dissolved well in methanol, DMSO, DMF but not in water, indicating that such a solubility increase from the assistance of acetic acid is limited by the volume and content of hydrophobic groups on the polymer chains and the polarity of the solvent used.

3.1.4.3 FT-IR Analysis

Infrared spectra for all neutral polymers were shown in **Figure 3.1.2**. It can be seen that a weak absorption, which can be attributed to the aldehyde end groups for **P2** and **P4-P6**, occurs at about 1680 cm^{-1}, indicating incomplete intermolecular condensation. Interestingly, it was also found that the ratio of *trans*-CH=CH (~970 cm^{-1}) group to *cis*-CH=CH (~875 cm^{-1}) group in the IR spectrum of **P2** was rather different from those of **P4**, **P5** and **P6**. A weak absorption peaked at 875 cm^{-1} (*cis*-CH=CH) was clearly visible for **P2** while no signals could be found at 970 cm^{-1} (*trans*-CH=CH), indicating that **P2** predominantly contains *cis*-CH=CH group under Wittig conditions. For **P4** with thiophene moiety in the conjugated backbone, on the contrary, a much more stronger absorption peaked appeared at 960 cm^{-1} (*trans*-CH=CH) compared with the peak at 876 cm^{-1} (*cis*-CH=CH). Meanwhile, an approximately identical IR

absorption intensity of *cis*-CH=CH group to *trans*-CH=CH group was observed for **P5** and **P6** which were also obtained through Wittig reaction. Therefore, it is concluded that the configuration of CH=CH group formed from Wittig reaction was highly related to the steric effect and the molecular structure of the reactant used. The ratio of *trans*- vs *cis*-configuration cannot be determined by FT-IR spectrum, which will be discussed in the next section.

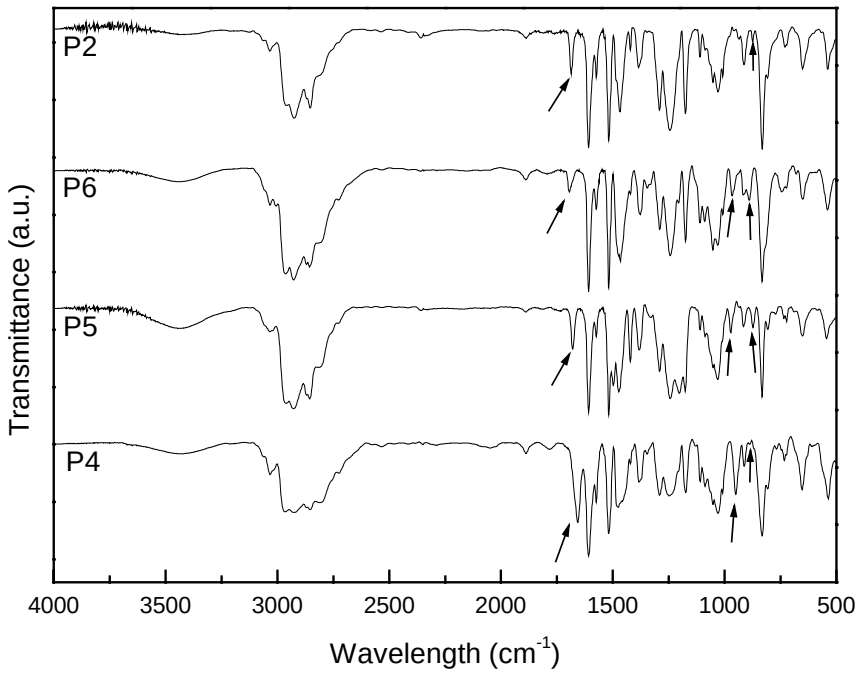

Figure 3.1.2 FT-IR spectra of the neutral PPVs

After quaternization, there are no obvious changes with the position of most peaks but greater changes with the intensity of some peaks compared with their respective neutral polymers (see **Figure 3.1.3**). Besides, a broad and strong self-associated absorption peak of water at 3400 cm^{-1} can be observed, which reflects strong

hydrophilicity of the resulting quaternized polymers.

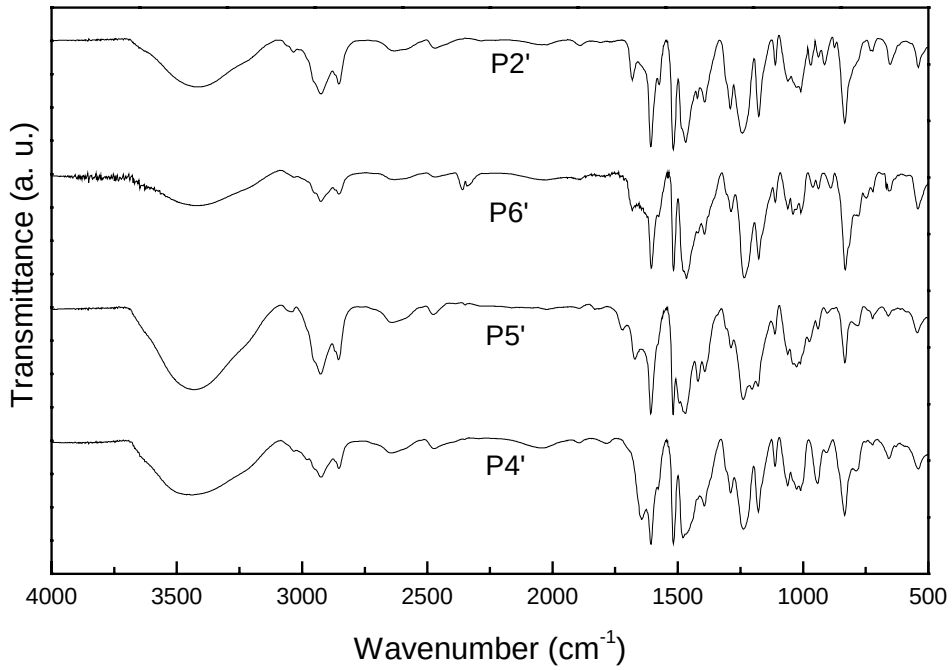

Figure 3.1.3 FT-IR spectra of the quaternized PPVs

3.1.4.4 Gel Permeation Chromatography (GPC)

The characterization of the molecular weights is often a problem for the ionic conjugated polymers.[16] The post-quaternization approach for the realization of water-solubility allows us to characterize the molecular weight at the stage of the neutral polymer. The molecular weights of the neutral polymers were measured by means of gel permeation chromatography (GPC) using THF as the eluant and polystyrene as the standards. The molecular weights of **P2** and **P4-P6** obtained through Wittig reaction are relatively lower, with the M_n of 4200, 8300, 7400, 8600 and M_w of 5300, 12000, 11000, 12000 respectively (see **Table 3.1.1**). The post-quaternization

method is especially useful for the analysis of the water-soluble polymers, since polyelectrolytes have a strong tendency to aggregate and adsorb on column fillers.

Table 3.1.1 GPC and Spectroscopic Data for all Neutral and Quaternized Polymers

polymer	GPC			content of	absorbance	emission	Φ_{pl}
	M_n [a]	M_w [a]	PDI[a]	*cis*-CH=CH (%)[b]	λ_{max} (nm)	λ_{max} (nm)	
P4[c]	4200	5 300	1.26	< 50	437	585	0.03
P5[c]	8300	12 000	1.45	55	437	524	0.40
P6[c]	7400	11 000	1.46	45	397	476	0.80
P2[c]	8600	12 000	1.40	80	392	500	0.55
P4'[d]	—	—	—		449	551	0.01
P5'[d]	—	—	—		404	508	0.18
P6'[d]	—	—	—		413	470	0.35
P2'[d]	—	—	—		370	484	0.28

[a] M_n, M_w and PDI of the polymers were determined by gel permeation chromatography using polystyrene standards. [b] The *cis*-CH=CH contents were estimated from the integration of $-OCH_2-$ signals in the ^{1}H NMR. [c]The spectroscopic data of neutral polymers were measured in THF and [d]those of quaternized polymers in methanol, using the quinine sulfate solution (ca. 1.0×10^{-5} M) in 0.10 M H_2SO_4 (Φ_f= 55%) as a standard.

3.1.4.5 Thermal Stability

Thermal properties of the polymers were studied by thermogravimetric analysis (TGA) under nitrogen atmosphere. The thermograms in **Figure 3.1.4** showed that the neutral polymers **P2** and **P4-P6** exhibited good thermal stability with a weight loss of 3% at 310 °C. For the quaternized samples (**Figure 3.1.4**), the degradation onsets for **P2'** and **P4'-P6'** decreased to 200 °C with the initial weight loss deriving from associated water. This variation can be explained by the lower stability of ethyl bromide than that of the other alkoxy side chains.[14] Although the thermal stability of quaternized polymers decreased, their degradation temperature at nearly 200 °C made them enough serve as

chemo or biosensors.

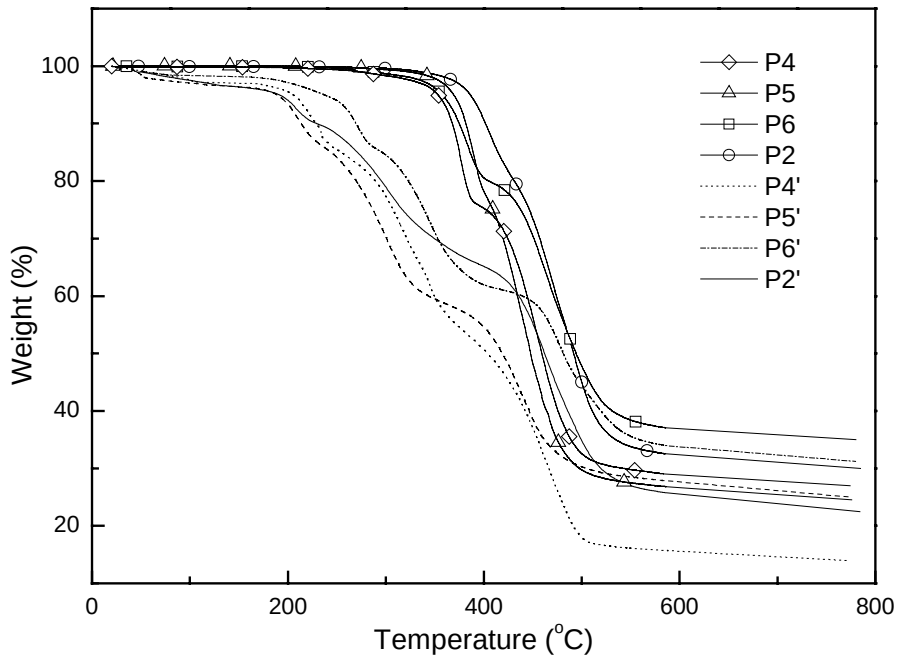

Figure 3.1.4 Thermalgravimetric analysis of the neutral and quaternized PPVs

Thermally induced phase transition behavior of the polymers was also investigated with the differential scanning calorimetry (DSC) in a nitrogen atmosphere. The representative DSC curves are shown in **Figure 3.1.5**. We could see that there are no obvious Tg appeared for **P5** and **P2**. **P4** exhibits a clear glass transition starting at ~47°C. In comparison with **P4**, the glass transition temperature, Tg, of **P6** is increased by ~10 ^{o}C to 57 ^{o}C. It is quite obvious that the increase of Tg is due to the structure difference between **P4** and **P6**, because the fluorene components in **P6** is much rigid than the thiophene components in **P4** so that the rotary free degree decreased much higher in **P6** than in **P4** which led to the enhanced Tg of **P6**.

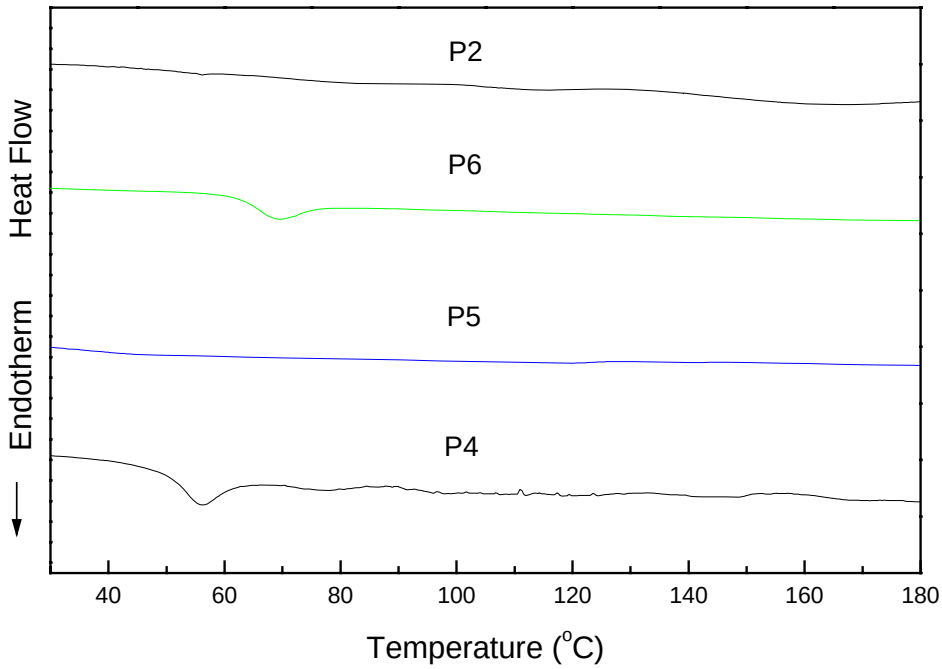

Figure 3.1.5 The DSC traces of P2 and P4-P6 in a nitrogen atmosphere

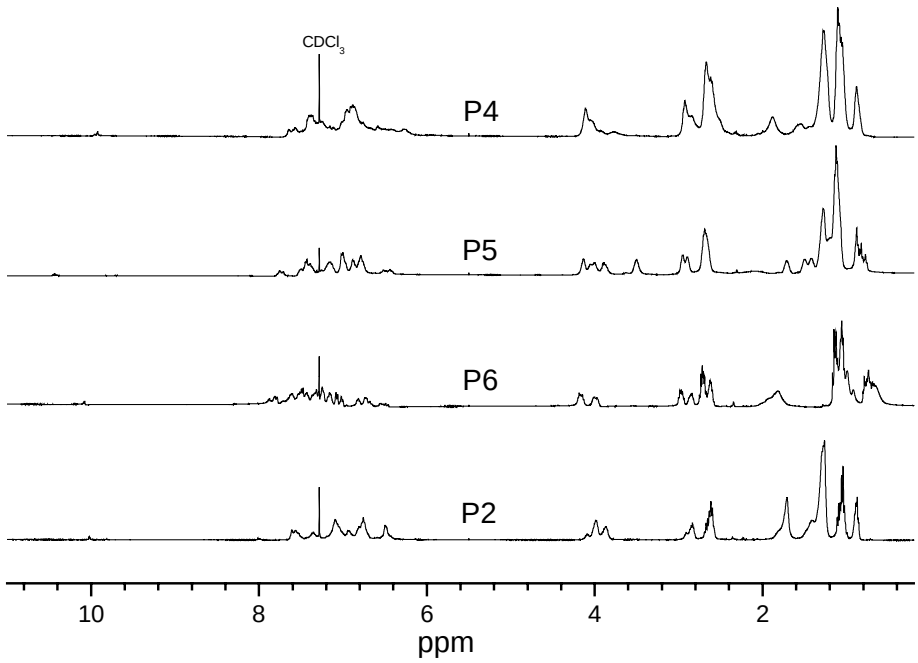

Figure 3.1.6 ^{1}H NMR spectra of the neutral polymers in chloroform-*d*

3.1.4.6 NMR Analysis

^{1}H NMR spectra of all the neutral and quaternized polymers were shown in **Figure 3.1.6** and **Figure 3.1.7** respectively. Integration ratios of the end aldehyde protons (about 10.00 ppm) to the -OCH_2CH_2N- protons for **P2** and **P4-P6** (3.00-2.75 ppm) were found to be about 1/24, 1/42, 1/36 and 1/32, corresponding to 12, 21, 18 and 16 phenyl rings in the backbone respectively. These results are in good agreement with those measured by GPC (Table 3.1.1). Our FT-IR analysis showed that **P2** adopted predominantly *cis*-CH=CH while *trans*-CH=CH was the dominated in **P4** and as for **P5-P6**, both *cis*-CH=CH and *trans*-CH=CH configurations were present. Such a result was also substantiated by ^{1}H NMR measurements. The ^{1}H NMR peaks of all the neutral polymers corresponding to –OCH_2– and –CH_2N– groups split into two parts, in which the downfield and upfield ones were caused by the *trans*- and *cis*-configurations respectively.[12] For **P6**, Clear separation between the two resonance signals near 4.2 and 4.0 ppm offered a convenient way to accurately estimate the relative *cis*-/*trans*-CH=CH contents. The ratio of *cis*- to *trans*-vinylic group for **P5** was determined by comparing the relative integrations of the –$OCH_2C_7H_{15}$ resonance from *cis*-confiuration at 3.50 ppm with the -OCH_2CH_2N- resonance between 3.00 ppm and 2.75 ppm. The ratio for **P2** has been reported in our previous work. However, although the two split peaks which were caused by the *trans*- and *cis*-vinylic groups on the signals of –OCH_2– and –CH_2N– groups in **P4** could be detected, they mixed together and made it difficult to calculate the ratio of *cis*- to *trans*-vinylic group. From the height of those corresponding peaks, we could only estimate the content of

trans-vinylic group was significantly higher than 50% in **P4**. All the results are shown in **Table 3.1.1**. The relative higher content of *cis*- configurations for **P2** (80%), compared to that of **P5** (55%), indicates that the steric effect due to bulky phenylene substitutent in the monomer significantly influence the formation of *trans*- and *cis*-vinyl group via Wittig reaction.

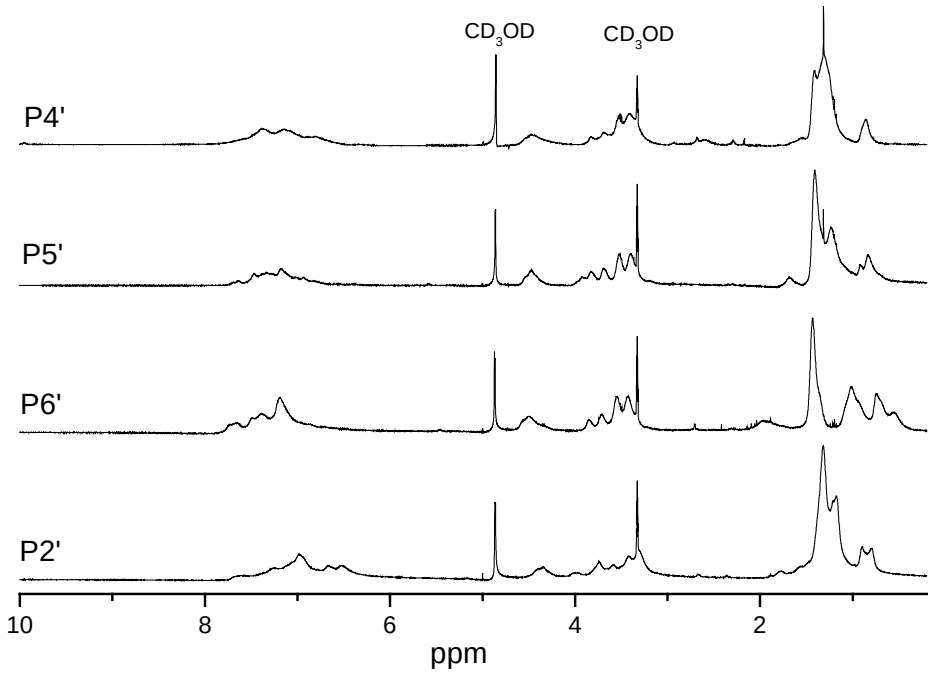

Figure 3.1.7 ^{1}H NMR spectra of the quaternized polymers in methanol-d_4

As shown in **Figure 3.1.7**, after quaterniztion with bromoethane, all proton peaks turns broadened, some of which could not be identified. **P2'** and **P4'-P6'** exhibit spectra in which all the signals from -OCH_2CH_2N-, -NCH_2CH_3 and -NCH_2CH_3 groups are downshifted. The quaternization degrees (QD) was determined from the ^{1}H NMR spectra by comparing the relative integrations of the aromatic peaks at 6.0-8.0 ppm (total aromatic and vinyl protons) with that of 0.5-2.0 ppm (total alkyl protons for

-$CH_2C_7H_{15}$ and –NCH_2CH_3 in **P4'**, -$OCH_2C_7H_{15}$ and -NCH_2CH_3 in **P5'**, -$CH_2C_5H_{11}$ and -NCH_2CH_3 in **P6'** or -$OCH_2C_9H_{19}$ and -NCH_2CH_3 in **P2'**[10]).[13] As a result, the QDs of **P2'** and **P4'-P6'** were calculated to be about 95%, 95%, 95%[10] and 90% respectively, which were close to the results from elemental analysis.

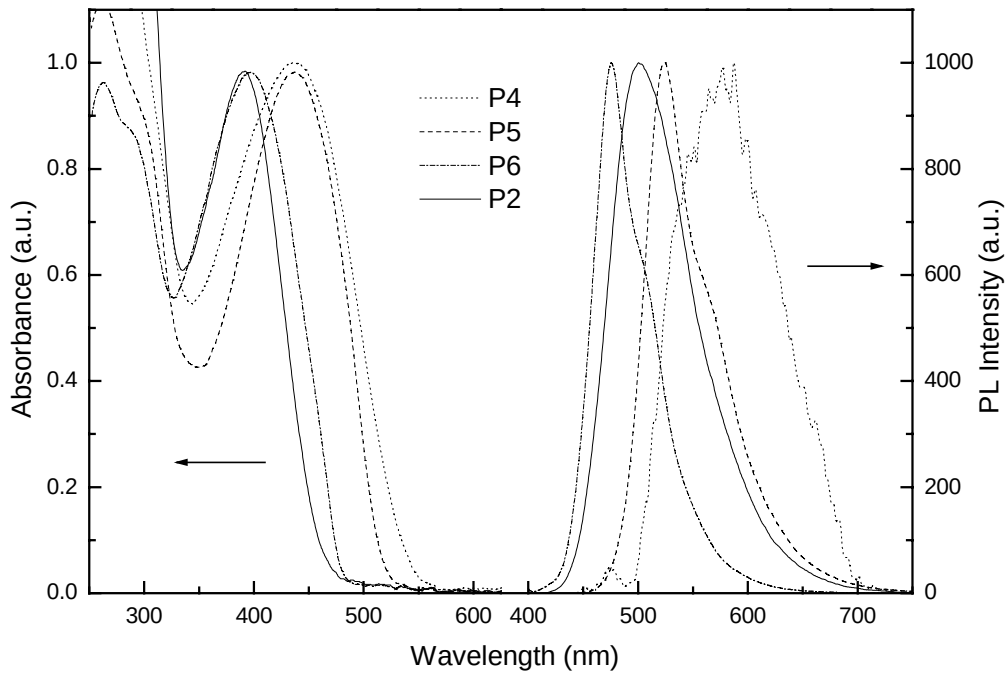

Figure 3.1.8 The UV-vis and PL spectra of the neutral polymers in $CHCl_3$

3.1.4.7 Optical Properties

The absorption and emission spectra of the neutral polymers in $CHCl_3$ are shown in **Figure 3.1.8**. **P4** and **P5** both showed a maximum absorption peak at 437 nm and **P6** and **P2** showed absorption maxima at 397 and 392 nm, respectively. These obvious blue-shifted UV-vis absorption wavelengths compared to that of MEH-PPV at 510 nm[9] are highly due to the lack of electron-donating ability of the phenyl substituent and the

fluorene unit in the alternating copolymer system.

The PL spectra showed an obvious change of emission maxima by the type of substituents and the alternating units in the main chain. In the PL spectra, the effects of phenyl substituent and fluorene unit in the copolymer systems were well consistent with the UV-vis absorption patterns of the polymers. Compared with the emission maximum at 595 nm for MEH-PPV[9], those for **P2** and **P4-P6** were blue-shifted to 585, 524 nm, 476 nm and 500 nm respectively. Such different distances of the blue shifts for the four neutral polymers can be attributed to the alternating units with different electronic properties, in which thiophene and alkoxylated phenyl units are electron rich moieties while phenyl-substituted benzene unit and alklated fluorene unit are electron deficient moieties in the alternating copolymer systems. Moreover, most of the polymers with phenyl-substituted phenylene unit showed extremely high PL efficiency in solution, the Φ_f which are 40% for **P5**, 80% for **P6** and 55% for **P2** (see **Table 3.1.1**). The highly enhanced PL efficiency of **P6** may be due to the non-electron-donating phenyl group and the introduction of highly fluorescent fluorene unit in the conjugated main chain. In addition, the emission spectrum of **P5** and **P6** were more featured than that of **P2**, indicating that **P2** emitted through an excited state of more twisted conformation, which may result from its high content of *cis*-vinylic group. However, **P4** showed dramatically lower PL efficiency (Φ = 3%) although **P4** also contains phenyl-substituted benzene unit, which can be explained by the existence of thiophene unit with poor fluorescence in the conjugated backbone.

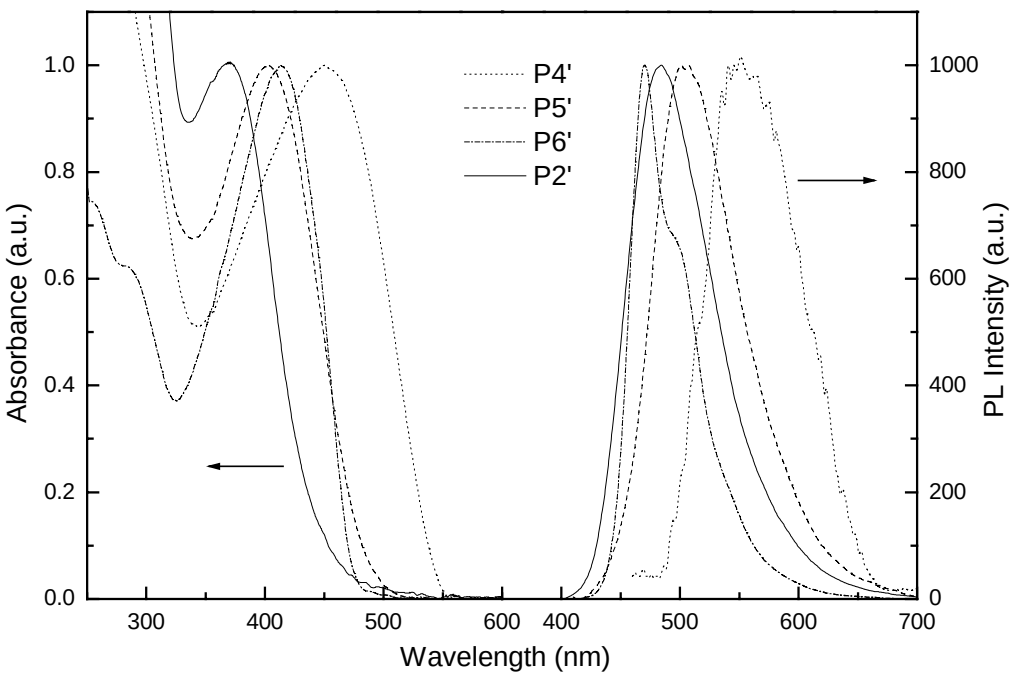

Figure 3.1.9 The UV-vis and PL spectra of the quaternized polymers in CH_3OH

The absorption and emission spectra of the quaternized polymers in methanol are shown in **Figure 3.1.9**. Quaternization was found to lead to more obvious blue-shifted UV-vis absorption and emission spectra of **P5'** and **P2'**. Such a blue-shift, attributed to the mutual electrostatic repulsion of positive charges pendent on the alternating benzene rings which leads to an increased torsion of the conjugated main chain and a decreased effective conjugation length, has been reported in other quaternized systems.[11,14] On the contrary, it is intriguing to find that after quaternization **P4'** and **P6'** showed red-shift absorption maxima at 449 and 414 nm and blue-shift emission maxima at 551 and 470 nm respectively. Such different shifts indicate that the thiophene and fluorene units, instead of the phenylene unit, in the conjugated main chain may highly influence the interaction of neighboring positive charges and

therefore the chain conformation. In addition, just as what we discovered in neutral polymers, the quaternized polymers **P2'** and **P4'-P6'** showed gradual increase of blue-shift of emission maxima compared with MPS-PPV (emission maxima at 590 nm),[2a] which are 551 nm (green-yellow), 508 nm (yellow-green), 470 nm (blue-green) and 484 nm (green) respectively.

Among all quaternized polymers, **P6'** showed the highest Φ_f at 35%, while **P5'** at 18% and **P2'** at 28%, indicating that introduction of highly fluorescent fluorene unit into the conjugated main chain surely enhanced the PL efficiency of such cationic PPV system. However, the significant reduction of PL efficiencies of quaternized phenyl-substituted polymers existed in this PPV system, compared with their corresponding neutral polymers. Considering the existence of bulky phenyl group in the polymer side chain and its highly steric effect on impeding the interchain and intrachain interaction, such PL efficiency decrease may not be simply explained by interchain or intrachain interaction. As we discussed in our previous work,[10] it is maybe the nonplanarization in the excited state of these cationic polymers and the coiled molecular structure of the polymer backbone which contains a lot of torsional defects that lead to such decreased PL efficiencies.[15]

3.1.5 Conclusions

In this work we synthesized amino-functionalized phenyl-substituted poly(*p*-phenylenevinylene) related copolymers containing thiophene, fluorene or alkoxylated or phenylated benzene unit through traditional Wittig reaction. Their

corresponding cationic light-emitting polymers were successfully obtained through a post-quaternization approach. Increasing steric effect of the monomer was found to enhance the *cis*-vinyl content in those copolymers synthesized from Wittig reaction. In addition, the acid-assisted water solubility of the amino-terminated PPV was dramatically limited by the existence of bulky hydrophobic group in the side chain. The neutral and quaternized polymers showed adjustable absorption and emission wavelengths by using aryl units with different electronic properties. The decrease of PL efficiency, compared with neutral polymers, still existed in those quaternized PPVs. **P6** and **P6'**, with fluorene unit, showed highest PL efficiencies among those neutral and quaternized PPVs respectively. Thus, introduction of fluorene unit into the main chain of ionic conjugated polymers could be anticipated to develop chemo or biosensors with high PL efficiency. Meanwhile, adding aryl units with different electronic properties into conjugated backbone can successfully adjust the emission wavelengths of PPV copolymers and consequently be beneficial to the study of their corresponding quenching behaviors.

References and Notes

1 Mitschke, U.; Baüerle, P. *J. Mater. Chem.* 2000, *10*, 1471.

2 (a) Chen, L.; McBranch, D. W.; Wang, H.-L.; Helgeson, R.; Wudl, F.; Whitten, D. G. *Proc. Natl. Acad. Sci. U. S. A.* **1999**, *96*, 12287. (b) Chen, L.; Xu, S.; McBranch, D.; Whitten, D. G. *J. Am. Chem. Soc.* **2000**, *122*, 9302. (c) Chen, L.; McBranch, D.; Wang, R.; Whitten, D. G. *Chem. Phys. Lett.* **2000**, *330*, 27. (d) Wang, J.; Wang, D. L.; Miller, E. K.; Moses, D.; Bazan; G. C.; Heeger, A. J. *Macromolecules* **2000**, *33*, 5153. (e) Wang, D. L.; Wang, J.; Moses, D.; Bazan; G. C.; Heeger, A. J. *Langmuir* **2001**, *17*, 1262. (f) Gaylord, B. S.; Wang, S.; Heeger, A. J.; Bazan, G. C. *J. Am. Chem. Soc.* **2001**, *123*, 6417. (g) Jones, R. M.; Bergstedt, T. S.; McBranch, D. W.; Whitten, D. G. *J. Am. Chem. Soc.* **2001**, *123*, 6726. (h) Stork, M.; Gaylord, B. S.; Heeger, A. J.; Bazan, G. C. *Adv. Mater.* **2002**, *14*, 361. (i) Wang, D.; Gong, X.; Heeger, P. S.; Rininsland, F.; Bazan, G. C.; Heeger, A. J. *Proc. Natl. Acad. Sci. U. S. A.* **2002**, *99*, 49. (j) Fan, C.; Plaxco, K. W.; Heeger, A. J. *J. Am. Chem. Soc.* **2002**, *124*, 5642.

3 Zhou, Q.; Swager, T. M. *J. Am. Chem. Soc.* **1995**, *117*, 12593.

4 Harrison, B. S.; Ramey, M. B.; Reynolds, J. R.; Schanze, K. S. *J. Am. Chem. Soc.* **2000**, *122*, 8561.

5 Gaylord, B. S.; Heeger, A. J.; Bazan, G. C. *Proc. Natl. Acad. Sci. U. S. A.* **2002**, *99*, 10954.

6 Spreitzer, H.; Becker, H.; Kluge, E.; Kreuder, W.; Schenk, H.; Demandt, R.; Schoo, H. *Adv. Mater.* **1998**, *10*, 1340.

7 (a) Wan, W. C.; Antoniadis, H.; Choong, V. E.; Razafitrimo, H.; Gao, Y.; Feld W. A.; Hsieh, B. R. *Macromolecules*, **1997**, *30*, 6567. (b) Hsieh, B. R.; Yu, Y.; Forsythe, E. W.; Schaaf, G. M.; Feld, W. A. *J. Am. Chem. Soc.* **1998**, *120*, 231.

8 Peng, Z.; Zhang, J.; Xu, B. *Macromolecules* **1999**, *32*, 5162.

9 Ahn, T,; Song, S.-Y.; Shim, H.-K. *Macromolecules* **2000**, *33*, 6764.

10 Fan, Q.-L.; Lu, S.; Lai, Y.-H.; Huang, W. *Macromolecules* **2000**, submitted.

11 Liu, B.; Yu, W.; Lai, Y. H.; Huang, W. *Macromolecules* **2002**, *35*, 4975.

12 (a) Liao, L.; Pang, Y.; Ding, L.; Karasz, F. E. *Macromolecules* **2001**, *34*, 7300. (b) Liao, L.; Pang, Y.; Ding, L.; Karasz, F. E. *Macromolecules* **2001**, *34*, 7300.

13 The QDs of **P4'-P6'** were calculated according to the following equations: $(42 + 6x)/24 = I_{0.5\text{-}2.0}/I_{6.0\text{-}8.0}$ for **P4'** and **P5'** and $(38 + 6x)/24 = I_{0.5\text{-}2.0}/I_{6.0\text{-}8.0}$ for **P6'**, where x is the QD, $I_{0.5\text{-}2.0}$ is the integration of the peaks at 0.5-2.0 ppm and $I_{6.0\text{-}8.0}$ is the integration of the peaks at 6.0-8.0 ppm. The QD of **P2'** has been reported in our previous work (see reference 10).

14 Balanda, P. B.; Ramey, M. B.; Reynolds, J. R. *Macromolecules* **1999**, *32*, 3970.

15 Oelkrug, D.; Tompert, A.; Gierschner, J.; Egelhaaf, H.-J.; Hanack, M.; Hohloch, M.; Steinhuber, E. *J. Phys. Chem. B* **1998**, *102*, 1902.

CHAPTER THREE

Part II: Fluorescence Quenching of Cationic Poly(*p*-phenylenevinylene)s with Different Contents of *cis*-and *trans*-Vinylic Linkages

3.2.1 Introduction

Water-soluble fluorescent π-conjugated polymers (WSCPs) such as sulfonated poly(*p*-phenylenevinylene) (MPS-PPV) has attracted much interest because of their potential application in the development of highly efficient chemo or biosensors.[1] Their sensibility results from their fluorescence which is highly quenched by a low concentration of quencher through electron or energy transfer due to facile energy migration along the conjugated backbone and relatively strong binding of quencher with WSCPs via electronstatic attraction.[2] Recent findings showed that their sensibility was significantly influenced by many factors, such as effective conjugated length,[3] size of conjugated polymer chain,[4] charge on quencher,[5] ionic strength,[4] pH values,[6] coujugated polymer concentration,[7,8] concentration of surfactant[9,10] or polyelectrolyte[11,12] and type of substrate introduced.[11] However, as far as we know, up to now the significant influence to the quenching efficiency by the conformation of conjugated backbone was never investigated.

PPV is very appropriate for sensors because of its good color tunability and easy enhancement of PL quantum efficiency to meet the requirement from energy and

electron transfer through introduction of suitable units into conjugated backbone. In corresponding synthetic ways to obtain required PPV ccopolymers, the *cis*-vinylic linkage was inevitably introduced into the conjugated backbone of those copolymers, which may influence their sensitivity. Our recent research has shown that the cationic phenyl-substituted PPV with *cis*-vinylic linkage in the backbone (quenched by $Fe(CN)_6^{4-}$ in aqueous solution) exhibited downward Stern-Volmer curve,[13] which was contrary to the typical upward curve of MPS-PPV (quenched by MV^{2+} in aqueous solution) occupied entirely by *trans*-vinylic linkage.[2] Their obvious difference in quenching effect showed that the sensitivity may be related to the structure of the vinylic group in conjugated backbone. To improve new sensors with high sensitivity, it appears necessary to investigate the effect of *cis*-/*trans*-vinylic group on quenching efficiency.

In this paper, we report on the quenching effects of $Fe(CN)_6^{4-}$ in water and methanol on cationic phenyl-substituted poly(*p*-phenylenevinylene) related copolymers with *cis*-vinylic group via Wittig reaction and PPV homopolymers with entire *trans*-vinylic group prepared from Gilch reaction. The quenching of those quaternized polymers in HCl aqueous and/or HCl methanol solution and unquaternized polymers in CH_3COOH aqueous and/or CH_3COOH methanol solution were highly investigated and successfully demonstrated that the existence of *cis*-vinylic group in conjugated backbone indeed lower the quenching efficiency.

3.2.2 Materials and Characterization Methods

3.2.2.1 Materials

All neutral and quaternized amino-functionalized PPV derivatives (**Scheme 3.2.1**) were synthesized via Wittig and Gilch reaction in our lab according to the procedure we reported previously.[13,14] The quencher, $K_4Fe(CN)_6$, was obtained from Aldrich Chemical Co. The Milli-Q water and methanol used in preparing the aqueous solutions of those polymers and quenchers was purged with nitrogen for 4 h before using.

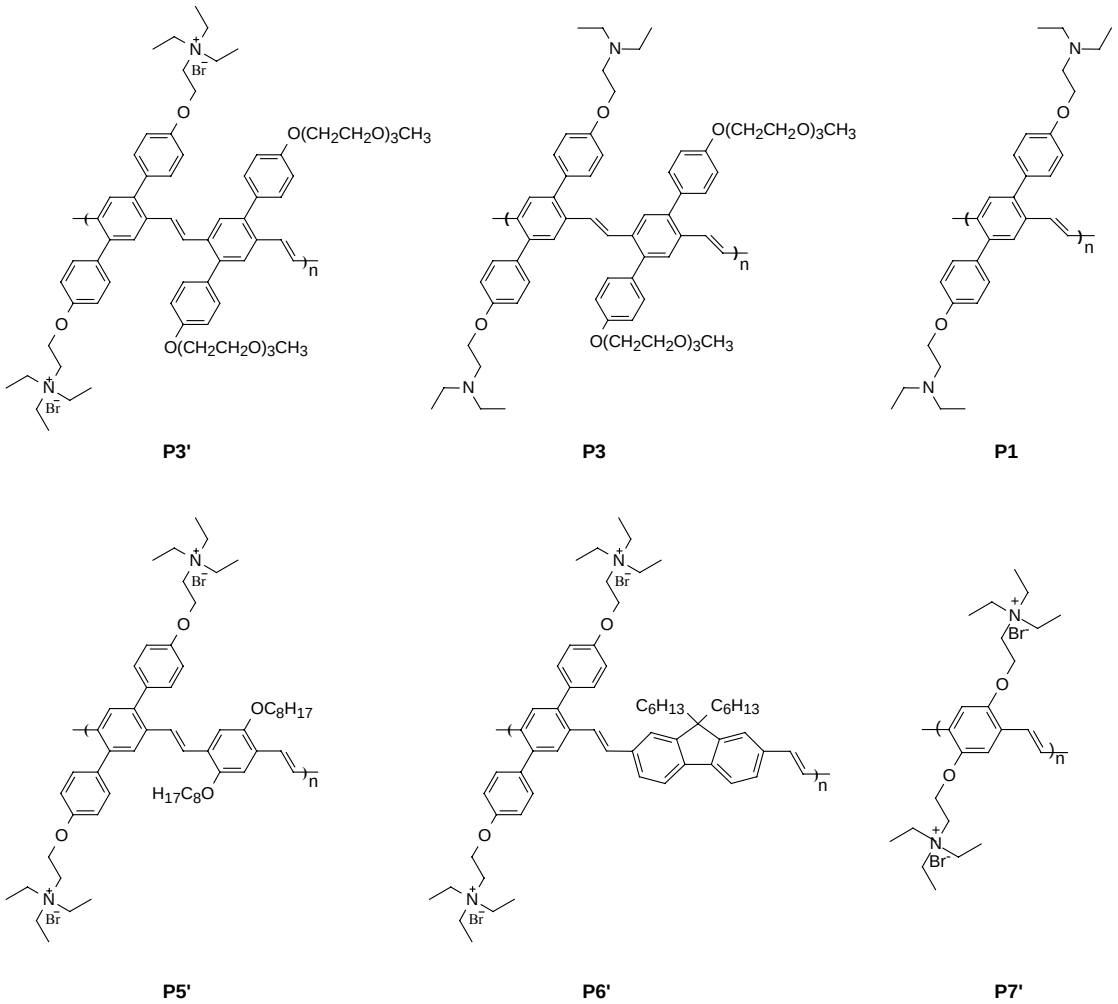

Scheme 3.2.1 Chemical structure of neutral and quaternized PPVs used in our investigation

3.2.2.2 Characterization Methods

UV-vis spectra were recorded on a Shimadzu 3101 PC spectrometer. Fluorescence measurement was carried out on a Perkin-Elmer LS 50B photoluminescence spectrometer with a xenon lamp as a light source. The quenching studies were realized *in situ* through comparing the photoluminescence intensities of the solutions at a series of detector and quencher concentration. All the quenched solutions were prepared after adding calculated amount of quencher solution into PPVs' solutions and purging with nitrogen for 1 min and immediately used to take their corresponding absorption spectra and emission spectra.

3.2.3 Results and Discussion

The fluorescence quenching generally includes static quenching and dynamic quenching. Each quenching behavior can be simply described by the Stern-Volmer equation[15]:

$$\frac{F_0}{F} = 1 + K_{sv}[Q] \tag{1}$$

In this equation, F_0 is the fluorescence intensity with no quencher present, F is the fluorescence intensity with quencher present, [Q] is the quencher concentration and K_{sv} is the Stern-Volmer constant. Both dynamic and static quenching follow linear Stern-Volmer plot (F_0/F~[Q]).

However, most fluorescent WSCPs exhibited upward Stern-Volmer curves and the concept of sphere-of-action was introduced into Stern-Volmer equation to account for

such upward curves:[4]

$$\frac{F_0}{F} = (1 + K_{sv}^{S}[Q])e^{\alpha V[Q]} \tag{2}$$

where K_{sv}^{S} is the static quenching constant, V is volume constant and α is used to account for the charge-induced enhancement of the local quencher concentration.

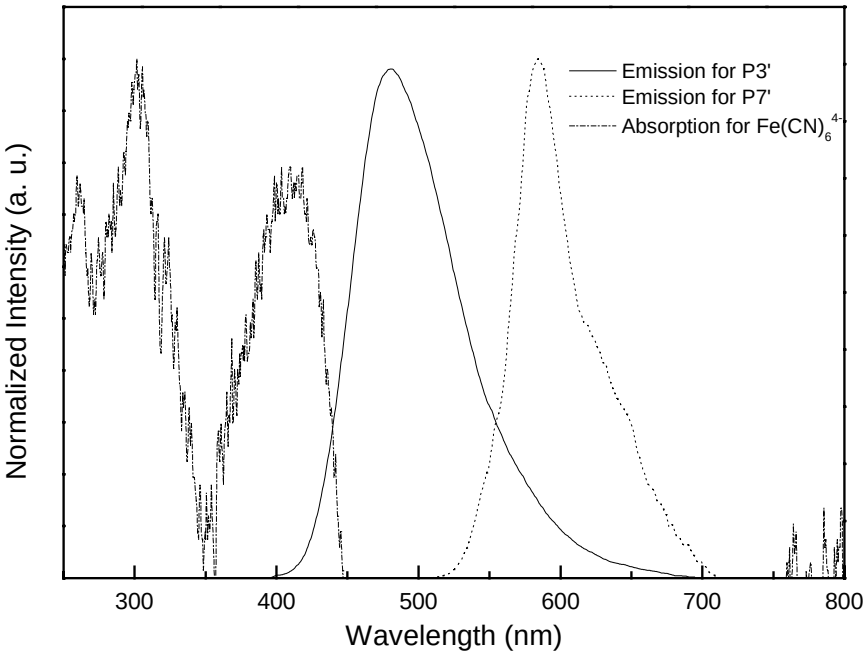

Figure 3.2.1 Absorption of $Fe(CN)_6^{4-}$ (10 μM) and emission spectra of P3' (1.25 μM) and P7' (1.25 μM) in aqueous solution

As we reported previously, **P3'** with 80% *cis*-vinylic group showed downward Stern-Volmer curve and the existence of unquenched fluorescence intensity when quenched by $Fe(CN)_6^{4-}$ in aqueous solution,[13] which was highly different with the general upward curves and complete quenching obtained in other fluorescent WSCPs. Such an incomplete quenching can be attributed to two possible reasons, one is incomplete energy transfer if the quenching mechanism was energy transfer, the other

is the existence of unquenched fluorophore which cannot be touched by $Fe(CN)_6^{4-}$.[15] To explain this downward curve, firstly we must investigate the quenching mechanism of this system. As we referred above, the fluorescence quenching of WSCPs was realized through two ways, energy or electron transfer between quencher and WSCPs. Harrison et al. have studied the quenching of PPP-NEt_3^+ by $Fe(CN)_6^{4-}$ and proposed that this quenching may occur by energy transfer.[7] To testify this proposition, **P7'** was chosen by our group to study the quenching. **Figure 3.2.1** showed the UV-vis absorption spectrum of $Fe(CN)_6^{4-}$ and the emission spectra of **P3'** and **P7'** in aqueous solution and **Figure 3.2.2** showed the Stern-Volmer plots of **P3'** and **P7'** quenched by $Fe(CN)_6^{4-}$ in aqueous solution. From **Figure 3.2.1**, we could see that there is only a little overlapping between the emission spectrum of **P3'** and the absorption spectrum of $Fe(CN)_6^{4-}$. Thus, if incomplete energy transfer was the real reason to lead to the incomplete quenching of **P3'** by $Fe(CN)_6^{4-}$, **P7'** will surely not be quenched by $Fe(CN)_6^{4-}$ through energy transfer because of no overlapping of the emission spectrum of **P7'** and the absorption spectrum of $Fe(CN)_6^{4-}$. However, from **Figure 3.2.2**, it can be seen that **P7'** was efficiently quenched by $Fe(CN)_6^{4-}$ and a typical upward Stern-Volmer curve was obtained, which clearly demonstrated that energy transfer was not the way to realize the quenching of **P7'**. Instead, it could be anticipated that it is electron transfer to result in the quenching of **P7'**. Therefore, although a little overlapping existed between the emission spectrum of **P3'** and the absorption spectrum of $Fe(CN)_6^{4-}$ and a little energy transfer existed between **P3'** and $Fe(CN)_6^{4-}$, electron transfer was the major way to realize the quenching of **P3'** and the incomplete

quenching of **P3'** did not result from the incomplete energy transfer. Thus we conclude that the existence of inaccessible fluorophore resulted in the downward Stern-Volmer curve of **P3'**.

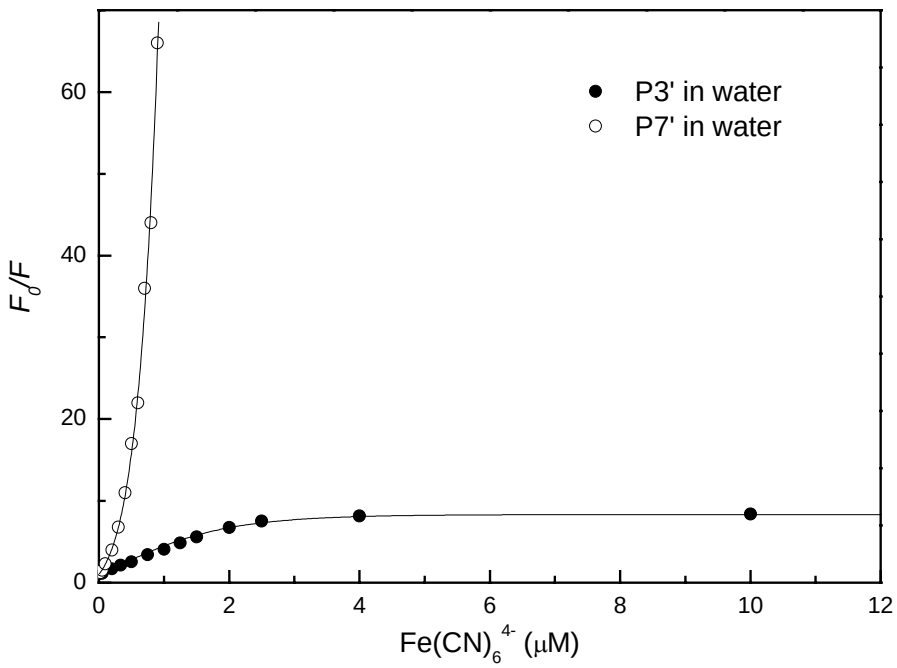

Figure 3.2.2 Stern-Volmer plot of P3' (1.25 μM) and P7' (1.25 μM) quenched by $Fe(CN)_6^{4-}$ in water

Generally, considering the inaccessible fluorophore, equation 1 was changed into

$$\frac{f_a F_0}{F-(1-f_a)F_0} = (1+K_{sv}[Q]) \tag{3}$$

$$f_a = \frac{F_{0a}}{F_{0a}+F_{0b}} \tag{4}$$

where F_{0a} is the fluorescence intensity from an accessible fluorophore, F_{0b} is the fluorescence intensity from an inaccessible fluorophore and f_a is the fraction of fluorescence from an accessible fluorophore. After rearrangement equation 4 became

$$F_0/(F_0 - F) = 1/(f_a K_{sv}[Q]) + 1/f_a \quad (5)$$

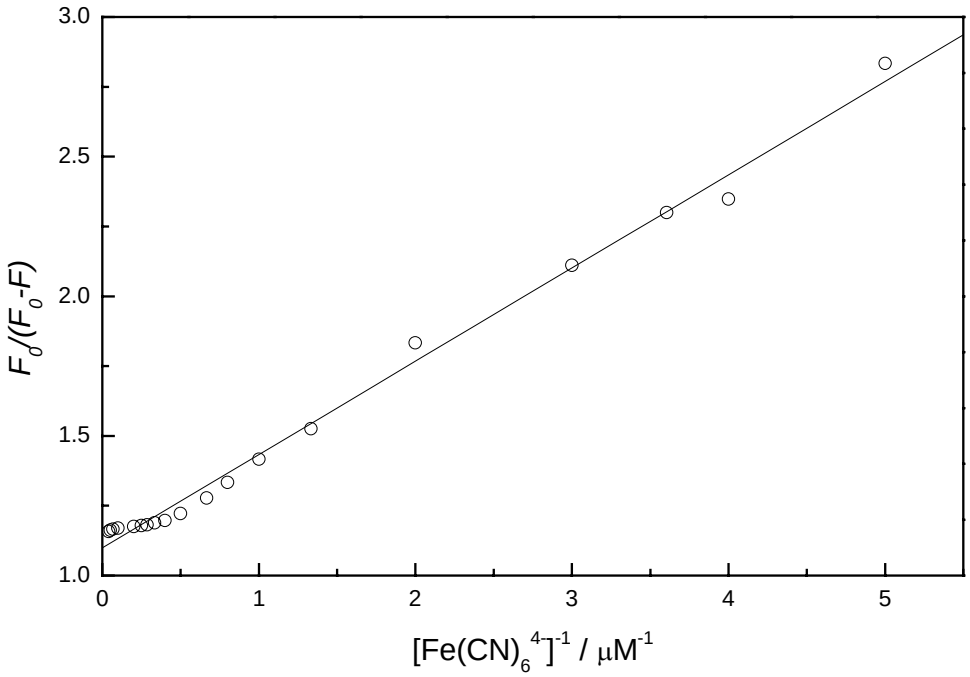

Figure 3.2.3 Modified Stern-Volmer plot of P3' (1.25 μM) in Figure 3.2.2

Thus a linear dependence of $F_0/(F_0 - F)$ on $1/[Q]$ can be obtained from equation 5. In **Figure 3.2.3**, the Stern-Vlomer plot of **P3'** according to equation 5 showed linearity when the value of 1/[Q] was high but nonlinearity when 1/[Q] was low. Meanwhile, equation 3 can not well fit the Stern-Volmer curve of **P3'** in **Figure 3.2.2** which indicated that other factors exited to influence the Stern-Volmer plot. Therefore, sphere-of-action was considered in our system and equation 3 was modified to describe the relationship between the fluorescence intensity and quencher concentration:

$$\frac{f_a F_0}{F - (1 - f_a)F_0} = (1 + K_{sv}[Q])e^{\alpha V[Q]} \quad (6)$$

After rearrangement equation 6 became

$$\frac{F_0}{F} = \frac{(1+K_{sv}[Q])e^{\alpha V[Q]}}{f_a + (1-f_a)(1+K_{sv}[Q])e^{\alpha V[Q]}} \quad (7)$$

With best fit on those Stern-Volmer curves by equation 7, the K_{sv}, f_a and αV values were obtained and listed in **Table 3.2.1**.

Table 3.2.1 Photoluminescence Quenching of Cationic PPVs by $Fe(CN)_6^{4-}$

	Solvent	Content of *cis*-vinylic group	K_{sv} (M^{-1})	αV	f_a
	H_2O		3.2×10^6	7.1×10^5	0.88
P3'	CH_3OH	80%	1.6×10^6	7.7×10^5	0.86
	HCl in H_2O		3.4×10^6	7.8×10^5	0.88
P3	CH_3COOH in H_2O	80%	3.4×10^6	7.6×10^5	0.89
P1	CH_3COOH in H_2O	—	4.0×10^6	7.0×10^5	—
P5'	CH_3OH	55%	2.0×10^6	8.0×10^5	0.94
P6'	CH_3OH	45%	2.2×10^6	8.1×10^5	0.95
P7'	H_2O	—	8.0×10^6	2.3×10^6	—

Now investigating the origin of the inaccessible fluorophore became very important to develop highly efficient chemo or biosensors. Interchain aggregation may be one of the possible factors which produce inaccessible fluorophore. We have reported that **P3'** had good solubility in methanol and poor solubility in water at room temperature and could be dissolved in warm water at 50 ^oC.[13] Thus, aggregation may exist in **P3'** aqueous solution and some fluorophore may be buried inside and cannot be touched by quencher and consequently the incomplete quenching appeared. The quenching of **P3'** by $Fe(CN)_6^{4-}$ in aqueous solution and methanol were compared with each other to show if aggregation play a major role on the inaccessible fluorophore of **P3'** in water. As we referred above that **P3'** had much better solubility in methanol than that in water, the solubility-induced aggregation of **P3'** in water was surely considered to be much

higher than in methanol, which means that the content of the unquaternized fluorophore in methanol will lower than that in water. **Figure 3.2.4** showed the Stern-Volmer plots of **P3'** quenched by $Fe(CN)_6^{4-}$ in methanol and water. In **Figure 3.2.4**, all the Stern-Volmer plots of **P3'** were downward curves, no matter whether **P3'** was in water or methanol, indicating the unquenched fluorophore of **P3'** in methanol still existed. Although the quenching efficiency of **P3'** in methanol (K_{sv} value) was a little lower than that in water, they had nearly the same content of unquenched fluorophore. Such an unchanged content of unquenched fluorophore of **P3'** in different solution demonstrated that the existence of unquenched fluorophore of **P3'** was not related to the solvent-induced aggregation.

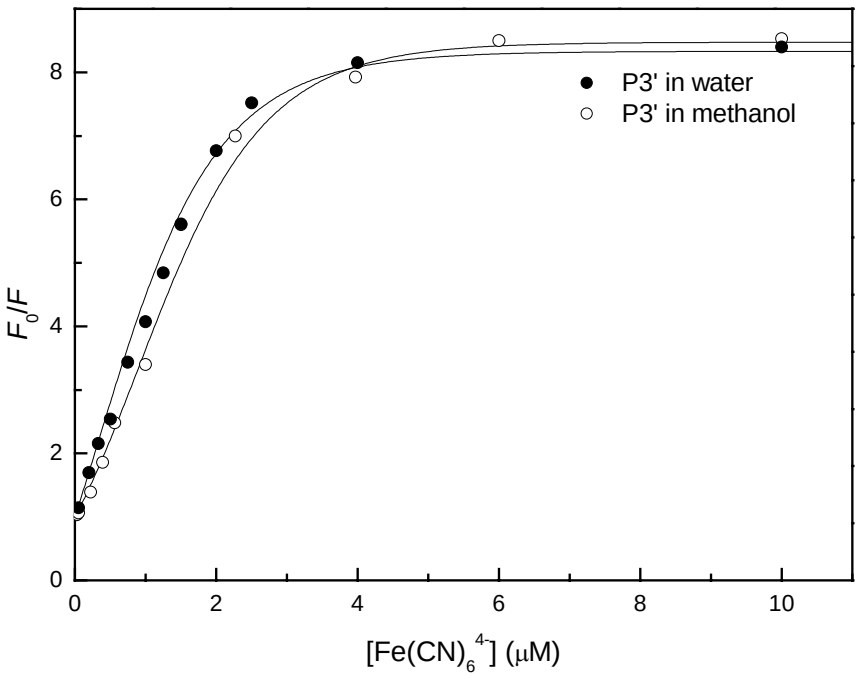

Figure 3.2.4 Stern-Volmer plot of P3' (1.25 μM) by $Fe(CN)_6^{4-}$ in water and methanol

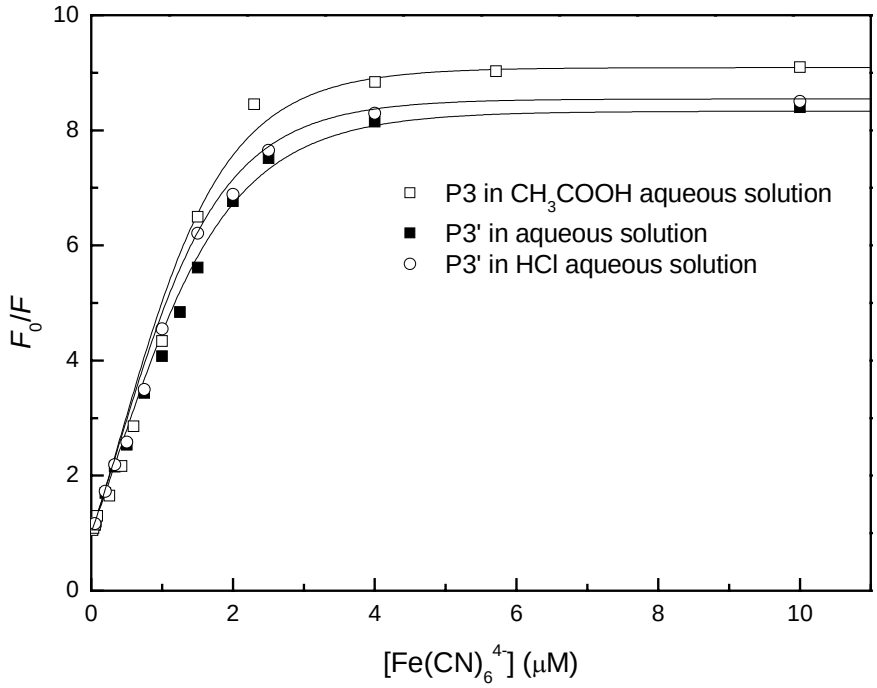

Figure 3.2.5 Stern-Volmer plot of quaternized polymer P3' (1.25 μM) by $Fe(CN)_6^{4-}$ in water and HCl aqueous solution (1 mM) and neutral polymer P3 (1.25 μM) in CH_3COOH aqueous solution (1 mM)

Previous study showed that the incomplete quaternization always exists in those quaternized polymers which was obtained through post-reaction from their corresponding neutral polymers.[16,17] Such an incomplete quaternization may be one of the explanation to the incomplete quenching that some fluorophore cannot touch with $Fe(CN)_6^{4-}$ by the traditional electrostatic attraction. It is well known that unquaternized amino group can be easily acidified by HCl or CH_3COOH to form ammonium ions and thus we could anticipated that adding acid will change unquaternized amino group into ammnium ions and decrease the content of inaccessible fluorophore through enhanced electrostatic attraction of **P3'**. Our previous work had shown that neutral conjugated polymer could be dissolved well in CH_3COOH aqueous solution.[17b] Therefore, to study

if the incomplete quenching resulted from the incomplete quaternization, the quenching of **P3'** in aqueous solution and HCl aqueous solution and neutral polymer in CH_3COOH aqueous solution was investigated. In **Figure 3.2.5**, the neutral polymer in CH_3COOH aqueous solution exhibits the highest K_{sv} value than those of quaternized polymer in aqueous solution and HCl aqueous solution which were nearly the same with each other. However, all the neutral and quaternized polymer showed downward Stern-Volmer curves and had the same content of inaccessible fluorophore, indicating that the enhancement of ionic content on the polymer chains did not increase the mutual interaction between the inaccessible fluorophore and quencher $Fe(CN)_6^{4-}$ and the incomplete quaternization was not the major reason to result in the existence of inaccessible fluorophore.

Based on those investigations above, it is reasonable to propose that the conformation of conjugated backbone in PPV be the main factor to form those inaccessible fluorophore. It is well known that the *cis*-/*trans*-vinylic linkage both exist in the PPV backbone obtained through Wittig reaction while 100% *trans*-vinylic linkage is formed through Gilch reaction. The different conformation may render PPVs to appear different quenching effect. Thus, for disclosing the relationship between the conformation of vinylic linkage and the quenching effect, it is necessary to compare the quenching of PPVs via Wittig reaction with that of PPVs via Gilch reaction. However, as we reported previously, the neutral polymer **P1**, synthesized from Gilch reaction, cannot be dissolved in any common organic solvent which blocked the further formation of its quaternized polymer via post-reaction.[13] Fortunately under

organic acid-assistance, **P1** can be well dissolved in water and methanol. Therefore the influence on quenching from the conformation of vinylic linkage can be investigated through comparing the quenching effect of the neutral polymers with each other in organic acid aqueous solution. **Figure 3.2.6** showed the Stern-Volmer plots of those neutral polymers in CH_3COOH aqueous solution.

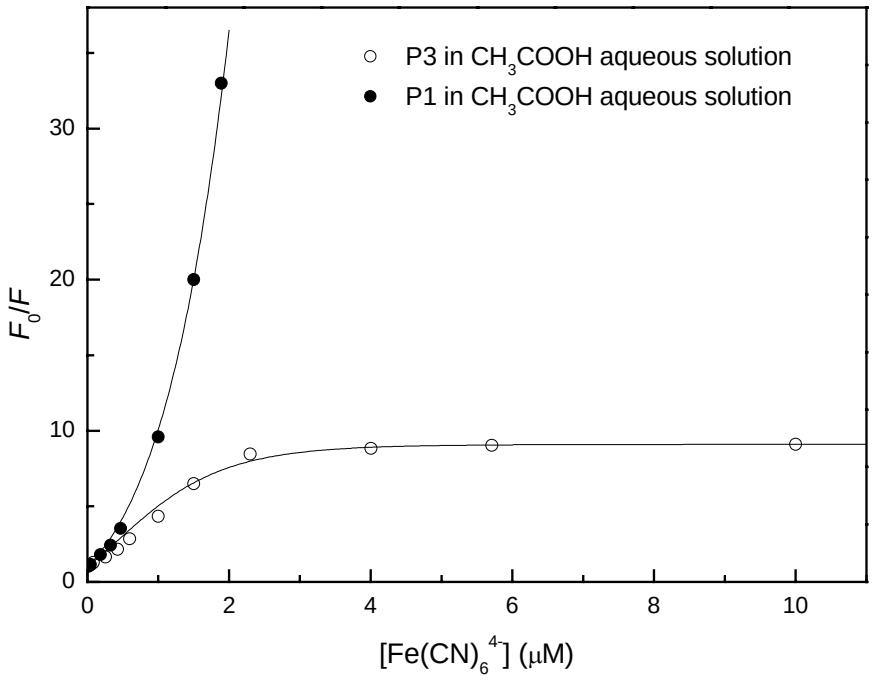

Figure 3.2.6 Stern-Volmer plot of P3 (1.25 μM) and P1 by $Fe(CN)_6^{4-}$ in CH_3COOH aqueous solution

In **Figure 3.2.6**, **P3** with *cis*- and *trans*-vinylic linkage showed a downward curve while **P1** with *trans*-vinylic linkage exhibited an upward curve, which dramatically demonstrated that the unquenched fluorophore in **P3'** was highly related to the existence of *cis*-vinylic linkage in its conjugated backbone. **Scheme 3.2.2** described the conformation of one unit of **P3** and **P1**. From **Scheme 3.2.2** we could see that

when *cis*-vinylic linkage existed, the steric effect from phenyl-substituted group became more and more obvious and the conformation of **P3** chain was more twisted (lower effective conjugated length) and disordered than that of **P1** with complete *trans*-vinylic linkage. We could anticipate that such a disorder made some fluorophore of **P3'** buried inside and meanwhile the steric effect from bulky phenyl group blocked the interaction between fluorophore and the arrested quencher through electrostatic attraction, all of which inevitably lead to the presence of unquenched fluorophore in **P3'**. Furthermore, the K_{sv} value of **P1** was higher than that of **P3'**, indicating the existence of shorter effective conjugated length in **P3'** conjugated chain.

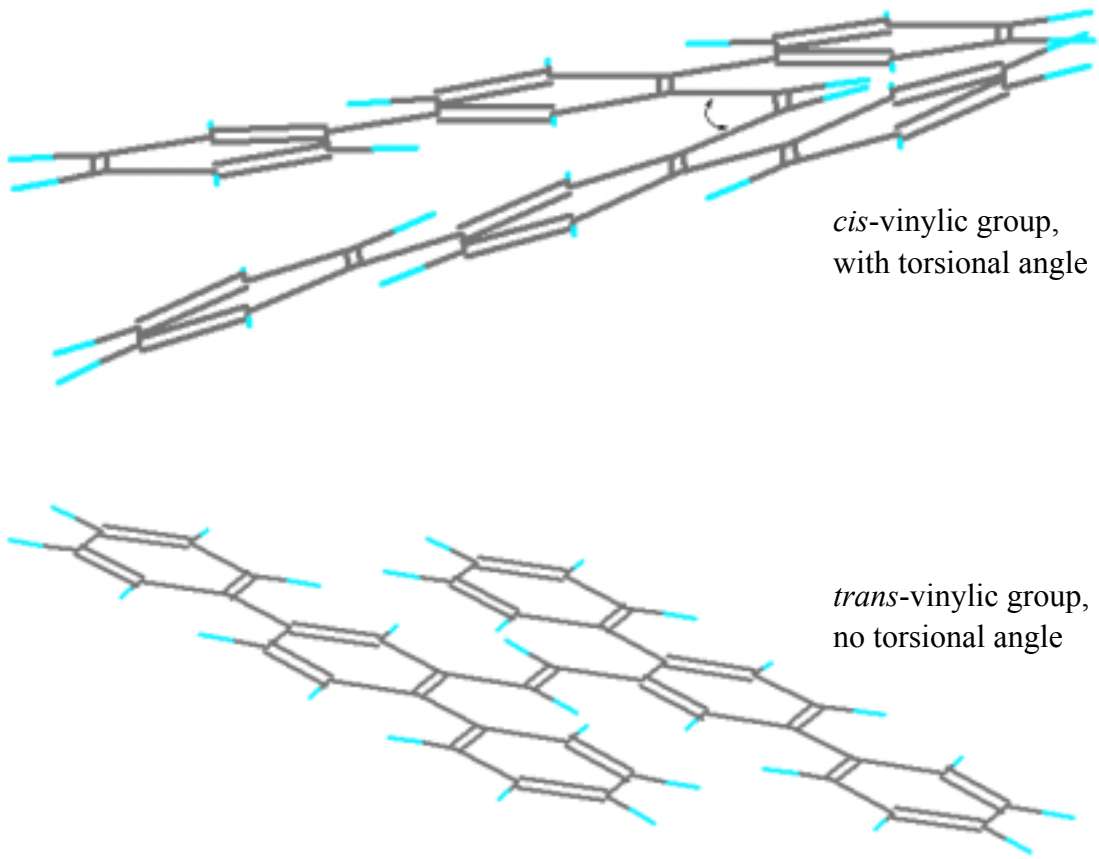

Scheme 3.2.2 The conformation of one unit of P3 and P1

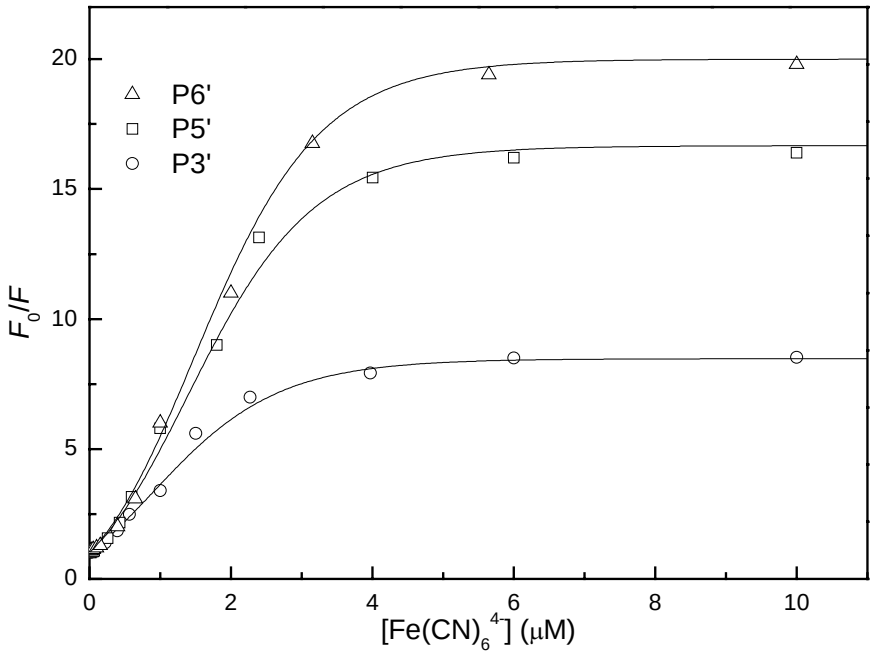

Figure 3.2.7 Stern-Volmer plot of P3', P5' and P6' by $Fe(CN)_6^{4-}$ in methanol

We also studied the influence on quenching effect from the different units in PPV conjugated backbone. The Stern-Volmer plots of cationic phenyl-substituted PPV related copolymers **P3'**, **P5'** and **P6'** obtained through Wittig reaction were shown in **Figure 3.2.7**. All the PPV copolymers with *cis*-vinylic linkage displayed downward curves which further indicated the quenching influence from *cis*-vinylic linkage. In **Table 3.2.1**, **P5'** and **P6'** with 55% and 45% *cis*-vinylic linkage respectively showed nearly the same content of accessible florophore at about 95%, both of which is higher than that (88%) of **P3'** with 80% *cis*-vinylic linkage. It is indicated that the content of inaccessible fluorophore was decreased accordingly with the decrease of the content of *cis*-vinylic group in PPV backbone. Meanwhile, the K_{sv} values of **P5'** and **P6'** were a little higher than that of **P3'**, which may also be explained by the existence of different

content of *cis*-vinylic linkage which lowers the effective conjugated length and thus decreases the quenching efficiency.

3.2.4 Conclusions

In summary, we studied the quenching effect of $Fe(CN)_6^{4-}$ on cationic PPV derivatives with *cis*- and/or *trans*-vinylic linkage and downward Stern-Volmer curves was found in PPVs with *cis*-/*trans*-vinylic linkage while upward Stern-Volmer curves in PPVs with all *trans*-vinylic linkage. Electron transfer, not energy transfer, was the major way to result in quenching of PPVs with *cis*-linkage and those downward curves presented the incomplete quenching from inaccessible fluorophore. After considering the inaccessible fluorophore and sphere-of-action effect, a modified Stern-Volmer equation was obtained to well fit the downward Stern-Volmer curve of PPVs with *cis*-linkage. The existence of *cis*-vinylic linkage was considered to be the key factor to produce such inaccessible fluorophore. Changing the molecular structures of alternating units in those PPV copolymers could significantly influence the corresponding quenching behavior and the content of inaccessible fluorophore.

References and Notes

1 McQuade, D. T.; Pullen, A. E.; Swager, T. M. *Chem. Rev.* **2000**, *100*, 2537.

2 Chen, L.; McBranch, D. W.; Wang, H.-L.; Helgeson, R.; Wudl, F.; Whitten, D. G. *Proc. Natl. Acad. Sci. U. S. A.* **1999**, *96*, 12287.

3 Gaylord, B. S.; Wang, S.; Heeger, A. J.; Bazan, G. C. *J. Am. Chem. Soc.* **2001**, *123*, 6417.

4 Wang, J.; Wang, D. L.; Miller, E. K.; Moses, D.; Bazan; G. C.; Heeger, A. J. *Macromolecules* **2000**, *33*, 5153.

5 Wang, D. L.; Wang, J.; Moses, D.; Bazan; G. C.; Heeger, A. J. *Langmuir* **2001**, *17*, 1262.

6 Fan, C.; Plaxco, K. W.; Heeger, A. J. *J. Am. Chem. Soc.* **2002**, *124*, 5642.

7 Harrison, B. S.; Ramey, M. B.; Reynolds, J. R.; Schanze, K. S. *J. Am. Chem. Soc.* **2000**, *122*, 8561.

8 Tan, C.; Pinto, M. R.; Schanze, K. S. *Chem. Commun.* **2002**, 446.

9 Chen, L.; McBranch, D.; Wang, R.; Whitten, D. G. *Chem. Phys. Lett.* **2000**, *330*, 27.

10 Chen, L.; Xu, S.; McBranch, D.; Whitten, D. G. *J. Am. Chem. Soc.* **2000**, *122*, 9302.

11 Jones, R. M.; Bergstedt, T. S.; McBranch, D. W.; Whitten, D. G. *J. Am. Chem. Soc.* **2001**, *123*, 6726.

12 Stork, M.; Gaylord, B. S.; Heeger, A. J.; Bazan, G. C. *Adv. Mater.* **2002**, *14*, 361.

13 Fan, Q.-L.; Lu, S.; Lai, Y.-H.; Huang, W. *Macromolecules* **2003**, submitted.

14 Fan, Q.-L.; Lu, S.; Lai, Y.-H.; Huang, W. *Langmuir* **2003**, submitted.

15 Lakowicz, J. R. in *Principles of Fluorescence Spectroscopy*, 2nd ed.; Plenum Press: New York, **1999**.

16 Balanda, P. B.; Ramey, M. B.; Reynolds, J. R. *Macromolecules* **1999**, *32*, 3970.

17 (a) Liu, B.; Yu, W.; Lai, Y.-H.; Huang, W. *Chem. Comm*. **2000**, 551. (b) Liu, B.; Yu, W.; Lai, Y.-H.; Huang, W. *Macromolecules* **2002**, *35*, 4975.

CHAPTER FOUR

Part I: Synthesis, Characterization and pH-Sensitive Optical Properties of Cationic Water-Soluble Poly(*p*-phenyleneethynylene)s

4.1.1 Introduction

Fluorescent water-soluble conjugated polymers (FWSCPs) containing charged groups have great potential as novel chemo or biosensors due to their amplified quenching of fluorescence upon electrostatic attraction by ionic quenchers.[1] Anionic water-soluble sulfonated poly(phenylene vinylene) (MPS-PPV), the first and most intensively studied FWSCP by scientists on fluorescence quenching, was reported that its fluorescence can be highly quenched by cationic electron acceptors, such as methyl viologen (MV^{2+}), through electron transfer and after grafting viologen on a biotin.[2] The detection of specific protein (avidin) was successfully realized via the fluorescence recovering upon the quencher removing from the conjugated chains by the formation of biodin-avidin complex. The utility of FWSCPs as biosensor builds up a very simple way to detect different types of biomolecules with high sensitivity, just through observing the fluorescence quenching/recovering procedure.

To develop FWSCP-based biosensors with high sensitivity, most researches were focused on the influence of local chemical environment on fluorescence quenching of FWSCPs and showed that the sensitivity of FWSCPs was tied up with the local chemical environment around them because their optical properties were strongly controlled by the conformation of conjugated main chains which varied according to the variation of chemical environment, such as ionic strength,[3] charge on quencher,[4] concentration of surfactant[5,6] or polyelectrolyte,[7,8] and type of substrate added.[7] All of

the above investigation was preceded in neutral chemical environment. However, it is well known that some biomolecules are alive and work in acid or base environment and detecting such biomolecules must be held at aqueous environment with different pH values. Recently Fan reported that changing pH value could control the protein's (analyte) charge state and thus tune the sensitivity of MPS-PPV (detector) over more than 6 orders of magnitude,[9] while the influence of pH on the optical properties of FWSCPs (detectors) themselves, which may change their sensitivity, was never investigated. Study on the variation of optical properties and sensitivities of FWSCPs in different pH aqueous solution is now becoming more and more significant to obtain good biosensors.

Anionic WSCPs, such as MPS-PPV, have been the subject of intensive studies recently.[2-7,9] However, theoretical and practical studies on cationic FWSCPs are rare,[8,10] which dramatically limits the use of WSCPs in detecting the anionic analytes through electrostatic attraction. Recently, cationic water-soluble polyfluorene was developed to identify anionic DNA through energy transfer and exhibited the wide perspective of cationic conjugated polymers as sensors.[11]

Poly(*p*-phenyleneethynylene) (PPE) is a kind of conjugated polymer which has been widely used to study optical property-structure relationship because of its good optical response on environmental variation through the facial changeable torsion angle and interchain aggregation. Its application as chemosensor has been widely reported by Swager's group.[12-16] Most recently the anionic water-soluble PPEs were utilized to study the contribution of polymer aggregation on sensitivity[17] and detect specific DNA.[18] Thus, it is reasonable to conceive that cationic water-soluble PPEs are good candidates for studying the variation of optical properties and sensitivity of FWSCPs at different pH values and developing novel good biosensors.

Herein we report the successful synthesis of cationic poly(phenyleneethynylene) (PPE) polyelectrolytes based on ammonium-functionalized groups. In an attempt to develop intrinsically water-soluble PPE polyelectrolytes, we synthesized three cationic PPE polymers containing respective side chains with different hydrophilicity. Their optical properties were investigated and compared with each other. The variation of optical properties and sensitivity of one water-soluble PPE according to different pH values and polymer concentrations were investigated and showed obvious pH-dependent fluorescence intensity and sensitivity of such a cationic PPE.

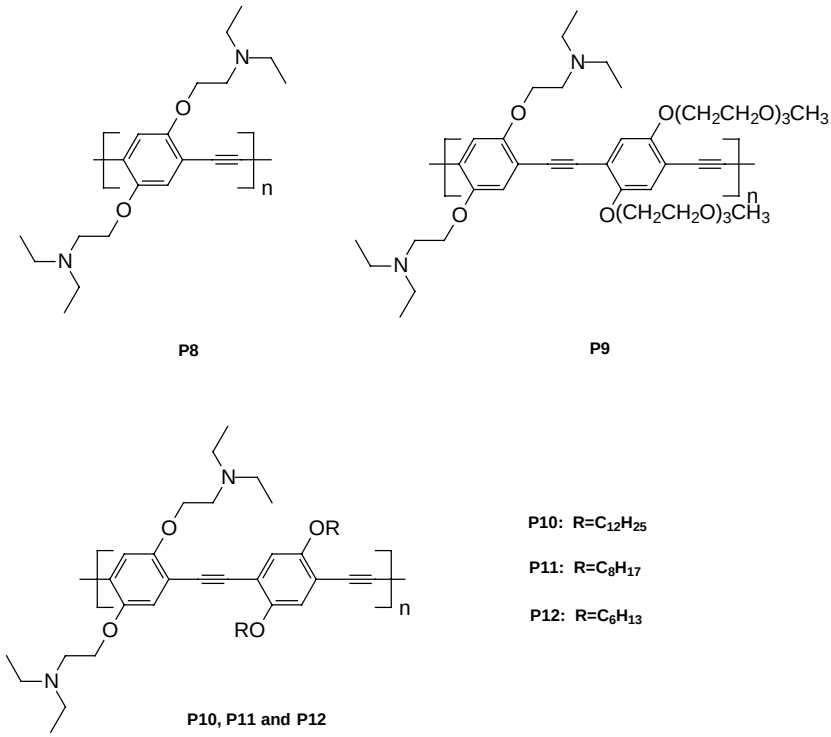

Figure 4.1.1 The designed neutral polymers for cationic PPEs

4.1.2 Molecular Design

In order to synthesize cationic PPEs, tertiary amine as the functional group was designed for the neutral polymer, which upon quaternization with bromoethane, could afford cationic polymers. To obtain water-soluble PPEs, tertiary amine group was introduced into every side chain. Because of the short alkoxy group (tertiary amine

group) on the side chain and the high rigidity of the PPE backbone, the molecular weight of the fully amino-functionalized PPE may not grow higher. To get high molecular weight, besides the tertiary amine groups in one moiety of side chains, long chains, tri(ethylene glycol)methyl ether groups with hydrophilic properties and alkoxy groups with hydrophobic properties, were added into the rest of side chains respectively. The chemical structures of the designed neutral polymers are illustrated in **Figure 4.1.1**.

4.1.3 Materials and Characterization Methods

4.1.3.1 Materials

All chemical reagents used were purchased from Aldrich Chemical Co. THF and Toluene was purified by distillation from sodium in the presence of benzophenone. Other organic solvents were used without any further purification.

4.1.3.2 Characterization Methods

The NMR spectra were collected on a Bruker Advance 400 spectrometer with tetramethylsilane as the internal standard. FT-IR spectra were recorded on a Bio-Rad FTS 165 spectrometer by dispersing samples in KBr. Mass spectra (MS) were obtained using a micromass VG 7035E mass spectrometer at an ionizing voltage of 70 eV. UV-vis spectra were recorded on a Shimadzu 3101 PC spectrometer. The concentrations of copolymer solutions were adjusted to about 0.01 mg/mL or less. Fluorescence measurement was carried out on a Perkin-Elmer LS 50B photoluminescence spectrometer with a xenon lamp as a light source. TGA measurements were performed on a TA Instruments Hi-Res TGA 2950 Thermogravimetric Analyzer at a heating rate of 10 °C/min under N_2. Elemental

microanalyses were carried out by the Microanalysis Laboratory of the National University of Singapore. Gel permeation chromatography (GPC) analysis was conducted with a Waters 2690 separation module equipped with a Waters 2410 differential refractometer HPLC system and three 5 μm Waters Styragel columns (pore size: 10^3, 10^4 and 10^5 Å) in series, using polystyrenes as the standard and tetrahydrofuran (THF) as the eluant at a flow rate of 1.0 mL/min and 35 °C.

The quenching behavior was studied by comparing the fluorescence intensities of polymer aqueous solutions in the presence of quenchers with different concentrations. The Milli-Q water used in preparing the aqueous solutions of those polymers and quenchers was purged with nitrogen for 4 h before using.

4.1.4 Results and Discussion

4.1.4.1 Synthesis of Monomers and Polymers

The preparation of monomers was shown in **Schemes 4.1.1.** 2,5-bis[3-(*N*,*N*-diethylamino)-1-oxapropyl)-1,4-diiodobenzene] (Monomer **8**) was prepared from 2,5-diiodohydroquinone by a reaction with 2-(diethylamino) ethyl chloride hydrochloride in refluxing acetone in the presence of excess anhydrous potassium carbonate. Consequently, treating Monomer **8** with trimethylsilyl acetylene afforded di(trimethylsilyl)ethynyl compounds which was further converted to the key Monomer **9** under base treatment. The 1,4-dialkoxybenzene obtained from 1,4-hydroquinone by reaction with 1-bromohexane, 1-bromooctane or 1-bromodedoxane in refluxing ethanol in the presence of C_2H_5ONa. 1,4-di{2-[2-(2-Methoxyethoxy)ethoxy]ethoxy}benzene was prepared from 2-[2-(2-Methoxyethoxy)ethoxy]ethyl-*p*-toluenesulfonate with 1,4-hydroquinone in refluxing acetone in the presence of excess anhydrous potassium carbonate. Direct

bromination of all the 1,4-alkoxybenzene with Br_2 in $CHCl_3$ afforded 2,5-bis(alkoxy)-1,4-dibromobenzene. 1,4-Diiodo-2,5-Bis{2-[2-(2-Methoxyethoxy) ethoxy]ethoxy}benzene was obtained through direct iodonation of 1,4-Di{2-[2-(2-Methoxyethoxy)ethoxy]ethoxy}benzene with I_2/KIO_3. Similarly, treating those dibromo or diiodo compounds with trimethylsilyl acetylene afforded di(trimethylsilyl)ethynyl compounds which were further converted to Monomer **10-13** under base treatment.

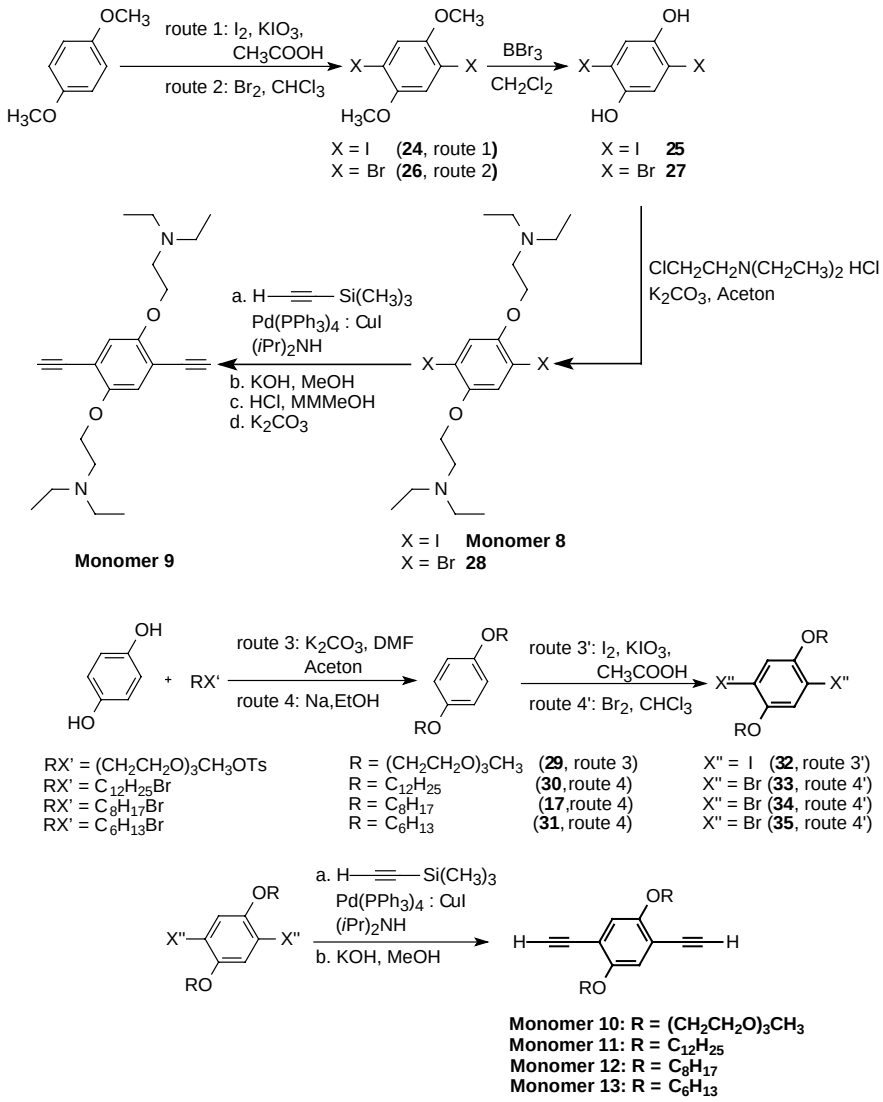

Scheme 4.1.1 The synthetic route for monomers

Syntheses of the polymers were outlined in **Scheme 4.1.2**. The preparation of neutral polymers **P8-P12** was accomplished via Heck-coupling reaction of corresponding Monomer **9-13** with Monomer **8** in the mixture of toluene and diisopropylamine solution in the presence of $Pd(PPh_3)_4$/CuI catalyst at 70 ^oC for one day. Conversion of the neutral polymers to the final cationic polymers was achieved by treating **P8-P12** with bromoethane in the mixture of dimethyl sulfoxide (DMSO) and tetrahydrofuran (THF) (1:4) at 50 ^oC for 5 days.[19,20]

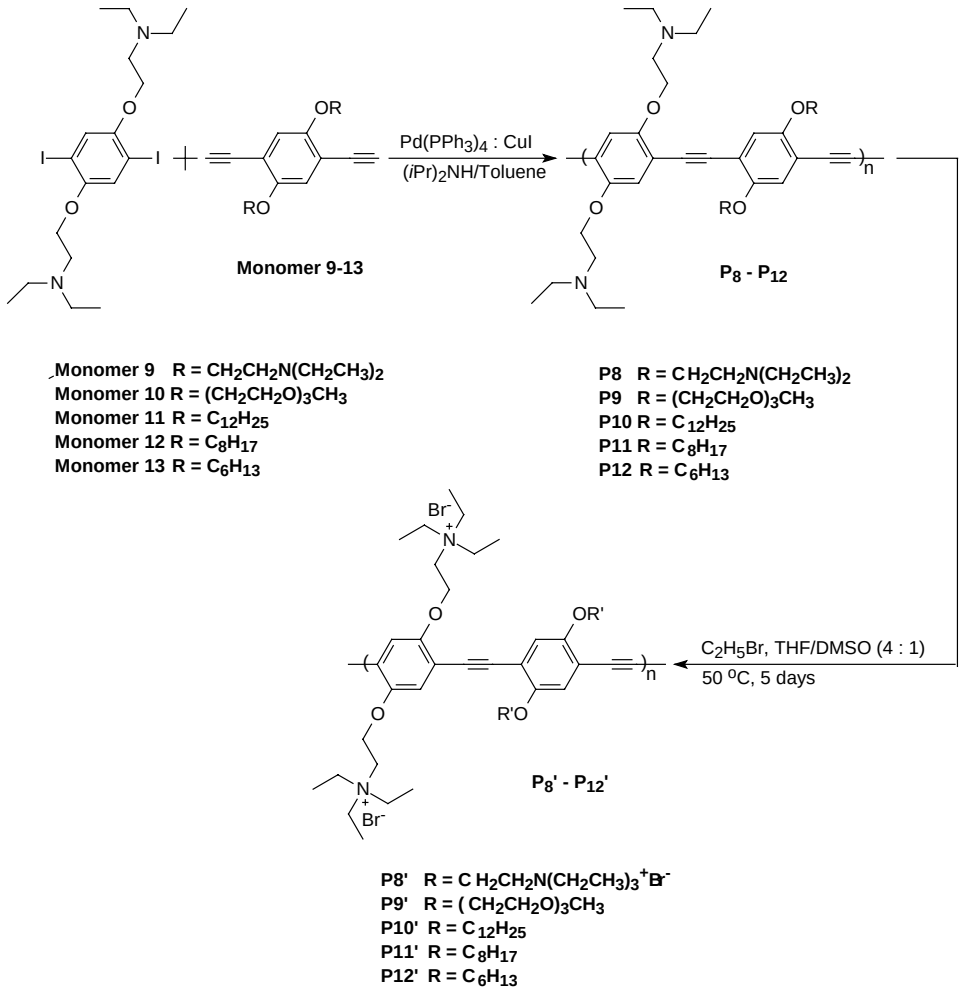

Scheme 4.1.2 The synthetic routes for neutral and quaternized PPEs

4.1.4.2 Solubility and Color Study

All of the neutral polymers **P8-P12** were readily soluble in common organic solvents

such as chloroform and THF but insoluble in methanol, DMSO and DMF. During the post-quaternization, the precipitates of **P11'** and **P12'** appeared in the mixture of THF/DMSO (4:1). Furthermore, it was found that the time needed for the appearance of precipitates of **P11'** and **P12'** increased in sequence. It is well known that the formation of quaternized groups would decrease the solubility of the neutral polymers in the main solvent THF. Thus, to some quaternized degrees, it is no doubt that the formed cationic polymers may precipitate from the mixture solvent. However, for **P10'**, its longer hydrophobic alkoxy side chains of the quaternized polymer compared to that of **P11'** and **P12'** made it obtain relatively better solubility in THF/DMSO mixture and the appearance of similar precipitate was denied. **P8'** and **P9'** exhibited good solubility in both methanol and water, while **P10'** was dissolved in methanol but not water due to the existence of long hydrophobic side chains. Therefore, the percentage increase of hydrophilic groups on the side chains is crucial to satisfy the water-solubility of the conjugated polymers. **P11'** and **P12'**, as we discussed above, showed poor solubility in any common solutions. Such an obvious difference in solubility among **P10'**, **P11'** and **P12'** suggested that the length of hydrophobic group, accompanied with quaternized group, may highly influence the solubility of corresponding conjugated polyelectrolytes. In the rest of this chapter, as a result, we focused on the investigation of the chemical and physical properties of **P8-P10** and their corresponding quaternized polymers **P8'-P10'** based on their good solubility.

For the neutral polymers, **P8** was a deep yellow powder and **P9-P12** were orange-yellow fibrous solids. All the quaternized samples **P8'-P12'** showed brown yellow color. Gel permeation chromatography revealed that all of the neutral polymers showed reasonably high molecular weight (see **Table 4.1.1**).

Table 4.1.1 Characterization of neutral polymers and uaternized polymers

polymer	GPC			absorbance (nm)			emission (nm)		
	M_n	M_w	PDI	$CHCl_3$	CH_3OH	H_2O	$CHCl_3$	CH_3OH	H_2O
P8	26 700	61 200	2.29	433	—	—	471	—	—
P9	20 300	46 700	2.30	430	—	—	470	—	—
P10	47 100	138 800	2.95	444	—	—	474	—	—
P11	31 000	77 600	2.50	—	—	—	—	—	—
P12	45 000	132 800	2.95	—	—	—	—	—	—
P8'	—	—	—	—	403	387	—	457	447
P9'	—	—	—	—	416	404	—	463	457
P10'	—	—	—	—	426	—	—	466	—

4.1.4.3 NMR Spectroscopy

^{1}H (see **Figure 4.1.2**) and ^{13}C (see **Figure 4.1.3**) NMR analyses indicated clearly that well-defined PPE derivatives have been indeed obtained. Furthermore, the quaternization degrees (QDs) of **P8'-P10'** could be determined by ^{1}H NMR spectra (see **Figure 4.1.4**).[20] As shown in **Figure 4.1.2**, the neutral polymer **P8** exhibits two well resolved peaks at 2.95, and 2.70 ppm corresponding to the methylene groups adjacent to the nitrogen (-$\boldsymbol{CH_2}$N-) atoms. After the treatment with bromoethane, all signals corresponding to -$\boldsymbol{CH_2}$N- split into two peaks, which arise from the quaternized (low field) and unquaternized components. The relative integrals of each pair of the split peaks can thus be used to estimate the QD of **P8'** which was 45%. But for **P9'** and **P10'**, the QD of **P9'** (85%) was determined by the relative integrals of the methylene (-$NCH_2\boldsymbol{CH_2}O$-) and methyl (-$NCH_2\boldsymbol{CH_3}$) peaks and that of **P10'** (95%) was calculated from the relative integrals of the methylene (in -$OCH_2\boldsymbol{CH_2}$N-) and methylene (in -N$\boldsymbol{CH_2}CH_3$) peaks. The higher QDs of **P9'** and **P10'** than that of **P8'**, combined with the deposition of **P8'** during its synthetic process, indicated that under the same quaternization conditions, the existence of longer side chains may be more beneficial to the completion of the quaternization.

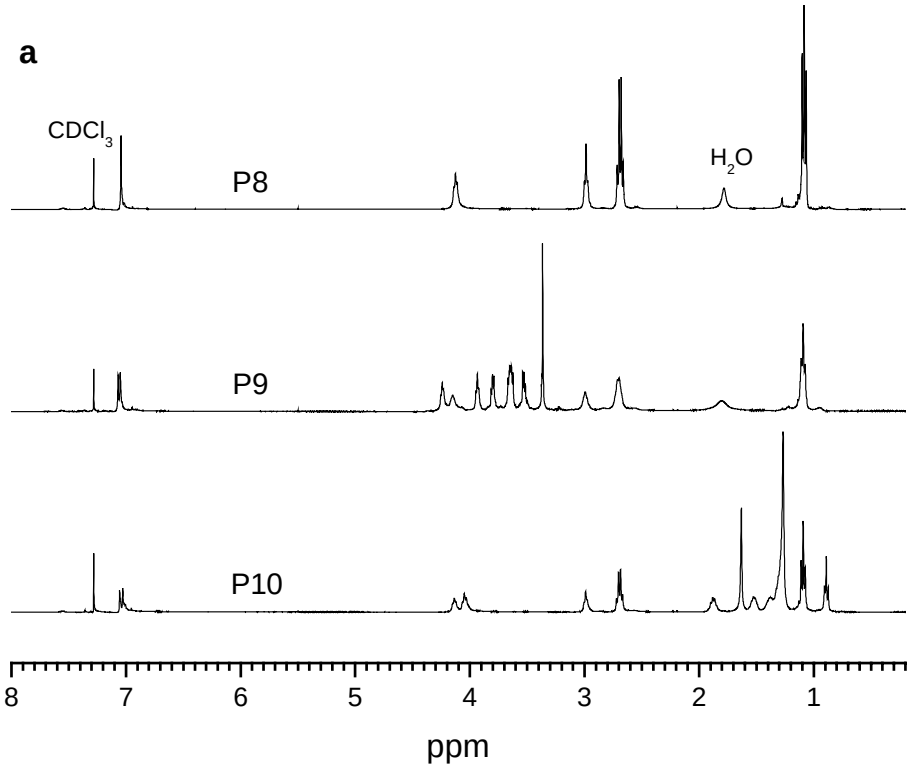

Figure 4.1.2. ^{1}H NMR spectra of neutral polymers P8-P10 in $CDCl_3$

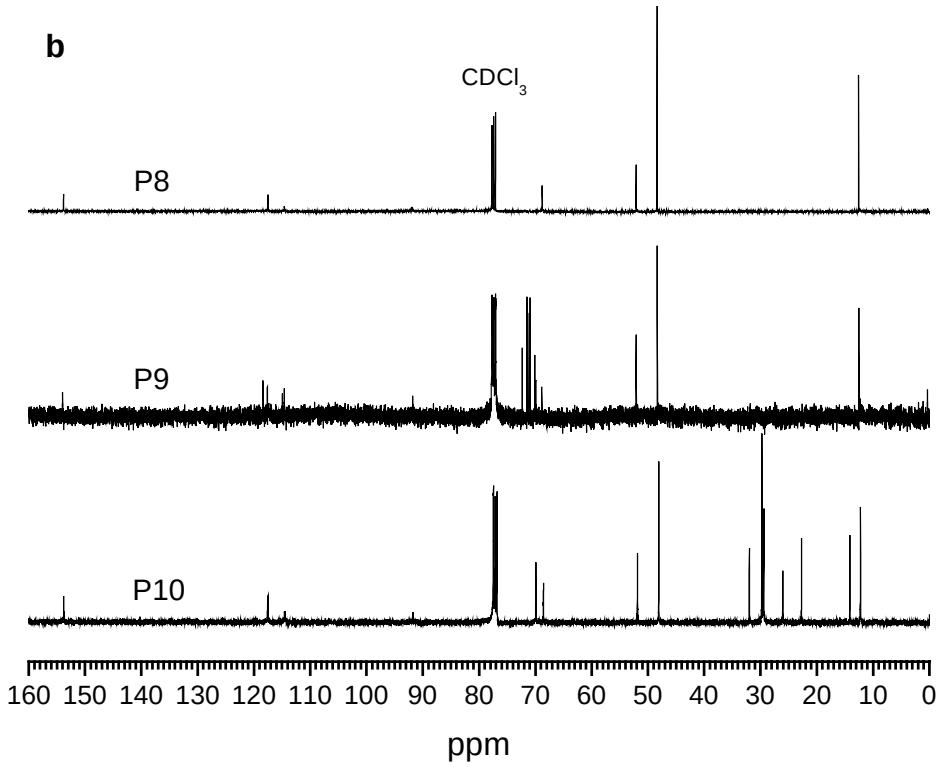

Figure 4.1.3 ^{13}C NMR spectra of neutral polymers P8-P10 in $CDCl_3$

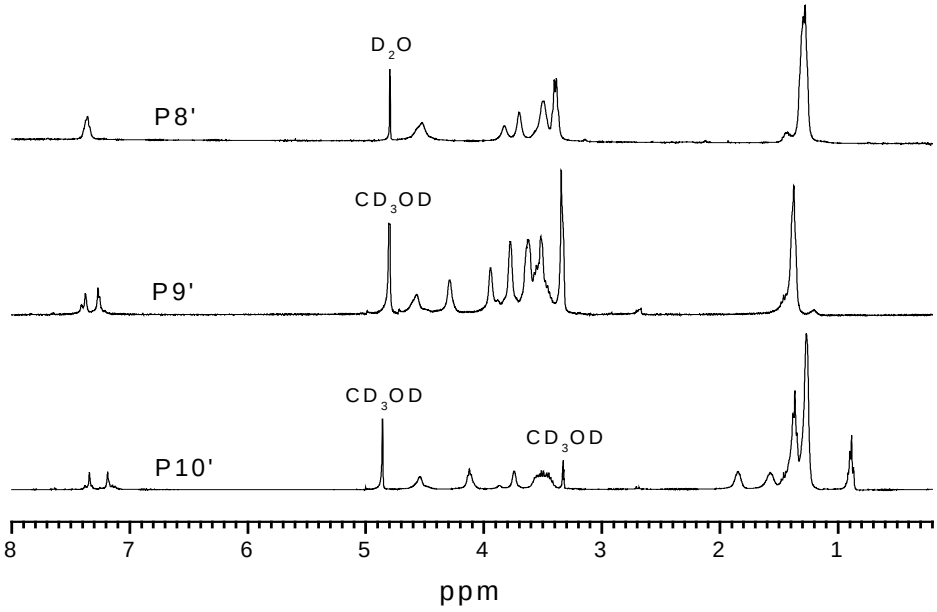

Figure 4.1.4 ^{1}H NMR spectra of quaternized polymers P8' in D_2O and P9'-P10' in CD_3OD

4.1.4.4 Thermal Stability

The thermal stability of the polymers in nitrogen was evaluated by thermogravimetric analysis (TGA). The thermograms are depicted in **Figure 4.1.5**. The neutral polymers possess common thermal stability. The onset degradation temperature of all polymers was nearly 200 ^oC in nitrogen. For **P9** and **P10**, it suffered two mass loss indicative of different side chain cleavage from the aromatic group in the molecular backbone. However, all the quaterized salts began decomposition at ca. 180 ^oC, with a small amount of water loss at lower temperatures. The quaternized polymers of **P9'** and **P10'** have three steps of mass loss. The first mass loss was from ethyl bromide, as reported by Reonolds.[19] The second transition occurred at 230 ^oC. The third major transition appeared in the vicinity of the first transition of the neutral polymer, again due to side chain cleavage. **P8**, in which all side chains are amino-terminated groups and its quternized polymer **P8'**, suffered only one mass loss starting at 195 ^oC and 180 ^oC,

respectively. Those T_d at nearly 200 ^oC of the quzternized polymers made them enough serve as chemo or biosensor because all of applications were proceeded at room temperature.

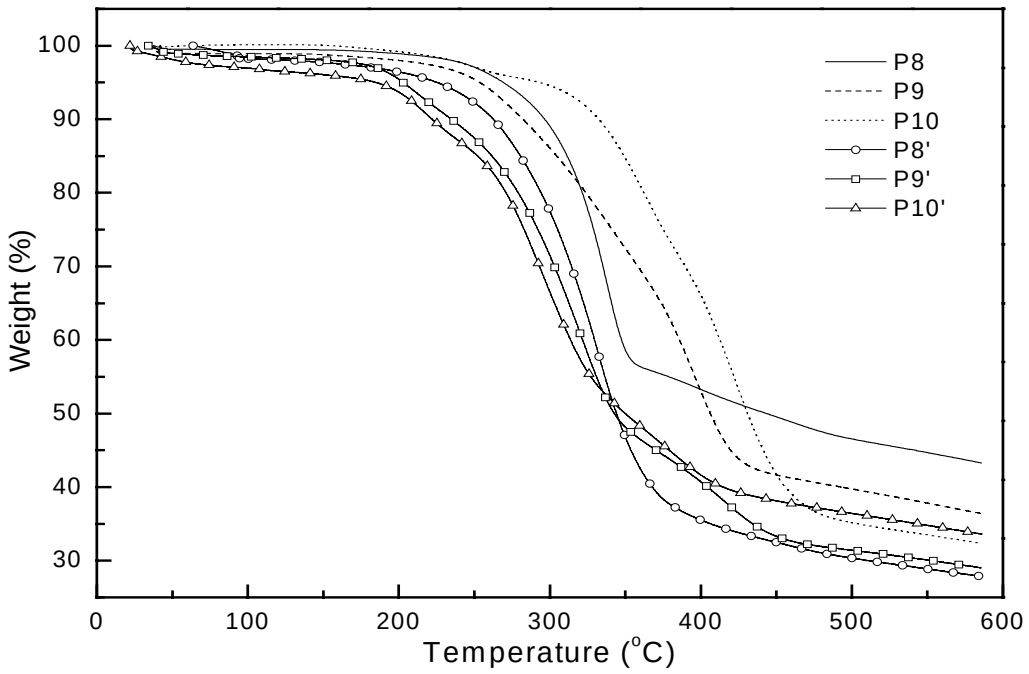

Figure 4.1.5 Thermalgravimetric analyses of the neutral and quaternized PPEs

4.1.4.5 Optical Properties

The UV-vis and photoluminescence spectra of the neutral polymers in $CHCl_3$ are shown in **Figure 4.1.6a**. **P8-P10** exhibit a strong absorption peak occurring at 433 nm, 430 nm and 444 nm respectively, while all the emission peaks of **P8-P10** appeared at about 472 nm with a vibronic band shoulder at 506 nm. All these absorption and emission spectra are almost identical to what Wrighton's group has reported previously,[21] indicating that the electronic properties of these conjugated polymers are predominantly governed by the rigid-rod and highly conjugated polymer backbone and ancillarily influenced by the nature of the attached side chains.

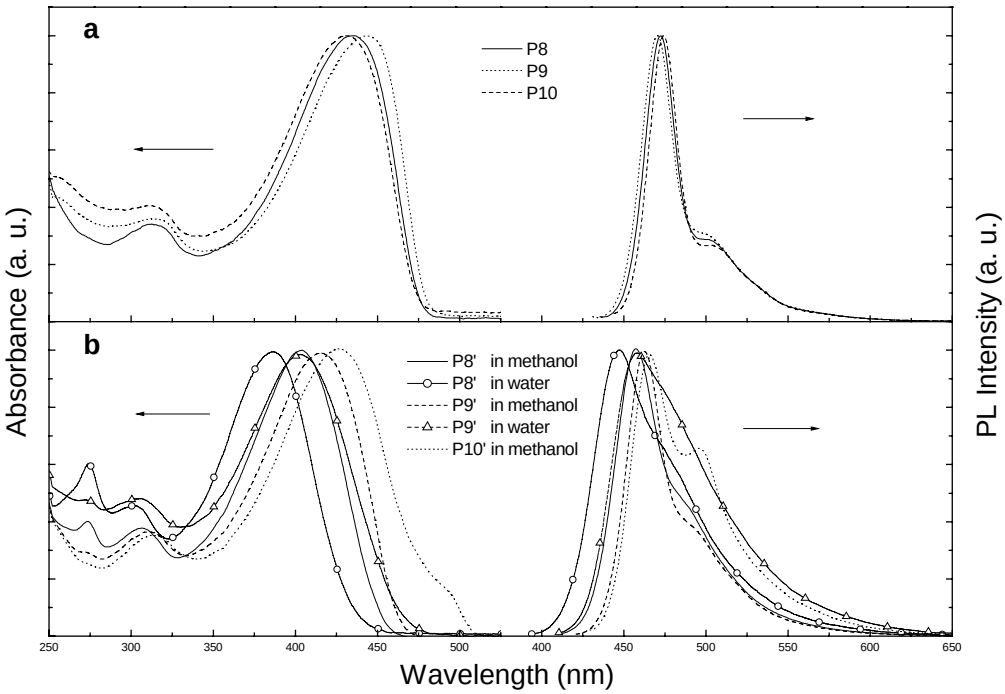

Figure 4.1.6 UV-vis absorption and PL emission spectra of (a) neutral polymers P8-P10 in chloroform and (b) quaternized polymers P8'-P10' in water or methanol

Figure 4.1.6b shows the UV-vis and photoluminescence spectra of the quaternized polymers in CH_3OH and water. In comparison with that of the neutral polymers, the absorption and emission peaks of all the quaternized polymers present obvious blue shift (detailed data please see **Table 4.1.1**), which may result from the mutual repulsion among the positive charges leading to a more twisted main chain conformation and therefore, a decreased effective conjugation length.[19,20] Meanwhile, the absorption and emission maxima of those quaternized polymers are remarkably dependent on the solvent, showing an obvious bathochromic shift with the decrease of solvent polarity. In methanol, the quarternized samples exhibit obviously different absorption and emission spectra, which may be due to the respective hydrophilicity of those polymer side chains that influences the interaction between the polymers and the solvent and therefore, the effective conjugation length. Interestingly, a new absorption shoulder

was observed at about 480 nm for **P10'**. Note that **P10'** has a hydrophilic-hydrophobic side chain pattern, the conjugated segments may have a strong tendency to form interchain aggregates. An aggregation absorption at about 470 nm has been previously observed by Swager in investigating the LB films of a series of PPE derivatives, which is quite close to the value in our system.[22] In addition, the formation of interchain aggregation can be further evidenced by the fact that such an absorption shoulder could disappear thoroughly by adding chloroform while showed no response to the introduction of water.

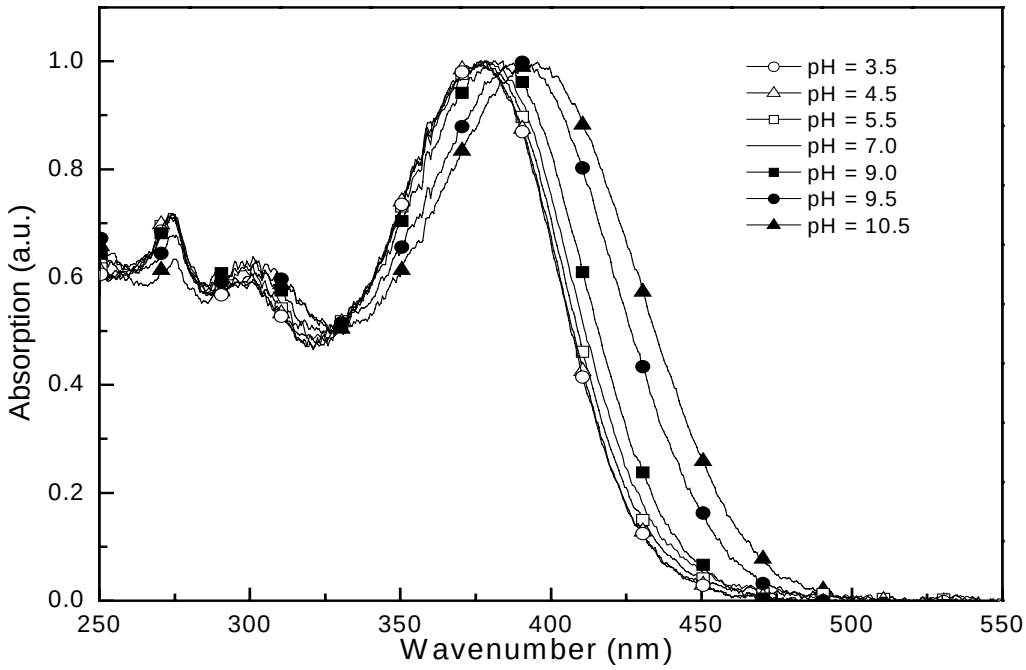

Figure 4.1.7 UV-vis absorption spectra of quaternized polymer P8' in aqueous solution with different pH values

4.1.4.6 pH-Sensitive Photoluminescence of P8'

Using water-soluble conjugated polymer to detect biomolecule in aqueous solution at different pH values is required in practical application. Here we study the influence of pH to the UV-vis and photoluminescence of **P8'**.

It was found that the yellow color of **P8'** aqueous solution at pH = 7 changed into light color when adding HCl aqueous solution and turned into deep yellow color after adding NaOH aqueous solution. This color tunability was very similar with that of water-soluble anionic polythiophene by changing the countercation, which dramatically indicated the obvious variation of UV-vis absorption of **P8'** through changing pH value.

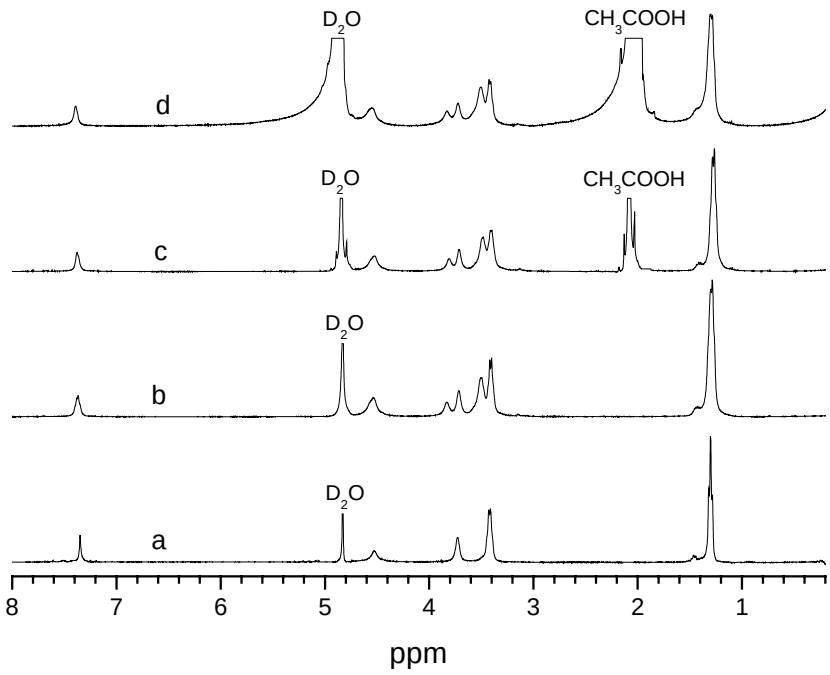

Figure 4.1.8 ^{1}H NMR spectra of (a) neutral polymer P8 in CD_3COOD/D_2O solution, (b) quaternized polymer P8' in D_2O, (c) quaternized polymer P8' in CD_3COOD/D_2O solution and (d) quaternized polymer P8' in D_2O after addition of NaOH solution and then neutralization by CH_3COOH solution.

Figure 4.1.7 showed the UV-vis absorption spectra of **P8'** in different pH values. In **Figure 4.1.7**, the absorption maximum was a little blue shifted when pH < 7.0 which indicated the formation of a more twisted main chain conformation. We considered that addition of HCl acidify unquaternized amino group in the side chain into cationic ammonium group and enhance the mutual repulsion among the positive charges which

formed a less effective conjugated length and therefore a blue shift of absorption maximum.[20b] In NMR spectra (**Figure 4.1.8**), when **P8'** was dissolved in acetic acid aqueous solution, all the signal corresponding to $–OCH_2$-, $-CH_2N$-, and $–NCH_2$- moved towards the lower field, which appeared similar with that of **P8'** in aqueous solution and indicated the interaction of acetic acid with unquaternized amino group. Thus when **P8'** was dissolved in acetic acid aqueous solution, it could be anticipated that the unquaternized amino group will move towards the lower field. But in **Figure 4.1.8**, there is little difference between the NMR spectra of **P8'** in aqueous solution and in acetic acid aqueous solution. It is noticeable that compared to those amino group in neutral polymer **P8**, the signal of unquaternized amino group in **P8'** has been drastically moved towards lower field, which may be explained by the mutual attraction between quaternized ammonium group and unquaternized amino group. Such a shift may higher than that from the interaction between unquaternized amino group and acetic acid and thus the influence of acid on the signal of unquaternized amino group in **P8'** was not obvious.

When pH > 7, the UV-vis peak of **P8'** red-shifted and broadened gradually with the increase of pH value. Meanwhile, after dropping NaOH aqueous solution into **P8'** solution, the color of **P8'** solution firstly changed into deep yellow color and then orange solid was precipitated from **P8'** solution, indicating the formation of interchain aggregation. To clarify whether the aggregation resulted from the destroyment of ammonium group under base environment and the decreased water solubility of **P8'**, the HCl solution was added to neutralize NaOH solution to pH = 7. Investigating showed that those produced precipitate was disappeared and redissolved in aqueous solution and correspondingly the UV-vis absorption spectrum was recovered into the pristine one, which demonstrated that the ammonium group was not damaged by

NaOH. Meanwhile, the non-changed NMR spectra of **P8'** before and after adding base and then acid in **Figure 4.1.8** further confirmed that the addition of NaOH is conducive to the formation of aggregation without damaging **P8'**.

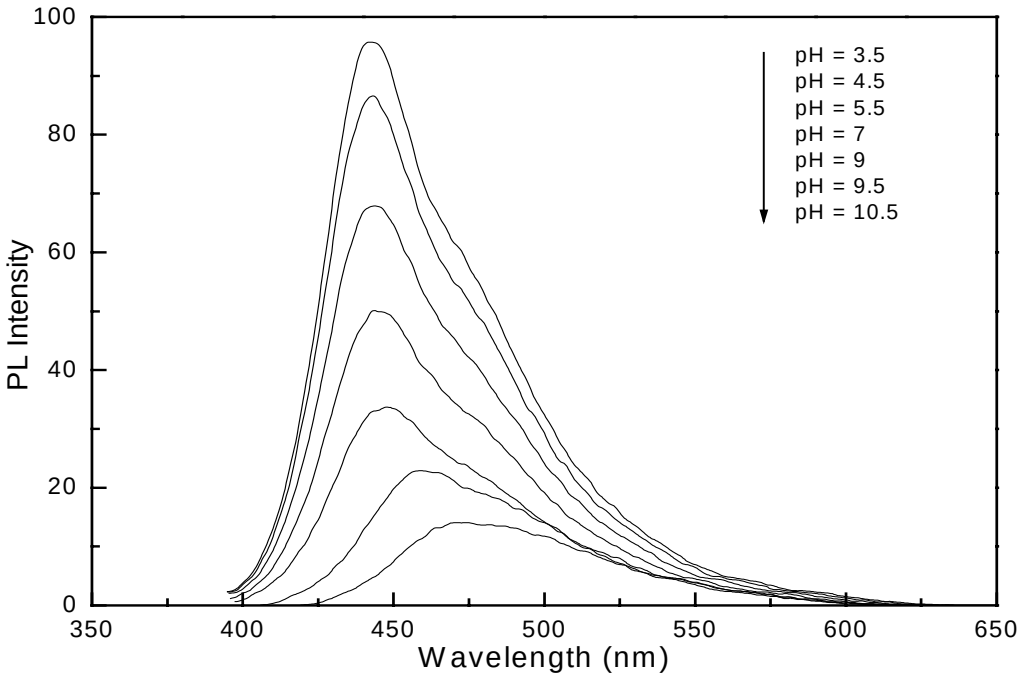

Figure 4.1.9 PL emission spectra of quaternized polymer P8' in aqueous solution with different pH values

Figure 4.1.9 showed the emissive spectra of **P8'** at different pH values. When **P8'** was in acidified environment, its fluorescence intensity enhanced and the emissive maxima did not shift while in base environment, its fluorescence intensity decreased and the emissive maxima red-shifted significantly.

To clarify the influence of pH values to fluorescence intensity of **P8'**, the plot of relative fluorescence intensity of **P8'** with the pH values was described in **Figure 4.1.10**. It is interesting to find that a titration-like curve was observed for the fluorescence of **P8'**. When pH < 7, the fluorescence of **P8'** enhanced gradually and reached a plateau at about pH = 3.5 while when pH > 7, the fluorescence intensity of

P8' started to decrease swiftly at pH = 8.0 and arrived to the nadir (1/3, compared with the pristine one) at about pH = 9.5. The pH region of changed fluorescence intensity in base environment was more narrow than that in acid environment, which significantly indicated the different mechanism of fluorescence change of **P8'** by H^+ and OH^-. When pH = 3.5, at which the enhancement of fluorescence intensity of **P8'** stopped, [H^+] is much higher than [unquaternized amino group] of **P8'**, indicating that the interaction between unquaternized amino group and H^+ was not the full reason to explain the increase of fluorescence intensity. Instead, there must exist some interaction between H^+ and fluorophore (conjugated segment) to influence its fluorescence. Because of its non-shift emissive maxima of **P8'** in different acid environment, it was suggested that the fluorescence enhancement of **P8'** in acid environment result from the existence of H^+, just as what surfactant functioned,[6] which may reduce the defects on the conjugated chain that can serve as trapping and nonradiative recombination sites. When pH > 7, **P8'** exhibited obvious red-shift of absorption and emissive maxima, broadened absorption peak, reduced fluorescence intensity, and precipitate formation after adding more OH^-, all of which could simply demonstrated that it was the formation of aggregation after adding OH^- to result in the reduced fluorescence of **P8'** at base environment. **Figure 4.1.10** also showed the emission spectra of **P8'** after adding acid and base with different sequence, which presented that the fluorescence intensity of **P8'** could be recovered to pristine one at pH = 7 via neutralization reaction. Further investigation (see **Inset** in **Figure 4.1.10**) exhibited that the fluorescence intensity of **P8'** did not vary after adding salt (sodium chloride), indicating that the existence of salt little influences the conformation of **P8'**, which is highly different with the general phenomenon that the adding of salt into aqueous solution of amphiphilies enhances formation of aggregates and micells. Such

a pH-dependent fluorescence of **P8'**, which has never been reported in other FWSCP systems, indicated that FWSCPs have the potential to be used as pH sensors and the sensitivity of FWSCPs may be adjusted by controlling pH value.

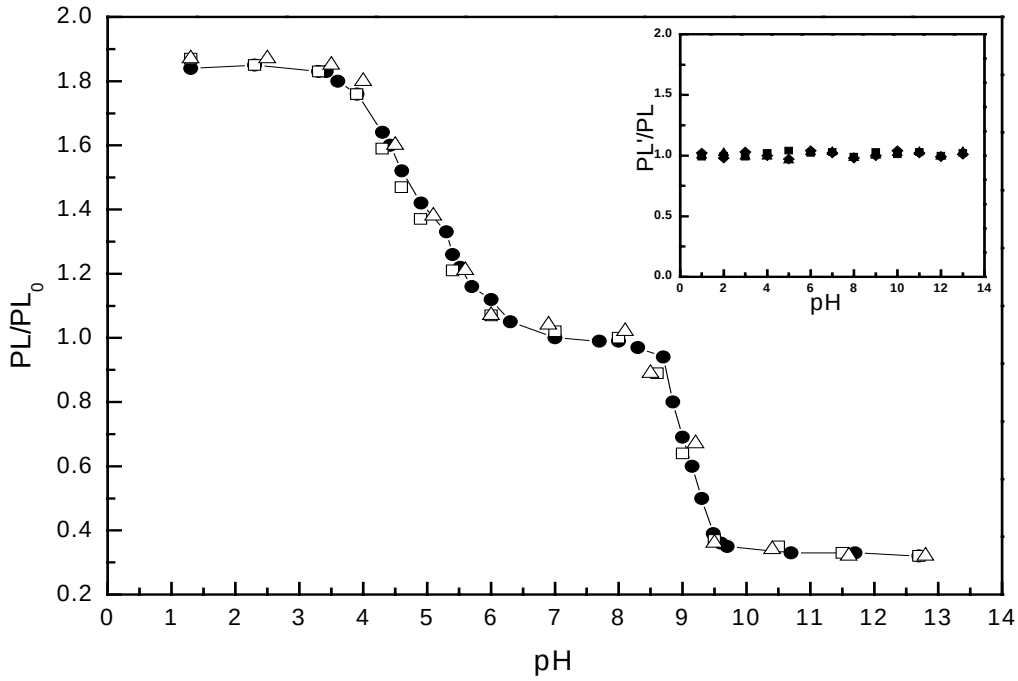

Figure 4.1.10 The curve of relative PL intensity of P8' in aqueous solution versus pH values which was adjusted by adding HCl and NaOH solution into P8' solution at pH = 7 respectively (–•–), adding HCl solution into P8' solution at pH = 1 (realized through adding NaOH solution) (□), adding NaOH solution into P8' solution at pH = 13 (realized through adding HCl solution) (Δ). Inset: the relative PL intensity of P8' at different pH environment after adding salt (sodium chloride) with different concentrations at 10^{-5} (■), 10^{-4} (▲) and 10^{-3} (♦) μM respectively

Further investigation showed that the pH-sensitive region of **P8'** was varied according to the concentration of **P8'** in aqueous solution. **Figure 4.1.11** showed the relative fluorescence intensity of **P8'** versus pH value at different concentrations of **P8'**. In **Figure 4.1.11**, when the concentration of **P8'** increased to 50 μM, the pH-sensitive region broadened accordingly, in which the fluorescence intensity of **P8'** increased to the highest at pH = 3 and decreased in the region from pH = 8.5 to 10. Such an

adjustable pH-sensitivity showed that the needed quantity of H^+ or OH^- to change the fluorescence of **P8'** was determined by the quantity of **P8'** in aqueous solution.

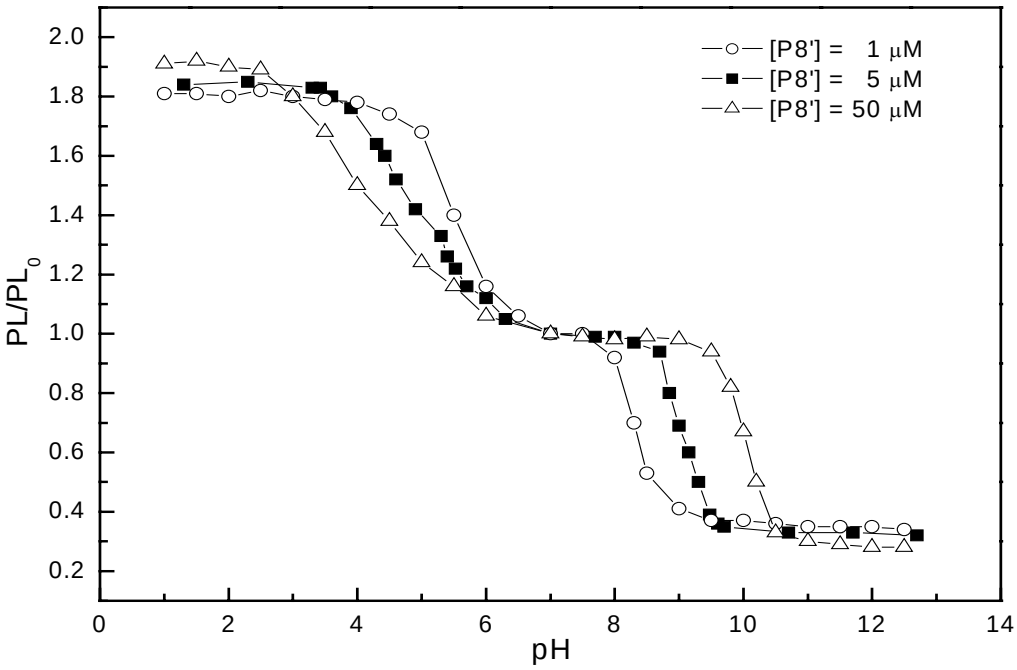

Figure 4.1.11 The curve of relative PL intensity versus pH value at different P8' concentration

4.1.4.7 Stern-Volmer Study at Different pH Values

Figure 4.1.12 showed the Stern-Volmer plot of **P8'** quenched by $Fe(CN)_6^{4-}$ in aqueous solution. The typical upward curve exhibited in **Figure 4.1.12** presented the existence of sphere-of-action, which could be described by equation 1:

$$\frac{F_0}{F} = (1 + K_{sv}^{S}[Q])e^{\alpha V[Q]} \tag{1}$$

where F_0 is the fluorescence intensity with no quencher present, F is the fluorescence intensity with quencher present, [Q] is the quencher concentration, K_{sv} is the Stern-Volmer constant and V is volume constant and α is used to account for the charge-induced enhancement of the local quencher concentration.

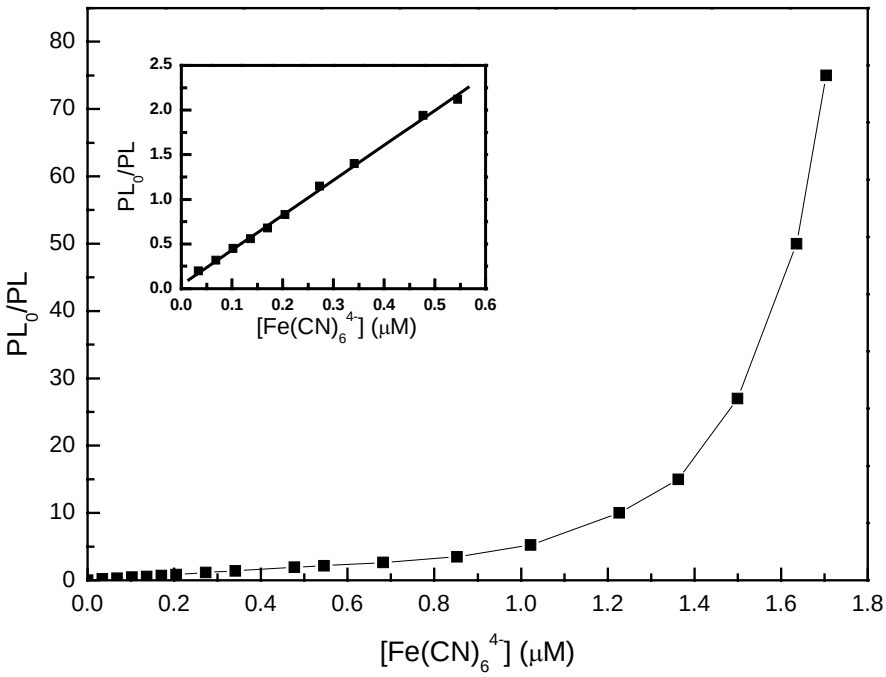

Figure 4.1.12 Stern-Volmer plot of P8' (5 μM) quenched by $Fe(CN)_6^{4-}$ in aqueous solution. Inset: the part of Stern-Volmer plot of P8' (5 μM) quenched by $Fe(CN)_6^{4-}$ at low concentration

The K_{sv} value of **P8'** versus pH value were depicted in **Figure 4.1.13**. When pH < 7, although the fluorescence intensity enhanced, the K_{sv} value was nearly unchanged, which indicating that H^+ little influenced the quenching efficiency of **P8'**. However, K_{sv} value started to increase at pH = 8 and reached the highest at pH = 9.5, which is ten times larger than the pristine one at pH = 7. Such an enhancement of K_{sv} value is well accorded with the decrease of fluorescence intensity of **P8'** at the same pH region, demonstrating clearly that the interchain aggregation is conducive to enhance the quenching efficiency. It has been reported that polymer aggregation is one part of reason to lead to fluorescence quenching[2] but whether polymer aggregation will lead to further amplification of fluorescence quenching through the occurring of interchain exciton migration is still a question. In our system, the aggregation of **P8'** in aqueous solution could be adjusted through adding OH^- with different quantity and the

correspondingly enhanced K_{sv} values confirmed the contribution of polymer aggregation on amplified quenching.

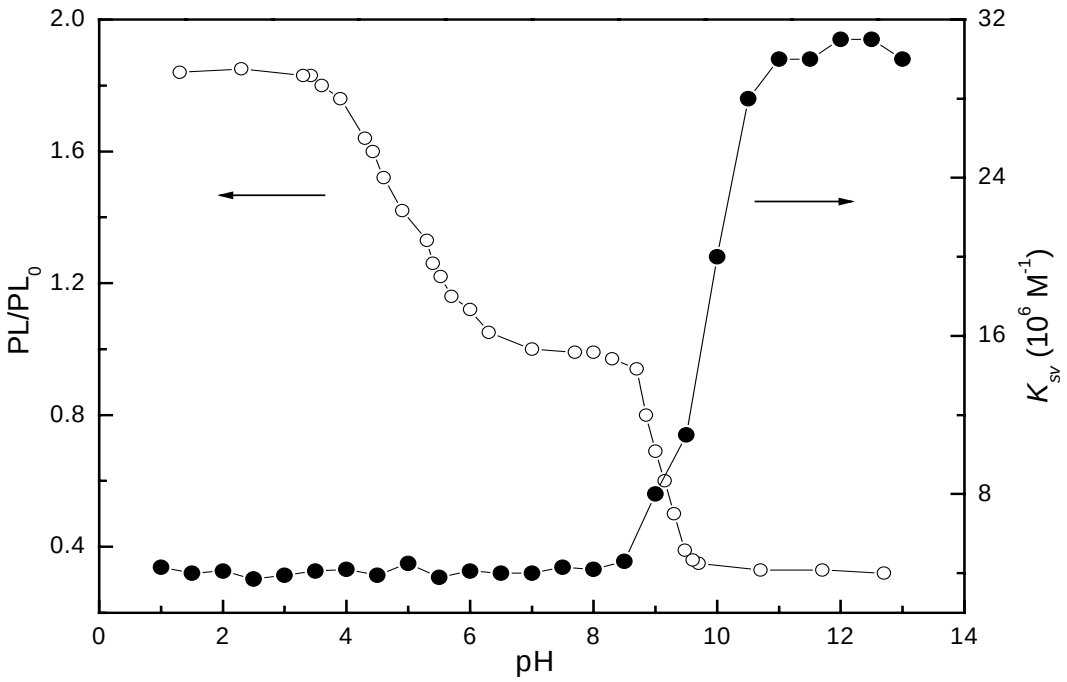

Figure 4.1.13 The plots of K_{sv} value and relative PL intensity of P8' (5 μM) versus pH value

The curves of K_{sv} values versus pH values at different concentrations of **P8'** were shown in **Figure 4.1.14**. It was seen that with the 10-fold increase of **P8'** concentration the K_{sv} value decreased nearly 10 folds simultaneously at pH = 7. However, the pH region for those upward K_{sv} values at higher **P8'** concentration was similar as that at lower concentration, the only difference of which is the onset and offset of the pH region for enhanced K_{sv}. All of those phenomena indicated that the K_{sv} value was stoichiometrically related to the polymer concentration. Further investigation of the effect of polymer concentration will be discussed in another paper.

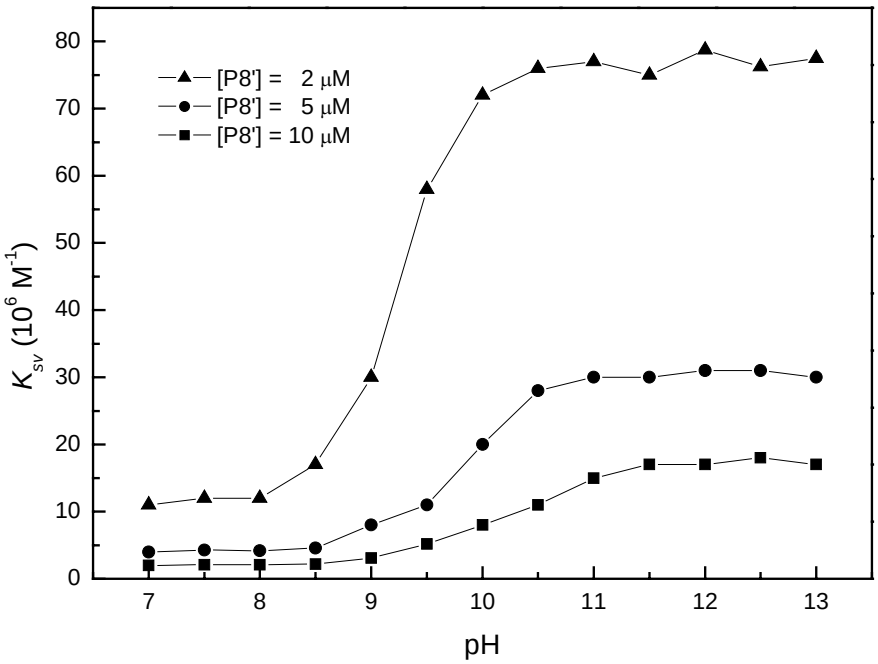

Figure 4.1.14 The plots of K_{sv} value of P8' versus pH value at different P8' concentration

4.1.5 Conclusions

In conclusion, we report on the successful synthesis and optical properties of a serious of water-soluble cationic PPE derivatives via post-quaternization. Excellent water-solublility was achieved by introducing more hydrophilic side chains. The electronic spectra of the quaternized polymers present a strong dependence on the nature of the substituents and the solvent. Intermolecular aggregation was observed for **P10'** in methanol, which may result from the presence of long chain hydrophobic groups. The fluorescence of **P8'** enhanced at acid environment and reduced at base environment, which exhibited a titration-like curve. The fluorescence enhancement of **P8'** when pH < 7 may result from the interaction between H^+ and **P8'** to reduce the trapping on the conjugated chain, while the reason for the fluorescence decrease of **P8'** was clearly attributed to the OH^--induced aggregation for **P8'**. Further investigation

showed that the pH-sensitive region could be tuned by changing the polymer concentration. The study of quenching of **P8'** by $Fe(CN)_6^{4-}$ at different pH values exhibited that the Stern-Volmer constant was retained in acid environment but highly increased at base environment due to the formation of interchain aggregation driven by OH^-. The K_{sv} value was found to be inverse proportional to the polymer concentration. Because of the highly influence of pH value on polymer fluorescence and K_{sv} value, such a significant variation must be considered for designing good biosensors.

References and Notes

1 McQuade, D. T.; Pullen, A. E.; Swager, T. M. *Chem. Rev.* **2000**, *100*, 2537.

2 Chen, L.; McBranch, D. W.; Wang, H.-L.; Helgeson, R.; Wudl, F.; Whitten, D. G. *Proc. Natl. Acad. Sci. U. S. A.* **1999**, *96*, 12287.

3 Wang, J.; Wang, D. L.; Miller, E. K.; Moses, D.; Bazan; G. C.; Heeger, A. J. *Macromolecules* **2000**, *33*, 5153.

4 Wang, D. L.; Wang, J.; Moses, D.; Bazan; G. C.; Heeger, A. J. *Langmuir* **2001**, *17*, 1262.

5 Chen, L.; McBranch, D.; Wang, R.; Whitten, D. G. *Chem. Phys. Lett.* **2000**, *330*, 27.

6 Chen, L.; Xu, S.; McBranch, D.; Whitten, D. G. *J. Am. Chem. Soc.* **2000**, *122*, 9302.

7 Jones, R. M.; Bergstedt, T. S.; McBranch, D. W.; Whitten, D. G. *J. Am. Chem. Soc.* **2001**, *123*, 6726.

8 Stork, M.; Gaylord, B. S.; Heeger, A. J.; Bazan, G. C. *Adv. Mater.* **2002**, *14*, 361.

9 Fan, C.; Plaxco, K. W.; Heeger, A. J. *J. Am. Chem. Soc.* **2002**, *124*, 5642.

10 Harrison, B. S.; Ramey, M. B.; Reynolds, J. R.; Schanze, K. S. *J. Am. Chem. Soc.* **2000**, *122*, 8561.

11 Gaylord, B. S.; Heeger, A. J.; Bazan, G. C. *Proc. Natl. Acad. Sci. U. S. A.* **2002**, *99*, 10954.

12 Zhou, Q.; Swager, T. M. *J. Am. Chem. Soc.* **1995**, *117*, 7017.

13 Zhou, Q.; Swager, T. M. *J. Am. Chem. Soc.* **1995**, *117*, 12593.

14 Yang, J.-S.; Swager, T. M. *J. Am. Chem. Soc.* **1998**, *120*, 5321.

15 Yang, J.-S.; Swager, T. M. *J. Am. Chem. Soc.* **1998**, *120*, 11864.

16 Kim, J.; McQuade, D. T.; McHugh, S. K.; Swager, T. M. *Angew. Chem. Int. Ed.*

2000, *39*, 3869.

17 Tan, C.; Mauricio, R. P.; Schanze, K. S. *Chem. Comm.* **2002**, 446.

18 DiCesare, N.; Pinto, M. R.; Schanze, K. S.; Lakowicz, J. R. *Langmuir* **2002**, *18*, 7785.

19 Balanda, P. B.; Ramey, M. B.; Reynolds, J. R. *Macromolecules* **1999**, *32*, 3970.

20 (a) Liu, B.; Yu, W.; Lai, Y. H.; Huang, W. *Chem. Comm*. **2000**, 551. (b) Liu, B.; Yu, W.; Lai, Y. H.; Huang, W. *Macromolecules* **2002**, *35*, 4975.

21 Weder, C.; Wrighton, M. S. *Macromolecules* **1996**, *29*, 5157.

22 Kim, J.; Swager, T. M. *Nature* **2001**, *411*, 1030.

CHAPTER FOUR

Part II: Polymer-Concentration-Dependent Photoluminescence Quenching of Poly(*p*-phenyleneethynylene) by $Fe(CN)_6^{4-}$ in Aqueous Solution

4.2.1 Introduction

Water-soluble conjugated polymers (WSCPs), a new class of polyelectrolytes which consist of both polyions and electronically active conjugated backbones, attract much interest because of the potential application in the development of highly efficient chemo or biosensors.[1] Recent findings showed that a low concentration of quencher is sufficient to quench the fluorescence from the conjugated segments through electron or energy transfer due to facile energy migration along the conjugated backbone and relatively strong binding of quencher with WSCPs via electrostatic attraction.[2]

Based on the fluorescence quenching effect, WSCPs were developed as biosensors to detect specific biomolecules such as proteins through combining quencher group with ligand group into one molecular structure.[2] Their biosensibility was realized through detecting the quenching and unquenching process of such conjugated polymers, which firstly formed conjugated polymer/quencher-ligand complex to quench the fluorescence and then formed quencher-ligand/bioacceptor complex to release quencher from conjugated polymer chain and therefore reactivate the fluorescence.

To improve their sensitivity, the fluorescence quenching of WSCPs has been and is

now being widely investigated. The initial research results showed that the efficiency of fluorescence quenching was influenced by many factors, such as effective conjugated length,[3] size of conjugated polymer chain,[4] charge on quencher,[5] ionic strength,[4] pH values,[6] conjugated polymer concentration,[7,8] concentration of surfactant[9,10] or polyelectrolyte[11,12] with counterions added into the WSCP system, and type of substrate introduced.[11] As a result, the sensitivity could be controlled by chemical (design and synthesis) or physical methods (change of system environment).

Recent reports showed that the sensitivity enhanced with the decrease of WSCP concentration.[7,8] Harrison et al. first reported that $Ru(phen')_3^{4-}$ and $Fe(CN)_6^{4-}$ quenched $PPP\text{-}NEt_3^+$ approximately 100-fold more efficiently when [$PPP\text{-}NEt_3^+$] decreased from 10 to 1 μM.[7] Similar phenomenon was also reported by Tan et al. on the $PPE\text{-}SO_3^-$ system quenched by MV^{2+}, in which when [$PPE\text{-}SO_3^-$] in methanol solution decreased from 10 to 1 μM, the Sterm-Volmer constant K_{sv} increased 10-fold stoichiometrically; while in aqueous solution, K_{sv} only increased 5-fold.[8] This phenomenon strongly suggested that changing the concentration of WSCP is desirable to obtain improved sensors because of its simplest way to tune the WSCP sensitivity without any chemical synthesizing route or addition of some extra materials. Subsequently, it was necessary to further investigate and explain the relationship between sensitivity and polymer concentration by a suitable theory.

In this paper, we study the fluorescence quenching of $PPE\text{-}NEt_3^+$ at different concentration by $Fe(CN)_6^{4-}$ in aqueous solution. Especially, we present a simple theory to explain the relationship between the static Stern-Volmer constant and the $PPE\text{-}NEt_3^+$

concentration. The possible influence of interchain aggregation on such a relationship was also discussed in this paper and showed that the theoretical results were significantly accorded with the experimental results without the existence of aggregation.

4.2.2 Materials and Characterization Methods

4.2.2.1 Materials

Water-soluble conjugated polymer, PPE-NEt_3^+ (**P8'**), was synthesized in our lab according to the procedure we reported previously.[13] The quencher, $K_4Fe(CN)_6$, was obtained from Aldrich Chemical Co. The Milli-Q water used in preparing the aqueous solutions of those polymers and quenchers was purged with nitrogen for 4 h before using.

4.2.2.2 Characterization Methods

UV-vis spectra were recorded on a Shimadzu 3101 PC spectrometer. Fluorescence measurement was carried out on a Perkin-Elmer LS 50B photoluminescence spectrometer with a xenon lamp as a light source. The quenching studies were realized *in situ* through comparing the photoluminescence intensities of the solutions at a series of detector and quencher concentration. All the investigations of optical properties and fluorescence quenching of PPE-NEt_3^+ were held at [PPE-NEt_3^+] ranging from 1 to 200 μM. All the quenched solutions were prepared after adding calculated amount of

quencher solution into PPE-NEt_3^+ solution and purging with nitrogen for 1 min and immediately used to take their corresponding absorption spectra and emission spectra with excitation at 386 nm. Prior to test those quenched solutions, the optical properties of pure PPE-NEt_3^+ solution were first studied according to the same procedure.

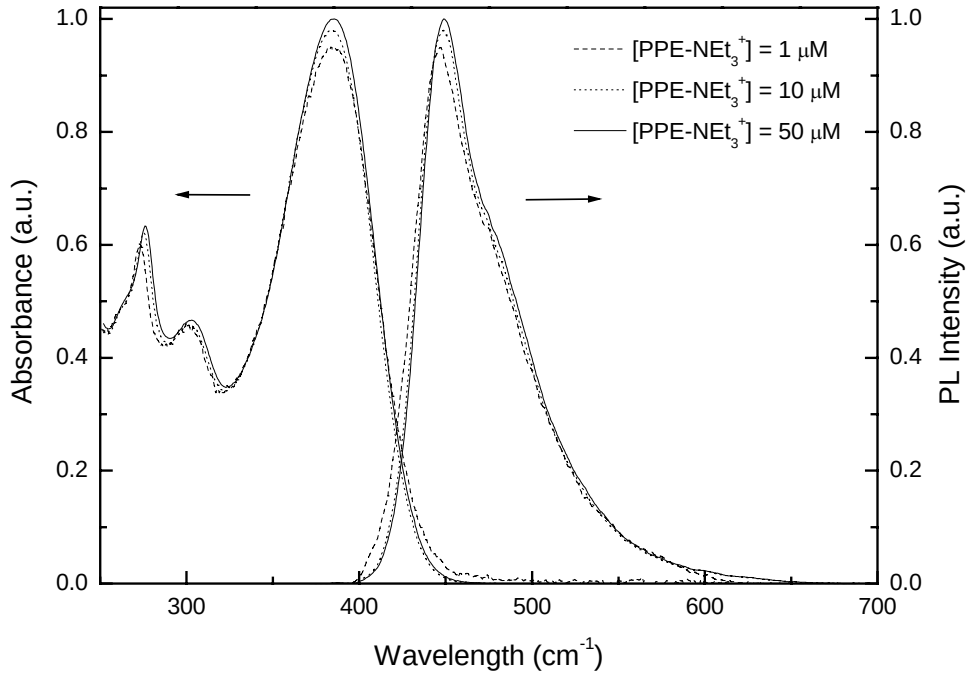

Figure 4.2.1 UV-vis absorption and emission spectra of PPE-NEt_3^+ in aqueous solution at different concentrations: [PPE-NEt_3^+] = 1, 10 and 50 μM

4.2.3 Results and Discussion

4.2.3.1 UV-vis Absorption and Emission

Figure 4.2.1 shows the selected UV-vis absorption and emission spectra of pure PPE-NEt_3^+ with different concentration (c = 1, 10 and 50 μM) in water. No spectra shift was observed with the increase of PPE-NEt_3^+ concentration, which indicates that

the conformation of pure PPE-NEt_3^+ polymer chain in water little changed at different concentrations ranging from 0.2 to 200 μM. Such a non-concentration dependence in absorption maxima of PPE-NEt_3^+ indicated that the polymer presented individual chain conformation at different concentrations, which may result from the mutual electrostatic repulsion among those rod-like PPE chains.

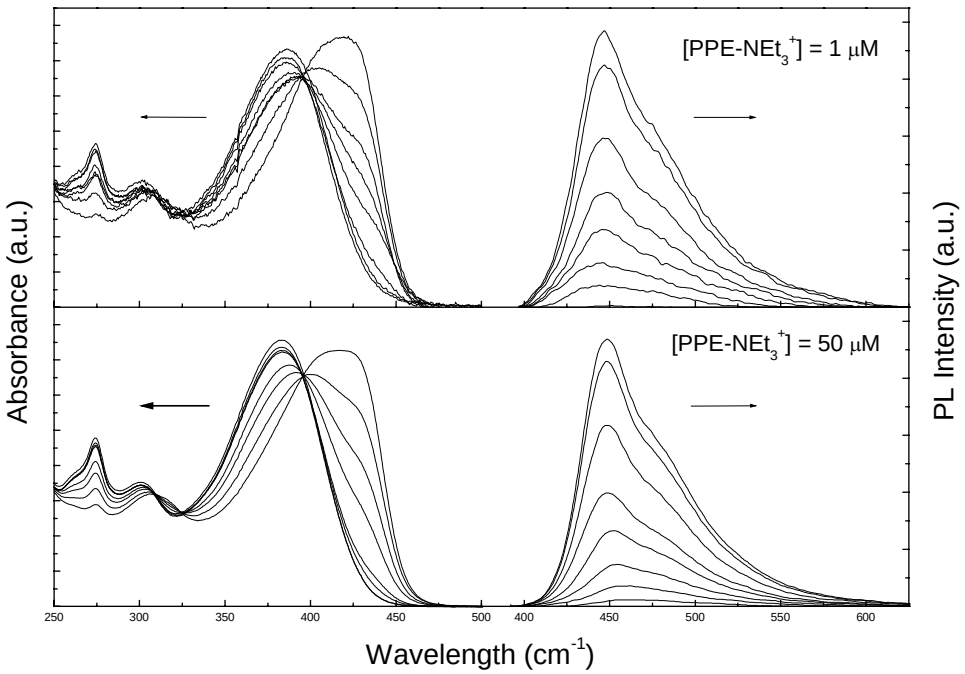

Figure 4.2.2 UV-vis absorption and emission spectra of PPE-NEt_3^+ in water quenched by added $Fe(CN)_6^{4-}$. [PPE-NEt_3^+] = 1 μM, [$Fe(CN)_6^{4-}$] = 0, 0.0025, 0.025, 0.05, 0.1, 0.15, 0.20 and 0.25 μM; [PPE-NEt_3^+] = 50 μM, [$Fe(CN)_6^{4-}$] = 0, 0.125, 1.25, 2.5, 5, 7.5, 10 and 12.5 μM. Absorption spectrum red-shifted and fluorenscence intensity decreased with increasing [$Fe(CN)_6^{4-}$].

Quenching study of PPE-NEt_3^+ by $Fe(CN)_6^{4-}$ in water was investigated. **Figure 4.2.2** shows the UV-vis and emission spectra of PPE-NEt_3^+ at 1 μM and 50 μM after addition of quencher $Fe(CN)_6^{4-}$ with different concentrations. As shown in **Figure 4.2.2**, the quencher-containing absorption and emission spectra of PPE-NEt_3^+ in such

two concentrations are nearly the same. The absorption at 426 nm in the UV-vis spectra of PPE-NEt_3^+ enhanced and formed a new peak gradually with the increase of $Fe(CN)_6^{4-}$ concentration, which clearly means that the quencher/polymer complex was formed. Its obvious red-shift, about 40 nm in comparison with the absorption maximum (386 nm) of pure PPE-NEt_3^+, may result from the quencher-induced longer conjugated length[13] or interchain aggregation.[2,8] It is noteworthy that despite the noticeable changes in the UV-vis absorption λ_{max} and efficient fluorescence quenching of PPE-NEt_3^+ by $Fe(CN)_6^{4-}$, PPE-NEt_3^+ with $Fe(CN)_6^{4-}$ showed nearly identical emission spectra with the emission peaks at λ_{max} = 446 nm, compared with the pristine emission spectra of pure PPE-NEt_3^+. This phenomenon is different with the quenching of PPE-SO_3^- by MV^{2+},[8] in which a new red-shifted absorption peak and broadened emission spectrum were observed due to PPE-SO_3^- aggregates induced by the addition of MV^{2+}. Thus it is unlikely to attribute the red-shift of absorption peak of PPE-NEt_3^+ to quenching-induced aggregation. Further investigation will be done in the future.

4.2.3.2 Stern-Volmer Studies

Figure 4.2.3 shows the selected Stern-Volmer plots for PPE-NEt_3^+ at different concentrations with $Fe(CN)_6^{4-}$ as the quencher. All the plots are linear at low concentrations, which is obeyed with equation 1:[14]

$$\frac{PL_0}{PL} = 1 + K_{sv}^{S}[Q] \qquad (1)$$

In this equation, PL_0 is the fluorescence intensity with no quencher present, PL is the

fluorescence intensity with quencher present, [Q] is the quencher concentration and K_{sv}^{S} is the static quenching Stern-Volmer constant. The high K_{sv}^{S} values (>10^6 M^{-1}) showed that the complex formation of PPE-NEt_3^+ and $Fe(CN)_6^{4-}$ via electrostatic interaction could effectively promote the sensibility of conjugated polymer to analyte.

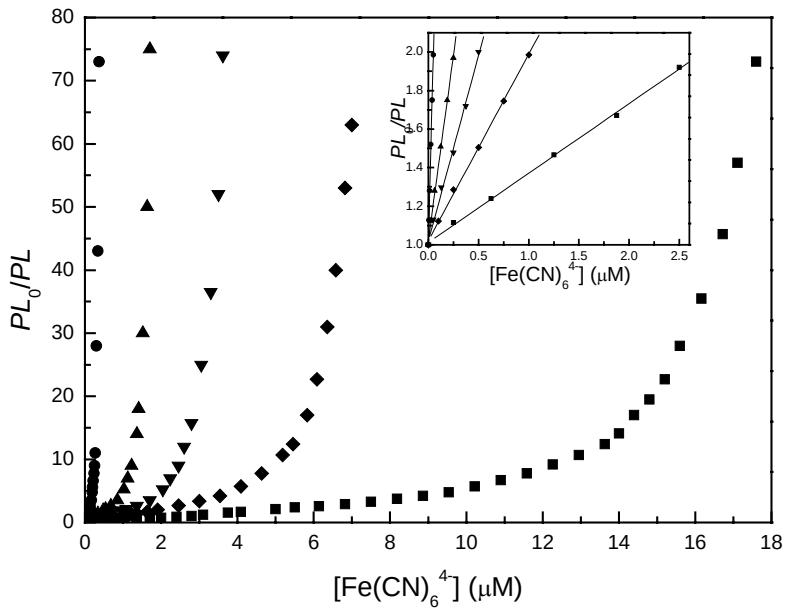

Figure 4.2.3 Stern-Volmer plots of PPE-NEt_3^+ at different concentrations quenched by $Fe(CN)_6^{4-}$. [PPE-NEt_3^+] = 1 μM (●), 5 μM (▲), 10 μM (▼), 20 μM (♦) and 50 μM (■). Inset: low quencher concentration regime and linear static Stern-Volmer fittings.

As the quencher concentration increased, the Stern-Volmer plots became superlinear, which could be explained by sphere-of-action quenching.[4] Thus a modified equation was used to describe the combination of static quenching with dynamic quenching containing the sphere-of-action:

$$\frac{PL_0}{PL} = (1 + K_{sv}^{S}[Q])e^{vN[Q]} = (1 + K_{sv}^{S}[Q])e^{\alpha V[Q]} \quad (2)$$

where v is the volume of sphere-of-action, N is Avogadro's number, volume constant V is defined as vN, and α is used to consider the charge-induced enhancement of the local quencher concentration.

It is interesting to find that the static quenching constant of PPE-NEt_3^+ for $Fe(CN)_6^{4-}$ increased with the concentration decrease of PPE-NEt_3^+. Such similar phenomenon was also reported on PPE-SO_3^- and PPP-NEt_3^+ systems,[7,8] which means that the static quenching constant K_{sv}^S was highly related to the concentration of detector used in detecting analyte. To further investigate this phenomenon, the plot of K_{sv}^S versus the reciprocal of PPE-NEt_3^+ concentration from 0.2 to 200 μM was described in **Figure 4.2.4**.

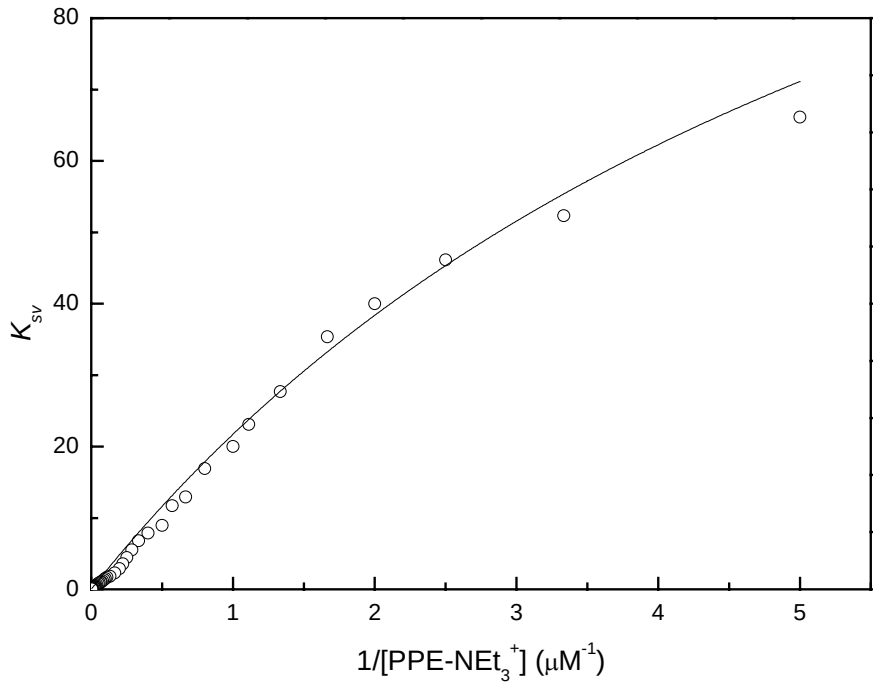

Figure 4.2.4 The plot of the static quenching constant K_{sv}^S versus the reciprocal of [PPE-NEt_3^+] ranging from 0.2 to 200 μM.

In **Figure 4.2.4**, K_{sv}^{S} is nearly in inverse proportion to PPE-NEt_3^+ concentration at high values (≥ 1 μM) while gradually deviating the linearity at low values (≤ 1 μM). Such a linear relationship was also presented in the quenching of PPE-SO_3^- by MV^{2+} in methanol.[8] To account for this phenomenon, the well-known concept of local concentration was introduced into the Stern-Volmer equation. PPE-NEt_3^+ chain acted as two roles in the quenching process. One role is that the main chain of PPE-NEt_3^+ is the fluorophore quenched by $Fe(CN)_6^{4-}$, the other is that its cationic side chain is the acceptor used to capture anionic $Fe(CN)_6^{4-}$ through electrostatic attraction and accordingly enhance the interaction between $Fe(CN)_6^{4-}$ and the main chain. The final effect of electrostatic attraction is that the homogenous dispersion of $Fe(CN)_6^{4-}$ in aqueous solution was destroyed and its local concentration near PPE-NEt_3^+ chain markedly enhanced. As a result, the quencher concentration $[Q]$ in equation 1 must be substituted by the real concentration, local quencher concentration $[Q]_{loc}$, and consequently a modified equation 3 was obtained:

$$\frac{PL_0}{PL} = 1 + K[Q]_{loc} \tag{3}$$

where K is the association constant of the interaction between the main chain and analyte. Assuming the captured analyte by polymer through electrostatic attraction was confined and dispersed homogenously in the volume controlled by polymer chain, the local concentration $[Q]_{loc}$ can be defined by equation 4:

$$[Q]_{loc} = \frac{[Q]_a}{[c]/N_p \times V_p} \tag{4}$$

where $[Q]_a$ is the concentration of attracted quencher, assuming dispersing in the

whole aqueous solution, $[c]$ is the concentration of repeat units in the whole aqueous solution, N_p is the polymerization degree, V_p is the volume controlled by one mol polymer chain, $[c]/N_p \times V_p$ is the ratio of all polymer-controlled volume to the whole volume of aqueous solution.

Accordingly, equation 3 changed into

$$\frac{PL_0}{PL} = 1 + \frac{N_p K}{[c]V_p}[Q]_a \tag{5}$$

$[Q]_a$ can be calculated from equation 6 and 7

$$K_b = \frac{[Q]_a}{[c_n][Q]_{na}} \tag{6}$$

$$[Q] = [Q]_a + [Q]_{na} \tag{7}$$

where K_b is the association constant, $[c_n]$ is the concentration of non-attracted ionic group in the whole solution, $[Q]_{na}$ is the concentration of non-attracted quencher in the whole solution, $[Q]$ is the pristine concentration of quencher before interaction with ionic group in the whole solution. After calculation, $[Q]_a$ is

$$[Q]_a = \frac{K_b[c_n]}{1 + K_b[c_n]}[Q] \tag{8}$$

Thus equation 5 became

$$\frac{PL_0}{PL} = 1 + \frac{N_p K}{[c]V_p}[Q]_a = 1 + \frac{N_p K}{[c]V_p} \times \frac{K_b[c_n]}{1 + K_b[c_n]}[Q] \tag{9}$$

Because we focused on the results when the quencher concentration was at low concentration, i.e. $[c_n] \gg [Q]$, thus $[c_n] \approx [c_n]_0 = n[c]$ where $[c_n]_0$ is the whole concentration of ionic group on the polymer side chain and n is the number of ionic group in one repeat unit (for PPE-NEt_3^+ investigated in this paper, n = 0.9), and the

above equation was rearranged into

$$\frac{PL_0}{PL} = 1 + \frac{N_p K}{[c]V_p} \times \frac{K_b n[c]}{1 + K_b n[c]}[Q] = 1 + \frac{nN_p KK_b}{V_p} \times \frac{1}{1 + nK_b[c]}[Q]$$
$$= 1 + \frac{nN_p KK_b}{V_p} \times \frac{1/[c]}{nK_b + 1/[c]}[Q] \quad (10)$$

Therefore, comparing equation 10 with equation 1, we can obtain

$$K_{sv}^{S} = \frac{nN_p KK_b}{V_p} \times \frac{1/[c]}{nK_b + 1/[c]} \quad (11)$$

Equation 11 describes the relationship between static quenching constant and detector concentration and can be utilized to determine the association constant K_b and K. From the best fit of equation 11 to the data in **Figure 4.2.4**, we obtained $K_b = 7.3 \times 10^6$ M^{-1}, $N_pK/V_p = 30$. Such a K_b contained the same order as the K_b for the bound complexes of $Ru(4,7\text{-}(SO_3C_6H_5)_2\text{-phen})_3^{4-}$ and poly-(amidoamine) family of starburst dendrimers,[15] and an order higher than that for the complex of $Ru(phen')_3^{4-}$ and $PPP\text{-}NEt_3^+$,[7] which implied that the binding constant K_b can be approximately estimated from equation 11, especially for those that can not be determined by the dependence of observed lifetime τ_{obs} on the host concentration.[16] Because of the rigid rod-like conformation of the polymer chain, the occupied volume of one polymer chain can be looked as a cylinder and thus V_p is described as

$$V_p = \frac{1}{4} N\pi a^2 L = \frac{1}{4} N\pi a^2 N_p l \quad (12)$$

where N is Avogadro's number, a is the diameter of the cylinder (~ 20 Å for $PPE\text{-}NEt_3^+$), L is the polymer length and l is the length of one repeater unit (~ 10 Å) in the main chain. After calculation, we obtained that the approximate value of K is 60 M^{-1}. The estimated K is nearly an order of magnitude lower than the K_{sv} for neutral

PPE derivatives quenched by MV^{2+}.[17] Such a much lower K value, compared with those K_{sv}^{S} values (10^6 M^{-1}), showed that the electrostatic interaction plays a major role to realize the significant high sensitivity of ionic conjugated polymer.[2]

In our PPE-NEt_3^+ system, it was discussed that this pure polymer presented physical property of individual chain at concentration ranging from 0.2 to 200 μM and the aggregation-induced quenching could be negligible at low quencher concentration. Based on the information listed above, we could consider that after adding quencher with low concentration, the individual chain properties at different PPE-NEt_3^+ concentration were similar with each other, and therefore V_p and K is stable with the change of detector concentration. Thus that K_{sv}^{S} is inverse proportional to PPE-NEt_3^+ concentration when nK_b » 1/[PPE-NEt_3^+], i.e. [PPE-NEt_3^+] » 1.5×10^{-7} M, could be inferred from equation 11.

$$K_{sv}^{S} = \frac{N_p K}{V_p} \times \frac{1}{[c]} \tag{13}$$

This theoretical inference is identical with the linear relationship of K_{sv}^{S} and 1/[PPE-NEt_3^+] obtained from the experimental results. We could anticipated that when nK_b » 1/[PPE-NEt_3^+], almost all quenchers were attracted to the polymer chains. As a result, when the original detector concentration decreased n-folds, correspondingly the quencher concentration with n-folds decrease was acquired to remain the local quencher concentration in the occupied volume of one polymer chain and obtain the same quenching effect. Finally, K_{sv}^{S} with n-folds enhancement is gained.

From **Figure 4.2.5** it was found that the fluorescence quenching effect at different PPE-NEt_3^+ concentrations is nearly the same when [$Fe(CN)_6^{4-}$]/[PPE-NEt_3^+] is

identical with each other, which further confirmed our theoretical anticipation. When 1/[c] is close to nK_b, only part of quencher was attracted to the polymer chains and as a result the linearity between K_{sv}^{S} and 1/[c] was destroyed and a downward curve was obtained.

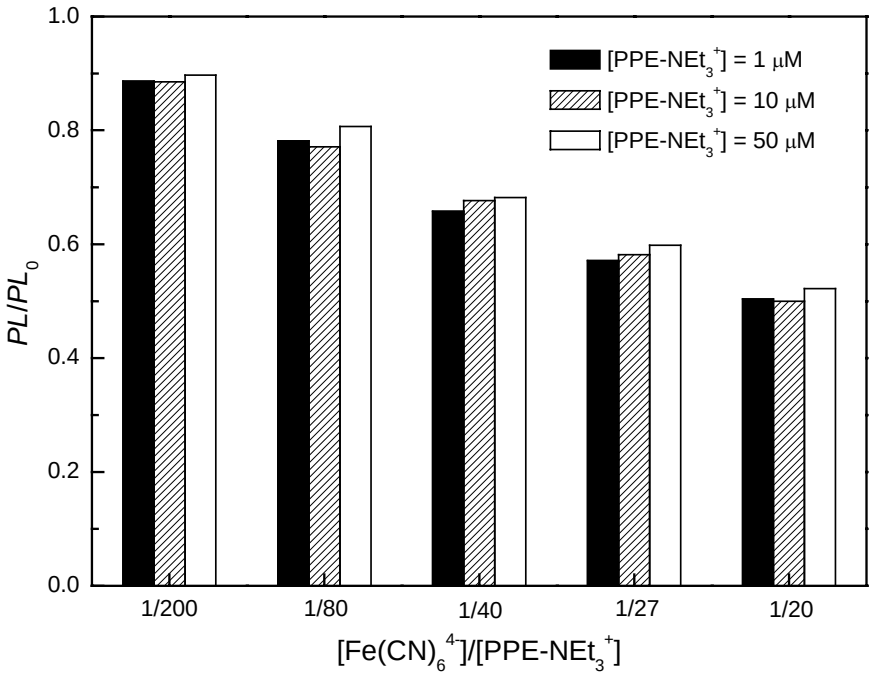

Figure 4.2.5 Fluorescence quenching of PPE-NEt$_3^+$ at different concentrations versus [Fe(CN)$_6^{4-}$]. [PPE-NEt$_3^+$] = 1, 10 and 50 μM. The concentration of Fe(CN)$_6^{4-}$ ranges from 1/200 to 1/20 in units of the ratio of [Fe(CN)$_6^{4-}$] to [PPE-NEt$_3^+$]

It is noteworthy that the successful explanation of the relationships between K_{sv}^{S} and 1/[c] in PPE-NEt$_3^+$ aqueous solution from equation 11 was gained under the environment without the existence of polymer aggregation. However, in many circumstances the influence to the relationship by aggregation of pure WSCPs in aqueous solution must be considered. Previous studies have showed that aggregation

of WSCPs always exists in water, even at low concentration of WSCPs. Such aggregation degree may be changed according to the WSCP concentration used and may influence the stability of K and V_p values and therefore destroy the relationship between K_{sv}^S and 1/[WSCP] obtained from equation 11. This influence from aggregation have been reported on the quenching of PPP-NEt_3^+ by $Ru(phen')_3^{4-}$ in aqueous solution.[7] The influence of aggregation to K and V_p could be considered as follows. It is well known that the intrachain exciton migration may occur when the existence of aggregation and lead to further amplified quenching, i.e., increased K value.[8] Also, the enhancement of aggregation reduces the occupied volume of all polymer chains and thereafter the V_p value. On the contrary, aggregation decreases the surface-of-volume ratio of polymer chains, which lowers polymer/quencher interactions and finally K value.[3] The influence of aggregation on the changes of K and V_p values is complicated, which is strongly based on the WSCP system and the solvent adopted.

4.2.4 Conclusions

In summary, we studied the fluorescence quenching of a water-soluble cationic poly(*p*-phenyleneethynylene) derivative at different concentrations by $Fe(CN)_6^{4-}$. A new UV-vis absorption peak appeared after adding $Fe(CN)_6^{4-}$, indicating that the polymer/quencher complex was formed. The static quenching constant K_{sv}^S of PPE-NEt_3^+ for $Fe(CN)_6^{4-}$ increased with the concentration decrease of PPE-NEt_3^+ and was observed inverse proportional to PPE-NEt_3^+ concentration ($\geq$ 1 μM) and deviation

of the linearity at lower concentration (≤ 1 μM) without the influence from aggregation. To account for this phenomenon, the concept of local quencher concentration was introduced into the Stern-Volmer equation and a new equation which successfully presented such a relationship between K_{sv}^{S} and [PPE-NEt_3^+] was obtained. The value of association constant for $Fe(CN)_6^{4-}$ binding to PPE-NEt_3^+ can be obtained from the equation ($K_b = 7.3 \times 10^6\ M^{-1}$).

References and Notes

1 McQuade, D. T.; Pullen, A. E.; Swager, T. M. *Chem. Rev.* **2000**, *100*, 2537.

2 Chen, L.; McBranch, D. W.; Wang, H.-L.; Helgeson, R.; Wudl, F.; Whitten, D. G. *Proc. Natl. Acad. Sci. U. S. A.* **1999**, *96*, 12287.

3 Gaylord, B. S.; Wang, S.; Heeger, A. J.; Bazan, G. C. *J. Am. Chem. Soc.* **2001**, *123*, 6417.

4 Wang, J.; Wang, D. L.; Miller, E. K.; Moses, D.; Bazan; G. C.; Heeger, A. J. *Macromolecules* **2000**, *33*, 5153.

5 Wang, D. L.; Wang, J.; Moses, D.; Bazan; G. C.; Heeger, A. J. *Langmuir* **2001**, *17*, 1262.

6 Fan, C.; Plaxco, K. W.; Heeger, A. J. *J. Am. Chem. Soc.* **2002**, *124*, 5642.

7 Harrison, B. S.; Ramey, M. B.; Reynolds, J. R.; Schanze, K. S. *J. Am. Chem. Soc.* **2000**, *122*, 8561.

8 Tan, C.; Pinto, M. R.; Schanze, K. S. *Chem. Commun.* **2002**, 446.

9 Chen, L.; McBranch, D.; Wang, R.; Whitten, D. G. *Chem. Phys. Lett.* **2000**, *330*, 27.

10 Chen, L.; Xu, S.; McBranch, D.; Whitten, D. G. *J. Am. Chem. Soc.* **2000**, *122*, 9302.

11 Jones, R. M.; Bergstedt, T. S.; McBranch, D. W.; Whitten, D. G. *J. Am. Chem. Soc.* **2001**, *123*, 6726.

12 Stork, M.; Gaylord, B. S.; Heeger, A. J.; Bazan, G. C. *Adv. Mater.* **2002**, *14*, 361.

13 Kim, B.; Chen, L.; Gong, J.; Osada, Y. *Macroolecules* **1999**, *32*, 3964.

14 Lakowicz, J. R. in *Principles of Fluorescence Spectroscopy*, 2nd ed.; Plenum Press: New York, **1999**.

15 Schwarz, P. F.; Turro, N.; Tomalia, D. A. *Journal of Photochemistry and Photobiology A: Chemistry* **1998**, *112*, 47.

16 Synder, S. W.; Scott, L. B.; Demas, J. N.; DeGraff, B. A. *J. Phys. Chem.* **1989**, *93*, 5265.

17 Zhou, Q.; Swager, T. M. *J. Am. Chem. Soc.* **1995**, *117*, 12593.

CHAPTER FOUR

Part III: Study on Optical Properties and Fluorescence Quenching of Cationic Water-Soluble Poly(*p*-phenyleneethynylene) under Complexation with Anionic Saturated Polyelectrolytes

4.3.1 Introduction

The attractive property of conjugated polymers based on their intense fluorescence is now highly focused on the potential application in biosensor field.[1] As noted by Chen et al., the fluorescence of water-soluble anionic conjugated polymer can be efficiently quenched by electron acceptor, methyl viologen (MV^{2+}), using electrostatic attraction as the binding force and by tethering MV^{2+} to a ligand which could bind to a specific biomolecule and observing the recoverability of fluorescence, a new class of biosensor was developed.[2] After that, Wang et al. formed a charge neutral complex (CNC) by combining conjugated polyelectrolyte and a saturated cationic polyelectrolyte at a 1:1 ratio (per repeat unit) to efficiently eliminate the influence on the fluorescence of conjugated polymers from nonspecific interaction between conjugated polyelectrolytes and biopolymers.[3] Recently, water-soluble cationic polyfluorene was developed to detect anionic DNA through energy transfer from conjugated chains to fluorophore grafted on another segment.[4] All the sensoric application referred to bi-polymer complexes, the optical properties of which were highly related to their conformation. However, up to now, there are no systematic studies for the relationship between sensitivity and conformation of conjugated polyelectrolytes.

Poly(*p*-phenyleneethynylene) (PPE) is a kind of conjugated polymer which has been widely used to study optical property-structure relationship because of its good optical

response on environmental variation through the facial changeable torsion angle and interchain aggregation. Its application as chemosensor has been widely reported by Swager's group.[5] Most recently the anionic water-soluble PPEs were utilized to study the contribution of polymer aggregation on sensitivity[6] and detect specific DNA.[7] Thus, it is reasonable to conceive that cationic water-soluble PPEs are good candidates for studying the variation of structure, optical properties and sensitivity of conjugated polymer-saturated polymer complexes.

Herein we report the study of optical properties and structures of polymer complexes prepared from the interaction between cationic conjugated polymer PPE-NEt_3Br and two oppositely charged saturated polymers, PAANa and PMAANa with different concentrations. It was showed that the complex structure was highly related to the structure of the saturated polymer chosen. The quenching effects of those complexes were also significantly determined by the structure of saturated polymer.

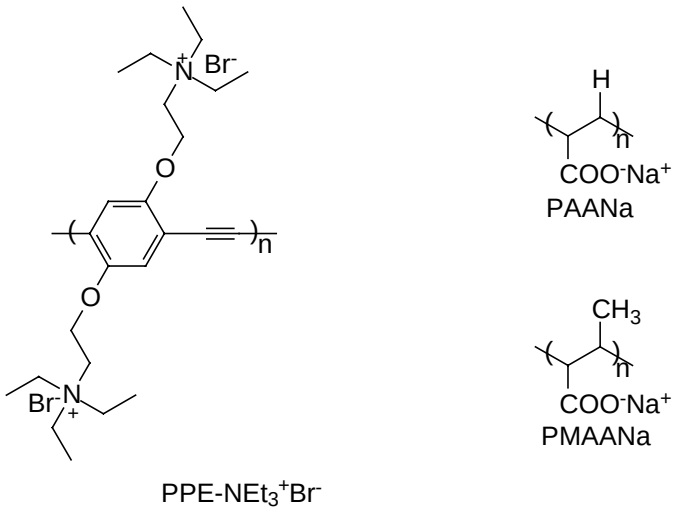

Scheme 4.3.1 Chemical structures of ionic polymers used in our investigation

4.3.2 Materials and Characterization Methods

4.3.2.1 Materials

Water-soluble conjugated polymer, PPE-NEt_3Br (**P8'**), was synthesized in our lab

according to the procedure we reported in Part I of Chapter 4. Poly(acrylic acid, sodium salt) (PAANa), poly(methyl acrylic acid, sodium salt) (PMAANa) and the quencher, $K_4Fe(CN)_6$, was obtained from Aldrich Chemical Co. All the chemical structures of the above ionic polymers were shown in **Scheme 4.3.1.** The Milli-Q water used in preparing the aqueous solutions of those polymers and quenchers was purged with nitrogen for 4 h before using.

4.3.2.2 Characterization Methods

UV-vis spectra were recorded on a Shimadzu 3101 PC spectrometer. Fluorescence measurement was carried out on a Perkin-Elmer LS 50B photoluminescence spectrometer with a xenon lamp as a light source. The quenching studies were realized *in situ* through comparing the photoluminescence intensities of the solutions at a series of polyelectrolyte complex and quencher concentrations. All the quenched solutions were prepared after adding calculated amount of quencher solution into PPE-NEt_3Br solution and purging with nitrogen for 1 min and immediately used to take their corresponding absorption spectra and emission spectra with excitation at 386 nm. Prior to test those quenched solutions, the optical properties of pure PPE-NEt_3Br solution were first studied according to the same procedure.

4.3.3 Results and Discussion

4.3.3.1 UV-vis Absorption and Emission of Polyelectrolyte Complex

Figure 4.3.1 showed the UV-vis absorption and emission spectra of a dilute aqueous solution (5 μM) of PPE-NEt_3Br in the presence of PAANa with different concentrations. In **Figure 4.3.1**, the absorption peak of PPE-NEt_3Br broadened and red shifted firstly according to the increase of [PAANa] and the corresponding maximum

reached the reddest at 387 nm when [PAANa]/[PPE-NEt_3Br] = 1.2. After further increasing the amount of PAANa, the absorption maximum blue shifted and recovered to the initial position at 381 nm. Such a variation of absorption peaks may be highly related to the variation of conjugation in the complexation. As **Figure 4.3.1** displayed, with the addition of PAANa into the aqueous solution of PPE-NEt_3Br, the pristine emission peak at 446 nm slightly red shifted to 453 nm and its fluorescence intensity steadily decreased with the [PAANa]/[PPE-NEt_3Br] ratio ongoing from 0 to 1.2. It is interesting to find that further increase of the [PAANa]/[PPE-NEt_3Br] ratio caused the emission maximum to return back to its original position and the fluorescence intensity to increase over the original one, which is well accorded with the corresponding change appeared in absorption spectra. Close association of π-systems of a conjugated polymer may induce a red-shifted aggregation-dominated emission spectrum and often cause a substantial decrease in PL quantum yield relative to isolated polymer chains. Thus, the spectra change shown in **Figure 4.3.1** is believed to originate from the aggregation of PPE-NEt_3Br main chains. The results suggested that the complex formation between oppositely charged polymer chains through Coulombic attraction is not a simple bichain combination but a cluster involving more than one PPE-NEt_3Br and PAANa chains, which is according to the [PAANa]/[PPE-NEt_3Br] ratio. After adding a small amount of PAANa, PAANa chain played a role as an anionic center to make PPE-NEt_3Br chains surround them and induce these conjugated chains to form interchain aggregation. When further increasing the amount of PAANa and finally PAANa was much more than PPE-NEt_3Br, the complex structure was changed. On the contrary, it could be anticipated that the aggregation of PPE-NEt_3Br chains was destroyed and PPE-NEt_3Br chain, instead of PAANa, served as the cationic center and was besieged by several PAANa chains. As a result, PPE-NEt_3Br chains were

separated with each other and existed in isolated state and recovered their optical properties as single chains. It is noteworthy that when the amount of PAANa continued enhancing, its fluorescence intensity increased obviously and exceeded the pristine one. Chen reported that adding surfactant into aqueous solution of PPV-SO_3^- significantly increased its fluorescence intensity because the surfactant could reduce the number of kink defects and frustrate the tendency of polymer chains to self-association.[8] Thus, we proposed that the enhancement of fluorescence intensity after adding enough amount of PAANa result from the same reason appeared in the interaction between conjugated polymer and appropriate surfactant.

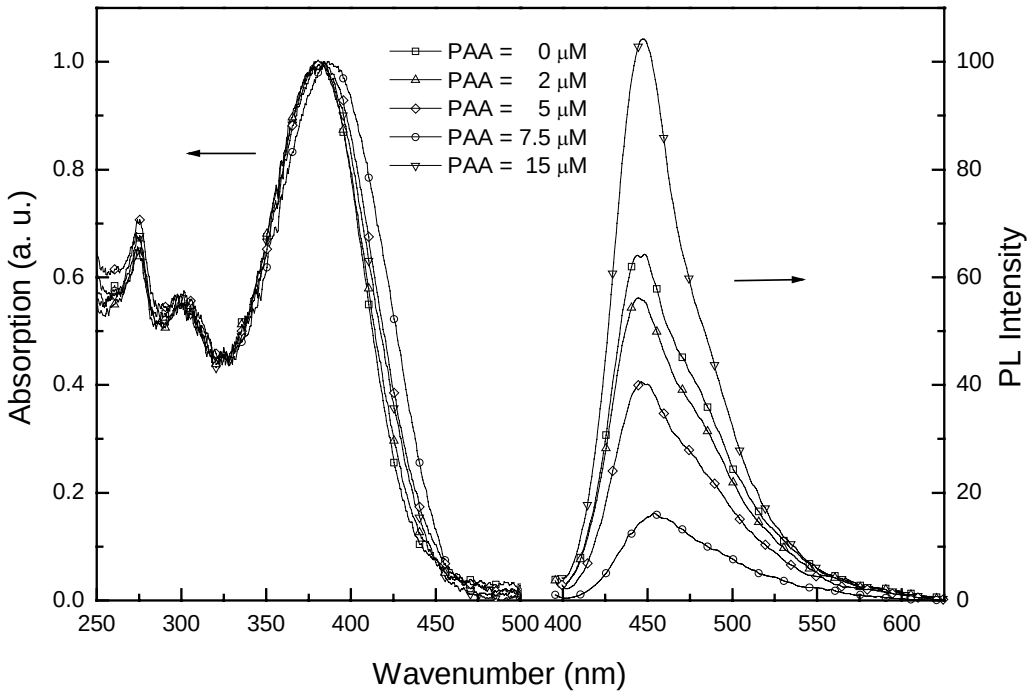

Figure 4.3.1 UV-vis absorption and emission spectra of PPE-NEt_3Br in the presence of PAANa with different concentration

However, further investigation showed that the structure of conjugated polymer-coil polymer complex was drastically influenced by the structure change of side group of the anionic saturated polymers. When PMAANa, instead of PAANa, was chosen to

form the complex with PPE-NEt_3Br, the results showed obvious difference with that of PAANa/PPE-NEt_3Br complex. In **Figure 4.3.2**, the absorption peak of PPE-NEt_3Br blue shifted gradually and became much narrower accompanied with the increase of the amount of PMAANa and the absorption maximum reached the bluest at 363 nm. Such an obvious blue-shift of PMAANa/PPE-NEt_3Br complex was contrast with the slight red-shift of PAANa/PPE-NEt_3Br complex, indicating the existence of different structure between the two complexes. The only structure difference between PAANa and PMAANa is the existence of methyl group in side chain of PMAANa and therefore it was suggested that the existence of methyl group in PMAANa result in a more twisted structure of PPE-NEt_3Br main chain and a correspondingly less effective conjugated length and a blue-shift absorption spectra when PMAANa chain entangled with PPE-NEt_3Br chain. Meanwhile, the obtained more twisted structure of PPE-NEt_3Br main chain and the methyl group itself could efficiently block the formation of interchain aggregation for PPE-NEt_3Br through steric effect. While for PAANa, the non-existence of methyl group in its side chain seemed to reduce the steric effect and be beneficial with interchain aggregation of PPE-NEt_3Br. It was also found that the absorption peak became narrow after adding PMAANa and we attribute this phenomenon to the reduced conformational disorder through the interaction between PMAANa and PPE-NEt_3Br.[8] The difference of the emission spectra between PMAANa/PPE-NEt_3Br and PAANa/PPE-NEt_3Br further demonstrated that the existence of bulky group in side chain significantly influence the structure of complex through electrostatic attraction. In **Figure 4.3.2**, the emission maxima obviously blue shifted from 446 nm to 419 nm and the obvious vibronic structure was disappeared after adding enough PMAANa, indicating the formation of shorter efficient conjugated length. Meanwhile, the emission spectra of PPE-NEt_3Br also showed gradually

enhanced fluorescence intensity after adding PMAANa without suffering the procedure of decreased fluorescence intensity, which is apparent after adding PAANa. Such an enhanced fluorescence intensity can also be explained by the reduced number of kink defects and the decreased self-association after adding PMAANa, just as what we discussed aon its absorption spectra.

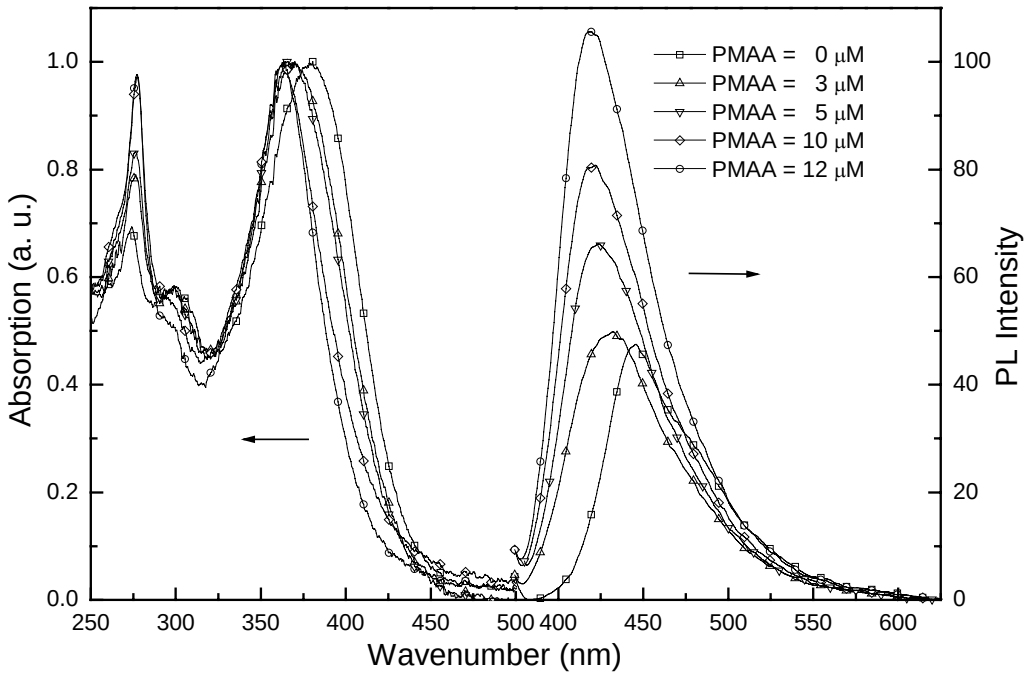

Figure 4.3.2 UV-vis absorption and emission spectra of PPE-NEt$_3$Br in the presence of PMAANa with different concentration

To further clarify the side-group-effect on the complex structure, curves of relative fluorescence intensity (the intensity ratio of PAANa/PPE-NEt$_3$Br or PMAA-PPE-NEt$_3$Br complexes to pure PPE-NEt$_3$Br in aqueous solution) vs. PAANa:PPE-NEt$_3$Br or PMAANa:PPE-NEt$_3$Br molar ratio ([PAANa]/[PPE-NEt$_3$Br] or [PMAANa]/[PPE-NEt$_3$Br]) were shown in **Figure 4.3.3**. When the PAANa:PPE-NEt$_3$Br reached 1.2, the fluorescence intensity decreased to the minimum at 0.2 (compared with the fluorescence intensity of the pristine PPE-NEt$_3$Br in aqueous

solution), indicating the formation of strongest aggregation. When the PAANa:PPE-NEt_3Br reached above 1.2, the fluorescence intensity increased gradually and reached the highest at [PAANa]:[PPE-NEt_3Br] ≈ 3.5, which means that the PAANa (low concentration)-induced aggregation of PPE-NEt_3Br was destroyed and nearly three PAANa chains is enough to obtain the saturation of the fluorescence intensity of PPE-NEt_3Br through entangling one PPE-NEt_3Br chain.

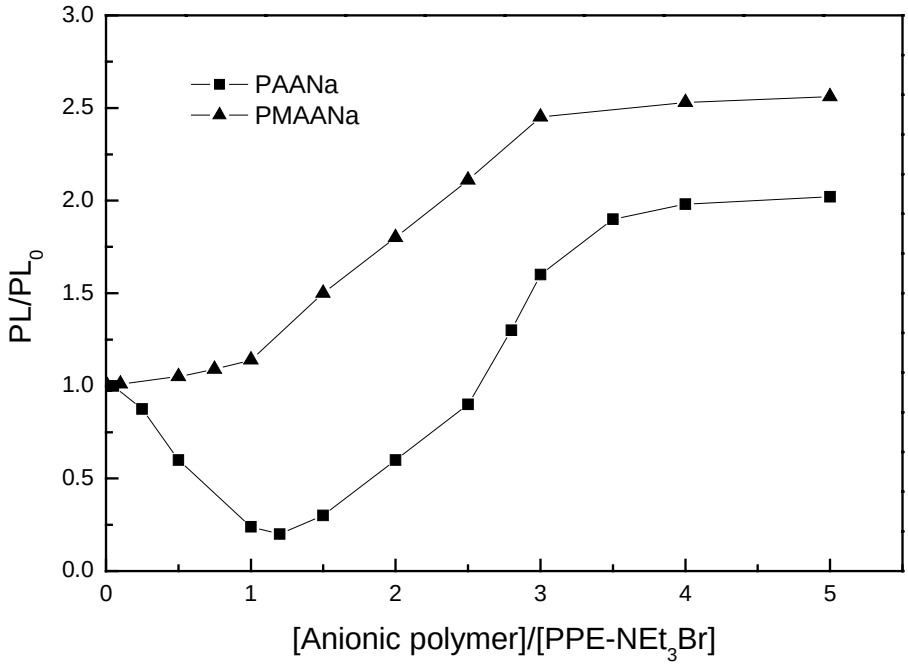

Figure 4.3.3 Curves of relative fluorescence intensity (the intensity ratio of PAANa/PPE-NEt_3Br complexes to pure PPE-NEt_3Br in aqueous solution) vs. PAANa:PPE-NEt_3Br or PMAANa:PPE-NEt_3Br molar ratio

For PMAANa/PPE-NEt_3Br complex, no decreased fluorescence intensity was found and the saturated fluorescence intensity was obtained at PMAANa:PPE-NEt_3Br ≈ 3. Meanwhile, the effect of PMAANa on fluorescence enhancement of PPE-NEt_3Br (FL/FL_0 = 2.4) was higher than that of PAANa (FL/FL_0 = 2.0), indicating that such an anionic polymer-induced fluorescence enhancement of conjugated polymers was highly related to the bulk of side group in those anionic polymers.

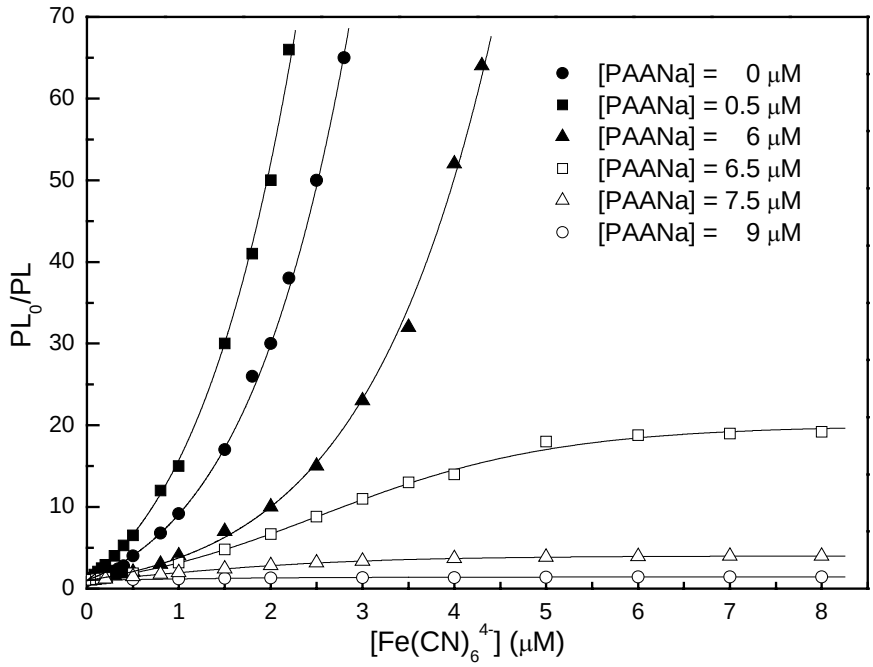

Figure 4.3.4 The Stern-Volmer plot of PAANa/PPE-NEt$_3$Br (5 μM) complex quenched by Fe(CN)$_6^{4-}$ in aqueous solution with different concentrations of PAANa

4.3.3.2 Stern-Volmer Study of PAANa/PPE-NEt$_3$Br and PMAANa/PPE-NEt$_3$Br Complexes

The fluorescence quenching study of biomolecules by suitable quencher has been widely used to investigate the conformation of corresponding biomolecules.[9] Thus, it is an appropriate way to study the structure of PAANa/PPE-NEt$_3$Br and PMAANa/PPE-NEt$_3$Br complex through quenching study of these complexes. Here we chose Fe(CN)$_6^{4-}$ as the anionic quencher to study related fluorescence quenching that have been widely used for quenching research.[10-12] **Figure 4.3.4** and **Figure 4.3.5** showed the Stern-Volmer plot of PAANa/PPE-NEt$_3$Br and PMAA-PPE-NEt$_3$Br complexes quenched by Fe(CN)$_6^{4-}$ in aqueous solution with different concentrations of PAANa and PMAANa respectively. It is interesting to find that there existed two kinds

of Stern-Volmer curves for the two complexes, the upward and downward curves. When PAANa:PPE-NEt_3Br ≤ 1.2 and PMAANa:PPE-NEt_3Br ≤ 1 , all Stern-Volmer curves presented upward curves, while when PAANa:PPE-NEt_3Br > 1.2 and PMAA:PPE-NEt_3Br > 1, all Stern-Volmer curves showed downward curves, which obviously indicated that there existed different structures of the complex in aqueous solution.

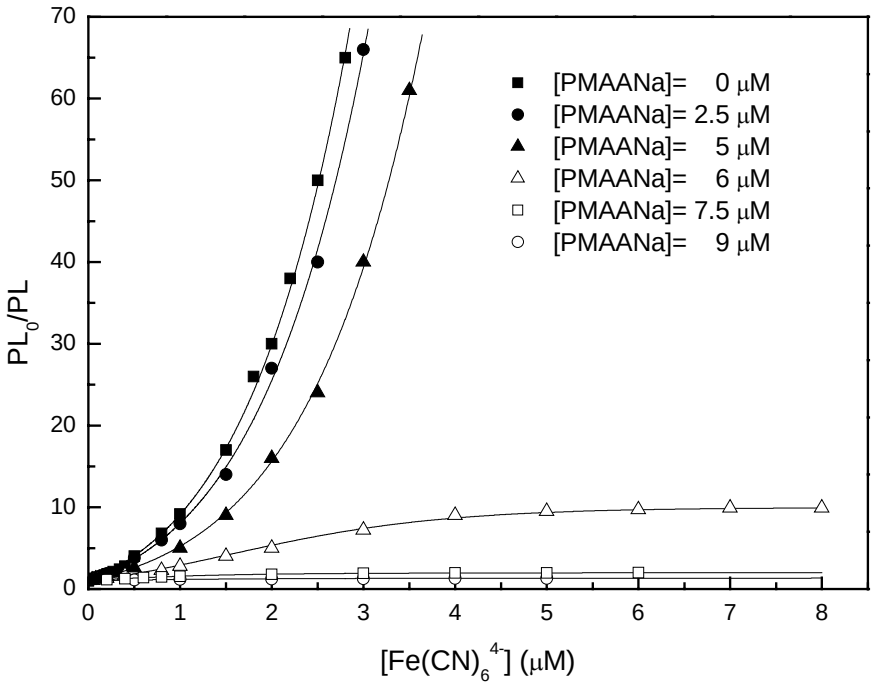

Figure 4.3.5 The Stern-Volmer plot of PMAANa/PPE-NEt_3Br (5μM) complex quenched by $Fe(CN)_6^{4-}$ in aqueous solution with different concentrations of PMAANa

For those upward curves, a modified Stern-Volmer equation 1, in which sphere-of-action was considered,[13] can be efficiently used to describe this phenomenon:

$$\frac{F_0}{F} = (1 + K_{sv}^{S}[Q])e^{\alpha V[Q]} \qquad (1)$$

where F_0 is the fluorescence intensity with no quencher present, F is the fluorescence

intensity with quencher present, [Q] is the quencher concentration, K_{sv}^{S} is the static quenching constant, V is volume constant and α is used to account for the charge-induced enhancement of the local quencher concentration.

Table 4.3.1 Photoluminescence quenching of complexes of PPE-NEt$_3^+$ and anionic saturated polymers by Fe(CN)$_6^{4-}$

[PAA] (μM)	K_{sv} (M^{-1})	αV (M^{-1})	f_a	[PMAA] (μM)	K_{sv} (M^{-1})	αV (M^{-1})	f_a
0.0	4.0×10^6	6.0×10^5	1	0.0	4.0×10^6	6.0×10^5	1
0.5	8.0×10^6	5.6×10^5	1	0.5	3.8×10^6	6.2×10^5	1
1.0	6.8×10^6	5.9×10^5	1	1.0	3.8×10^6	6.0×10^5	1
2.5	5.0×10^6	5.8×10^5	1	2.5	3.6×10^6	5.8×10^5	1
5.0	2.2×10^6	5.6×10^5	1	4.0	2.4×10^6	5.6×10^5	1
6.0	1.2×10^6	5.4×10^5	1	5.0	1.9×10^6	5.9×10^5	1
6.5	1.0×10^6	5.0×10^5	0.95	6.0	1.0×10^6	5.4×10^5	0.90
7.5	6.2×10^5	4.4×10^5	0.75	7.5	3.4×10^5	4.9×10^5	0.50
9.0	2.0×10^5	4.2×10^5	0.30	9.0	8.0×10^4	4.6×10^5	0.20
10	0	0	0	10	0	0	0
12	0	0	0	12	0	0	0

In **Figure 4.3.4 and Figure 4.3.5**, those downward curves could be efficiently explained by the existence of inaccessible fluorophore,[9] which results in part of unquenched fluorescence (the platform in those downward curves). Therefore, considering the inaccessible fluorophore and sphere-of-action in our system, equation 2 was modified to describe the relationship between the fluorescence intensity and quencher concentration (please see Part II of Chapter 3):

$$\frac{f_a F_0}{F-(1-f_a)F_0} = (1+K_{sv}[Q])e^{\alpha V[Q]} \tag{2}$$

where f_a is the fraction of fluorescence from an accessible fluorophore. After rearrangement equation 2 became

$$\frac{F_0}{F} = \frac{(1+K_{sv}[Q])e^{\alpha V[Q]}}{f_a+(1-f_a)(1+K_{sv}[Q])e^{\alpha V[Q]}} \tag{3}$$

With best fit on those Stern-Volmer curves by equation 2 or 3, the K_{sv}, f_a and αV values were obtained and listed in **Table 4.3.1**.

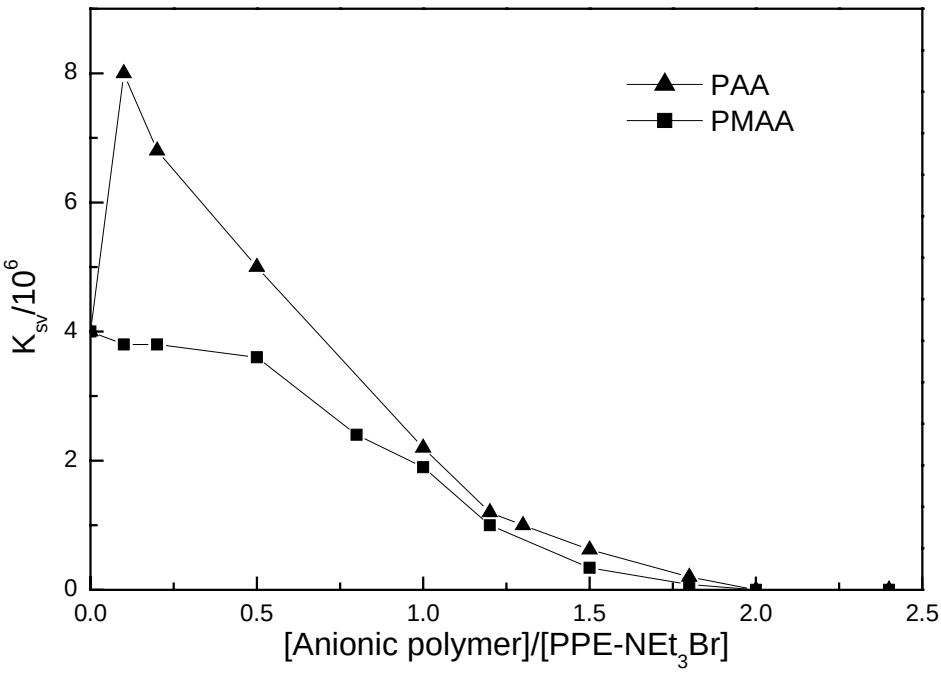

Figure 4.3.6 The K_{sv}^S values of PPE-NEt$_3$Br at different concentrations of those ionic polymers, PAANa and PMAANa

Figure 4.3.6 showed the K_{sv}^S values of PPE-NEt$_3$Br at different concentrations of those ionic polymers, PAANa and PMAANa. For PAANa- PPE-NEt$_3$Br complex, the K_{sv}^S value enhanced initially and then decreased swiftly to zero, which showed a sharp peak at about 0.1 of PAANa:PPE-NEt$_3$Br. Such gradually enhanced K_{sv}^S values when PAANa:PPE-NEt$_3$Br < 0.1 could be reasonably explained by the formation of interchain aggregation which enhances the conjugated effect and the energy migration among the interchains and therefore increases the quenching effect.[6,14] It is noticeable that although the lowest fluorescence intensity of this complex, i.e., the highest aggregation was happened at PAANa:PPE-NEt$_3$Br = 1.2, its corresponding K_{sv}^S value was not the highest in our system. It is well known that electrostatic attraction was the

major driving force to obtain amplified K_{sv}^{S} values for ionic conjugated polymers. Thus, although adding anionic PAANa could form aggregation of PPE-NEt_3Br which is conducive to increase the fluorescence quenching effect, the enhanced concentration of negative charge on PAANa simultaneously neutralized the positive charge on PPE-NEt_3Br chains and led to the decreased electrostatic attraction between PPE-NEt_3Br and anionic quencher $Fe(CN)_6^{4-}$ and consequently the lowered fluorescence quenching effect.[8] Thus it could be anticipated that when the fluorescence intensity decreased to the minimum based on the formation of aggregation, the decreased quenching effect from the decreased electrostatic attraction was much higher than the enhanced quenching effect from the enhanced aggregation, and as a result the total effect showed decreased K_{sv}^{S} value. When PAANa:PPE-NEt_3Br = 2.5, the K_{sv}^{S} value dramatically lowered to zero, which could be explained by two reasons: one is the lowered electrostatic attraction as we discussed above, the other is the formation of inaccessible fluorophore which was deeply buried by PAANa chains. For PMAANa/PPE-NEt_3Br complex, no enhanced K_{sv}^{S} value was observed according to the increased PMAANa concentration. Instead, its K_{sv}^{S} value decreased followed by two steps. When PMAANa:PPE-NEt_3Br < 0.5, all the K_{sv}^{S} value decreased slowly attributing to the decreased effective conjugated length inferred from absorption spectra which lowered the quenching efficiency. As PMAANa:PPE-NEt_3Br > 0.5, K_{sv}^{S} value decreased swiftly, which could also be explained by the neutralization effect from anionic PMAANa chains and the formation of inaccessible fluorophore in this system, as we discussed in PAANa/PPE-NEt_3Br system. The different variation of K_{sv}^{S} values in PAANa/PPE-NEt_3Br and PMAANa/PPE-NEt_3Br complexes indicated that the structure variation of the added anionic polymer could significantly influence the sensitivity of conjugated polymers with counterions. Furthermore, the study disclosed

that choosing appropriate ionic polymer and controlling its concentration to form complex with ionic conjugated polymers might efficiently increase its biosensitivity.

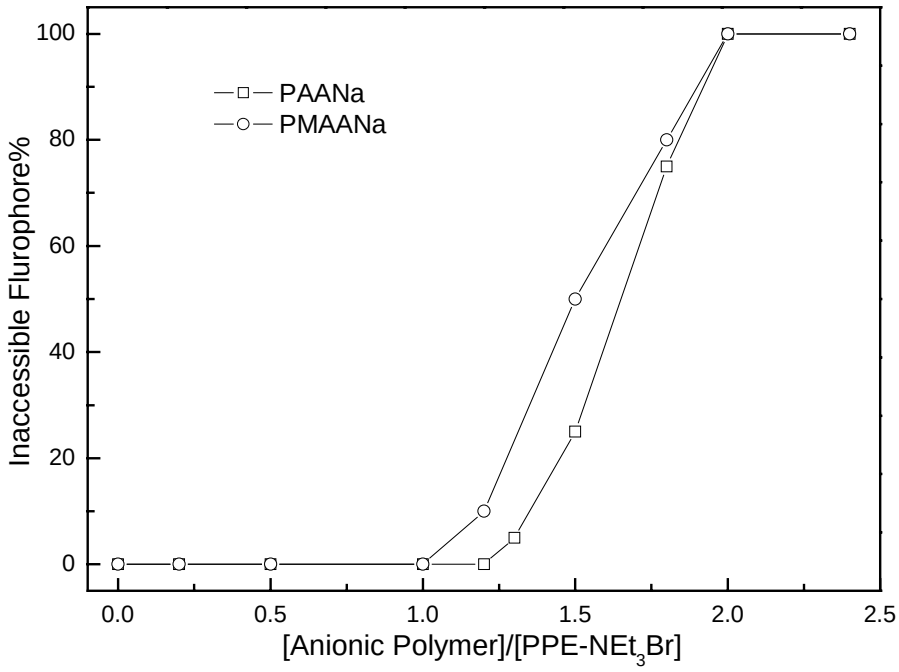

Figure 4.3.7 The percentage of inaccessible fluorophore vs the relative concentration of PAANa and PMAANa

To further investigate the structure of those complexes, the percentage of inaccessible fluorophore vs the relative concentration of PAANa and PMAANa was depicted in **Figure 4.3.7**. The inaccessible fluorophore in PAANa/PPE-NEt_3Br complex started to be formed at PAANa:PPE-NEt_3Br ≈ 1.2. Such a data is very close to the PAANa:PPE-NEt_3Br ratio for obtaining the lowest fluorescence intensity of such a complex, indicating the formation of part of the buried PPE-NEt_3Br chain surrounded by PAANa chains. Compared with **Figure 4.3.6**, it could be found that although the K_{sv}^{S} value fluctuated when PAANa:PPE-NEt_3Br < 1.2, the inaccessible fluorophore still not existed. It could be imagined that when PAANa:PPE-NEt_3Br < 1.2, all the rod-like conjugated chains besieged the PAANa chain and could be easily touched by

quencher. Although at the same time the increased concentration of anionic group enhanced the neutralization of cationic groups on PPE-NEt_3Br and hence decreased its sensitivity through lowering electrostatic attraction, the whole fluorescence still could be quenched completely at higher concentration of $Fe(CN)_6^{4-}$. When PAANa:PPE-NEt_3Br > 1.2, inaccessible fluorophore was produced which clearly means that part of the PPE-NEt_3Br chains started to be surrounded by PAANa chains and some was deeply buried and can not be touched by quencher. When PAANa:PPE-NEt_3Br = 2.5, inaccessible fluorophore reached 100%, indicating that all conjugated chains have been isolated from quenchers by the surrounded PAANa chains. It is noticeable that although all PPE-NEt_3Br chains was screened by PAANa chains when PAANa:PPE-NEt_3Br = 2.5, the fluorescence intensity of such a complex was continued enhancing until PAANa:PPE-NEt_3Br = 3.5. Such a concentration difference showed that the disappearance of interchain aggregation is not the reason for the enhanced fluorescence intensity. PMAANa/PPE-NEt_3Br complex showed the similar curve for inaccessible fluorophore as PAANa/PPE-NEt_3Br complex. Previous figures for PMAANa/PPE-NEt_3Br complex cannot give out the concentration value of PMAANa at which the mutation of complex structure was happened. But in **Figure 4.3.7**, we could see clearly that inaccessible fluorophore in PMAANa/PPE-NEt_3Br complex started to appear at PMAANa:PPE-NEt_3Br = 1, which indicated the mutation of complex structure happened at this point.

4.3.4 Conclusions

In summary, we studied the optical properties and quenching behaviors of complexations of PPE-NEt_3Br with the oppositely charged polymer PAANa and PMAANa in aqueous solution. It was showed that addition of few PAANa induced the

PPE-NEt_3Br chain to vary from isolated state to aggregated state and then recovered to isolated state through increasing the amount of PAANa, which exhibited an obvious fluctuation of fluorescence intensity and K_{sv} values. While after adding PMAANa, PPE-NEt_3Br still exhibited the similar mutation of complex structure just as what appeared in PAANa/PPE-NEt_3Br complex except that more twisted conjugated main chain and no aggregation was formed. Such a significant structure difference showed that a little change of the structure of those anionic polymers will significantly influence the conformation and hence the optical and quenching properties of ionic conjugated polymers. Investigation of the percentage of inaccessible fluorescence is a good way to obtain the complex structure information that the mutation point for PAANa/PPE-NEt_3Br complex was at PAANa:PPE-NEt_3Br = 1.2, which is amount to the corresponding result from the variation of its fluorescence intensity, and that for PMAANa/PPE-NEt_3Br complex is at PMAANa:PPE-NEt_3Br = 1. Investigation of the sensitivity of those complexes showed that adding an appropriate amount of PAANa will be beneficial to enhance the K_{sv} value resulting from the PAANa-induced aggregation while no similar phenomenon was found in PMAANa/PPE-NEt_3Br system, which further demonstrated that the sensitivity of conjugated polymers could be controlled by the structure of the complexes formed between rod-like conjugated polyelectrolyte and oppositely charged polymers and thus by the structure of those oppositely charged polymers utilized in our system. Therefore, in practical application to develop good sensors with high sensitivity, it is important to choose a polyelectrolyte with suitable structure as biosensor platform and control its amount for obtaining complexes with good seistivity.

References and Notes

1 McQuade, D. T.; Pullen, A. E.; Swager, T. M. *Chem. Rev.* **2000**, *100*, 2537.

2 Chen, L.; McBranch, D. W.; Wang, H.-L.; Helgeson, R.; Wudl, F.; Whitten, D. G. *Proc. Natl. Acad. Sci. U. S. A.* **1999**, *96*, 12287.

3 Wang, D.; Gong, X.; Heeger, P. S.; Rininsland, F.; Bazan, G. C.; Heeger, A. J. *Proc. Natl. Acad. Sci. U. S. A.* **2002**, *99*, 49.

4 Gaylord, B. S.; Heeger, A. J.; Bazan, G. C. *Proc. Natl. Acad. Sci. U. S. A.* **2002**, *99*, 10954.

5 (a) Zhou, Q.; Swager, T. M. *J. Am. Chem. Soc.* **1995**, *117*, 7017. (b) Zhou, Q.; Swager, T. M. *J. Am. Chem. Soc.* **1995**, *117*, 12593. (c) Yang, J.-S.; Swager, T. M. *J. Am. Chem. Soc.* **1998**, *120*, 5321. (d) Yang, J.-S.; Swager, T. M. *J. Am. Chem. Soc.* **1998**, *120*, 11864. (e) Kim, J.; McQuade, D. T.; McHugh, S. K.; Swager, T. M. *Angew. Chem. Int. Ed.* **2000**, *39*, 3869.

6 Tan, C.; Pinto, M. R.; Schanze, K. S. *Chem. Commun.* **2002**, 446.

7 Kushon, S. A.; Ley, Kevin D.; Bradford, K.; Jones, R. M.; McBranch, D.; Whitten, D. *Langmuir*, **2002**, *18*, 7245.

8 Chen, L.; Xu, S.; McBranch, D.; Whitten, D. G. *J. Am. Chem. Soc.* **2000**, *122*, 9302.

9 Lakowicz, J. R. in *Principles of Fluorescence Spectroscopy*, 2nd ed.; Plenum Press: New York, 1999.

10 Harrison, B. S.; Ramey, M. B.; Reynolds, J. R.; Schanze, K. S. *J. Am. Chem. Soc.* **2000**, *122*, 8561.

11 Schwarz, P. F.; Turro, N.; Tomalia, D. A. *Journal of Photochemistry and Photobiology A: Chemistry* **1998**, *112*, 47.

12 Fan, Q-L.; Lu, S.; Lai, Y-H.; Huang, W. *Macromolecules* **2003**, revised.

13 Wang, J.; Wang, D. L.; Miller, E. K.; Moses, D.; Bazan; G. C.; Heeger, A. J. *Macromolecules* **2000**, *33*, 5153.

14 Fan, Q-L.; Lu, S.; Huang, W. *Macromolecules* **2003**, submitted.

CHAPTER FIVE

EXPERIMENTAL SECTION

5.1 General

5.1.1 Instrumentation

All melting points (mp) were determined on an Electrothermal IA 9300 Digital Melting-point Apparatus and are uncorrected. The ^{1}H NMR spectra were determined in $CDCl_3$ (unless otherwise stated) on a Bruker ACF 300 (300 MHz) Fourier transform spectrometer. All chemical shifts are reported in ppm downfield from tetramethyl silane as the internal standard. All ^{13}C NMR spectra were determined in $CDCl_3$ at room temperature on a Bruker ACF 400 spectrometer. Infrared spectra were recorded on a Bio-Rad FTS 165 spectrometer by dispersing samples in KBr. Elemental microanalyses were carried out by the Microanalysis Lab of the National University of Singapore. All evaporations were carried out under reduced pressure on a rotary evaporator at ca. 40 ^{o}C. All organic layers were washed with water (unless otherwise stated) and were dried with anhydrous sodium sulfate or magnesium sulfate.

5.2 Monomers and Polymers Synthesized in Chapter 2

5.2.1 2,5-Dibromo-1,4-phenylenemethylene diacetate (1)

26.4 g (0.1 mol) of 2,5-dibromo-*p*-xylene, 36.0 g (0.2 mol) of NBS and a catalytic amount of AIBN as a initiator were added into 200 mL of benzene. The reaction mixture was reflux for 3 h under nitrogen atmosphere. When cooling to room temperature the mixture was filtered. The obtained filtrate was rotary evaporated and then directly added into 200 mL of acetic acid with 33 g (0.4 mol) of sodium acetate

without purification. The mixture was refluxed for 12 h and the acetic acid was rotary evaporated. The residue was added into 200 mL of water, extracted with chloroform and dried with anhydrous magnesium sulfate. The solution was filtered and concentrated. The resulting crude product was purified by recrystallization from ethanol to give 23.0 g of white crystals (yield 60.5%). Mp: 162–3 ^{o}C. ^{1}H NMR ($CDCl_3$, ppm): δ 7.62 (s, 2H), 5.16 (s, 4H), 2.18 (s, 6H). ^{13}C NMR ($CDCl_3$, ppm): δ 170.77, 137.31, 133.67, 122.28, 65.16, 21.20.

5.2.2 2,5-Dibromo-1,4- bishydroxymethylbenzene (2)

A 22.8 g (0.06 mol) sample of diacetate **1** was added into 300 mL mixed solvent of ethanol-water (1:1) containing 20 g (0.5 mol) of sodium hydroxide. The mixture was refluxed for 4 h with stirring. After cooling to room temperature, ethanol was evaporated through a rotary evaporator. The residue was filtered and washed with water three times. The crude product was purified by recrystallization from ethanol to give 14.5 g of white crystals (yield 82%). Mp: 214-5 ^{o}C. ^{1}H NMR (DMSO-d_6, ppm): δ 7.65 (s, 2H), 5.54 (t, 2H, J = 8.0 Hz), 4.50 (d, 6H, J = 8.0 Hz). ^{13}C NMR (DMSO-d_6, ppm): δ 142.35, 132.01, 120.79, 62.86.

5.2.3 2,5-Dibromo-1,4- bis(2-tetrahydropyranyloxymethyl)benzene (3)

A 11.84 g (0.04 mol) sample of diol compound **2**, 7.39 g (0.088 mol) of 3,4-dihydro-2*H*-pyran, a catalytic amount of *p*-toluic acid and 200 mL of dichloromethane were charged in a 500 mL round-bottom flask. The mixture was stirred under nitrogen protection at room temperature for 3 h. The reaction mixture was washed with saturated sodium bicarbonate water solution twice, water three times, brine once and then the organic layer was dried over anhydrous magnesium sulfate.

The residue was subjected to purification by chromatography on silica gel using hexane/ethyl acetate (20:1) as eluent. After the solvent was evaporated, white crystals (18.0 g, yield 97%) were finally obtained. Mp: 105–6 ^{o}C. ^{1}H NMR ($CDCl_3$, ppm): δ 7.67 (s, 2H), 4.80 (d, 2H, *J* = 20 Hz), 4.78 (s, 2H), 4.56 (d, 2H, *J* = 20 Hz), 3.91 (m, 2H), 3.58 (m, 2H), 1.94 - 1.47 (m, 12H). ^{13}C NMR ($CDCl_3$, ppm): δ 138.93, 132.73, 121.64, 98.86, 68.16, 62.58, 30.83, 25.77, 19.65.

5.2.4 4-(3-[*N,N*-diethylamino]-1-oxapropyl) bromobenzene (4)

A 500 mL round-bottom flask with magnetic stirring bar was charged with anhydrous potassium carbonate (124 g, 0.9 mol), 4-bromophenol (52 g, 0.3 mol), and 300 mL of acetone. The stirred mixture was sparged with nitrogen for 15 min and then refluxed for about 30 min. After 30 min refluxing, 2-chlorotriethylamine hydrochloride (62 g, 0.36 mol) was added into the round-bottom flask and the mixture was then refluxed for 3 days. The precipitate mixture was filtered away and the filtrate was rotary evaporated. The residue was poured into water and extracted with ether three times, and the combined organics were washed with 10% aqueous sodium hydroxide twice, water twice, and brine once. The solution was dried over magnesium sulfate, filtered and stripped of solvent by rotary evaporation to yield crude oil. The crude product was dissolved in 200 mL methanol and the solution was sparged with dry hydrochloride gas for 30 min. After methanol was rotary evaporated a brown solid was obtained, added into 300 mL acetone, stirred, filtered and washed with acetone three times to yield pure white solid of hydrochloride salt of **3** (60 g, yield 65%). Mp: 240-1 ^{o}C. ^{1}H NMR (D_2O, ppm): δ 7.43 (d, 2H, *J* = 8.0 Hz), 6.87 (d, 2H, *J* = 8.0 Hz), 4.28 (t, 2H, *J* = 4.8 Hz), 3.52 (t, 2H, *J* = 4.8 Hz), 3.26 (m, 4H), 1.25 (t, 6H, *J* = 7.2 Hz).

The pure product (46.28 g, 0.15 mol) was dissolved into 150 mL water and then

aqueous potassium carbonate solution (30 g K_2CO_3 in 150 mL water) was dropwise added into the solution at room temperature. The resulting organic layer was extracted with ether three times, washed with water twice and brine once, dried with magnesium sulfate, filtered and concentrated to get pure oily liquid **4** quantitatively. ^{1}H NMR ($CDCl_3$, ppm): δ 7.32 (d, 2H, *J* = 8.0 Hz), 6.76 (d, 2H, *J* = 8.0 Hz), 3.97 (t, 2H, *J* = 4.8 Hz), 2.84 (t, 2H, *J* = 4.8 Hz), 2.62 (q, 4H, *J* = 4.8 Hz), 1.17 (t, 6H, *J* = 7.2 Hz). ^{13}C NMR ($CDCl_3$, ppm): δ 158.42, 132.55, 116.75, 113.14, 67.33, 52.11, 48.25, 12.31.

5.2.5 2,5-Bis[4'-2-(*N,N*-diethylamino)ethoxy phenyl]-1,4-bis(hydroxymethyl) benzene (5)

A Grignard reagent of 4-(3-[*N,N*-diethylamino]-1-oxapropyl) magnesium bromobenzene (0.06 mol), prepared from the reaction of 16.32 g (0.06 mol) of **4** with 1.584 g (0.066 mol) of Mg in 60 mL of dry tetrahydrofuran (THF), was added dropwise into a solution of **3** (9.28 g, 0.02 mol) in 40 mL of THF containing a catalytic amount of tetrakis-(triphenylphosphine)-palladium(0) over a period of 1 h. After refluxing for 12 h, the reaction mixture was quenched with saturated aqueous ammonium chloride solution and extracted with ethyl acetate. The extract was washed with water three times, with brine once, and then was dried over anhydrous magnesium sulfate. After the solvent was removed, the residue was added into 200 mL of 1 M HCl and stirred for 1 h at room temperature. The water solution was washed with ethyl acetate for three times and then 1 M potassium carbonate was added dropwisely into the solution until all the organic oily product was precipitated from the water layer. The organic layer was extracted with chloroform and the extract was wash with water three times, with brine once, and then was dried over anhydrous magnesium sulfate. After the solvent was removed the residue was recrystallized in hexane-chloroform to

afford 6 g of white crystals (yield 58%). Mp: 80-2 ^{o}C. MS: *m/z* 520.3. ^{1}H NMR ($CDCl_3$, ppm): δ 7.46 (s, 2H), 7.35 (d, 4H, *J* = 8.0 Hz), 6.98 (d, 4H, *J* = 8.0 Hz), 4.67 (s, 4H), 4.12 (t, 4H, *J* = 6.4 Hz), 2.93 (t, 4H, *J* = 6.4 Hz), 2.68 (q, 8H, *J* = 7.2 Hz), 1.11 (t, 12H, *J* = 7.2 Hz). ^{13}C NMR ($CDCl_3$, ppm): δ 158.17, 139.87, 137.37, 132.50, 130.27, 130.12, 114.25, 66.48, 62.87, 51.68, 47.70, 11.67. Anal. Calcd for $C_{32}H_{44}N_2O_4$: C, 73.81; H, 8.52; N, 5.38. Found: C, 73.30; H, 8.52; N, 5.19.

5.2.6 2,5-Bis[4'-2-(*N,N*-diethylamino)ethoxyphenyl]-1,4-bis(chloromethyl)benzene dihydrochloride (Monomer 1)

A 5.20 g (0.01 mol) sample of **5** was dissolved in 100 mL methanol and then 50 mL saturated hydrochloride methanol solution was poured into the solution at room temperature. After stirred for 30 min, the solution was concentrated and dropwise added into 400 mL acetone under violent stirring. The obtained crude white precipitate was filtered and washed with acetone for three times. Mp: 222-3 ^{o}C. ^{1}H NMR (D_2O, ppm): δ 7.35 (s, 2H), 7.33 (d, 4H, *J* = 8.0 Hz), 7.06 (d, 4H, *J* = 8.0 Hz), 4.51 (s, 4H), 4.35 (t, 4H, *J* = 4.0 Hz), 3.56 (t, 4H, *J* = 4.0 Hz), 3.28 (t, 8H, *J* = 4.4 Hz), 1.26 (t, 12H, *J* = 7.6 Hz).

The crude product was directly added into 10 mL $SOCl_2$ under nitrogen protection at 0 ^{o}C and stirred for 10 min. The ice bath was removed and the reaction mixture was continued stirring at room temperature for 3 h. The $SOCl_2$ was removed under vacuum evaporation and then the residue was added into 100 mL acetone, stirred for 2 h, filtered and then washed with acetone three times. The crude product was recrystallized with ethanol to afford 5 g of white crystals with a yield of 79%. Mp: 180-2 ^{o}C. MS: *m/z* (-2HCl) 556.3. ^{1}H NMR ($CDCl_3$, ppm): δ 12.45 (br, 2H), 7.42 (s, 2H), 7.41 (d, 4H, *J* = 8.4 Hz), 7.02 (d, 4H, *J* = 8.4 Hz), 4.63 (t, 4H, *J* = 4.0 Hz), 4.52

(s, 4H), 3.54 (m, 4H), 3.32 (m, 8H), 1.50 (t, 12H, J = 7.2 Hz). ^{13}C NMR ($CDCl_3$, ppm): δ 157.33, 141.25, 135.74, 133.45, 132.94, 130.97, 114.95, 63.26, 51.08, 47.64, 44.31, 9.04. Anal. Calcd for $C_{32}H_{44}Cl_4N_2O_2$: C, 60.96; H, 7.03; N, 4.44; Cl, 22.49. Found: C, 60.79; H, 6.99; N, 4.20; Cl, 23.05.

5.2.7 {2,5-Bis[4'-2-(*N*,*N*-diethylamino)ethoxyphenyl]-1,4-xylene}bis(triphenyl-phosphonium chloride) dihydrochloride (Monomer 2)

A solution of 3.15 g (5 mmol) of monomer **1** and 2.88 g (11 mmol) of triphenylphosphine in 10 mL of DMF was heated to reflux for 24 h with stirring. The resulting mixture was poured into diethyl ether. The precipitate was filtered and recrystallized in dioxane-ethanol to afford 5.15 g of white crystals (yield 89%). Mp: 272-4 ^{o}C. ^{1}H NMR (D_2O, ppm): δ 11.35 (br, 2H) 7.88 (t, 6H, J = 8.0 Hz), 7.63 (m, 12H), 7.44 (m, 12H), 6.85 (s, 2H), 6.81 (d, 4H, J = 8.4 Hz), 6.54 (d, 4H, J = 8.4 Hz) 5.12 (d, 4H, J = 16 Hz) 4.48 (s, 4H), 3.51 (s, 4H), 3.25 (q, 8H, J = 6.4 Hz), 1.31 (t, 12H, J = 8.8 Hz). ^{13}C NMR (D_2O, ppm): δ 157.33, 142.43, 135.78, 135.04, 134.30, 131.94, 130.60, 130.47, 126.24, 117.59, 116.72, 115.40, 62.43, 51.29, 48.69, 27.58, 27.09, 8.71. Anal. Calcd for $C_{68}H_{74}Cl_4N_2O_2P_2{\cdot}4.5H_2O$: C, 66.07; H, 6.77; N, 2.27; Cl, 11.47. Found: C, 65.97; H, 6.94; N, 2.55; Cl, 12.08.

5.2.8 4-Decyloxy bromobenzene (6)

Sodium ethoxide was prepared by adding 2.53 g (110 mmol) of sodium into 50 mL of anhydrous ethanol. After all the sodium disappeared, 17.3 g (100 mmol) of 4-bromophenol in 30 mL of anhydrous ethanol was added dropwise. To the stirred mixture, 24.31 g (110 mmol) of 1-bromidecane in 30 mL of anhydrous ethanol was added. After stirring for 24 h with refluxing, the ethanol was evaporated at reduced

pressure. The brownish residue was added into 300 mL of water, extracted with ethyl acetate, and dried with anhydrous magnesium sulfate. The pure product was obtained through silicon-gel chromatography using hexane as eluent to afford 28.2 g of colorless liquid (yield 90%). ^{1}H NMR ($CDCl_3$, ppm): δ 7.32 (d, 2H, *J* = 8.0 Hz), 6.76 (d, 2H, *J* = 8.0 Hz), 3.97 (t, 2H, *J* = 4.8 Hz), 1.80 (m, 2H), 1.65-1.20 (m, 16H), 0.91 (t, 3H, *J* = 8.0 Hz).

5.2.9 2,5-Bis(4'-decyloxy phenyl)-*p*-xylene (7)

A Grignard reagent of 4-decyloxy magnesium bromobenzene (0.06 mol), prepared from the reaction of 18.78 g (0.06 mol) of **6** with 1.584 g (0.066 mol) of Mg in 60 mL of dry tetrahydrofuran (THF), was added dropwise into a solution of 2,5-dibromo-p-xylene (5.28 g, 0.02 mol) in 40 mL of THF containing a catalytic amount of tetrakis-(triphenylphosphine)-palladium(0) over a period of 1 h. After refluxing for 12 h, the reaction mixture was quenched with saturated aqueous ammonium chloride solution and extracted with ethyl acetate. The extract was washed with water three times, with brine once, and then was dried over anhydrous magnesium sulfate. After the solvent was removed by rotary evaporation, the residue was recrystallized in hexane-chloroform to afford 8.55 g of white crystals (yield 75%). Mp: 73-4 ^{o}C. ^{1}H NMR ($CDCl_3$, ppm): δ 7.32 (d, 4H, *J* = 8.0 Hz), 7.16 (s, 2H), 6.95 (d, 4H, *J* = 8.0 Hz), 3.97 (t, 4H, *J* = 4.8 Hz), 2.29 (s, 6H), 1.80 (m, 4H), 1.67-1.23 (m, 32H), 0.91 (t, 6H, *J* = 7.6 Hz). ^{13}C NMR ($CDCl_3$, ppm): δ 158.50, 140.61, 134.35, 133.04, 132.30, 130.64, 114.48, 68.48, 32.30, 29.98, 29.72, 26.50, 23.07, 20.37, 14.49.

5.2.10 2,5-Bis(4'-decyloxy phenyl)-1,4-phenylenemethylene diacetate (8)

5.70 g (10 mmol) of **7**, 3.6 g (20 mmol) of NBS and a catalytic amount of AIBN as a

initiator were added into 40 mL of benzene. The reaction mixture was reflux for 3 h under nitrogen atmosphere. When cooling to room temperature the mixture was filtered. The obtained filtrate was rotary evaporated and then directly added into 40 mL of acetic acid with 3.3 g (40 mmol) of sodium acetate without purification. The mixture was refluxed for 12 h and the acetic acid was rotary evaporated. The residue was added into 100 mL of water, extracted with chloroform and dried with anhydrous magnesium sulfate. The solution was filtered and concentrated. The resulting crude product was purified through silica gel chromatography using hexane/ethyl acetate (3:1) as eluent. The white product (3.4 g, yield 50%) was obtained by crystallization after most of the solvent was removed under reduced pressure. Mp: 123-4 ^{o}C. ^{1}H NMR ($CDCl_3$, ppm): δ 7.44 (s, 2H), 7.33 (d, 4H, *J* = 7.6 Hz), 6.97 (d, 4H, *J* = 7.6 Hz), 5.07 (s, 4H), 3.97 (t, 4H, *J* = 7.2 Hz), 2.07 (s, 6H), 1.50 (m, 4H), 1.44-1.26 (m, 32H), 0.93 (t, 6H, *J* = 7.6 Hz).

5.2.11 2,5-Bis(4'-decyloxy phenyl)-1,4-bishydroxymethylbenzene (9)

A 3.2 g (4.66 mmol) sample of diacetate **8** was added into 40 mL mixed solvent of ethanol-water (1:1) containing 2 g (50 mmol) of sodium hydroxide. The mixture was refluxed for 4 h with stirring. After cooling to room temperature, ethanol was evaporated through a rotary evaporator. The residue was filtered and washed with water three times. The crude product was purified by recrystallization from ethanol to give 2.4 g of white crystals (yield 86%). Mp: 145-6 ^{o}C. ^{1}H NMR ($CDCl_3$, ppm): δ 7.45 (s, 2H), 7.30 (d, 4H, *J* = 7.2 Hz), 6.97 (d, 4H, *J* = 7.2 Hz), 4.68 (d, 4H, *J* = 4.8 Hz), 4.02 (t, 4H, *J* = 5.2 Hz), 1.82 (m, 4H), 1.64-1.23 (m, 32H), 0.91 (t, 6H, *J* = 7.2 Hz). ^{13}C NMR ($CDCl_3$, ppm): δ 159.04, 140.52, 137.90, 132.76, 130.86, 130.62, 114.79, 68.53, 63.52, 32.29, 29.97, 29.81, 29.71, 26.48, 23.06, 14.48.

5.2.12 2,5-Bis(4'-decyloxy phenyl)-1,4-diformylbenzene (Monomer 3)

A 2.01 g (3.3 mol) sample of diol compound **9**, 2.56 g (10 mmol) of pyridium chlorochromate (PCC), 1.0 g of 4Å freshly dried molecular sieves, 1.0 g of silicon gel, and 100 mL of dry methylene chloride were charged into 150 mL round-bottom flask. The mixture was cooled to 0 ^{o}C in an ice bath and stirred for another 12 h. The solvent was evaporated and the residue was run through a silicon gel column eluted with methylene chloride. After the solvent was evaporated, yellow crystals (1.8 g, yield 90%) were obtained. Mp: 90-1 ^{o}C. MS: *m/z* 598.4. ^{1}H NMR ($CDCl_3$, ppm): δ 10.11 (s, 2H), 8.09 (s, 2H), 7.37 (d, 4H, *J* = 7.5 Hz), 7.08 (d, 4H, *J* = 7.2 Hz), 4.05 (t, 4H, *J* = 6.6 Hz), 1.85 (m, 4H), 1.57-1.25 (m, 32H), 0.90 (t, 6H, *J* = 4.8 Hz). ^{13}C NMR ($CDCl_3$, ppm): δ 192.59, 160.11, 144.24, 136.94, 131.68, 130.51, 128.93, 115.19, 68.66, 32.29, 29.96, 29.79, 29.71, 29.64, 26.45, 23.07, 14.48. Anal. Calcd for $C_{40}H_{54}O_4$: C, 80.22; H, 9.09. Found: C, 80.48; H, 9.32.

5.2.13 2,5-Bis(4'-methyloxy phenyl)-*p*-xylene (10)

A Grignard reagent of 4-methyloxy magnesium bromobenzene (0.06 mol), prepared from the reaction of 18.78 g (0.06 mol) of 4-bromoanisole with 1.584 g (0.066 mol) of Mg in 60 mL of dry tetrahydrofuran (THF), was added dropwise into a solution of 2,5-dibromo-p-xylene (5.28 g, 0.02 mol) in 40 mL of THF containing a catalytic amount of tetrakis-(triphenylphosphine)-palladium(0) over a period of 1 h. After refluxing for 12 h, the reaction mixture was quenched with saturated aqueous ammonium chloride solution and extracted with ethyl acetate. The extract was washed with water three times, with brine once, and then was dried over anhydrous magnesium sulfate. After the solvent was removed by rotary evaporation, the residue was recrystallized in hexane-chloroform to afford 8.55 g of white crystals (yield 75%). Mp:

160-1 ^{o}C. ^{1}H NMR ($CDCl_3$, ppm): δ 7.32 (d, 4H, J = 7.2 Hz), 7.15 (s, 2H), 6.99 (d, 4H, J = 7.2 Hz), 3.88 (s, 6H), 2.29 (s, 6H). ^{13}C NMR ($CDCl_3$, ppm): δ 158.94, 140.59, 134.58, 133.08, 132.32, 130.70, 113.93, 55.70, 20.36.

5.2.14 2,5-Bis(4'-hydroxy phenyl)-*p*-xylene (11)

A 6.36 g (0.02 mol) sample of compound **10** was dissolved in CH_2Cl_2 (100 mL) in a 250 mL round-bottom flask fitted with a condenser. The reaction mixture was cooled to –80 ^{o}C in a dry ice-acetone bath. 12 g (0.048 mol) tribromoboron in 50 mL CH_2Cl_2 was added slowly through the condenser. After the addition, a drying tube was attached on the top of the condenser, and the mixture was allowed to warm to room temperature. The mixture was stirred at room temperature for 24 h and then carefully hydrolyzed with H_2O (100 mL). The aqueous layer was separated and extracted with ether three times. The combined organic phases were extracted with water three times, brine once and then dried by anhydrous $MgSO_4$. After the solvent was evaporated, the crude product was recrystallized with benzene to afford white crystals (5 g, yield 86%). Mp: 217-8 ^{o}C. ^{1}H NMR (DMSO-d_6, ppm): δ 9.43 (br, 2H), 7.20 (d, 4H, J = 8.0 Hz), 7.02 (s, 2H), 6.82 (d, 4H, J = 8.0 Hz), 2.20 (s, 6H). ^{13}C NMR (DMSO-d_6, ppm): δ 157.15, 140.56, 132.80, 132.62, 132.39, 130.87, 115.81, 20.64.

5.2.15 2-[2-(2-Methoxyethoxy)ethoxy]ethyl-*p*-toluenesulfonate (12)

21 g (0.11 mol) of toluenesulfonyl chloride was added dropwise to a THF solution of 16.4 g (0.1 mol) of tri(ethylene glycol) monoethyl ether and 20.2 g (0.2 mol) of triethylamine at 0 ^{o}C. After stirring for 12 h, the reaction mixture was filtered and the filtrate was evaporated and the residue was then extracted with CH_2Cl_2/10% HCl and the organic layer was concentrated under reduced pressure. The crude extract was

purified by silica gel column chromatography using hexane/ethyl acetate (1:1) as eluent to give the desired product as a viscous oil (30 g, yield 94%). ^{1}H NMR ($CDCl_3$, ppm): δ 7.82 (d, 2H, *J* = 7.2 Hz), 7.35 (d, 2H, *J* = 7.2 Hz), 4.17 (t, 2H, *J* = 4.8 Hz), 3.70 (t, 2H, *J* = 4.8 Hz), 3.56 (m, 6H), 3.50 (t, 2H, *J* = 4.8 Hz), 3.32 (s, 3H), 2.47 (s, 3H). ^{13}C NMR ($CDCl_3$, ppm): δ 145.18, 133.39, 130.19, 128.26, 72.21, 71.01, 70.81, 69.66, 68.96, 59.25, 21.91.

5.2.16 2,5-Bis{4'-2-[2-(2-Methoxyethoxy)ethoxy]ethoxy phenyl}-*p*-xylene (13)

A 10.5 g (0.033 mol) sample of compund **12** was added to a solution (60 mL of acetone/ 2 mL of DMF) of 4.35 g of compound **11** (0.015 mol) and 6.2 g of potassium carbonate (0.045 mol), and the mixture was allowed to reflux for 3 days. The reaction mixture was filtered and the filtrate was evaporated and then the residue was extracted with CH_2Cl_2/H_2O and the organic layer was dried over $MgSO_4$ and concentrated under reduced pressure. The crude extract was purified by silica gel column chromatography using hexane/ethyl acetate (1:2) as eluent to give the desired product as white crystals (8.3 g, yield 95%). Mp: 71-2 ^{o}C. ^{1}H NMR ($CDCl_3$, ppm): δ 7.29 (d, 4H, *J* = 7.2 Hz), 7.12 (s, 2H), 6.94 (d, 4H, *J* = 7.2 Hz), 4.21 (t, 4H, *J* = 4.8 Hz), 3.88 (t, 4H, *J* = 4.8 Hz), 3.75 (t, 4H, *J* = 4.8 Hz), 3.68 (m, 8H), 3.56 (t, 4H, *J* = 4.8 Hz), 3.38 (s, 6H) 2.24 (s, 6H). ^{13}C NMR ($CDCl_3$, ppm): δ 158.15, 140.57, 134.77, 133.04, 132.28, 130.65, 114.65, 72.37, 71.27, 71.10, 70.99, 70.21, 67.91, 59.41, 20.33.

5.2.17 2,5-Bis{4'-2-[2-(2-Methoxyethoxy)ethoxy]ethoxyphenyl}-1,4-phenylenem-ethylene diacetate (14)

5.82 g (10 mmol) of **13**, 3.74 g (21 mmol) of NBS and a catalytic amount of AIBN as a initiator were added into 40 mL of benzene. The reaction mixture was reflux for 6 h

under nitrogen atmosphere. When cooling to room temperature the mixture was filtered. The obtained filtrate was rotary evaporated and then directly added into 40 mL of acetic acid with 3.3 g (40 mmol) of sodium acetate without purification. The mixture was refluxed for 12 h and the acetic acid was rotary evaporated. The residue was added into 100 mL of water, extracted with chloroform and dried with anhydrous magnesium sulfate. The solution was filtered and concentrated. The resulting crude product was purified through silica gel chromatography using hexane/ethyl acetate (1:3) as eluent. The viscous oil (3.2 g, yield 46%) was obtained after most of the solvent was removed under reduced pressure. ^{1}H NMR ($CDCl_3$, ppm): δ 7.41 (s, 2H), 7.31 (d, 4H, *J* = 8.4 Hz), 7.00 (d, 4H, *J* = 8.4 Hz), 5.07 (s, 4H), 4.20 (t, 4H, *J* = 4.8 Hz), 3.91 (t, 4H, *J* = 4.8 Hz), 3.78 (t, 4H, *J* = 4.8 Hz), 3.70 (m, 8H), 3.58 (t, 4H, *J* = 4.8 Hz), 3.40 (s, 6H) 2.06 (s, 6H). ^{13}C NMR ($CDCl_3$, ppm): δ 171.03, 158.79, 141.33, 133.70, 132.72, 131.78, 130.64, 114.94, 72.37, 71.28, 71.09, 70.99, 70.15, 67.97, 64.52, 59.41, 21.35.

5.2.18 2,5-Bis{4'-2-[2-(2-Methoxyethoxy)ethoxy]ethoxy phenyl}-1,4-bishydroxy-methyl benzene (15)

A 2.1 g (3 mmol) sample of diacetate **14** was added into 40 mL mixed solvent of ethanol-water (1:1) containing 1 g (25 mmol) of sodium hydroxide. The mixture was refluxed for 4 h with stirring. After cooling to room temperature, ethanol was evaporated through a rotary evaporator. Concentrated hydrochloric acid was added dropwise to the above solution until pH of the suspension changed to 7. This solution was extracted with ethyl acetate, and the organic layer was washed with water and brine and then dried by anhydrous $MgSO_4$. After the solvent was evaporated, the viscous liquid (1.8 g, 98%) was obtained. ^{1}H NMR ($CDCl_3$, ppm): δ 7.45 (s, 2H), 7.30 (d, 4H, *J* = 8.0 Hz), 6.97 (d, 4H, *J* = 8.0 Hz), 4.68 (d, 4H, *J* = 4.8 Hz), 4.20 (t, 4H, *J* =

5.2 Hz), 3.91 (t, 4H, J = 4.8 Hz), 3.78 (t, 4H, J = 4.8 Hz), 3.70 (m, 8H), 3.58 (t, 4H, J = 4.8 Hz), 3.40 (s, 6H). ^{13}C NMR ($CDCl_3$, ppm): δ 158.62, 140.36, 137.87, 133.23, 130.77, 130.64, 114.90, 72.34, 71.25, 71.07, 70.96, 70.17, 67.92, 63.34, 59.40.

5.2.19 2,5-Bis{4'-2-[2-(2-methoxyethoxy)ethoxy]ethoxyphenyl}-1,4-diformylbenzene (Monomer 4)

A 1.54 g (2.5 mol) sample of diol compound **15**, 1.92 g (7.5 mmol) of pyridium chlorochromate (PCC), 1.0 g of 4Å freshly dried molecular sieves, 1.0 g of silicon gel, and 50 mL of dry methylene chloride were charged into 150 mL round-bottom flask. The mixture was cooled to 0 ^{o}C in an ice bath and stirred for another 12 h. The solvent was evaporated and the residue was run through a silicon gel column eluted with methylene chloride. After the solvent was evaporated, yellow crystals (1.4 g, yield 92%) were obtained. Mp: 82-3 ^{o}C. MS: *m/z* 610.3. ^{1}H NMR ($CDCl_3$, ppm): δ 10.09 (s, 2H), 8.09 (s, 2H), 7.37 (d, 4H, J = 8.0 Hz), 7.08 (d, 4H, J = 8.0 Hz), 4.23 (t, 4H, J = 4.8 Hz), 3.93 (t, 4H, J = 4.8 Hz), 3.80 (t, 4H, J = 4.8 Hz), 3.72 (m, 8H), 3.59 (t, 4H, J = 4.8 Hz), 3.41 (s, 6H). ^{13}C NMR ($CDCl_3$, ppm): δ 192.50, 159.76, 144.20, 136.93, 131.68, 130.53, 129.34, 115.33, 72.36, 71.31, 71.10, 71.00, 70.09, 68.06, 59.44. Anal. Calcd for $C_{34}H_{42}O_{10}$: C, 66.87; H, 6.93. Found: C, 67.08; H, 6.94.

5.2.20 Poly{2,5-bis[4'-2-(*N,N*-diethylamino)ethoxyphenyl]-1,4-phenylenevinylene} (P1)

A 0.315 g (0.5 mmol) sample of monomer 1 was added into 30 mL of anhydrous THF in a 50 mL round-bottom flask. To this stirred solution was added dropwise 4 mL of 1.0 M solution of potassium *tert*-butoxide (4 mmol) in anhydrous THF at room temperature. The mixture was stirred at ambient temperature for 24 h. The reaction

mixture was then poured into 200 mL of methanol with stirring. The resulting green precipitate was washed with deionized water and dried under vacuum to afford 0.21 g (yield 87%) of a green powder. ^{1}H NMR ($CDCl_3$, ppm): δ 7.48-7.13 (br, 6H, Ar-*H* and *trans*-vinyl protons), 7.08-6.75 (br, 6H, Ar-*H*), 4.58-4.09 (br, 4H, -OCH_2CH$_2$N-), 3.68-3.44 (br, 4H, -OCH$_2$CH_2N-), 3.43-3.00 (br, 8H, -NCH_2CH$_3$), 1.59-1.18 (br, 12H, -NCH$_2$CH_3). FT-IR (KBr pellet, cm^{-1}): 3400 (br), 3034, 2967, 2930, 2872, 2806, 1608, 1575, 1517, 1485, 1383, 1290, 1243, 1176, 1110, 1052, 1031, 975, 904, 834, 736, 656, 541. Anal. Calcd for $(C_{32}H_{40}N_2O_2)_n$: C, 79.30; H, 8.32; N, 5.78. Found: C, 76.01; H, 7.95; N, 6.03.

5.2.21 Poly{2,5-bis(4'-decyloxy phenyl)-1,4-phenylenevinylene-*alt*-2,5-bis[4'-2-(*N,N*-diethylamino)ethoxy phenyl]-1,4-phenylenevinylene} (P2)

A solution of 0.476 g (7 mmol) of sodium ethoxide in 7 mL of anhydrous ethanol was added to a stirred solution of 1.00 g (0.87 mmol) of triphenylphosphonium chloride monomer **2** and 0.518 g (0.87 mmol) of diformyl monomer **3** in 10 mL of dry chloroform and 10 mL of anhydrous ethanol. The mixture was stirred for 12 h and then it was poured into 200 mL of methanol. The orange polymer powder was collected by filtration and further purified by a Soxhlet extraction in methanol for 3 days. The polymer yield was 0.61 g (yield 67%). ^{1}H NMR ($CDCl_3$, ppm): δ 7.73-7.46 (br, Ar-*H*), 7.46-7.24 (br, Ar-*H* and *trans*-vinyl protons), 7.24-6.97 (br, Ar-*H*), 6.97-6.87 (br, Ar-*H*), 6.87-6.65 (br, Ar-*H*), 6.59-6.36 (br, *cis*-vinyl protons), 4.20-4.06 (br, -OCH_2- in *trans*-vinyl groups), 4.06-3.93 (br, -OCH_2C$_9$H$_{19}$- in *cis*-vinyl protons), 3.93-3.79 (br, -OCH_2- in *cis*-vinyl protons), 3.03-2.76 (m, 4H, -OCH$_2$CH_2N-), 2.76-2.52 (m, 8H, -NCH_2CH$_3$), 1.96-1.59 (br, 8H, -OCH$_2$CH_2CH_2-), 1.57-1.18 (br, 24H, -(CH_2)$_6$CH$_3$), 1.18-0.96 (m, 12H, -NCH$_2$CH_3), 0.96-0.79 (br, 6H, -(CH$_2$)$_6$CH_3). ^{13}C NMR ($CDCl_3$,

ppm): δ 158.71, 139.35, 134.60, 133.15, 131.97, 130.90, 130.10, 114.33, 68.27, 66.79, 52.16, 48.20, 32.29, 29.97, 29.83, 29.72, 26.51, 23.02, 14.46, 12.31. FT-IR (KBr pellet, cm^{-1}): 3406 (br), 3034, 2961, 2924, 2853, 2808, 1686, 1609, 1574, 1518, 1468, 1422, 1385, 1292, 1246, 1175, 1111, 1053, 1030, 1009, 937, 914, 875, 831, 731, 652, 540. Anal. Calcd for $(C_{72}H_{94}N_2O_4)_n$: C, 82.24; H, 9.01; N, 2.66. Found: C, 81.50; H, 8.70; N, 2.87.

5.2.22 Poly(2,5-Bis{4'-2-[2-(2-methoxyethoxy)ethoxy]ethoxy phenyl}-1,4-phenylenevinylene-*alt*-2,5-bis[4'-2-(*N,N*-diethylamino)ethoxy phenyl]-1,4-phenylenevinylene) (P3)

A solution of 0.476 g (7 mmol) of sodium ethoxide in 7 mL of anhydrous ethanol was added to a stirred solution of 1.00 g (0.87 mmol) of triphenylphosphonium chloride monomer **2** and 0.529 g (0.87 mmol) of diformyl monomer **4** in 10 mL of dry chloroform and 10 mL of anhydrous ethanol. The mixture was stirred for 12 h and then it was poured into 200 mL of methanol. The orange polymer powder was collected by filtration and further purified by a Soxhlet extraction in methanol for 3 days. The polymer yield was 0.58 g (yield 63%). ^{1}H NMR ($CDCl_3$, ppm): δ 7.68-7.46 (br, Ar-*H*), 7.43-7.22 (br, Ar-*H* and *trans*-vinyl protons), 7.22-6.99 (br, Ar-*H*), 6.99-6.88 (br, Ar-*H*), 6.88-6.65 (br, Ar-*H*), 6.58-6.33 (br, *cis*-vinyl protons), 4.28-3.44 (br, 28H, -OCH_2-), 3.43-3.26 (br, 6H, -OCH_3), 3.03-2.77 (m, 4H, -OCH_2CH_2N-), 2.77-2.50 (m, 8H, -NCH_2CH_3), 1.26-0.95 (m, 12H, -NCH_2CH_3). ^{13}C NMR ($CDCl_3$, ppm): δ 158.44, 158.33, 139.37, 134.58, 133.25, 131.93, 130.90, 129.98, 114.45, 72.29, 71.18, 71.02, 70.91, 70.10, 67.79, 66.78, 59.34, 52.16, 48.14, 12.31. FT-IR (KBr pellet, cm^{-1}): 3477 (br), 3032, 2964, 2926, 2875, 2820, 1686, 1608, 1573, 1520, 1471, 1422, 1379, 1353, 1293, 1246, 1203, 1178, 1111, 1064, 1032, 1009, 915, 875, 833, 808, 733, 651, 540.

Anal. Calcd for $(C_{66}H_{82}N_2O_{10})_n$: C, 74.55; H, 7.77; N, 2.63. Found: C, 73.15; H, 7.39; N, 3.50.

5.2.23 Poly{2,5-bis(4'-decyloxy phenyl)-1,4-phenylenevinylene-*alt*-2,5-bis[4'-2-(*N,N,N*-triethylammonium)ethoxy phenyl]-1,4-phenylenevinylene} Dibromide (P2') via Postpolymerization Alkylation of Poly{2,5-bis(4'-decyloxy phenyl)-1,4-phenylenevinylene-*alt*-2,5-bis[4'-2-(*N,N*-diethylamino)ethoxy phenyl]-1,4-phenylenevinylene}

A 50 mL round-bottom flask with a magnetic spin bar was charged with **P2** (0.420 g, 0.4 mmol based on repeat). The polymer was dissolved in 20 mL of THF. To this was added bromoethane (0.436 g, 4 mmol) and 5 mL of DMSO. The solution was stirred at 50 ^{o}C for 3 days, at which time most of the bromoethane and THF was evaporated. Polymer was precipitated in 100 mL of acetone, collected by centrifugation and dried overnight in vacuo at 50 ^{o}C (0.38 g, yield 75%). ^{1}H NMR (CD_3OD, ppm): δ 7.90-6.10 (br, 24H, Ar-*H* and vinyl protons), 4.71-3.00 (br, -OCH_2- and -NCH_2-), 2.00-0.60 (br, 54.8H, -(CH_2)$_8$CH_3 and -NCH$_2$CH_3). ^{13}C NMR (CD_3OD, ppm): δ 159.82, 158.55, 140.08, 135.93, 135.16, 133.16, 131.80 (br), 115.66, 69.24, 63.63, 62.86, 57.35, 55.15, 52.33, 33.08, 30.73, 30.44, 27.23, 23.72, 14.57, 9.35, 8.18. FT-IR (KBr pellet, cm^{-1}): 3409 (br), 3033, 2926, 1684, 1608, 1574, 1518, 1469, 1422, 1393, 1292, 1243, 1177, 1111, 1060, 1025, 1009, 937, 915, 875, 833, 728, 652, 540. Anal. Calcd for $(C_{72}H_{94}N_2O_4{\cdot}1.8C_2H_5Br{\cdot}3H_2O)_n$: C, 69.76; H, 8.44; N, 2.15; Br, 11.05. Found: C, 67.96; H, 7.58; N, 1.93, Br, 12.59.

5.2.24 Poly(2,5-Bis{4'-2-[2-(2-methoxyethoxy)ethoxy]ethoxy phenyl}-1,4-phenylenevinylene-*alt*-2,5-bis[4'-2-(*N,N,N*-triethylammonium)ethoxy phenyl]-1,4-phen-

ylenevinylene) Dibromide (P3') via Postpolymerization Alkylation of Poly(2,5-Bis-{4'-2-[2-(2-methoxyethoxy)ethoxy]ethoxyphenyl}-1,4-phenylenevinylene-*alt*-2,5-bis-[4'-2-(*N*,*N*-diethylamino)ethoxy phenyl]-1,4-phenylene vinylene)

A 50 mL round-bottom flask with a magnetic spin bar was charged with **P3** (0.425 g, 0.4 mmol based on repeat). The polymer was dissolved in 20 mL of THF. To this was added bromoethane (0.436 g, 4 mmol) and 5 mL of DMSO. The solution was stirred at 50 ^{o}C for 3 days, at which time most of the bromoethane and THF was evaporated. Polymer was precipitated in 100 mL of acetone, collected by centrifugation and dried overnight in vacuo at 50 ^{o}C (0.35 g, yield 68%). ^{1}H NMR (CD_3OD, ppm): δ 7.80 - 6.20 (br, 24H, Ar-*H* and vinyl protons), 4.60 - 3.20 (br, -OCH_2- and -NCH_2-), 1.80 - 0.80 (br, 17.1H, -(CH_2)$_8$CH_3 and -NCH$_2$CH_3). ^{13}C NMR (CD_3OD, ppm): δ 159.57, 158.49, 140.28, 135.79, 135.30, 132.91, 131.79 (br), 130.54, 115.67, 72.99, 71.77, 71.57, 71.38, 70.79, 68.65, 63.57, 62.95, 59.15, 57.30, 55.11, 52.26, 9.35, 8.14. FT-IR (KBr pellet, cm^{-1}): 3429 (br), 3032, 2979, 2926, 2879, 2824, 1686, 1608, 1574, 1520, 1470, 1422, 1395, 1353, 1293, 1246, 1178, 1111, 1062, 1029, 1009, 941, 919, 875, 835, 786, 733, 651, 540. Anal. Calcd for $(C_{66}H_{82}N_2O_{10}\cdot 1.7C_2H_5Br\cdot 5H_2O)_n$: C, 62.27; H, 7.57; N, 2.09; Br, 10.15. Found: C, 60.38; H, 6.59; N, 1.71; Br, 11.54.

5.3 Monomers and Polymers Synthesized in Chapter 3

5.3.1 3-Octylthiophene (16)

The Grignard **r**eagent of 1-magnesium bromodecane (0.10 mol), prepared from the reaction of 16.3 g (0.1 mol) of 1-bromodecane with 2.64 g (0.11 mol) of Mg in 300 mL of dry was slowly added dropwise into a solution of 3-bromothiophene (13.0 g, 0.08 mol) and [1,3-bis (diphenylphosphino)propane]dichloronickel (II) (0.438 g, 0.8 mmol) in 300 mL of dry ether cooled by ice-water bath. After the addition, the mixture was

stirred at room temperature overnight, and then refluxed for another 10 h. The reaction mixture was then cooled and quenched by saturated ammonium chloride aqueous solution. The aqueous layer was extracted with ether and the combined extracts were dried over magnesium sulfate. After removing the solvent, the residue was distilled under reduced pressure (80 ^{o}C/0.1 mmHg) to afford a colorless liquid product (13.3 g, yield 85%). ^{1}H NMR ($CDCl_3$, ppm): δ 7.29 (d, 1H, *J* = 4.8 Hz), 7.00 (m, 2H), 2.68 (t, 2H, *J* = 8.0 Hz), 1.67 (m, 2H), 1.34 (m, 10H), 0.95 (t, 3H, *J* = 8.4 Hz).

5.3.2 2,5-Diformyl-3-octylthiophene (Monomer 5).

A solution of *n*-butyllithium (63 mmol, 39 mL) in hexane was added slowly to a mixture of TMEDA (6.97 g, 60 mmol) and 3-octylthiophene (5.88 g, 30 mmol) in 200 mL of hexane under nitrogen protection. The mixture was stirred at 40 ^{o}C for 30min and then refluxed for 2 h. After addition of dried THF (150 mL), the mixture was cooled to –78 ^{o}C. Excess DMF (7.46 g, 102 mmol) was added dropwise under nitrogen over 15 minute. The mixture was warmed to reach room temperature and was poured into 400 mL of aqueous HCl dilute solution under vigorous stirring. After neutralization with saturated $NaHCO_3$ solution, the organic layer was extracted several times with ether and dried over anhydrous magnesium sulfate. After the solvent was evaporated under reduced pressure, the residue was purified through flash silicon-gel chromatography using hexane/ethyl acetate (9:1) as eluent to afford 5.14 g of orange liquid (yield 68%). ^{1}H NMR ($CDCl_3$, ppm): δ 10.15 (s, 1H), 9.94 (s, 1H), 7.65 (s, 1H), 2.97 (t, 2H, *J* = 8.0 Hz), 1.70 (m, 2H), 1.41-1.18 (m, 10H), 0.88 (t, 3H, *J* = 8.4 Hz). ^{13}C NMR ($CDCl_3$, ppm): δ 183.78, 183.39, 152.44, 148.27, 143.69, 137.59, 32.16, 31.57, 29.64, 29.59, 29.50, 28.88, 22.98, 14.42. Anal. Calcd for $C_{14}H_{20}O_2S$: C, 66.63; H, 7.99; S, 12.70. Found: C, 66.12; H, 7.62; S, 12.87.

5.3.3 1,4-Dioctyloxybenzene (17)

Sodium ethoxide was prepared by adding 2.53 g (110 mmol) of sodium into 50 mL of anhydrous ethanol. After all the sodium disappeared, 5.5 g (50 mmol) of hydroquinone in 10 mL of anhydrous ethanol was added dropwise. To the stirred mixture, 21.23 g (110 mmol) of octyl bromide in 10 mL of anhydrous ethanol was added. After stirring for 24 h with refluxing, the ethanol was evaporated at reduced pressure. The brownish residue was added into 300 mL of water, extracted with ethyl acetate, and dried with anhydrous magnesium sulfate. The white product (15.2 g, yield 91%) was obtained by recrystallization in ethanol after most of the solvent was removed under reduced pressure. ^{1}H NMR ($CDCl_3$, ppm): δ 6.82 (s, 4H), 3.88 (t, 4H, J = 4.8 Hz), 1.76 (m, 4H), 1.53-1.18 (m, 20H), 0.88 (t, 6H, J = 8.0 Hz).

5.3.4 2,5-Dioctyloxy-1,4-bisbromomethylbenzene (18)

A mixture of 10.02 g (30 mmol) of **17** and 2.7 g (90 mmol) of paraformaldehyde were mixed with 100 mL of acetic acid. To this mixture was added HBr (30 wt% in acetic acid, 27 g, 100 mmol). The reaction mixture was stirred at room temperature overnight. The reaction was poured into water, and the light yellow precipitate was filted, washed with a large amount of saturated sodium bicarbonate water solution, water and ethanol, and then dried to give 10.1 g (65%) pure product as white solid. ^{1}H NMR ($CDCl_3$, ppm): δ 6.86 (s, 2H), 4.55 (s, 4H), 4.00 (t, 4H, J = 5.6 Hz), 1.82 (m, 4H), 1.50 (m, 4H), 1.41-1.23 (m, 16H), 0.91 (t, 6H, J = 7.6 Hz).

5.3.5 2,5-Dioctyloxy-1,4-phenylenemethylene diacetate (19)

A 5.2g (10 mmol) sample of **18**, 3.28g (40 mmol) of anhydrous sodium acetate and 100 mL of acetate acid were charged in a 250 mL round-bottom flask. The mixture was

heated to 140 ^{o}C through an oil bath and kept at this temperature for one day with stirring. After cooling to room temperature, the mixture was poured into 300 mL of water. This solution was extracted with chloroform three times and the resulted organic layer was washed with water and brine and then dried with anhydrous $MgSO_4$. The solvent was evaporated by rotary evaporation, and the residue was purified by recrystallization in ethanol to afford 3.8 g (yield 80%) of white crystals. Mp: 65-6 ^{o}C. ^{1}H NMR ($CDCl_3$, ppm): δ 6.90 (s, 2H), 5.14 (s, 4H), 3.95 (t, 4H, J = 5.6 Hz), 2.10 (s, 6H), 1.77 (m, 4H), 1.45 (m, 4H), 1.41-1.23 (m, 16H), 0.89 (t, 6H, J = 7.6 Hz).

5.3.6 2,5-Dioctyloxy-1,4-bishydroxymethylbenzene (20)

A 2.39 g (5 mmol) sample of **19** was added into 100 mL of mixed solvent of ethanol-water (1:1) containing 1.6 g (40 mmol) of sodium hydroxide. The mixture was refluxed for 4 h with stirring. After cooling to room temperature, ethanol was evaporated through a rotary evaporator. Concentrated hydrochloric acid was added dropwise to the above solution until pH of the suspension changed to 7. This solution was extracted with ethyl acetate, and the organic layer was washed with water and brine and then dried by anhydrous $MgSO_4$. After the solvent was evaporated, the crude product was purified by recrystallization from ethyl acetate to give 1.77 g (yield 90%) of white crystals. Mp: 104-5 ^{o}C. ^{1}H NMR ($CDCl_3$, 400 MHz, ppm) δ 6.84 (s, 2H), 4.68 (s, 4H), 3.96 (t, 4H, J = 5.6 Hz), 1.79 (m, 4H), 1.55-1.20 (m, 20H), 0.91 (t, 6H, J = 7.6 Hz).

5.3.7 2,5-Dioctyloxy-1,4-diformylbenzene (Monomer 6)

A 1.58 g (4 mol) sample of diol compound **20**, 3.45 g (16 mmol) of pyridium chlorochromate (PCC), 1.0 g of 4Å freshly dried molecular sieves, 1.0 g of silicon gel,

and 100 mL of dry methylene chloride were charged into 150 mL round-bottom flask. The mixture was cooled to 0 ^{o}C in an ice bath and stirred for another 12 h. The solvent was evaporated and the residue was run through a silicon gel column eluted with methylene chloride. After the solvent was evaporated, yellow crystals (1.48 g, yield 95%) were obtained. Mp: 76-7 ^{o}C. ^{1}H NMR ($CDCl_3$, ppm): δ 10.54 (s, 2H), 7.45 (s, 2H), 4.11 (t, 4H, J = 7.6 Hz), 1.85 (m, 4H), 1.49 (m, 4H), 1.43-1.25 (m, 16H), 0.92 (t, 6H, J = 7.6 Hz). ^{13}C NMR ($CDCl_3$, ppm): δ 191.40, 155.66, 129.74, 112.07, 69.69, 32.16, 29.66, 29.58, 29.44, 26.41, 23.02, 14.45. Anal. Calcd for $C_{24}H_{38}O_4$: C, 73.81; H, 9.81. Found: C, 74.07; H, 9.87.

5.3.8 9,9-Di-*n*-hexylfluorene (21)

9.97 g (0.06 mol) of fluorene was dissolved in 200 mL of THF in a round-bottom flask. When the solution was cooled to –78 ^{o}C, a solution of 1.6 M *n*-butyllithium (0.15 mol, 94 mL) in hexane was added slowly into the solution under nitrogen protection. After stirring for 30 min, 24.75 g (0.15 mol) of *n*-bromohexane was added into the solution. After the addition, the mixture was stirred at room temperature overnight and the solvent was rotary evaporated. The residue was subjected to purification by chromatography on silica gel using hexane as eluent to afford 19 g (95%) of a colorless liquid. ^{1}H NMR ($CDCl_3$, ppm): δ 7.75 (d, 2H, J = 7.2 Hz), 7.39 (m, 6H), 2.00 (m, 4H), 1.27-1.05 (m, 12H), 0.82 (t, 6H, J = 7.2 Hz), 0.67 (m, 4H).

5.3.9 2,7-Bis(acetyloxymethyl)-9,9-di-*n*-hexylfluorene (22)

A mixture of 6.68 g (0.02 mol) of **21** and 6 g (0.2 mol) of paraformaldehyde were mixed with 50 mL of acetic acid. To this mixture was added HBr (30 wt% in acetic acid, 108 g, 0.4 mol). The reaction mixture was stirred at room temperature overnight.

The reaction was poured into water, and the light yellow precipitate was filtered, washed with a large amount of saturated sodium bicarbonate water solution, water and ethanol, and then dried to give crude product as white solid. The crude product, 6.56 g (0.08 mol) of anhydrous sodium acetate and 100 mL of acetate acid were directly charged in a 250 mL round-bottom flask. The mixture was heated to 140 ^{o}C through an oil bath and kept at this temperature for one day with stirring. After cooling to room temperature, the mixture was poured into 300 mL of water. This solution was extracted with chloroform three times and the resulted organic layer was washed with water and brine and then dried with anhydrous $MgSO_4$. The solvent was evaporated by rotary evaporation, and the residue was purified through silica gel chromatography from hexane/ethyl acetate (6:1) as eluent to afford 5.1 g (yield 53%) of colorless liquid. ^{1}H NMR ($CDCl_3$, ppm): δ 7.68 (d, 2H, J = 7.2 Hz), 7.32 (m, 4H), 5.19 (s, 4H), 2.12 (s, 6H), 1.95 (m, 4H), 1.18-1.00 (m, 12H), 0.76 (t, 6H, J = 7.2 Hz), 0.62 (m, 4H).

5.3.10 2,7-Bis(hydroxymethyl)-9,9-di-*n*-hexylfluorene (23)

A 3.82 g (8 mmol) sample of **22** was added into 50 mL of mixed solvent of ethanol-water (1:1) containing 2.56 g (64 mmol) of sodium hydroxide. The mixture was refluxed for 4 h with stirring. After cooling to room temperature, ethanol was evaporated through a rotary evaporator. Concentrated hydrochloric acid was added dropwise to the above solution until pH of the suspension changed to 7. This solution was extracted with ethyl acetate, and the organic layer was washed with water and brine and then dried by anhydrous $MgSO_4$. After the solvent was evaporated, the viscous liquid was obtained (2.98 g, yield 95%). ^{1}H NMR ($CDCl_3$, ppm): δ 7.71 (d, 2H, J = 7.2 Hz), 7.35 (m, 4H), 5.32 (s, 2H), 4.82 (s, 4H), 2.00 (m, 6H), 1.23-1.00 (m, 12H), 0.79 (t, 6H, J = 7.2 Hz), 0.62 (m, 4H).

5.3.11 2,7-Diformyl-9,9-Di-*n*-hexylfluorene (Monomer 7)

A 2.76 g (7 mmol) sample of diol compound **23**, 6.02 g (28 mmol) of pyridium chlorochromate (PCC), 1.0 g of 4Å freshly dried molecular sieves, 2.0 g of silicon gel, and 100 mL of dry methylene chloride were charged into 150mL round-bottom flask. The mixture was cooled to 0 ^{o}C in an ice bath and stirred for another 12h. The solvent was evaporated and the residue was run through a silicon gel column eluted with methylene chloride. After evaporation of the solvent using rotary evaporator, a pure white liquid was obtained with the yield of 2.46 g (90%). MS: *m/z* 390.2. ^{1}H NMR ($CDCl_3$, ppm): δ 10.12 (s, 2H), 7.94 (s, 6H), 2.05 (m, 6H), 1.18-0.94 (m, 12H), 0.76 (t, 6H, J = 7.2 Hz), 0.56 (m, 4H). ^{13}C NMR ($CDCl_3$, ppm): δ 190.50, 153.30, 146.03, 136.88, 130.70, 123.81, 121.72, 55.99, 40.42, 31.81, 29.88, 24.17, 22.86, 14.29. Anal. Calcd for $C_{27}H_{34}O_2$: C, 83.03; H, 8.77. Found: C, 83.16; H, 8.82.

5.3.12 2,5-Bis(4'-decyloxy phenyl)-1,4-diformylbenzene (Monomer 3)

This compound was synthesized according to the same procedure which was reported in chapter 2.

5.3.13 {2,5-bis[4'-2-(*N,N*-diethylamino)ethoxyphenyl]-1,4-xylene}bis(triphenyl-phosphonium chloride) dihydrochloride (Monomer 2)

This monomer was synthesized according to the same procedure which was reported in chapter 2.

5.3.14 Poly{3-octyl-2,5-thiophenediyl-vinylene-*alt*-2,5-bis[4'-2-(*N,N*-diethylamino)ethoxy phenyl]-1,4-phenylenevinylene} (P4)

A solution of 0.476 g (7 mmol) of sodium ethoxide in 7 mL of anhydrous ethanol was

added to a stirred solution of 1.00 g (0.87 mmol) of triphenylphosphonium chloride Monomer **2** and 0.218 g (0.87 mmol) of diformyl Monomer **5** in 10 mL of dry chloroform and 10 mL of anhydrous ethanol. The mixture was stirred for 12 h and then it was poured into 200 mL of methanol. The orange polymer powder was collected by filtration and further purified by a Soxhlet extraction in methanol for 3 days. The polymer yield was 0.25 g (yield 41%). ^{1}H NMR ($CDCl_3$, ppm): δ 7.80-6.00 (br, Ar-*H* and *trans*-/*cis*-vinyl protons), 4.30-3.50 (br, -OCH_2-), 3.10-2.30 (br, -OCH$_2$CH_2N- and -NCH_2CH$_3$), 2.00-1.76 (br, -ArCH_2-), 1.70-0.95 (br, -CH_2-), 0.98-0.75 (br, -CH_3). ^{13}C NMR ($CDCl_3$, ppm): δ 158.74, 158.57, 140.10-132.00 (m), 131.19, 131.01, 130.10-121.00 (m), 114.62, 67.02, 52.26, 48.26, 32.26, 31.24, 29.82, 29.65, 28.81, 23.03, 14.47, 12.33. FT-IR (KBr pellet, cm^{-1}): 3430 (br), 3030, 2965, 2925, 2854, 2809, 1656, 1608, 1574, 1516, 1476, 1379, 1291, 1246, 1174, 1111, 1029, 958, 913, 879, 832, 731, 653, 537. Anal. Calcd for $(C_{46}H_{60}N_2O_2S)_n$: C, 78.36; H, 8.58; N, 3.97; S, 4.55. Found: C, 76.98; H, 8.97; N, 3.82; S, 5.06.

5.3.15 Poly{2,5-bisoctyl-*p*-phenylenevinylene-*alt*-2,5-bis[4'-2-(*N,N*-diethylamino)ethoxy phenyl]-1,4-phenylenevinylene} (P5)

A solution of 0.476 g (7 mmol) of sodium ethoxide in 7 mL of anhydrous ethanol was added to a stirred solution of 1.0 g (0.87 mmol) of triphenylphosphonium chloride Monomer **2** and 0.338 g (0.87 mmol) of diformyl Monomer **6** in 10 mL of dry chloroform and 10 mL of anhydrous ethanol. The mixture was stirred for 12 h and then it was poured into 200 mL of methanol. The orange polymer powder was collected by filtration and further purified by a Soxhlet extraction in methanol for 3 days. The polymer yield was 0.31 g (yield 42.5%). ^{1}H NMR ($CDCl_3$, ppm): δ 7.83-7.61 (br, Ar-*H*), 7.59-7.07 (br, Ar-*H* and *trans*-vinyl protons), 7.07-6.67 (br, Ar-*H*), 6.61-6.36

(br, *cis*-vinyl protons), 4.24-3.77 (br, -OCH_2-), 3.60-3.37 (br, -OCH_2-(connecting to benzene unit directly) in *cis*-vinyl protons), 3.10-2.80 (br, -OCH_2CH_2N-), 2.80-2.52 (br, -NCH_2CH_3), 1.87-1.61 (br, -CH_2-), 1.61-0.98 (br, -CH_2-), 0.98-0.65 (br, -CH_3). ^{13}C NMR ($CDCl_3$, ppm): δ 158.72, 151.50, 150.85, 140.10, 139.35, 138.80, 135.55, 133.70, 133.15, 131.90, 131.50, 130.80, 128.00, 126.70, 125.20, 114.56, 69.27, 67.06, 52.24, 48.23, 32.21, 32.11, 29.60, 26.44, 23.01, 14.45, 12.36. FT-IR (KBr pellet, cm^{-1}): 3437 (br), 3030, 2959, 2927, 2856, 2810, 1678, 1516, 1472, 1422, 1382, 1291, 1243, 1203, 1176, 1111, 1031, 973, 914, 873, 833, 723, 652, 544. Anal. Calcd for $(C_{56}H_{78}N_2O_4)_n$: C, 79.77; H, 9.32; N, 3.32. Found: C, 78.49; H, 8.81; N, 2.86.

5.3.16 Poly{9,9-*n*-dihexyl-2,7-fluorenediyl-vinylene-*alt*-2,5-bis[4'-2-(*N*,*N*-diethyl-amino)ethoxy phenyl]-1,4-phenylenevinylene} (P6)

A solution of 0.476 g (7 mmol) of sodium ethoxide in 7 mL of anhydrous ethanol was added to a stirred solution of 1.00 g (0.87 mmol) of triphenylphosphonium chloride Monomer **2** and 0.338 g (0.87 mmol) of diformyl Monomer **7** in 10 mL of dry chloroform and 10 mL of anhydrous ethanol. The mixture was stirred for 12 h and then it was poured into 200 mL of methanol. The orange polymer powder was collected by filtration and further purified by a Soxhlet extraction in methanol for 3 days. The polymer yield was 0.55 g (yield 75%). ^{1}H NMR ($CDCl_3$, ppm): δ 8.01-6.91 (br, Ar-*H* and *trans*-vinyl protons), 6.90-6.61 (br, Ar-*H*), 6.61-6.42 (br, *cis*-vinyl protons), 4.35-4.08 (br, -OCH_2- in *trans*-vinyl protons), 4.08-3.90 (br, -OCH_2- in *cis*-vinyl protons), 3.11-2.91 (br, -OCH_2CH_2N- in *trans*-vinyl protons), 2.91-2.79 (br, -OCH_2CH_2N- in *cis*-vinyl protons), 2.79-2.54 (br, -NCH_2CH_3), 2.13-1.57 (br, -CH_2-), 1.24-0.84 (br, -CH_2-), 0.84-0.45 (br, -CH_3). ^{13}C NMR ($CDCl_3$, ppm): δ 158.62, 152.02, 141.10, 140.31, 137.20, 136.51, 135.35, 133.40, 131.50, 130.53, 128.00, 125.14,

122.02, 120.27, 114.59, 67.06, 55.21, 52.26, 52.15, 48.27, 41.10, 31.78, 30.11, 24.17, 22.99, 14.35, 12.29. FT-IR (KBr pellet, cm^{-1}): 3437 (br), 3031, 2963, 2926, 2856, 2810, 1681, 1606, 1574, 1518, 1466, 1378, 1290, 1242, 1175, 1049, 1031, 965, 914, 878, 831, 742, 651, 540. Anal. Calcd for $(C_{59}H_{74}N_2O_2)_n$: C, 84.04; H, 8.85; N, 3.32. Found: C, 83.06; H, 8.66; N, 3.35.

5.3.17 Poly{2,5-bis(4'-decyloxy phenyl)-1,4-phenylenevinylene-*alt*-2,5-bis[4'-2-(*N,N*-diethylamino)ethoxy phenyl]-1,4-phenylenevinylene} (P2)

This polymer was synthesized according to the same procedure which was reported in chapter 2.

5.3.18 Poly{3-octyl-2,5-thiophenediyl-vinylene-*alt*-2,5-bis[4'-2-(*N,N,N*-triethyl-ammonium)ethoxy phenyl]-1,4-phenylenevinylene} Dibromide (P4') via Postpoly-merization Alkylation of Poly{3-octyl-2,5-thiophenediyl-vinylene-*alt*-2,5-bis-[4'-2-(*N,N*-diethylamino)ethoxy phenyl]-1,4-phenylenevinylene}

A 50 mL round-bottom flask with a magnetic spin bar was charged with **P4** (0.352 g, 0.5 mmol based on repeat). The polymer was dissolved in 20 mL of THF. To this was added bromoethane (0.545 g, 5 mmol) and 5mL of DMSO. The solution was stirred at 50 ^{o}C for 3 days, at which time most of the bromoethane and THF was evaporated. Polymer was precipitated in 100 mL of acetone, collected by centrifugation and dried overnight in vacuo at 50 ^{o}C (0.3 g, yield 65%). ^{1}H NMR (CD_3OD, ppm): δ 7.90-6.10 (br, Ar-*H* and *trans*-/*cis*-vinyl protons), 4.70-4.00 (br, -OCH_2-), 4.00-3.00 (br, -OCH_2CH_2N- and -NCH_2CH_3), 2.00-1.00 (br, -ArCH_2- and -CH_2- and –NCH_2CH_3), 0.98-0.75 (br, -CH_3). ^{13}C NMR (CD_3OD, ppm): δ 157.54, 140.30-133.10 (m), 131.30, 130.10-126.00 (br), 114.65, 62.63, 61.83 56.30, 54.11, 51.45, 32.00, 30.95, 29.40,

28.03, 22.70, 13.49, 8.31, 7.09. FT-IR (KBr pellet, cm^{-1}): 3437 (br), 3032, 2970, 2924, 2853, 2642, 2472, 1643, 1607, 1574, 1516, 1476, 1390, 1289, 1238, 1178, 1112, 1026, 952, 910, 834, 726, 658, 539. Anal. Calcd for $(C_{46}H_{60}N_2O_2S{\cdot}1.9C_2H_5Br{\cdot}1.5H_2O)_n$: C, 63.69; H, 7.78; N, 2.98; S, 3.41; Br, 16.17. Found: C, 62.77; H, 7.75; N, 2.67; S, 3.86; Br, 17.50.

5.3.19 Poly{2,5-bisoctyl-*p*-phenylenevinylene-*alt*-2,5-bis[4'-2-(*N,N,N*-triethylammonium)ethoxy phenyl]-1,4-phenylenevinylene} Dibromide (P5') via Postpolymerization Alkylation of Poly{2,5-bisoctyl-*p*-phenylenevinylene-*alt*-2,5-bis[4'-2-(*N,N*-diethylamino)ethoxy phenyl]-1,4-phenylenevinylene}

A 50 mL round-bottom flask with a magnetic spin bar was charged with **P5** (0.337 g, 0.4 mmol based on repeat). The polymer was dissolved in 20 mL of THF. To this was added bromoethane (0.436 g, 4 mmol) and 5 mL of DMSO. The solution was stirred at 50 ^{o}C for 3 days, at which time most of the bromoethane and THF was evaporated. Polymer was precipitated in 100 mL of acetone, collected by centrifugation and dried overnight in vacuo at 50 ^{o}C (0.29 g, yield 68%). ^{1}H NMR (CD_3OD, ppm): δ 7.85-6.15 (br, Ar-*H* and vinyl protons), 4.68-4.19 (br, -OCH_2-), 4.07-3.07 (br, -OCH_2- and –NCH_2-), 2.00-0.50 (br, -CH_2- and -CH_3). ^{13}C NMR (CD_3OD, ppm): δ 157.57, 151.05, 140.10, 135.93, 134.75, 131.34, 130.77, 130.05, 128.00, 114.71, 69.57, 62.78, 61.95, 56.32, 54.14, 51.42, 31.94, 29.39, 26.39, 22.70, 13.55, 8.33, 7.08. FT-IR (KBr pellet, cm^{-1}): 3429 (br), 3040, 2954, 2926, 2854, 2640, 2475, 1670, 1514, 1469, 1418, 1383, 1286, 1239, 1201, 1112, 1178, 1112, 1026, 970, 940, 874, 833, 721, 660, 544. Anal. Calcd for $(C_{56}H_{78}N_2O_4{\cdot}1.9C_2H_5Br{\cdot}2H_2O)_n$: C, 66.12; H, 8.49; N, 2.58; Br, 13.98. Found: C, 64.23; H, 7.66; N, 2.22, Br, 15.86.

5.3.20 Poly{9,9-*n*-dihexyl-2,7-fluorenediyl-vinylene-*alt*-2,5-bis[4'-2-(*N,N,N*-triethylammonium)ethoxy phenyl]-1,4-phenylenevinylene} Dibromide (P6') via Postpolymerization Alkylation of Poly{9,9-*n*-dihexyl-2,7-fluorenediyl-vinylene-*alt*-2,5-bis[4'-2-(*N,N*-diethylamino)ethoxy phenyl]-1,4-phenylenevinylene}

A 50 mL round-bottom flask with a magnetic spin bar was charged with **P6** (0.337 g, 0.4 mmol based on repeat). The polymer was dissolved in 20 mL of THF. To this was added bromoethane (0.436 g, 4 mmol) and 5 mL of DMSO. The solution was stirred at 50 ^{o}C for 3 days, at which time most of the bromoethane and THF was evaporated. Polymer was precipitated in 100 mL of acetone, collected by centrifugation and dried overnight in vacuo at 50 ^{o}C (0.33 g, yield 78%). ^{1}H NMR (CD_3OD, ppm): δ 7.93-6.15 (br, Ar-*H* and vinyl protons), 4.70-4.14 (br, -OCH_2-), 4.00-3.04 (br, -OCH_2- and –NCH_2-), 2.20-0.25 (br, -CH_2- and -CH_3). ^{13}C NMR (CD_3OD, ppm): δ 157.65, 151.76, 141.11, 140.18, 137.22, 134.73, 131.45, 130.82, 130.26, 127.69, 120.07, 114.71, 62.69, 61.86, 56.35, 54.13, 51.49, 40.41, 31.56, 29.63, 23.84, 22.49, 13.40, 8.31, 7.04. FT-IR (KBr pellet, cm^{-1}): 3428 (br), 3030, 2965, 2924, 2853, 2630, 2467, 1680, 1605, 1575, 1514, 1465, 1394, 1287, 1235, 1177, 1060, 1006, 973, 914, 883, 829, 742, 654, 540. Anal. Calcd for $(C_{59}H_{74}N_2O_2{\cdot}1.9C_2H_5Br{\cdot}H_2O)_n$: C, 70.61; H, 8.07; N, 2.62; Br, 14.21. Found: C, 68.69; H, 6.98; N, 2.37, Br, 15.12.

5.3.21 Poly{2,5-bis(4'-decyloxy phenyl)-1,4-phenylenevinylene-*alt*-2,5-bis[4'-2-(*N,N,N*-triethylammonium)ethoxy phenyl]-1,4-phenylenevinylene} Dibromide (P2') via Postpolymerization Alkylation of Poly{2,5-bis(4'-decyloxy phenyl)-1,4-phenylenevinylene-*alt*-2,5-bis[4'-2-(*N,N*-diethylamino)ethoxy phenyl]-1,4-phenylenevinylene}

This quaternized polymer was synthesized according to the same procedure that was

reported in chapter 2.

5.4 Monomers and Polymers Synthesized in Chapter 4

5.4.1 2,5-Diiodo-1,4-dimethoxybenzene (24)

13.8 g (0.1 mol) of 1,4-Dimethoxybenzene, 8.56 g (0.04 mol) of KIO_3 and 27.94 g (0.11 mol) of I_2 were added into a solution of acetic acid (500 mL), 98% H_2SO_4 (5 mL), and H_2O (50 mL). The reaction mixture was stirred at reflux for 24 h and then cooled to room temperature. Aqueous Na_2SO_4 (20%) was added until the brown color of iodine had disappeared, and the acetic acid was evaporated under reduced pressure. The residue was poured into 200 mL water and the mixture was extracted with ethyl acetate three times, and the obtained organic layer was washed with water two times, and brine once. The combined organic layers were dried over $MgSO_4$. After the solvent was evaporated, the crude solid was recrystallized with hexane/chloroform to afford pure product as colorless crystals (29 g, yield 75%). Mp: 172-3 ^oC. ^1H NMR ($CDCl_3$, ppm): δ 7.23 (s, 2H), 3.86 (s, 6H).

5.4.2 1,4-Diiodo-2,5-hydroquinone (25)

19.5 g (0.05 mol) of 2,5-Diiodo-1,4-dimethoxybenzene was dissolved in 250 mL CH_2Cl_2 in a 500 mL round-bottom flask fitted with a condenser. The reaction mixture was cooled to –80 ^oC in a dry ice-acetone bath. 26.3 g (0.105 mol) of BBr_3 dissolved in 105 mL CH_2Cl_2 was added dropwise through the condenser. After the addition, a drying tube was attached on the top of the condenser, and the mixture was allowed to warm to room temperature. The mixture was stirred at room temperature for 12 h and then carefully hydrolyzed with 200 mL H_2O. The aqueous layer was separated and extracted with ether three times. The combined organic phases were extracted with

NaOH (200 mL, 2 N), and then the NaOH solution was neutralized with dilute HCl (1 N) in ice bath. The precipitate was collected and dried, and recrystallized from acetic acid to afford brown crystals (14.5 g, yield 80%). Mp: 198-200 ^{o}C. ^{1}H NMR (DMSO-d_6, ppm): δ 9.82 (s, 2H), 7.15 (s, 2H).

5.4.3 1,4-Bis[3-(*N,N*-diethylamino)-1-oxapropyl]-2,5-diiodobenzene (Monomer 8)

A 250 mL round-bottom flask with magnetic stirring bar was charged with anhydrous potassium carbonate (24.84 g, 0.18 mol), 1,4-Diiodo-2,5-hydroquinone (10.86 g, 0.03 mol), and 150 mL of acetone. The stirred mixture was sparged with nitrogen for 15 min and then refluxed for about 30 min. After 30 min refluxing, 2-chlorotriethylamine hydrochloride (12.38 g, 0.072 mol) was added into the round-bottom flask and the mixture was then refluxed for 3 days. The precipitate mixture was filtered away and the filtrate was rotary evaporated. The residue was poured into water and extracted with ether three times, and the combined organics were washed with 10% aqueous sodium hydroxide twice, water twice, and brine once. The solution was dried over magnesium sulfate, filterd and stripped of solvent by rotary evaporation to yield crude solid. The crude product was recrystallized with hexane to afford colorless crystals (12 g, yield 71%). Mp: 76-8 ^{o}C. MS: *m/z* 559.9. ^{1}H NMR ($CDCl_3$, ppm): δ 7.23 (s, 2 H), 4.02 (t, 4 H, J = 6.4 Hz), 2.93 (t, 4 H, J = 6.4 Hz), 2.67 (q, 8 H, J = 6.4 Hz), 1.10 (t, 12 H, J = 6.8 Hz). ^{13}C NMR ($CDCl_3$, ppm) δ 153.4, 123.4, 86.5, 69.8, 52.0, 48.4, 12.6. Anal. Calcd for $C_{18}H_{30}I_2N_2O_2$: C, 38.59; H, 5.40; N, 5.00; I, 45.30. Found: C, 38.99; H, 5.32; N, 4.84.

5.4.4 1,4-Dibromo-2,5-dimethoxybenzene (26)

In a round-bottom flask equipped with a water condenser was added 13.8 g (0.1 mol) of 1,4-dimethoxybenzene and 200 mL of $CHCl_3$ under argon. The mixture was stirred until all solids disappeared. Into the solution was added dropwise 12.4 mL (0.24 mol) of bromine mixed with 80 mL of $CHCl_3$ at 0 ^oC. After the addition, the mixture was warmed up to room temperature and stirred for 12 h. HBr gas was collected in saturated aqueous NaOH as it evolved. The mixture was poured into 100 mL of water and neutralized by adding aqueous K_2CO_3 with vigorous stirring until the solution turned colorless. The organic layer was washed with water three times, brine once and dried over $MgSO_4$. The solvent was stripped using rotary evaperator and the obtained crude product was recrystallized from ethanol to afford colorless crystals (24 g, yield 81%). ^1H NMR ($CDCl_3$, ppm): δ 7.19 (s, 2H), 3.80 (s, 6H).

5.4.5 1,4-Dibromohydroquinone (27)

14.8 g (0.05 mol) of 2,5-Dibromo-1,4-dimethoxybenzene was dissolved in 250 mL CH_2Cl_2 in a 500 mL round-bottom flask fitted with a condenser. The reaction mixture was cooled to –80 ^oC in a dry ice-acetone bath. 26.3 g (0.105 mol) of BBr_3 dissolved in 150 mL CH_2Cl_2 was added dropwise through the condenser. After the addition, a drying tube was attached on the top of the condenser, and the mixture was allowed to warm to room temperature. The mixture was stirred at room temperature for 12 h and then carefully hydrolyzed with 200 mL H_2O. The aqueous layer was separated and extracted with ether three times. The organic layer was then washed with water twice, brine once and dried over $MgSO_4$. After the solvent was evaporated under reduced pressure, the residue was recrystallized from acetic acid to afford light brown crystals (12 g, 90%). ^1H NMR (DMSO-d_6, ppm): δ 7.28 (s, 2H), 4.95 (br, 2H).

5.4.6 2,5-Bis[3-(*N,N*-diethylamino)-1-oxapropyl]-1,4-dibromobenzene (28)

A 500 mL round-bottom flask with magnetic stirring bar was charged with anhydrous potassium carbonate (33.12 g, 0.24 mol), 1,4-Dibromohydroquinone (10.72 g, 0.04 mol), and 300 mL of acetone. The stirred mixture was sparged with nitrogen for 15 min and then refluxed for about 30 min. After 30 min refluxing, 2-chlorotriethylamine hydrochloride (16.51 g, 0.096 mol) was added into the round-bottom flask and the mixture was then refluxed for 3 days. The precipitate mixture was filtered away and the filtrate was rotary evaporated. The residue was poured into water and extracted with ether three times, and the combined organics were washed with 10% aqueous sodium hydroxide twice, water twice, and brine once. The solution was dried over magnesium sulfate, filtered and stripped of solvent by rotary evaporation to yield crude solid. The crude product was recrystallized using ethanol/water to afford 11 g of white crystals (yield 59%). Mp: 66-7 ^{o}C. ^{1}H NMR ($CDCl_3$, ppm): δ 7.14 (s, 2H), 4.03 (t, 4H, J = 5.6 Hz), 2.92 (t, 4H, J = 5.6 Hz), 2.67 (q, 8H, J = 5.6 Hz), 1.09 (t, 12 H, J = 7.2 Hz).

5.4.7 1,4-Diethynyl-2,5-bis[3-(*N,N*-diethylamino)-1-oxapropyl]benzene (Monomer 9)

A 4.66 g (0.01 mol) sample of 2,5-Bis[3-(*N,N*-diethylamino)-1-oxapropyl]-1,4-dibromobenzene, 0.35 g (0.5 mmol) of $PdCl_2(PPh_3)_2$ and 0.0952 g (0.5 mmol) of CuI were dissolved in 40 mL of diisopropylamine. 2.156 g (0.022 mol) of (trimethylsilyl)acetylene was added into the vigorously stirred solution at room temperature under nitrogen protection. After the addition was finished, the reaction mixture was stirred at reflux for 3 h. After the solvent was evaporated under reduced pressure, the residue was poured into 100 mL of water and extracted with chroloform

three times. The combined organic layer was washed with water twice, brine once and dried over $MgSO_4$. After the mixture was filtered, 5 mL of hydrazine dissolved in10 mL of water monohydrate was poured into the filtrate and stirred vigorously for 12 h. The organic layer was separated and washed with water three times, brine once and dried over $MgSO_4$. After the solvent was evaporated, the residue was dissolved in a mixture of KOH (1 g in 2 mL of water) and 100 mL of methanol and stirred at room temperature for 1 h. After evaporation of the solvent, the mixture was subjected to a $CHCl_3/H_2O$ workup. The organic phases were combined and dried over $MgSO_4$. The solvent was removed under reduced pressure, and the deep black residue was added into 100 ml of saturated HCl methanol solution and stirred for 30 min at room temperature. The solvent was evaporated and the crude product was recrystallized with ethanol to afford light yellow crystals (3.1 g, yield 72%). Mp: 230-1 ^{o}C. ^{1}H NMR (D_2O, ppm): δ 7.17 (s, 2H), 4.34 (t, 4H, *J* = 5.2 Hz), 3.84 (s, 2H), 3.58 (t, 4H, *J* = 4.8 Hz), 3.32 (q, 8H, *J* = 7.2 Hz), 1.28 (t, 12 H, *J* = 7.2 Hz).

The above compound was dissolved in 50 mL of water and K_2CO_3 aqueous solution (3 g in 50 mL water) was added dropwise at room temperature and stirred for 30 min. After the stirring, the obtained light yellow organic layer was separated and the water layer was extracted with chloroform three times. The combined organic layers were wash with water twice, brine once and dried over $MgSO_4$. The mixture was filtered and the filtrate was evaporated using rotary evaporator to afford yellow crystals (2.49 g, yield 97%). Mp: 70-1 ^{o}C. MS: *m/z* 356.2. ^{1}H NMR ($CDCl_3$, ppm): δ 6.99 (s, 2 H), 4.07 (t, 4 H, *J* = 6.0 Hz), 3.34 (s, 2 H), 2.93 (t, 4 H, *J* = 6.0 Hz), 2.66 (q, 8 H, *J* = 7.2 Hz), 1.09 (t, 12 H, *J* = 7.2 Hz). ^{13}C NMR ($CDCl_3$, ppm) δ 154.4, 118.0, 113.6, 83.0, 80.1, 68.7, 51.9, 48.3, 12.4. Anal. Calcd for $C_{22}H_{32}N_2O_2$: C, 74.12; H, 9.05; N, 7.86. Found: C, 74.05; H, 8.99; N, 7.73.

5.4.8 2-[2-(2-Methoxyethoxy)ethoxy]ethyl-*p*-toluenesulfonate (12)

This compound was synthesized according to the same procedure which was reported in chapter 2.

5.4.9 1,4-Di{2-[2-(2-Methoxyethoxy)ethoxy]ethoxy}benzene (29)

A 13.8 g (0.044 mol) sample of 2-[2-(2-Methoxyethoxy)ethoxy]ethyl-*p*-toluene-sulfonate was added to a solution (60 mL of acetone/ 2 mL of DMF) of 2.2 g of hydroquinone (0.02 mol) and 8.28 g of potassium carbonate (0.06 mol), and the mixture was allowed to reflux for 3 days. The reaction mixture was filtered and the filtrate was evaporated and then the residue was extracted with CH_2Cl_2/H_2O and the organic layer was dried over $MgSO_4$ and concentrated under reduced pressure. The crude extract was purified by silica gel column chromatography using hexane/ethyl acetate (1:1) as eluent to give the desired product as colorless oil (7.5 g, yield 93%). ^{1}H NMR ($CDCl_3$, ppm): δ 6.81 (s, 4H), 4.02 (t, 4H, J = 4.8 Hz), 3.79 (t, 4H, J = 4.8 Hz), 3.74-3.55 (m, 12H), 3.51 (t, 4H, J = 4.8 Hz), 3.32 (s, 6H).

5.4.10 1,4-Didodecyloxybenzene (30)

Sodium ethoxide was prepared by adding 2.53 g (110 mmol) of sodium into 50 mL of anhydrous ethanol. After all the sodium disappeared, 5.5 g (50 mmol) of hydroquinone in 10 mL of anhydrous ethanol was added dropwise. To the stirred mixture, 27.39 g (110 mmol) of 1-bromododecane in 10 mL of anhydrous ethanol was added. After stirring for 24 h with refluxing, the ethanol was evaporated at reduced pressure. The brownish residue was added into 300 mL of water, extracted with ethyl acetate, and dried with anhydrous magnesium sulfate. The white product (18 g, yield 81%) was obtained by recrystallization in ethanol after most of the solvent was removed under

reduced pressure. Mp: 75-6 ^{o}C. ^{1}H NMR ($CDCl_3$, ppm): δ 6.82 (s, 4H), 3.88 (t, 4H, *J* = 4.8 Hz), 1.76 (m, 4H), 1.53-1.18 (m, 36H), 0.88 (t, 6H, *J* = 8.0 Hz).

5.4.11 1,4-Dioctyloxybenzene (17)

This compound was synthesized according to the same procedure which was reported in chapter 2.

5.4.12 1,4-Dihexyloxybenzene (31)

Sodium ethoxide was prepared by adding 2.53 g (110 mmol) of sodium into 50 mL of anhydrous ethanol. After all the sodium disappeared, 5.5 g (50 mmol) of hydroquinone in 10 mL of anhydrous ethanol was added dropwise. To the stirred mixture, 18.15 g (110 mmol) of 1-bromohexane in 10 mL of anhydrous ethanol was added. After stirring for 24 h with refluxing, the ethanol was evaporated at reduced pressure. The brownish residue was added into 300 mL of water, extracted with ethyl acetate, and dried with anhydrous magnesium sulfate. The white product (12.1 g, yield 87%) was obtained by recrystallization in ethanol after most of the solvent was removed under reduced pressure. Mp: 44-5 ^{o}C. ^{1}H NMR ($CDCl_3$, ppm): δ 6.82 (s, 4H), 3.88 (t, 4H, *J* = 4.8 Hz), 1.76 (m, 4H), 1.53-1.18 (m, 12H), 0.88 (t, 6H, *J* = 8.0 Hz).

5.4.13 1,4-Diiodo-2,5-Bis{2-[2-(2-Methoxyethoxy)ethoxy]ethoxy}benzene (32)

4.02 g (0.01 mol) of **29**, 0.856 g (0.004 mol) of KIO_3 and 2.794 g (0.011 mol) of I_2 were added into a solution of acetic acid (50 mL), 98% H_2SO_4 (0.5 mL), and H_2O (5 mL). The reaction mixture was stirred at reflux for 24 h and then cooled to room temperature. Aqueous Na_2SO_4 (20%) was added until the brown color of iodine had disappeared, and the acetic acid was evaporated under reduced pressure. The residue

was poured into 200 mL water and the mixture was extracted with ethyl acetate three times, and the obtained organic layer was washed with water two times, and brine once. The combined organic layers were dried over $MgSO_4$. After the solvent was evaporated, the residue was purified by silica gel column chromatography using hexane/ethyl acetate (1:2) as eluent to give the desired product as white solid (4.2 g, yield 64%). Mp: 36-7 ^oC. MS: *m/z* 654.0. ^1H NMR ($CDCl_3$, ppm): δ 7.26 (s, 2H), 4.12 (t, 4H, *J* = 4.8 Hz), 3.88 (t, 4H, *J* = 4.8 Hz), 3.79 (t, 4H, *J* = 4.8 Hz), 3.71 (m, 8H), 3.59 (t, 4H, *J* = 4.8 Hz), 3.40 (s, 6H). ^{13}C NMR ($CDCl_3$, ppm): δ 153.57, 123.96, 86.83, 72.38, 71.56, 71.16, 71.00, 70.73, 70.02, 59.44. Anal. Calcd for $C_{20}H_{32}I_2O_8$: C, 36.72; H, 4.93. Found: C, 37.15; H, 4.88.

5.4.14 2,5-Bis(dodecyloxy)-1,4-dibromobenzene (33)

In a round-bottom flask equipped with a water condenser was added 13.38 g (0.03 mol) of **30** and 150 mL of CCl_3 under argon. The mixture was stirred until all solids disappeared. Into the solution was added dropwise 11.52 g (0.072 mol) of bromine mixed with 30 mL of CCl_3 at 0 ^oC. After the addition, the mixture was warmed up to room temperature and stirred for 12 h. HBr gas was collected in saturated aqueous NaOH as it evolved. The mixture was poured into 100 mL of water and neutralized by adding aqueous K_2CO_3 with vigorous stirring until the solution turned colorless. The organic layer was washed with water three times, brine once and dried over $MgSO_4$. The solvent was stripped using rotary evaperator and the obtained crude product was recrystallized from ethanol to afford colorless crystals (15 g, yield 83%). Mp: 80-1 ^oC. ^1H NMR ($CDCl_3$, ppm): δ 7.09 (s, 2H), 3.94 (t, 4H, *J* = 5.6 Hz), 1.82 (m, 4H), 1.53-1.20 (m, 36H), 0.91 (t, 6H, *J* = 7.6 Hz).

5.4.15 2,5-Bis(octyloxy)-1,4-dibromobenzene (34)

In a round-bottom flask equipped with a water condenser was added 10.02 g (0.03 mol) of compound **17** and 150 mL of CCl_3 under argon. The mixture was stirred until all solids disappeared. Into the solution was added dropwise 11.52 g (0.072 mol) of bromine mixed with 30 mL of CCl_3 at 0 ^oC. After the addition, the mixture was warmed up to room temperature and stirred for 12 h. HBr gas was collected in saturated aqueous NaOH as it evolved. The mixture was poured into 100 mL of water and neutralized by adding aqueous K_2CO_3 with vigorous stirring until the solution turned colorless. The organic layer was washed with water three times, brine once and dried over $MgSO_4$. The solvent was stripped using rotary evaperator and the obtained crude product was recrystallized from ethanol to afford colorless crystals (12 g, yield 81%). Mp: 66-7 ^oC. ^1H NMR ($CDCl_3$, ppm): δ 7.09 (s, 2H), 3.94 (t, 4H, J = 5.6 Hz), 1.82 (m, 4H), 1.53-1.20 (m, 20H), 0.91 (t, 6H, J = 7.6 Hz).

5.4.16 2,5-Bis(hexyloxy)-1,4-dibromobenzene (35)

In a round-bottom flask equipped with a water condenser was added 8.34 g (0.03 mol) of **31** and 150 mL of CCl_3 under argon. The mixture was stirred until all solids disappeared. Into the solution was added dropwise 11.52 g (0.072 mol) of bromine mixed with 30 mL of CCl_3 at 0 ^oC. After the addition, the mixture was warmed up to room temperature and stirred for 12 h. HBr gas was collected in saturated aqueous NaOH as it evolved. The mixture was poured into 100 mL of water and neutralized by adding aqueous K_2CO_3 with vigorous stirring until the solution turned colorless. The organic layer was washed with water three times, brine once and dried over $MgSO_4$. The solvent was stripped using rotary evaperator and the obtained crude product was recrystallized from ethanol to afford colorless crystals (11 g, yield 84%). Mp: 63-4 ^oC.

^{1}H NMR ($CDCl_3$, ppm): δ 7.08 (s, 2H), 3.99 (t, 4H, *J* = 4.8 Hz), 1.82 (m, 4H), 1.52 (m, 4H), 1.37 (m, 8H), 0.94 (t, 6H, *J* = 8.0 Hz).

5.4.17 1,4-Diethynyl-2,5-Bis{2-[2-(2-Methoxyethoxy)ethoxy]ethoxy}benzene (Monomer 10)

A 3.27 g (5 mmol) sample of **32**, 0.175g (0.5 mmol) of $PdCl_2(PPh_3)_2$ and 0.0475 g (0.5 mmol) of CuI were dissolved in 20 mL of diisopropylamine. 1.078 g (0.011 mol) of (trimethylsilyl)acetylene was added into the vigorously stirred solution at room temperature under nitrogen protection. After the addition was finished, the reaction mixture was stirred at reflux for 3 h. 5 g of silica gel was added into the mixture and the solvent was removed under reduced pressure. The residue was passed through a silica gel column using ethyl acetate as eluent. The evaporation of the solvent led to a yellow solid and the solid was dissolved in a mixture of KOH (1 g in 2 mL of water) and 100 mL of methanol and stirred at room temperature for 1 h. The mixture was filtered and the solvent was evaporated using rotary evaporator. The residue was dissolved in chloroform and washed with water three times, brine once and dried over $MgSO_4$. After the solvent was evaporated the obtained crude product was purified by silica gel column chromatography using hexane/ethyl acetate (1:3) as eluent to give the desired product as deep yellow solid (1.8 g, yield 80%). Mp: 51-2 ^oC. ^{1}H NMR ($CDCl_3$, ppm): δ 7.00 (s, 2H), 4.17 (t, 4H, *J* = 4.8 Hz), 3.90 (t, 4H, *J* = 4.8 Hz), 3.79 (t, 4H, *J* = 4.8 Hz), 3.69 (m, 8H), 3.57 (t, 4H, *J* = 4.8 Hz), 3.41 (s, 6H), 3.35 (s, 2H).

5.4.18 1,4-Diethynyl-2,5-bis(dodecyloxy)benzene (Monomer 11)

A 3.02 g (5 mmol) sample of **33**, 0.175 g (0.5 mmol) of $PdCl_2(PPh_3)_2$ and 0.0475 g (0.5 mmol) of CuI were dissolved in 20 mL of diisopropylamine. 1.078 g (0.011 mol)

of (trimethylsilyl)acetylene was added into the vigorously stirred solution at room temperature under nitrogen protection. After the addition was finished, the reaction mixture was stirred at reflux for 3 h. 5 g of silica gel was added into the mixture and the solvent was removed under reduced pressure. The residue was passed through a silica gel column using ethyl acetate as eluent. The evaporation of the solvent led to a yellow solid and the solid was dissolved in a mixture of KOH (1 g in 2 mL of water) and 100 mL of methanol and stirred at room temperature for 1 h. The mixture was filtered and the solvent was evaporated using rotary evaporator. The residue was dissolved in chloroform and washed with water three times, brine once and dried over $MgSO_4$. After the solvent was evaporated the obtained crude product was recrystallized from hexane-$CHCl_3$ twice to afford yellow crystals (2 g, yield 81%). Mp: 80-1 ^{o}C. ^{1}H NMR ($CDCl_3$, ppm): δ 6.99 (s, 2H), 4.00 (t, 4H, J = 4.8 Hz), 3.38(s, 2H), 1.82 (m, 4H), 1.58-1.23 (m, 36H), 0.93 (t, 6H, J = 8.0 Hz).

5.4.19 1,4-Diethynyl-2,5-bis(octyloxy)benzene (Monomer 12)

A 2.46 g (5 mmol) sample of **34**, 0.175 g (0.5 mmol) of $PdCl_2(PPh_3)_2$ and 0.0475 g (0.5 mmol) of CuI were dissolved in 20 mL of diisopropylamine. 1.078 g (0.011 mol) of (trimethylsilyl)acetylene was added into the vigorously stirred solution at room temperature under nitrogen protection. After the addition was finished, the reaction mixture was stirred at reflux for 3 h. 5 g of silica gel was added into the mixture and the solvent was removed under reduced pressure. The residue was passed through a silica gel column using ethyl acetate as eluent. The evaporation of the solvent led to a yellow solid and the solid was dissolved in a mixture of KOH (1 g in 2 mL of water) and 100 mL of methanol and stirred at room temperature for 1 h. The mixture was filtered and the solvent was evaporated using rotary evaporator. The residue was

dissolved in chloroform and washed with water three times, brine once and dried over $MgSO_4$. After the solvent was evaporated the obtained crude product was recrystallized from ethanol twice to afford yellow crystals (1.4 g, yield 73%). Mp: 65-6 ^oC. ^1H NMR ($CDCl_3$, ppm) δ 6.99 (s, 2H), 4.00 (t, 4H, *J* = 4.8 Hz), 3.35(s, 2H), 1.82 (m, 4H), 1.58-1.23 (m, 20H), 0.93 (t, 6H, *J* = 8.0 Hz).

5.4.20 1,4-Diethynyl-2,5-bis(hexyloxy)benzene (Monomer 13)

A 2.18 g (5 mmol) sample of **35**, 0.175 g (0.5 mmol) of $PdCl_2(PPh_3)_2$ and 0.0475 g (0.5 mmol) of CuI were dissolved in 20 mL of diisopropylamine. 1.078 g (0.011 mol) of (trimethylsilyl)acetylene was added into the vigorously stirred solution at room temperature under nitrogen protection. After the addition was finished, the reaction mixture was stirred at reflux for 3 h. 5 g of silica gel was added into the mixture and the solvent was removed under reduced pressure. The residue was passed through a silica gel column using ethyl acetate as eluent. The evaporation of the solvent led to a yellow solid and the solid was dissolved in a mixture of KOH (1 g in 2 mL of water) and 100 mL of methanol and stirred at room temperature for 1 h. The mixture was filtered and the solvent was evaporated using rotary evaporator. The residue was dissolved in chloroform and washed with water three times, brine once and dried over $MgSO_4$. After the solvent was evaporated the obtained crude product was recrystallized from methanol twice to afford yellow crystals (1.3 g, yield 80%). Mp: 72-4 ^oC. ^1H NMR ($CDCl_3$, ppm): δ 7.06 (s, 2H), 4.03 (t, 4H, *J* = 4.8 Hz), 3.35(s, 2H), 1.79 (m, 4H), 1.53 (m, 4H), 1.35 (m, 8H), 0.91 (t, 6H, *J* = 8.0 Hz).

5.4.21 Poly{2,5-Bis[3-(*N*,*N*-diethylamino)-1-oxapropyl]-*p*-phenyleneethynylene} (P8)

Under argon protection, diisopropylamine/toluene (3:7, 35 mL) was added to a 50 mL round-bottom flask containing a 0.272 g (0.765 mmol) sample of Monomer **9**, 0.420 g (0.75 mmol) of 1,4-Bis[3-(N,N-diethylamino)-1-oxapropyl]-2,5-diiodobenzene (Monomer **8**), 51.9 mg (0.045 mmol)of $Pd(PPh_3)_4$ and 42.8 mg (0.225 mmol) of CuI. The mixture was heated at 70 ^oC for 24 h and then subjected to a $CHCl_3/H_2O$ workup. The combined organic phase was washed with water NH_4OH (50%) twice, water twice, brine once and dried over $MgSO_4$.The solution was removed *in vacuo*, and the residue was redissolved in 10 mL of $CHCl_3$ and reprecipitated in methanol twice, The mixture was filtered to afford 0.42 g of a yellow solid (yield 85%). ^1H NMR ($CDCl_3$, ppm): δ 7.04 (s, 2 H), 4.12 (t, 4 H), 2.95 (t, 4 H), 2.70 (q, 8 H), 1.08 (t, 12 H). ^{13}C NMR ($CDCl_3$, ppm): δ 153.8, 117.5, 114.6, 91.9, 68.8, 52.1, 48.4, 12.6. FT-IR (KBr pellet, cm^{-1}): 3429 (br), 3055, 2967, 2930, 2872, 2816, 2199, 1512, 1464, 1426, 1379, 1275, 1211, 1042, 953, 860, 802, 740, 717, 510. Anal. Calcd for $C_{20}H_{30}N_2O_2$: C, 72.69; H, 9.15; N, 8.48. Found: C, 71.95; H, 8.68; N, 8.04.

5.4.22 Poly(2,5-Bis[3-(N,N-diethylamino)-1-oxapropyl]-*p*-phenyleneethynylene-*alt*-2,5-bis{2-[2-(2-Methoxyethoxy)ethoxy]ethoxy}-*p*-phenyleneethynylene) (P9)

Under argon protection, diisopropylamine/toluene (3:7, 35 mL) was added to a 50 mL round-bottom flask containing a 0.344 g (0.765 mmol) sample of monomer **3**, 0.420 g (0.75 mmol) of 1,4-Bis[3-(N,N-diethylamino)-1-oxapropyl]-2,5-diiodobenzene (Monomer **8**), 51.9 mg (0.045 mmol)of $Pd(PPh_3)_4$ and 42.8 mg (0.225 mmol) of CuI. The mixture was heated at 70 ^oC for 24 h and then subjected to a $CHCl_3/H_2O$ workup. The combined organic phase was washed with water NH_4OH (50%) twice, water twice, brine once and dried over $MgSO_4$.The solution was removed *in vacuo*, and the residue was redissolved in 10 mL of $CHCl_3$ and reprecipitated in methanol twice, The mixture

was filtered to afford 0.48 g of a yellow solid (yield 85%). ^{1}H NMR ($CDCl_3$, ppm): δ 7.07 (s, 2 H), 7.04 (s, 2 H), 4.24 (br, 4 H), 4.15 (br, 4 H), 3.93 (br, 4 H), 3.80 (br, 4 H), 3.65 (br, 8 H), 3.53 (br, 4 H), 3.36 (s, 6 H), 2.99 (br, 4 H), 2.71 (br, 8 H), 1.09 (t, 12 H). ^{13}C NMR ($CDCl_3$, ppm): δ 153.8, 118.1, 117.5, 114.9, 114.6, 92.0, 72.1, 71.7, 71.2, 71.0, 70.5, 70.3, 68.8, 52.0, 48.4, 12.6. FT-IR (KBr pellet, cm^{-1}): 3483 (br), 3056, 2967, 2929, 2873, 2816, 2200, 1510, 1456, 1425, 1372, 1277, 1218, 1107, 1042, 953, 858, 803, 741, 717, 512. Anal. Calcd for $C_{42}H_{62}N_2O_{10}$: C, 66.82; H, 8.28; N, 3.71. Found: C, 64.15; H, 7.90; N, 3.28.

5.4.23 Poly{2,5-Bis[3-(N,N-diethylamino)-1-oxapropyl]-*p*-phenyleneethynylene-*alt*-2,5-bis(dedocyloxy)-*p*-phenyleneethynylene} (P10)

Under argon protection, diisopropylamine/toluene (3:7, 35 mL) was added to a 50 mL round-bottom flask containing a 0.378 g (0.765 mmol) sample of Monomer **11**, 0.420 g (0.75 mmol) of 1,4-Bis[3-(N,N-diethylamino)-1-oxapropyl]-2,5-diiodobenzene (Monomer **8**), 51.9 mg (0.045 mmol)of $Pd(PPh_3)_4$ and 42.8 mg (0.225 mmol) of CuI. The mixture was heated at 70 ^{o}C for 24 h and then subjected to a $CHCl_3/H_2O$ workup. The combined organic phase was washed with water NH_4OH (50%) twice, water twice, brine once and dried over $MgSO_4$.The solution was removed *in vacuo*, and the residue was redissolved in 10 mL of $CHCl_3$ and reprecipitated in methanol twice, The mixture was filtered to afford 0.52 g of a yellow solid (yield 87%). ^{1}H NMR ($CDCl_3$, ppm): δ 7.06 (s, 2 H), 7.03 (s, 2 H), 4.14 (br, 4 H), 4.05 (br, 4 H), 2.99 (br, 4 H), 2.70 (q, 8 H), 1.88 (br, 4 H), 1.52 (br, 4 H), 1.43-1.22 (br, 32 H), 1.09 (t, 12 H), 0.89 (t, 6 H). ^{13}C NMR ($CDCl_3$, ppm): δ 153.7, 117.5, 114.6, 91.9, 70.0, 68.8, 51.9, 48.3, 32.0, 29.8, 29.7, 29.5, 29.4, 26.0, 22.7, 14.1, 12.2. FT-IR (KBr pellet, cm^{-1}): 3446 (br), 3057, 2964, 2924, 2868, 2815, 2200, 1510, 1463, 1428, 1386, 1278, 1213, 1043, 955, 861, 804,

740, 721, 511. Anal. Calcd for $C_{52}H_{82}N_2O_4$: C, 78.15; H, 10.34; N, 3.51. Found: C, 76.64; H, 9.80; N, 3.08.

5.4.24 Poly{2,5-Bis[3-(N,N-diethylamino)-1-oxapropyl]-*p*-phenyleneethynylene-*alt*-2,5-bis(octyloxy)-*p*-phenyleneethynylene} (P11)

Under argon protection, diisopropylamine/toluene (3:7, 35 mL) was added to a 50 mL round-bottom flask containing a 0.292 g (0.765 mmol) sample of Monomer **12**, 0.420 g (0.75 mmol) of 1,4-Bis[3-(N,N-diethylamino)-1-oxapropyl]-2,5-diiodobenzene (Monomer **8**), 51.9 mg (0.045 mmol)of $Pd(PPh_3)_4$ and 42.8 mg (0.225 mmol) of CuI. The mixture was heated at 70 ^oC for 24 h and then subjected to a $CHCl_3/H_2O$ workup. The combined organic phase was washed with water NH_4OH (50%) twice, water twice, brine once and dried over $MgSO_4$.The solution was removed *in vacuo*, and the residue was redissolved in 10 mL of $CHCl_3$ and reprecipitated in methanol twice, The mixture was filtered to afford 0.48 g of a yellow solid (yield 93%). ^1H NMR ($CDCl_3$, ppm): δ 7.06 (s, 2 H), 7.03 (s, 2 H), 4.14 (br, 4 H), 4.05 (br, 4 H), 2.99 (br, 4 H), 2.70 (q, 8 H), 1.88 (br, 4 H), 1.52 (br, 4 H), 1.43-1.20 (br, 16 H), 1.09 (t, 12 H), 0.89 (t, 6 H). ^{13}C NMR ($CDCl_3$, ppm): δ 153.7, 117.5, 114.6, 91.9, 70.0, 68.8, 51.9, 48.3, 32.0, 29.8, 29.7, 29.5, 29.4, 26.0, 22.7, 14.1, 12.2. FT-IR (KBr pellet, cm^{-1}): 3437 (br), 3057, 2964, 2926, 2855, 2815, 2200, 1510, 1465, 1426, 1385, 1274, 1211, 1039, 861, 803, 722, 510. Anal. Calcd for $C_{44}H_{66}N_2O_4$: C, 76.92; H, 9.68; N, 4.08. Found: C, 74.28; H, 9.04; N, 3.31.

5.4.25 Poly{2,5-Bis[3-(*N,N*-diethylamino)-1-oxapropyl]-*p*-phenyleneethynylene-*alt*-2,5-bis(hexyloxy)-*p*-phenyleneethynylene} (P12)

Under argon protection, diisopropylamine/toluene (3:7, 35 mL) was added to a 50 mL

round-bottom flask containing a 0.249 g (0.765 mmol) sample of Monomer **13**, 0.420 g (0.75 mmol) of 1,4-Bis[3-(N,N-diethylamino)-1-oxapropyl]-2,5-diiodobenzene (Monomer **8**), 51.9 mg (0.045 mmol)of $Pd(PPh_3)_4$ and 42.8 mg (0.225 mmol) of CuI. The mixture was heated at 70 ^oC for 24 h and then subjected to a $CHCl_3/H_2O$ workup. The combined organic phase was washed with water NH_4OH (50%) twice, water twice, brine once and dried over $MgSO_4$.The solution was removed *in vacuo*, and the residue was redissolved in 10 mL of $CHCl_3$ and reprecipitated in methanol twice, The mixture was filtered to afford 0.42 g of a yellow solid (yield 89%). ^1H NMR ($CDCl_3$, ppm): δ 7.06 (s, 2 H), 7.03 (s, 2 H), 4.14 (br, 4 H), 4.05 (br, 4 H), 2.99 (br, 4 H), 2.70 (q, 8 H), 1.88 (br, 4 H), 1.52 (br, 4 H), 1.43-1.22 (br, 8 H), 1.09 (t, 12 H), 0.89 (t, 6 H). FT-IR (KBr pellet, cm^{-1}): 3454 (br), 3057, 2958, 2928, 2865, 2815, 2200, 1510, 1466, 1423, 1383, 1275, 1209, 1038, 950, 858, 803, 717, 509. Anal. Calcd for $C_{40}H_{58}N_2O_4$: C, 76.15; H, 9.27; N, 4.44. Found: C, 73.22; H, 8.54; N, 3.79.

5.4.26 Poly{2,5-Bis[3-(*N,N,N*-triethylammonium)-1-oxapropyl]-*p*-phenyleneethynylene} dibromide (P8') via Postpolymerization Alkylation of Poly{2,5-Bis[3-(N,N-diethylamino)-1-oxapropyl]-*p*-phenyleneethynylene}

A 50 mL round-bottom flask with a magnetic spin bar was charged with **P8** (0.33 g, 1mmol based on repeat). The polymer was dissolved in 20 mL of THF. To this was added bromoethane (1.09 g, 10 mmol) and 5 mL of DMSO. The solution was stirred at 50 ^oC for 3 days. Yellow precipitate was produced and filtered and dried to get 0.41 g of the desired product (yield 75%). ^1H NMR (D_2O, ppm): δ 7.26 (br, 2 H), 4.44 (br, 4 H), 3.73 (br, 1.8 H), 3.60 (br, 2.2 H), 3.40 (br, 4.3 H), 3.31 (br, 5.4 H), 1.20 (br, 12 H). ^{13}C NMR (D_2O, ppm): δ 153.3, 117.6, 114.1, 91.4, 64.8, 63.6, 58.5, 56.0, 54.3, 51.4, 49.5, 9.1, 7.6. FT-IR (KBr pellet, cm^{-1}): 3458 (br), 3056, 2970, 2947, 2870, 2659, 2484,

2202, 1510, 1467, 1422, 1397, 1275, 1216, 1059, 1020, 951, 864, 785, 715, 520. Anal. Calcd for $C_{20}H_{30}N_2O_2 \cdot 0.9C_2H_5Br \cdot 0.5H_2O$: C, 59.84; H, 8.18; N, 6.40; Br, 16.44. Found: C, 58.04; H, 7.35; N, 5.55; Br, 17.87.

5.4.27 Poly(2,5-Bis[3-(*N,N,N*-triethylammonium)-1-oxapropyl]-*p*-phenyleneethynylene-*alt*-2,5-bis{2-[2-(2-Methoxyethoxy)ethoxy]ethoxy}-*p*-phenyleneethynylene) Dibromide (P9') via Postpolymerization Alkylation of Poly(2,5-Bis[3-(*N,N*-diethylamino)-1-oxapropyl]-*p*-phenyleneethynylene-*alt*-2,5-bis{2-[2-(2-methoxyetho-xy)ethoxy]ethoxy}-*p*-phenyleneethynylene)

A 50 mL round-bottom flask with a magnetic spin bar was charged with **P9** (0.302 g, 0.4 mmol based on repeat). The polymer was dissolved in 20mL of THF. To this was added bromoethane (0.436 g, 4 mmol) and 5 mL of DMSO. The solution was stirred at 50 ^{o}C for 3 days, at which time most of the bromoethane and THF was evaporated. Polymer was precipitated in 100 mL of acetone, collected by centrifugation and dried overnight in vacuo at 50 ^{o}C (0.3 g, yield 77%). ^{1}H NMR (CD_3OD, ppm): δ 7.37 (br, 2 H), 7.27 (br, 2 H), 4.57 (br, 4 H), 4.29 (br, 4 H), 3.94 (br), 3.78 (br), 3.63 (br), 3.52 (br), 3.35 (br), 1.37 (br, 17.1 H). ^{13}C NMR (CD_3OD, ppm): δ 153.3, 152.7, 118.1, 117.9, 114.3, 92.3, 91.4, 72.5, 71.5, 71.3, 71.0, 69.7, 64.8, 63.6, 60.0, 58.6, 56.2, 54.2, 51.8, 49.5, 9.2, 7.4. FT-IR (KBr pellet, cm^{-1}): 3430 (br), 3056, 2980, 2932, 2880, 2650, 2483, 2203, 1508, 1464, 1423, 1398, 1275, 1218, 1097, 1052, 1026, 949, 852, 790, 716, 527. Anal. Calcd for $C_{42}H_{62}N_2O_{10} \cdot 1.7C_2H_5Br \cdot H_2O$: C, 56.91; H, 7.63; N, 2.92; Br, 14.18. Found: C, 58.77; H, 7.75; N, 2.67; Br, 15.50.

5.4.28 Poly{2,5-Bis[3-(*N,N,N*-triethylammonium)-1-oxapropyl]-*p*-phenyleneethynylene-*alt*-2,5-bis(dodecyloxy)-*p*-phenyleneethynylene} dibromide (P10') via

Postpolymerization Alkylation of Poly{2,5-Bis[3-(*N,N*-diethylamino)-1-oxapropyl] -*p*-phenyleneethynylene-*alt*-2,5-bis(dodecyloxy)-*p*-phenyleneethynylene}

A 50 mL round-bottom flask with a magnetic spin bar was charged with **P10** (0.319 g, 0.4 mmol based on repeat). The polymer was dissolved in 20 mL of THF. To this was added bromoethane (0.436 g, 4 mmol) and 5 mL of DMSO. The solution was stirred at 50 ^{o}C for 5 days. Polymer was precipitated in 200 mL of acetone, collected by centrifugation and dried overnight in vacuo at 50 ^{o}C (yield 79%). ^{1}H NMR (CD_3OD, ppm): δ 7.34 (br, 2 H), 7.19 (br, 2 H), 4.54 (br, 4 H), 4.12 (br, 4 H), 3.74 (br, 4 H), 3.51 (br, 11.8 H), 1.85 (br, 4 H), 1.57 (br, 4 H), 1.37 (br), 1.27 (br), 0.89 (br, 6 H). ^{13}C NMR (CD_3OD, ppm): δ 154.2, 153.3, 117.8, 114.9, 91.2, 70.3, 64.8, 54.3, 51.3, 49.3, 32.1, 29.8, 29.6, 26.3, 22.8, 13.5, 8.7, 7.2. FT-IR (KBr pellet, cm^{-1}): 3420 (br), 3056, 2968, 2924, 2853, 2627, 2475, 2203, 1510, 1467, 1422, 1392, 1271, 1214, 1057, 1020, 947, 863, 798, 718, 517. Anal. Calcd for $C_{52}H_{82}N_2O_4 \cdot 1.9C_2H_5Br \cdot 2.5H_2O$: C, 63.75; H, 9.25; N, 2.66 Br, 14.44. Found: C, 61.68; H, 8.47; N, 2.78; Br, 14.92.

5.4.29 Poly{2,5-Bis[3-(*N,N,N*-triethylammnium)-1-oxapropyl]-*p*-phenyleneethy-nylene-*alt*-2,5-bis(octyloxy)-*p*-phenyleneethynylene} dibromide (P11') via Postpolymerization Alkylation of Poly{2,5-Bis[3-(*N,N*-diethylamino)-1-oxapropyl]-*p*-phenyleneethynylene-*alt*-2,5-bis(octyloxy)-*p*-phenyleneethynylene}

A 50 mL round-bottom flask with a magnetic spin bar was charged with **P11** (0.343 g, 0.5mmol based on repeat). The polymer was dissolved in 20 mL of THF. To this was added bromoethane (0.545 g, 5 mmol) and 5 mL of DMSO. The solution was stirred at 50 ^{o}C for 5 days. Yellow precipitate was produced and filtered and dried to get 0.37 g of the desired product (yield 82%).

5.4.30 Poly{2,5-Bis[3-(*N,N,N*-triethylammnium)-1-oxapropyl]-*p*-phenyleneethynylene-*alt*-2,5-bis(hexyloxy)-*p*-phenyleneethynylene} dibromide (P12') via Postpolymerization Alkylation of Poly{2,5-Bis[3-(*N,N*-diethylamino)-1-oxapropyl]- *p*-phenyleneethynylene-*alt*-2,5-bis(hexyloxy)-*p*-phenyleneethynylene}

A 50 mL round-bottom flask with a magnetic spin bar was charged with **P12** (0.315 g, 0.5 mmol based on repeat). The polymer was dissolved in 20 mL of THF. To this was added bromoethane (0.545 g, 5 mmol) and 5 mL of DMSO. The solution was stirred at 50 ^{o}C for 5 days. Yellow precipitate was produced and filtered and dried to get 0.30 g of the desired product (yield 71%).

CHAPTER SIX

CONCLUSION REMARKS

In summary, three series of water-soluble cationic conjugated polyelectrolytes have been synthesized and characterized. Their applications as sensors have been investigated.

The first series of water-soluble polymers containing three cationic green light-emitting poly(*p*-phenylvinylene)s (PPVs) were successfully synthesized through a post-quaternization approach. Two traditional polymerization techniques, Gilch and Wittig reactions, were employed and found to produce two types of polymer structures, in which *trans*- and *cis*-vinyl was the dominant composition respectively. Although the Gilch product was insoluble in common organic solvents, its interesting acid-assisted and reversible solubility make it very promising for application as green emissive material in light-emitting diodes. Increase of hydrophilicity of the side chains was found to be beneficial to water solubility of the polymers. The optical properties of those polymers were studied, which showed a solvent-dependent conjugation length. Quaterizaition also resulted in the more twisted conformation of the polymer main chain. The conformation change may be responsible for the decrease in quantum efficiency of the polymers in solution. The bulky phenyl rings successfully suppressed interchain interactions, as evidenced by the absence of intermolecular dimmer and excimer. Quenching studies on water-soluble polymer showed that efficient fluorescence quenching can be achieved by using an anionic quencher $Fe(CN)_6^{4-}$, which is very useful in chemo- and biosensor applications. However, a modified Stern-Volmer plot demonstrated that some of the fluophores can not be accessible to the quencher, probably due to a twisted conformation or intermolecular aggregation.

Based on the results obtained from the first series of conjugated polyelectrolytes and to further study and develop novel sensors with good sensitivity, we synthesized amino-functionalized phenyl-substituted poly(*p*-phenylenevinylene) related copolymers containing thiophene, fluorene or alkoxylated or phenylated benzene unit through traditional Wittig reaction. Their corresponding cationic light-emitting polymers were successfully obtained through a post-quaternization approach. Increasing steric effect of the monomer was found to enhance the *cis*-vinyl content in those copolymers synthesized from Wittig reaction. In addition, the acid-assisted water solubility of the amino-terminated PPV was dramatically limited by the existence of bulky hydrophobic group in the side chain. The decrease of PL efficiency, compared with neutral polymers, still existed in those quaternized PPVs. Those polymers, with fluorene unit, showed highest PL efficiencies among those neutral and quaternized PPVs respectively. Thus, introduction of fluorene unit into the main chain of ionic conjugated polymers could be anticipated to develop chemo or biosensors with high PL efficiency. Meanwhile, adding aryl units with different electronic properties into conjugated backbone can successfully adjust the emission wavelengths of PPV copolymers and consequently be beneficial to the study of their corresponding quenching behaviors.

Moreover, we studied the quenching effect of $Fe(CN)_6^{4-}$ on cationic PPV derivatives with *cis*- and/or *trans*-vinylic linkage and downward Stern-Volmer curves was found in PPVs with *cis*-/*trans*-vinylic linkage while upward Stern-Volmer curves in PPVs with all *trans*-vinylic linkage. Electron transfer, not energy transfer, was the major way to result in quenching of PPVs with *cis*-linkage and those downward curves presented the incomplete quenching from inaccessible fluorophore. After considering the inaccessible fluorophore and sphere-of-action effect, a modified Stern-Volmer equation

was obtained to well fit the downward Stern-Volmer curve of PPVs with *cis*-linkage. The existence of *cis*-vinylic linkage was considered to be the key factor to produce such inaccessible fluorophore. Changing the molecular structures of alternating units in those PPV copolymers could significantly influence the corresponding quenching behavior and the content of inaccessible fluorophore. All the results indicate that choosing appropriate molecular structures is very important to obtain sensors with good sensitivity.

The third series of polymers were successfully designed for the study of influence of chemical and physical environments on the quenching behaviours of conjugated polyelectrolytes. We report on the successful synthesis and optical properties of a serious of water-soluble cationic poly(p-phenyleneethynylene)s (PPEs) via post-quaternization. Excellent water-solublility was also achieved by introducing more hydrophilic side chains. The electronic spectra of the quaternized polymers present a strong dependence on the nature of the substituents and the solvent. Intermolecular aggregation was observed for the polymer with hydrophobic side chain in methanol, which may result from the presence of long chain hydrophobic groups. The fluorescence of water-soluble PPE (PPE-NEt_3^+) enhanced at acid environment and reduced at base environment, which exhibited a titration-like curve. The fluorescence enhancement of PPE-NEt_3^+ when pH < 7 may result from the interaction between H^+ and PPE-NEt_3^+ to reduce the trapping on the conjugated chain, while the reason for the fluorescence decrease of PPE-NEt_3^+ was clearly attributed to the OH^--induced aggregation for PPE-NEt_3^+. Further investigation showed that the pH-sensitive region could be tuned by changing the polymer concentration. The study of quenching of PPE-NEt_3^+ by $Fe(CN)_6^{4-}$ at different pH values exhibited that the Stern-Volmer constant (K_{sv}) was retained in acid environment but highly increased at base

environment due to the formation of interchain aggregation driven by OH^-. The K_{sv} value was found to be inverse proportional to the polymer concentration. Because of the highly influence of pH value on polymer fluorescence and K_{sv} value, such a significant variation must be considered for designing good biosensors.

Furthermore, we studied the fluorescence quenching of PPE-NEt_3^+ at different concentrations by $Fe(CN)_6^{4-}$. A new UV-vis absorption peak appeared after adding $Fe(CN)_6^{4-}$, indicating that the polymer/quencher complex was formed. K_{sv} of PPE-NEt_3^+ for $Fe(CN)_6^{4-}$ increased with the concentration decrease of PPE-NEt_3^+ and was observed inverse proportional to PPE-NEt_3^+ concentration (≥ 1 μM) and deviation of the linearity at lower concentration (≤ 1 μM) without the influence from aggregation. To account for this phenomenon, the concept of local quencher concentration was introduced into the Stern-Volmer equation and a new equation which successfully presented such a relationship between K_{sv} and [PPE-NEt_3^+] was obtained. The value of association constant for $Fe(CN)_6^{4-}$ binding to PPE-NEt_3^+ can be obtained from the equation ($K_b = 7.3 \times 10^6\ M^{-1}$).

We also studied the optical properties and quenching behaviors of complexations of PPE-NEt_3Br with the oppositely charged polymer PAANa and PMAANa in aqueous solution. It was showed that addition of few PAANa induced the PPE-NEt_3Br chain to vary from isolated state to aggregated state and then recovered to isolated state through increasing the amount of PAANa, which exhibited an obvious fluctuation of fluorescence intensity and K_{sv} values. While after adding PMAANa, PPE-NEt_3Br still exhibited the similar mutation of complex structure just as what appeared in PAANa/PPE-NEt_3Br complex except that more twisted conjugated main chain and no aggregation was formed. Such a significant structure difference showed that a little change of the structure of those anionic polymers will significantly influence the

conformation and hence the optical and quenching properties of ionic conjugated polymers. Investigation of the percentage of inaccessible fluorescence is a good way to obtain the complex structure information that the mutation point for PAANa/PPE-NEt_3Br complex was at PAANa : PPE-NEt_3Br = 1.2, which is amount to the corresponding result from the variation of its fluorescence intensity, and that for PMAANa/PPE-NEt_3Br complex is at PMAANa : PPE-NEt_3Br = 1. Investigation of the sensitivity of those complexes showed that adding an appropriate amount of PAANa will be beneficial to enhance the K_{sv} value resulting from the PAANa-induced aggregation while no similar phenomenon was found in PMAANa/PPE-NEt_3Br system, which further demonstrated that the sensitivity of conjugated polymers could be controlled by the structure of the complexes formed between rod-like conjugated polyelectrolyte and oppositely charged polymers and thus by the structure of those oppositely charged polymers utilized in our system. Therefore, in practical application to develop good sensors with high sensitivity, it is important to choose a polyelectrolyte with suitable structure as biosensor platform and control its amount which is used to form complex with oppositely charged conjugated polyelectrolyte.

All the results have demonstrated that those water-soluble conjugated polyelectrolytes with PPV and PPE structures have exhibited great potentials in sensory application and theoretical study on quenching mechanism. Further investigation of the optical properties and quenching behaviors of those water-soluble conjugated polymers is on the rise in our group.